VOLUME 114 NUMBER 3

THE ASTROPHYSICAL JOURNAL

AN INTERNATIONAL REVIEW OF SPECTROSCOPY AND ASTRONOMICAL PHYSICS

NOVEMBER 1951

THE NONRADIAL OSCILLATIONS OF GASEOUS STARS AND THE ... OF BETA CANIS MAJORIS ... 373
THE POSSIBLE INFLUENCE OF INTERSTELLAR CLOUDS ON ... Lyman Spitzer, Jr., and ... 385
ON THE DIFFERENCE IN CHEMICAL COMPOSITION BETWEEN ... VELOCITY STARS M. Schwarzschild, L. Spitzer, and ... 398
CONTINUOUS EMISSION FROM PLANETARY NEBULAE Lyman Spitzer, Jr. ... 407
THE STRUCTURE OF THE PLANETARY NEBULA IC 418 O. C. Wilson ... 431
THE ANALYSIS OF AURORAL EMISSION BANDS FROM THE 431
A TWO-ENERGY SOURCE SOLAR MODEL ... 438
ON THE INTENSITY OF Ti LINES AT DIFFERENT POINTS OF THE ... F. ... 443
THE PHYSICAL THEORY OF METEORS. II. ASTEROIDAL ... Richard N. Thomas ... 449
LABORATORY STUDIES OF THE λ 4050 GROUP OF COMETARY ... 466
TRANSITION PROBABILITIES OF FORBIDDEN LINES ... 469
THE ... STARS William H. McCrea ... 473
THE ... SPECTROSCOPIC BINARY BD +48°4220 O. C. ... 487
A FUNDING LIST OF HIGH-LUMINOSITY STARS. II ... 492
PROPER MOTIONS FOR THIRTY-THREE BLUE STARS IN HIGH ... TUBE William J. Luyten ... 498
A STUDY OF THE CONCENTRATION OF EARLY-TYPE STARS ... 499
THE LIGHT-CURVE AND THE COLOR OF VESTA ... 500
PHOTOMETRY OF ZETA AURIGAE IN THE 1947–1948 ECLIPSE ... 505
THE ECLIPSING BINARY U SAGITTAE ... 515
ON THE COLOR-MAGNITUDE DIAGRAM OF THE PLEIADES H. L. ... 522
NOTE ON OLIN J. EGGEN'S OBSERVATIONS OF THE PLEIADES ... 544
NOTES—
Transition Probabilities for C_I and A_I ... 546
On the Spectrum of AC Andromedae ... 546
A Useful Luminosity Discriminant in the Late K and Early M Giants W. S. ... 548
REVIEWS ... 549
INDEX ... 553

THE UNIVERSITY OF CHICAGO PRESS
CHICAGO, ILLINOIS, U.S.A.

November 1951 Vol. 114, No. 3

THE ASTROPHYSICAL JOURNAL

AN INTERNATIONAL REVIEW OF SPECTROSCOPY AND ASTRONOMICAL PHYSICS

The Astrophysical Journal is published bimonthly by the University of Chicago at the University of Chicago Press, 5750 Ellis Avenue, Chicago 37, Illinois, during July, September, November, January, March, and May. Two volumes are published per year, one beginning with the January issue and the other beginning with the July issue. The subscription price is $6.00 per volume or $12.00 per year; the price of single copies is $3.00. (Orders for service of less than a volume will be charged at the single copy rate.) Postage is prepaid by the publishers on all orders from the United States and its possessions. No extra charge is made for postage to countries in the Pan American Postal Union. Postage is charged extra as follows: for Canada, 20 cents per volume, 40 cents per year (total $6.20 per volume, $12.40 per year); on single copies 5 cents (total $3.05); for all other countries in the Postal Union, 50 cents per volume, $1.00 per year (total $6.50 per volume, $13.00 per year), on single copies 10 cents (total $3.10). Subscriptions are payable in advance. Please make all remittances payable to The University of Chicago Press. In United States currency or its equivalent by postal or express money orders or bank drafts.

The following is an authorized agent:

For the British Empire, except North America and Australasia: The Cambridge University Press, Bentley House, 200 Euston Road, London, N.W. 1, England. Prices of yearly subscriptions and of single copies may be had on application.

Claims for missing numbers should be made within the month following the regular month of publication. The publishers expect to supply missing numbers free only when issues have been lost in transit, and when the reserve stock will permit.

Business correspondence should be addressed to The University of Chicago Press, Chicago 37, Illinois.

Communications for the editors and manuscripts should be addressed to: W. W. Morgan, Editor of The Astrophysical Journal, Yerkes Observatory, Williams Bay, Wisconsin.

Line drawings and photographs should be made by the author, and all marginal notes such as co-ordinates, wave lengths, etc., should be included in the cuts. It will not be possible to set up such material in type.

One copy of the corrected galley proof should be returned as soon as possible to the editor, Yerkes Observatory, Williams Bay, Wisconsin. Authors should take notice that the manuscript will not be sent to them with the proof.

The cable address is "Observatory, Williamsbay, Wisconsin."

The articles in this journal are indexed in the *International Index to Periodicals*, New York, N.Y.

Applications for permission to quote from this journal should be addressed to The University of Chicago Press, and will be freely granted.

Microfilms of complete journal volumes are available to regular subscribers only and may be obtained at the end of the year. Orders and inquiries should be addressed to University Microfilms, 313 North First Street, Ann Arbor, Michigan.

Notice to subscribers: If you change your address, please notify us and your local postmaster immediately.

Entered as second-class matter, July 22, 1930, at the Post-Office at Chicago, Ill., under the Act of March 3, 1879.
Acceptance for mailing at special rate of postage provided for in United States Postal Act of October 3, 1917, Section 1103, amended February 28, 1925.

[PRINTED IN U.S.A.]

THE ASTROPHYSICAL JOURNAL

An International Review of Spectroscopy and Astronomical Physics

FOUNDED IN 1895 BY GEORGE E. HALE AND JAMES E. KEELER

VOLUME 114

JULY–NOVEMBER, 1951

THE UNIVERSITY OF CHICAGO PRESS
CHICAGO, ILLINOIS

CAMBRIDGE UNIVERSITY PRESS, LONDON

PUBLISHED JULY, SEPTEMBER, NOVEMBER, 1951

COMPOSED AND PRINTED BY THE UNIVERSITY OF CHICAGO PRESS
CHICAGO, ILLINOIS, U.S.A.

CONTENTS

NUMBER 1

THE MAGNETICALLY VARIABLE STAR HD 125248. Horace W. Babcock 1

THE SPECTRUM OF XX OPHIUCHI IN 1949 AND 1950. Paul W. Merrill 37

THE SPECTRAL CHANGES OF VV CEPHEI OUTSIDE ECLIPSE. Dean B. McLaughlin . . 47

THE ATMOSPHERES OF A-TYPE SUBDWARFS AND 95 LEONIS. Joseph W. Chamberlain and Lawrence H. Aller 52

SPECTROPHOTOMETRY OF EARLY A-TYPE STARS. William Buscombe 73

IONIZED HYDROGEN REGIONS IN PLANETARY NEBULAE. Thornton Page and Jesse L. Greenstein 98

NEGATIVE HYDROGEN IONS IN PLANETARY NEBULAE. Jesse L. Greenstein and Thornton Page 106

THE THEORY OF THE FLUCTUATIONS IN BRIGHTNESS OF THE MILKY WAY. III. S. Chandrasekhar and G. Münch 110

AN ANALYSIS OF GALACTIC STRUCTURE IN THE DIRECTION OF AQUILA. Ralph L. Calvert 123

AN ANALYSIS OF THE MILKY WAY IN PERSEUS. David S. Heeschen 132

PHOTOELECTRIC STUDIES. VIII. POSITIONAL EFFECT IN PHOTOMULTIPLIERS AND SOME REVISED MAGNITUDES IN THE NORTH POLAR SEQUENCE AND HARVARD REGION C 12. Olin J. Eggen 141

THE STRUCTURE OF THE SOLAR ATMOSPHERE AS DEDUCED FROM LIMB-DARKENING MEASURES. A Keith Pierce and Lawrence H. Aller 145

A ROTATIONAL ANALYSIS OF THE γ-SYSTEM OF THE *TiO* MOLECULE. John G. Phillips . . 152

NOTES

A NOTE ON THE SPECTRUM OF RR TELESCOPII. Karl G. Henize and Dean B. McLaughlin 163

NUMBER 2

THE EVOLUTION OF GALAXIES AND STARS. C. F. von Weizsäcker 165

A THEORY OF INTERSTELLAR POLARIZATION. Lyman Spitzer, Jr., and John W. Tukey . 187

THE POLARIZATION OF STARLIGHT BY ALIGNED DUST GRAINS. Leverett Davis, Jr., and Jesse L. Greenstein 206

POLARIZATION OF STELLAR RADIATION. III. THE POLARIZATION OF 841 STARS. W. A. Hiltner 241

THE CONDITION FOR TURBULENCE IN ROTATING STARS. T. G. Cowling 272

ON THE VARIATION OF TURBULENT VELOCITIES IN STELLAR AND SOLAR ATMOSPHERES. Su-shu Huang 287

PHOTOELECTRIC STUDIES OF FIVE ECLIPSING BINARIES. C. M. Huffer and Zdeněk Kopal 297

COUDÉ RADIAL VELOCITIES OF TU CASSIOPEIAE, DT CYGNI, AND U VULPECULAE. Roscoe F. Sanford 331

RADIAL VELOCITIES OF FF AQUILAE. Roscoe F. Sanford 335

DISPLACED HELIUM LINES IN THE SPECTRUM OF BD+11°4673. Paul W. Merrill . . . 338

AN EMISSION BAND SYSTEM ATTRIBUTED TO THE MOLECULE NH^+. M. W. Feast . . . 344

CHARACTERISTICS OF SOLAR FLARES. Robert S. Richardson 356

SOME OBSERVATIONS OF DARK FILAMENTS IN PROMINENCES. Yngve Öhman 367

NOTES

THE SPECTROSCOPIC BINARY 47 ANDROMEDAE. P. D. Jose 370

REVIEWS 371

NUMBER 3

THE NONRADIAL OSCILLATIONS OF GASEOUS STARS AND THE PROBLEM OF BETA CANIS MAJORIS. P. Ledoux 373

THE POSSIBLE INFLUENCE OF INTERSTELLAR CLOUDS ON STELLAR VELOCITIES. Lyman Spitzer, Jr., and Martin Schwarzschild 385

ON THE DIFFERENCE IN CHEMICAL COMPOSITION BETWEEN HIGH- AND LOW-VELOCITY STARS. M. Schwarzschild, L. Spitzer, Jr., and R. Wildt 398

CONTINUOUS EMISSION FROM PLANETARY NEBULAE. Lyman Spitzer, Jr., and Jesse L. Greenstein 407

THE STRUCTURE OF THE PLANETARY NEBULA IC 418. O. C. Wilson and Lawrence H. Aller 421

THE ANALYSIS OF AURORAL EMISSION BANDS FROM THE $A^2\Pi$ STATE OF N_2^+. A. B. Meinel 431

A TWO-ENERGY SOURCE SOLAR MODEL. I. Epstein 438

ON THE INTENSITY OF *Ti* LINES AT DIFFERENT POINTS OF THE SUN'S RADIUS. V. Barocas and G. Righini 443

THE PHYSICAL THEORY OF METEORS. II. ASTROBALLISTIC HEAT TRANSFER. Richard N. Thomas and Fred L. Whipple 448

LABORATORY STUDIES OF THE λ 4050 GROUP OF COMETARY SPECTRA. A. E. Douglas . . 466

TRANSITION PROBABILITIES OF FORBIDDEN LINES. Donald E. Osterbrock 469

THE *Ba* II STARS. William P. Bidelman and Philip C. Keenan 473

THE Of-TYPE SPECTROSCOPIC BINARY BD+40°4220. O. C. Wilson and Arthur Abt . . 477

A FINDING LIST OF HIGH-LUMINOSITY STARS. II. Luis Münch 482

PROPER MOTIONS FOR THIRTY-THREE BLUE STARS IN HIGH GALACTIC LATITUDE. Willem J. Luyten and William C. Miller 488

A STUDY OF THE CONCENTRATION OF EARLY-TYPE STARS IN CYGNUS. Nancy G. Roman 492

THE LIGHT-CURVE AND THE COLOR OF VESTA. C. Bruce Stephenson 500

PHOTOMETRY OF ZETA AURIGAE IN THE 1947–1948 ECLIPSE. Frank Bradshaw Wood . . 505

THE ECLIPSING BINARY U SAGITTAE. D. H. McNamara 513

ON THE COLOR-MAGNITUDE DIAGRAM OF THE PLEIADES. H. L. Johnson and W. W. Morgan 522

NOTE ON OLIN J. EGGEN'S OBSERVATIONS OF THE PLEIADES. Joel Stebbins 544

NOTES

TRANSITION PROBABILITIES FOR C_2 AND N_2^+. Harrison Shull 546

ON THE SPECTRUM OF AC ANDROMEDAE. Guido Münch 546

A USEFUL LUMINOSITY DISCRIMINANT IN THE LATE K AND EARLY M GIANTS. W. S. Fitch and W. W. Morgan 548

REVIEWS 549

INDEX 553

THE ASTROPHYSICAL JOURNAL

AN INTERNATIONAL REVIEW OF SPECTROSCOPY AND ASTRONOMICAL PHYSICS

VOLUME 114 NOVEMBER 1951 NUMBER 3

THE NONRADIAL OSCILLATIONS OF GASEOUS STARS AND THE PROBLEM OF BETA CANIS MAJORIS*

P. LEDOUX†
Princeton University Observatory
Received June 5, 1951

ABSTRACT

The general characteristics of the nonradial oscillations of a rotating star are summarized and compared with the observations of β Canis Majoris. It is shown that the existence of two periods very close to each other as well as a phase shift of a quarter-period between the broadening of the lines and the corresponding radial velocity can be accounted for if the oscillation corresponds to a spherical harmonic of degree 2 in a rotating star. However, for free oscillations, the sign of the phase shift is opposite to the one observed when the periods are in the correct ratio, and vice versa.

Forced oscillations are briefly discussed, and, although they offer a possibility of removing this discrepancy, a quantitative analysis presents difficulties due to the proximity of the hypothetical companion.

I. INTRODUCTION

In a recent paper, O. Struve[1] has discussed radial observations of β Canis Majoris extending over a period of more than forty years. His results confirm Meyer's interpretation[2] in terms of two harmonic radial-velocity-curves, V_1 and V_2, of very close periods τ_1 and τ_2, giving rise to a beat oscillation of period τ_3. According to Struve, the shortest period, $\tau_1 = 0.25002246$ day, and the corresponding amplitude, $A_1 = 5.8$ km/sec, have remained constant, while, as far as τ_2 and A_2 are concerned, the observations are best represented by adopting the values $\tau_2 = 0.2513015$ day and $A_2 = 4.2$ km/sec for the period 1909–1931 and $\tau_2' = 0.2513003$ day and $A_2' = 2.0$ km/sec for the period 1931–1948. The corresponding beat periods are $\tau_3 = 49.12$ and $\tau_3' = 49.17$ days.

Furthermore, the absorption lines exhibit a variation in width with the same period τ_2 as V_2, but with a phase lag of a quarter-period; that is, the maximum broadening occurs when V_2 goes through zero from positive to negative values. Struve's discussion suggests also that this broadening has changed with the amplitude A_2.

* This research was supported in part by funds of the Eugene Higgins Trust allocated to Princeton University.

† On leave from the Institut d'Astrophysique, Cointe-Sclessin, Belgium; associé du Fonds national de la Recherche scientifique.

[1] *Ap. J.*, **112**, 520, 1950.

[2] *Pub. A.S.P.*, **46**, 202, 1934.

The explanation proposed by Struve requires the presence of a companion of very small dimensions and high density, one of the periods corresponding to the orbital motion and the other to an oscillation excited by resonance in the main component. This hypothesis raises difficulties which we will discuss later, but first we review the properties of the free oscillations of a rotating gaseous star.

II. THEORY OF FREE OSCILLATIONS

a) EQUATIONS OF MOTION, PERIODS, AND DISPLACEMENTS

It seems unlikely that purely radial oscillations are significant in this connection, as it would be difficult to explain both the very close periods and the observed broadening of the lines on such a theory. On the other hand, for nonradial oscillations, we know[3] that there will exist groups of oscillations of very close periods, provided that the star is in slow rotation.

In this case, if we suppose that the dependence with respect to the time t is of the form $\exp i\sigma t$, the Eulerian equation of motion, with respect to axis rotating with the angular velocity of the star $\vec{\Omega}$, can be written

$$-\sigma^2\,\delta\mathbf{r}+2i\sigma\,(\vec{\Omega}\times\delta\mathbf{r})=-\frac{1}{\rho}\operatorname{grad}P'+\frac{\rho'}{\rho^2}\operatorname{grad}P+\operatorname{grad}U', \tag{1}$$

where $\delta\mathbf{r}$ is the displacement and the other symbols have their usual meaning, the primes denoting the Eulerian variations of the corresponding variables. If Ω is small, so that we can neglect all its powers greater than the first, the components of this equation in polar co-ordinates are

$$-\sigma^2\,\delta r-2i\sigma\Omega r\sin^2\theta\,\delta\phi=-\frac{1}{\rho}\frac{\partial P'}{\partial r}+\frac{\rho'}{\rho^2}\frac{\partial P}{\partial r}+\frac{\partial U'}{\partial r}, \tag{2}$$

$$-\sigma^2 r\,\delta\theta-2i\sigma\Omega\cos\theta\, r\sin\theta\,\delta\phi=-\frac{1}{\rho}\frac{\partial P'}{r\,\partial\theta}+\frac{\partial U'}{r\,\partial\theta}, \tag{3}$$

$$-\sigma^2 r\sin\theta\,\delta\phi+2i\sigma\Omega\sin\theta\,\delta r+2i\sigma\Omega\cos\theta\, r\,\delta\theta=-\frac{1}{\rho}\frac{\partial P'}{r\sin\theta\,\partial\phi}+\frac{\partial U'}{r\sin\theta\,\partial\phi}, \tag{4}$$

where the equilibrium values of the variables can be taken equal to their values in a purely spherical nonrotating configuration.

We must take into account the equation of continuity,

$$\rho'=-\operatorname{div}\rho\,\delta\mathbf{r}, \tag{5}$$

and the adiabatic relation,

$$P'=-\frac{\gamma P}{\rho}\operatorname{div}\delta\mathbf{r}-\delta\mathbf{r}\cdot\operatorname{grad}P=\frac{\gamma P}{\rho}\rho'-\delta\mathbf{r}\left(\operatorname{grad}P-\frac{\gamma P}{\rho}\operatorname{grad}\rho\right). \tag{6}$$

We can suppose that δr, ρ', P', and U' are expanded in series of spherical harmonics and consider only the general term,

$$F(r,\theta,\phi)=f(r)P_s^m(\cos\theta)\,e^{\pm im\phi}. \tag{7}$$

These solutions must satisfy the boundary conditions

$$\delta r=0 \qquad \text{at} \qquad r=0,$$

[3] T. G. Cowling and R. A. Newing, *Ap. J.*, **109**, 149, 1949; also P. Ledoux, *Mém. Soc. R. Sci. Liége*, 4th ser., **9**, 263, 1949.

$$P' + \delta r \cdot \operatorname{grad} P = 0\,, \qquad \frac{\partial U'}{\partial r} + \frac{s+1}{r}\, U' = 0\,, \qquad \text{at} \qquad r = R\,. \tag{8}$$

If we denote, by a suffix zero, the solutions for $\Omega = 0$, we can easily verify that the corresponding displacements $\delta r_{k,0}$ are orthogonal:

$$\int_0^M \delta r_{k,0} \cdot \delta r^*_{l,0}\, dm = \int_0^M (\delta r_{k,0}\, \delta r^*_{l,0} + r^2 \delta\theta_{k,0}\, \delta\theta^*_{l,0} + r^2 \sin^2\theta\, \delta\phi_{k,0}\, \delta\phi^*_{l,0})\, dm = 0\,, \tag{9}$$
$$(k \neq l)\,.$$

If we retain the terms in Ω, $\sigma_{k,0}$ is increased by a small amount σ'_k and $\delta r_{k,0}$ by a small vector $\delta r'_k$, which can be represented by a series in terms of $\delta r_{i,0}$,

$$\delta r_k = \delta r_{k,0} + \sum_i a_{k,i}\, \delta r_{i,0}\,.$$

Then equations (5) and (6) and Poisson's equation give

$$\rho'_k = \rho'_{k,0} + \sum_i a_{k,i}\, \rho'_{i,0}\,, \qquad P'_k = P'_{k,0} + \sum_i a_{k,i}\, P'_{i,0}\,, \qquad U'_k = U'_{k,0} + \sum_i a_{k,i}\, U'_{i,0}\,.$$

Introducing these expressions into equation (1) and keeping first-order terms only, we obtain

$$2\sigma_{k,0}\sigma'_k\, \delta r_{k,0} = 2i\sigma_{k,0}\, (\vec{\Omega} \times \delta r_{k,0}) - \sum_i a_{k,i}\, (\sigma^2_{k,0} - \sigma^2_{i,0})\, \delta r_{i,0}\,.$$

If we multiply the components of this equation, respectively, by $\delta r^*_{k,0}$, $r\delta\theta^*_{k,0}$, $r \sin\theta\, \delta\phi^*_{k,0}$, integrate the sum over the whole mass, and use relation (9), we find

$$\sigma'_k = \frac{i \int_0^M (\vec{\Omega} \times \delta r_{k,0}) \cdot \delta r^*_{k,0}\, dm}{\int_0^M (\delta r_{k,0} \cdot \delta r^*_{k,0})\, dm}\,, \tag{10}$$

which is identical to the formula obtained by T. G. Cowling and R. A. Newing[3] from the application of Rayleigh's principle.

The displacements $\delta r_{k,0}$ can be deduced from equations (2), (3), and (4) with $\Omega = 0$. Furthermore, T. G. Cowling's discussion of the polytropic case[4] has shown that, even for harmonics of small degree ($s = 2, 3, \ldots$) a reasonable approximation can be obtained by neglecting U'. In that case, using equations (2) and (6) and the following definitions,

$$y = \frac{P'}{\rho}\,, \qquad g = -\frac{1}{\rho}\frac{\partial P}{\partial r}\,, \qquad A = \frac{1}{\gamma P}\frac{\partial P}{\partial r} - \frac{1}{\rho}\frac{\partial \rho}{\partial r}\,, \tag{11}$$

we have

$$\delta r_{k,0} = \frac{1}{\sigma^2_{k,0} - gA}\left(\frac{\partial y}{\partial r} - yA\right) P^m_s e^{\pm im\phi} = a(r)\, P^m_s e^{\pm im\phi}\,, \tag{2'}$$

$$r\,\delta\theta_{k,0} = \frac{y}{\sigma^2_{k,0}\, r}\frac{\partial P^m_s}{\partial\theta}\, e^{\pm im\phi} = b(r)\frac{\partial P^m_s}{\partial\theta}\, e^{\pm im\phi}\,, \tag{3'}$$

[4] *M.N.*, **101**, 367, 1941; cf. also Z. Kopal, *Ap. J.*, **109**, 509, 1949; and E. Sauvenier-Goffin, *Bull. Soc. R. Sci. Liège*, **20**, 20, 1951.

$$r \sin\theta \, \delta\phi_{k,0} = \frac{\pm imy}{\sigma_{k,0}^2 r} \frac{P_s^m}{\sin\theta} e^{\pm im\phi} = \pm im\, b(r) \frac{P_s^m}{\sin\theta} e^{\pm im\phi}. \tag{4'}$$

Introducing these expressions into equation (10) and making use of well-known properties of the spherical harmonics, we obtain

$$\sigma_k' = \pm m\Omega \frac{\int_0^R \rho (2ab + b^2) r^2 dr}{\int_0^R \rho [a^2 + s(s+1) b^2] r^2 dr} = \pm m\Omega C_k, \tag{10'}$$

where C_k is a constant for a given mode. For the homogeneous compressible model, this expression reduces to the known value,[5]

$$\sigma_k' = \pm m\Omega \frac{2a_k + 1}{a_k^2 + s(s+1)}, \qquad \text{where} \qquad a_k = \frac{3\sigma_k^2}{4\pi G\rho}. \tag{12}$$

Since, for a given value of the degree s, the rank m can take the values $0, 1, 2, \ldots, s$, we now have $(2s+1)$ frequencies $\sigma_{k,m}$ associated with each frequency $\sigma_{k,0}$ of the nonrotating star,

$$\sigma_{k,m} = \sigma_{k,0} \pm m\Omega C_k, \qquad (m = 1, 2, \ldots, s).$$

We can limit our discussion here to the case $s = 2$, which is the most interesting one, and, if we neglect the nonsymmetrical oscillations corresponding to $m = 1$, we are left with three frequencies σ and $\sigma \pm 2\Omega C$ for each mode. The first one is the frequency of a stationary oscillation symmetrical with respect to the axis of rotation, while the other two correspond, respectively, to waves traveling in the opposite or the same direction as the rotation of the star with relative angular velocities $\mp(\sigma/2 \pm \Omega C)$. But, since our axes are themselves rotating with velocity Ω, the absolute angular velocities are, respectively, $\mp[\sigma/2 \mp \Omega(1 - C)]$ and the corresponding frequencies for observers at rest are

$$\sigma, \qquad \sigma - 2\beta\Omega, \qquad \sigma + 2\beta\Omega, \qquad \text{where} \qquad \beta = 1 - C. \tag{13}$$

b) DISCUSSION OF THE VALUES OF C

In the case of an incompressible fluid, C is just equal to $\frac{1}{2}$, but it is already appreciably smaller for the homogeneous compressible model, in which case equation (12) gives the maximum value $C \simeq \frac{1}{4}$ for the lowest stable mode. In more general cases the value of C will depend on the behavior of a and b through the star. To discuss this dependence, let us consider equation (2') and the equation obtained in developing the last two members of equation (6),

$$\frac{dy}{dr} - yA = (\sigma^2 - gA)\, a, \tag{14}$$

$$\frac{d}{dr}(r^2 a) + \frac{1}{\gamma P} \frac{\partial P}{\partial r} r^2 a = \left[\frac{s(s+1)}{\sigma^2} - \frac{\rho r^2}{\gamma P}\right]. \tag{15}$$

With the help of the following definitions:

$$v = r^2 a P^{1/\gamma}, \qquad w = \rho y P^{-1/\gamma},$$

these equations become

$$r^2 \frac{dw}{dr} = (\sigma^2 - gA)\, \rho P^{-2/\gamma} v, \tag{16}$$

[5] Ledoux, *op. cit.*, p. 283.

$$\frac{dv}{dr} = \left[\frac{s(s+1)}{\sigma^2} - \frac{\rho r^2}{\gamma P}\right] \rho^{-1} P^{2/\gamma} w . \tag{17}$$

A general discussion of the equations with respect to the stability cannot be attempted here, but equations (16) and (17) show that if A is positive everywhere—that is, if the star is convectively stable in all its parts—there is no solution with σ^2 negative (instability) which satisfies the boundary conditions.

We will limit ourselves to this case, because regions of small extent, with slightly superadiabatic gradients, will not affect our conclusions for the modes in which we are interested.

These equations have regular singularities at $r = 0$ and $r = R$; and, taking the boundary conditions (8) into account, one finds that near the center, where A varies as r, one has the asymptotic relations

$$y \to \sigma^2 r a \to r^s \quad \text{or} \quad b \to a \to r^{s-1} ; \qquad (r \to 0) , \tag{18}$$

while near the surface, where A becomes infinite, one finds immediately

$$y \to g a \quad \text{or} \quad b \to \frac{a}{a} \qquad (r \to R) , \tag{19}$$

if a is defined by

$$\sigma^2 = \frac{4\pi G \bar{\rho}}{3} a . \tag{20}$$

As $\rho r^2/\gamma P$ varies in a monotonic fashion from zero at the center to $+\infty$ at the surface, the bracket in equation (17) vanishes once in the interval $0 < r < R$, let us say at r_v. On the other hand, gA varies also from 0 to ∞ but is not necessarily monotonic, so that there are either one or an odd number of points r_w where the bracket in equation (16) vanishes. At these points, r_v and r_w, the equations have regular singularities where v and w have true maxima or minima.

For a given value of s, the solutions can be divided into two groups, according to the relative positions of the points r_v and r_w nearest the center; and Cowling's nomenclature for the polytropes can be adopted here, too. If the point r_w occurs first—and this is certainly the case for σ^2 small enough—the first node of w (or P') is nearer the center than the first node of v (or δr). This class of solutions comprises the g oscillations, for which σ^2 tends toward zero as the number of nodes increases indefinitely. On the other hand, when a point r_v occurs first—and this is certainly the case for σ^2 large enough—we have the p oscillations, for which σ^2 tends toward infinity as the number of nodes increases. There is one oscillation called f by Cowling, which has no node in $0 < r < R$ and separates these two classes.

For the standard model, which can be considered typical in this respect, the value of a_f is of the order of 10, and we can conclude from equations (18) and (19) that, except for the high g modes, b will always be smaller than a, especially near the surface. In that case the definition (10′) shows that C will be of the order of $\overline{(2b/a)}$, or 0.2 for the standard model. When b tends to become of the same order of magnitude as a or larger (g oscillations), the product (ab) changes sign along the radius, and its integral in equation (10′) tends to vanish, so that even in this case C can never become much larger than $\frac{1}{4}$. For instance, the numerical integrations[4] carried out for the standard model with $s = 2$ and $\gamma = \frac{5}{3}$ give

$$a_f = 8.69 , \qquad a_{g_1} = 4.72 , \qquad a_{g_2} = 2.92 ; \tag{21}$$

and, using the values of the corresponding amplitudes in equation (10′), one finds

$$C_f = 0.179 , \qquad C_{g_1} = 0.146 , \qquad C_{g_2} = 0.137 . \tag{22}$$

Unfortunately, we have no numerical information on the p oscillations except for the homogeneous compressible model; but we know that the corresponding a_p increase, a_{p_1} being probably of the order of 15, while the C_p will slowly decrease.

III. COMPARISON WITH THE OBSERVATIONS

a) PERIODS

According to Struve, β Canis Majoris, which is of spectral type B, has some giant characteristics, and we will adopt for its mean density, $\bar{\rho}$, a value of the order of 0.02, which is about one-tenth the density of a main-sequence star of the same type.[6] With an observed period of 0.25 day, this gives, according to definition (20), a value for a of the order of 15.

A comparison with the theoretical values (21) points toward the p_1 oscillation rather than the f or one of the g oscillations. However, some of the stars belonging to this class of variables are members of the main sequence and have only slightly shorter periods, so that the corresponding a's would be of the order of 2–2.5, which would imply g oscillations in these cases. This is not very satisfactory, but the giant characteristics of β Canis Majoris might be due to a distended photosphere caused by some surface agency,[7] which would leave its mean density closer to that of the main-sequence stars.

Perhaps at this preliminary stage the only significant feature as far as the periods are concerned is that they fall in the range of theoretical values corresponding to simple modes, which do not require a too complicated mechanism for their excitation or maintenance.

As the two traveling waves will have the same general properties, we can already suspect that we will have to identify the two observed oscillations with the stationary pulsation and one or the other of the traveling waves. According to the set of values (13), the corresponding frequencies would differ in either case by an amount of the order of 2Ω, which should be equal to the observed beat frequency. For instance, for the f mode of the standard model, the difference would be 1.642Ω. If we put this equal to 49 days, we find a period of rotation for β Canis Majoris of the order of 80 days, corresponding to linear velocities at the equator of the order of 8–10 km/sec.

b) MEAN VELOCITY COMPONENT ALONG THE LINE OF SIGHT AND BROADENING

Let us consider the combined effects of the rotation and the oscillation on the absorption lines. Apart from terms wholly negligible—of the order of Ω/σ—we can obtain the velocities at the surface by multiplying equations (2′), (3′), and (4′) by $i\sigma e^{i\sigma t}$, putting $r = R$, $s = 2$, and $m = 0$ or 2. The two corresponding real solutions differ only by an angle $\pi/2$ in the argument, and it is sufficient to discuss one of them for each of the two values of m. We obtain

$$\left.\begin{aligned} v_{r,0} &= \tfrac{1}{2} A_0 (3\cos^2\theta - 1)\cos\sigma t\,, \\ v_{\theta,0} &= -3B_0 \cos\theta \sin\theta \cos\sigma t\,, \\ v_{\psi,0} &\simeq 0\,. \end{aligned}\right\} \quad (m = 0) \tag{23}$$

With $A_0 = \sigma a_0(R)$, $B_0 = \sigma b_0(R)$,

$$\left.\begin{aligned} v_{r,2} &= 3A_2 \sin^2\theta \cos[(\sigma \mp 2\beta\Omega)t \pm 2\psi]\,, \\ v_{\theta,2} &= 6B_2 \sin\theta \cos\theta \cos[(\sigma \mp 2\beta\Omega)t \pm 2\psi]\,, \\ v_{\psi,2} &= \mp 6B_2 \sin\theta \sin[(\sigma \mp 2\beta\Omega)t \pm 2\psi]\,. \end{aligned}\right\} \quad (m = 2) \tag{24}$$

[6] G. P. Kuiper, *Ap. J.*, **88**, 429 and 472, 1938; according to Dr. Kuiper, the temperatures around B, as given there, are too low and should be raised by one subclass.

[7] Cf. O. Struve and P. Swings, *Ap. J.*, **94**, 99, 1941.

With $A_2 = \sigma a_2(R)$, $B_2 = \sigma b_2(R)$. In these expressions, ψ is now the longitude measured from a fixed direction coinciding, at $t = 0$, with the origin of ϕ.

Let us suppose that the line of sight makes an angle θ_0 with the axis of rotation, and we define a new right-handed system of fixed co-ordinates (x, y, z), x being along the origin of ψ, and z along the axis of rotation. If the velocity component along the line of sight V_i is counted positively away from us, as is usual in the observations, we find, for the stationary oscillation ($m = 0$),

$$V_{i,0} = \left\{ \left[\frac{A_0}{2}(1 - 3z^2)\, x + 3B_0 z^2 x \right] \sin\theta_0 + \left[\frac{A_0}{2}(1 - 3z^2)\, z + 3B_0 z\,(z^2 - 1) \right] \cos\theta_0 \right\} \cos\sigma t\,, \tag{25}$$

and, for the traveling waves ($m = 2$),

$$\begin{aligned} V_{i,2} = {} & [3A_2(z^2 - 1)\, x - 6B_2 z^2 x] \cos[(\sigma \mp 2\beta\Omega)\, t \pm 2\psi] \sin\theta_0 \\ & \mp 6B_2 y \sin[(\sigma \mp 2\beta\Omega)\, t \pm 2\psi] \sin\theta_0 \\ & - (3A_2 - 6B_2)(1 - z^2) \cos[(\sigma \mp 2\beta\Omega)\, t \pm 2\psi] \cos\theta_0 \\ & + y\Omega \sin\theta_0\,, \end{aligned} \tag{26}$$

where we have included the velocity of rotation.

In turn, these co-ordinates can be expressed in terms of polar co-ordinates d and Θ in the plane normal to the line of sight, as this facilitates the integrations on the visible disk,

$$\begin{aligned} x &= d \cos\Theta \cos\theta_0 + \sqrt{(1 - d^2)} \sin\theta_0\,, \\ y &= d \sin\Theta\,, \\ z &= \sqrt{(1 - d^2)} \cos\theta_0 - d \cos\Theta \sin\theta_0\,, \end{aligned} \tag{27}$$

Θ being measured from the projection of the origin of ψ.

1. *The stationary oscillation* ($m = 0$).—In this case, according to equation (25), all the terms oscillate in phase, and, using the transformation (27), one has, for the mean radial velocity over the whole disk,

$$\bar{V}_{i,0} = -\left(\tfrac{2}{3} - \sin^2\theta_0\right)\left[\tfrac{1}{5}(A_0 + 3B_0) + \frac{\delta}{16}(3A_0 + 6B_0)\right](\tfrac{1}{2} + \tfrac{1}{3}\delta)^{-1} \cos\sigma t\,, \tag{28}$$

where δ is the coefficient of limb darkening, so that the intensity at each point of the disk is

$$I = I_0[1 + \delta\sqrt{(1 - d^2)}]\,. \tag{29}$$

Of course, there are also brightness variations along the surface due to the oscillation itself; but at this stage the theory could not give any useful information on this point, and we know from the observations that these variations are very small in any case and not likely to offset our qualitative conclusions.

From equation (28) we see that $\bar{V}_{i,0}$ vanishes for a value of θ_0 close to 54°, the whole effect then reducing to a broadening of the lines with a period π/σ equal to half the period of the velocity variation and in phase with $|\cos\sigma t|$. However, if we consider a line of sight near the pole or the equator and assume that B_0 is approximately equal to $A_0/8$, as for the f oscillation, we find that the amplitude of $\bar{V}_{i,0}$ is of the order of $A_0/3$ or $A_0/6$ for θ_0 equal to 0 and $\pi/2$, respectively, and its period in both cases is $2\pi/\sigma$. A rough esti-

mate made on the basis of the observed amplitudes of β Canis Majoris shows that in these cases, assuming δ to be of the order of $\frac{3}{4}$, the broadening of the lines due to the oscillation is very small.

2. *The traveling waves* ($m = 2$).—As far as $V_{i,2}$ is concerned, the algebra becomes rather complicated if θ_0 is kept as a parameter, and we shall limit ourselves here to the cases corresponding to $\theta_0 = 0$ and $\theta_0 = \pi/2$. This is sufficient, as the solution changes progressively from one form to the other as θ_0 varies from 0 to $\pi/2$. If the line of sight is along the axis of rotation ($\theta_0 = 0$), $V_{i,2}$ becomes

$$V_{i,2} = -(3A_2 - 6B_2)\sqrt{(1-d^2)}\, d^2 \cos[(\sigma \mp 2\beta\Omega)t \pm 2\Theta]. \tag{30}$$

The mean value $\bar{V}_{i,2}$ vanishes because of the integration with respect to Θ from 0 to 2π, and the lines will simply be broadened and their mean wave lengths will not vary in the course of time. If we combine this result with the corresponding case for $V_{i,0}$, the lines would appear more or less broad, with a periodic asymmetry of period $2\pi/\sigma$ more or less marked according to the relative amplitudes of the two oscillations.

If the line of sight is in the equatorial plane, equation (26) in terms of d and Θ becomes, if we expand the factors containing the time,

$$\begin{aligned} V_{i,2} = &-\{(3A_2 - 6B_2)[1 - d^2(1 + \sin^2\Theta)] + 6B_2\}(1-d^2)^{1/2} \\ &\times \cos[(\sigma \mp 2\beta\Omega)t - \pi] \pm [2(3A_2 - 6B_2)(1-d^2) + 6B_2]\, d \sin\Theta \sin \\ &\times [(\sigma \mp 2\beta\Omega)t] + \Omega R d \sin\Theta. \end{aligned} \tag{31}$$

The interesting point here is that the component of velocity along the line of sight can be divided into two parts, which are 90° out of phase. The first part, when integrated over all the disk, gives a mean component

$$\bar{V}_{i,2} = [\tfrac{2}{5}(A_2 + 3B_2) + \tfrac{3}{8}\delta(A_2 + 2B_2)](\tfrac{1}{2} + \tfrac{1}{3}\delta)^{-1} \cos[(\sigma \mp 2\beta\Omega)t - \pi], \tag{32}$$

which in the observations will appear as a variable radial velocity of period $(2\pi/\sigma)(1 \pm 2\beta\Omega/\sigma)$ and amplitude approximately equal to A_2 if we suppose again that $B_2 \simeq A_2/8$ and $\delta = \frac{3}{4}$. Since this should correspond to the observed radial velocity V_2, A_2 should be of the order of 2–4 km/sec.

The second term of $V_{i,2}$, being proportional to sin Θ, vanishes when integrated over the whole disk and thus corresponds only to a periodic broadening of the lines 90° out of phase with the corresponding radial velocity (32), and it will combine with the broadening due to the rotation represented by the third term.

If the equatorial linear velocity (ΩR) is small compared to the amplitude of the oscillation, the broadening will vary as $|\sin(\sigma \mp 2\beta\Omega)t|$, and its period will be only half that of the radial-velocity-curve. But if (ΩR) is of the same order of magnitude as the amplitude or larger, the broadening will have the same period as the radial-velocity-curve. Essentially what happens is that the rotation appears reinforced at a given phase and then decreased half a period later.[8] According to our previous estimates, (ΩR) here would be of the order of $3A_2$, and, combining the two last terms of equation (31) with $B_2 \simeq A_2/8$, we find for the component $V'_{i,2}$, giving rise to the broadening,

$$V'_{i,2} = A_2\left\{3 + (5.25 - 4.5d^2)\cos\left[(\sigma \mp 2\beta\Omega)t \mp \frac{\pi}{2}\right]\right\} d \sin\Theta. \tag{33}$$

If we consider, on the visible disk, sectors of 45°, each divided into ten parts which contribute equally to the formation of the lines, assuming the same law of darkening as before, the values taken by $V'_{i,2}$ at the center of each of these subdivisions are given in Table 1.

From this table we see that the total effective range of velocities at the phases of

[8] Cf. Struve and Swings, *op. cit.*, p. 103, end of second paragraph.

maximum and minimum broadening are, respectively, of the order of +10 to −10 km/sec and +2 to −2 km/sec. Although these figures are rather small, the corresponding variation might be sufficient to give rise to a differential effect such as the one observed. Furthermore, it is satisfactory that, on this picture, the broadening and the amplitude of the corresponding radial velocity are strongly correlated, as suggested by the observations.

However, there is a major difficulty as to the sign of the phase shift Φ_1 of the broadening with respect to the radial velocity. Since the broadening is associated with the longest period, we see from Table 2, where the results are summarized, that, to represent

TABLE 1

VALUES OF $V'_{1,2}$ AT PHASES $\Phi \equiv [(\sigma \mp 2\beta\Omega)t \mp \pi/2] = 0$ or π

θ	d									
	0.2	0.346	0.456	0.542	0.621	0.692	0.759	0.822	0.889	0.959
0° $\Phi=0$	0	0	0	0	0	0	0	0	0	0
0° $\Phi=\pi$	0	0	0	0	0	0	0	0	0	0
45° $\Phi=0$	+3.42	+5.66	+ 7.07	+ 7.96	+ 8.58	+ 8.95	+ 9.11	+ 9.08	+ 8.86	+ 8.36
45° $\Phi=\pi$	−0.88	−1.26	− 1.27	− 1.06	− 0.68	− 0.14	+ 0.55	+ 1.38	+ 2.46	+ 3.84
90° $\Phi=0$	+4.84	+8.00	+10.00	+11.27	+12.14	+13.55	+12.88	+12.84	+12.53	+11.82
90° $\Phi=\pi$	−1.24	−1.78	− 1.80	− 1.50	− 0.96	− 0.19	+ 0.48	+ 1.95	+ 3.18	+ 5.44
135° $\Phi=0$	+3.42	+5.66	+ 7.07	+ 7.96	+ 8.58	+ 8.95	+ 9.11	+ 9.08	+ 8.86	+ 8.36
135° $\Phi=\pi$	−0.88	−1.26	− 1.27	− 1.06	− 0.68	− 0.14	+ 0.55	+ 1.38	+ 2.46	+ 3.84
180° $\Phi=0$	0	0	0	0	0	0	0	0	0	0
180° $\Phi=\pi$	0	0	0	0	0	0	0	0	0	0
225° $\Phi=0$	−3.42	−5.66	− 7.07	− 7.96	− 8.58	− 8.95	− 9.11	− 9.08	− 8.86	− 8.36
225° $\Phi=\pi$	+0.88	+1.26	+ 1.27	+ 1.06	+ 0.68	+ 0.14	− 0.55	− 1.38	− 2.46	− 3.84
270° $\Phi=0$	−4.84	−8.00	−10.00	−11.27	−12.14	−13.55	−12.88	−12.84	−12.53	−11.82
270° $\Phi=\pi$	+1.24	+1.78	+ 1.80	+ 1.50	+ 0.96	+ 0.19	− 0.48	− 1.95	− 3.18	− 5.44
315° $\Phi=0$	−3.42	−5.66	− 7.07	− 7.96	− 8.58	− 8.95	− 9.11	− 9.08	− 8.86	− 8.36
315° $\Phi=\pi$	+0.88	+1.26	+ 1.27	+ 1.06	+ 0.68	+ 0.14	− 0.55	− 1.38	− 2.46	− 3.84

TABLE 2

THEORETICAL PREDICTIONS ON THE THEORY OF NONRADIAL OSCILLATIONS

m	Type of Oscillation	Periods	θ_0: Direction of Line of Sight	$\bar{V}_1$	Broadening	Φ_1
0	Stationary (P_2^0)	τ_0	0° (polar axis)	$A_0/3$	Very small	0
			54°	0	Large, variable with period $=\tau_0/2$	−
			90° (equator)	$A_0/6$	Very small	0
2	Wave traveling in the same direction as the rotation ($P_2^2 e^{-2i\phi}$)	$\tau_0-2\beta\Omega$	0° (polar axis)	0	Large, constant	−
			90° (equator)	A_2	Large, variable with period $=\tau_0-2\beta\Omega$	$-\pi/2$
	Wave traveling in the opposite direction ($P_2^2 e^{+2i\phi}$)	$\tau_0+2\beta\Omega$	0° (polar axis)	0	Large, constant	−
			90° (equator)	A_2	Large, variable with period $=\tau_0+2\beta\Omega$	$+\pi/2$

the observations, we should take the stationary oscillation and the wave traveling in the opposite direction to the rotation, assuming the line of sight to be close to the equatorial plane. But then the broadening is advanced by one-quarter period with respect to the radial velocity. In other words, the maximum broadening would occur when the radial velocity V_2 goes through zero from negative to positive values, which is contrary to the observations. Of course, the wave traveling in the same direction as the rotation would give us the right phase shift, but then the periods stand in the wrong ratio. Thus, although free oscillations, corresponding to P_2^0 and P_2^2, give us periods very close to one another and a possibility of accounting for the periodic broadening, the last discrepancy forces us to reject them as an explanation. Furthermore, even if one of the set of solutions of Table 2 was in complete agreement with observations, it would still be very difficult, for purely free oscillations, to explain why one of the traveling waves would be excited and not the other.

IV. FORCED OSCILLATIONS

Let us suppose that, as suggested by Struve, the main star of mass M, radius R, and mean density $\bar{\rho}$ has a very small companion of mass m describing a circular orbit of radius a with the angular velocity ω, then

$$\omega^2 = \frac{4\pi G\bar{\rho}}{3}\left(\frac{R}{a}\right)^3. \tag{34}$$

The gravitational potential of m at a point r, θ, or ψ with respect to the absolute axis defined previously, can be written, provided that r is less than a, in the form

$$U_2' = \frac{Gm}{a}\sum_{s=1}^{\infty}\left(\frac{r}{a}\right)^s\left\{P_s(\mu)P_s(0) + 2\sum_{m=1}^{s}\frac{(s-m)!}{(s+m)!}P_s^m(\mu)P_s^m(0)\cos m(\omega t - \psi)\right\} \tag{35}$$

if the mass m coincides at $t = 0$ with the origin of ψ. Since $P_s(0) = 0$, if s is odd and $P_s^m(0) = 0$ if $(s - m)$ is odd, U_2' will contain only terms which are symmetrical with respect to the equator.

The first nonzero term in equation (35) is proportional to P_1^1 and corresponds to the displacement of the center of gravity of M around m. In Struve's hypothesis, this is supposed to account for the velocity V_1 of β Canis Majoris.[9] But the only other term capable of giving rise to an oscillation of very close period is one in P_3^1, P_3^3 being the most likely. However, as it would be a forced oscillation, it is difficult to see why the two periods would not be exactly equal. On the other hand, the resulting motion would not differ very much from the corresponding free oscillation which is in resonance. But then, even in the most favorable case, when the line of sight is in the equatorial plane, the corresponding velocity component would be

$$\begin{aligned} V_{i,3} = &-\left\{\tfrac{3}{2}(5d^2\cos^2\Theta - 1)[A_3 + (B_3 - A_3)d^2] + 15B_3d^2(1-d^2)\cos^2\Theta\right\}\cos\omega t \\ &+\left\{\tfrac{3}{2}(5d^2\cos^2\Theta - 1)(A_3 - B_3) - 6B_3\right\}d(1-d^2)^{1/2}\sin\Theta\sin\omega t \\ &+\Omega Rd\sin\Theta, \end{aligned} \tag{36}$$

if we include the component due to the rotation of M. Since B_3 is appreciably smaller than A_3, the first two terms will change sign for approximately $d^2 = \frac{1}{5}\cos^2\Theta$. As a result, the average radial velocity over the whole disk will be very small, and the resulting broad-

[9] In a paper on 12 Lacertae, which the author had the privilege of reading before its publication, O. Struve suggests that the binary motion might account for the velocity V_2 rather than for V_1, the associated broadening being due to some kind of turbulence on the hemisphere facing m. However, in the case of β Canis Majoris, at any rate, this would not facilitate the explanation.

ening, which will be important, will vary with the period π/ω, equal to half the period of the corresponding radial velocity, whatever be the value of Ω. It is only in the case of the oscillation corresponding to P_2^2 that, as we have seen, its combination with the rotation can give a period for the broadening which is equal to the period of the corresponding radial velocity.

Furthermore, if we use the same data as before for β Canis Majoris, we find from formula (34) that the agreement between observed and theoretical periods would require a value of a/R of the order of 0.4 or, if we put $(a/R) = 1$, a value of $\bar{\rho}$ fifteen times greater than the value previously adopted. This seems unreasonable in both cases. An analysis of the light-variation[10] precise enough to decide whether these two periods are also present in the light-curve would be particularly useful in this respect, as one would not expect any light-variation associated with the orbital motion, since any eclipsing effect would probably be negligible.

On the other hand, if we assume that the ratio m/M is so small that the motion of the center of gravity of M is negligible, then the first term in equation (35) which could give rise to resonance is the term in P_2^2. First, the observed frequency in this case would be 2ω, and, to bring its value as given by equation (34) into agreement with the observations, a/R would have to be of the order of 0.625. This already seems more reasonable, since, if we suppose, for instance, that the main component is built on the standard model, then 97 per cent of its mass would already lie inside the orbit of the companion. On the other hand, an increase in $\bar{\rho}$ by a factor of 3.7, which is equivalent to a decrease in radius by a factor of 1.6, would make $a/R \simeq 1$. Changes of this magnitude are perhaps not ruled out entirely. The only other oscillation of very close period which could represent V_1 is the one in P_2. But the corresponding term in equation (35) is not periodic and would result only in a permanent deformation. However, as the amplitude of P_2^2 increases, the linear approximation breaks down, and one might expect some transfer of energy from P_2^2 to P_2 due to their nearly equal periods. Nevertheless, it seems somewhat unlikely that this could amplify P_2 to the extent observed, unless there is an incipient instability toward this mode of the same type as the vibrational instability, which in cepheids leads to radial pulsations. In any case, the corresponding period, τ_1, would be practically equal to that of the free oscillation.

The forced oscillation P_2^2 corresponds here to a wave traveling in the same direction as the revolution of m, and it is probable that the rotation of M, although much slower, will also be in the same sense. In that case, we know from our previous discussion that the phase shift between broadening and radial velocity will have the right sign. As to the corresponding period τ_2', it must be equal to π/ω, since P_2^2 is a forced oscillation. Although τ_2' must be very close to the free period τ_2 of P_2^2, it is probable that the small difference needed to have $\tau_2' > \tau_1$, as required by the observations, is not excluded. Of course, if this is the case, the fact that the broadening has the largest period in β Canis Majoris is purely accidental, and one would expect the reverse to occur in other stars.

The variations in pressure and temperature in the reversing layer could also affect the lines, although one might be tempted to think that their amplitude would be small, as are the changes in luminosity. However, in order to decide on this point, a detailed study of the conditions in the external layers would be necessary, and such a study is beyond the scope of this paper.

On the other hand, the investigation of A. B. Underhill[11] gives the impression that motions must be mainly responsible for the line profiles. In this respect, one must expect that the general nonuniform velocity field corresponding to P_2^2 would also be accompanied by an appreciable turbulence.

The fact that the companion has to be so very close to the main star if, in fact, it does

[10] E. A. Fath, *Lick Obs. Bull.*, **17**, 116, 1935.

[11] *Ap. J.*, **104**, 388, 1946.

not share a common photosphere with it[12] makes a precise discussion rather difficult. On the other hand, the observed changes in the amplitude and period of V_2 may be connected with this.

Of course, we need much more observational data, especially on other stars of the same type, before we can reach any definite conclusion, but it is hoped that this analysis in terms of nonradial oscillations will help in the search for a final explanation.

It is a pleasure to record here the many interesting discussions which I had with Dr. M. Schwarzschild in the course of this work.

[12] Cf., in this respect, Hoyle and Lyttleton's theory of the cepheids, *M.N.*, **103**, 21, 1943.

THE POSSIBLE INFLUENCE OF INTERSTELLAR CLOUDS ON STELLAR VELOCITIES*

LYMAN SPITZER, JR., AND MARTIN SCHWARZSCHILD
Princeton University Observatory
Received June 29, 1951

ABSTRACT

Gravitational encounters between stars and interstellar clouds produce a much shorter relaxation time of the galaxy in the solar neighborhood than do star-star encounters. This result is caused by the much larger masses of the interstellar clouds as compared with stars. In the extreme case that the largest cloud complexes acting as gravitational units should have masses of the order of a million solar masses, it is found that low-velocity stars may have been speeded up appreciably by star-cloud encounters during 3×10^9 years. This speedup of the stars, which is the same for stars of all masses, arises from the tendency of the encounters to act toward equipartition of energy between clouds and stars, though at the present time equipartition must be far from reached. If the masses of the large cloud complexes are, in fact, high enough to make the star-cloud encounters sufficiently effective, one may suppose that all low-velocity population I stars have been formed from interstellar clouds with initial average velocities equal to those of the present clouds and that the present differences in the velocity dispersions of population I stars have been caused entirely by star-cloud encounters. Under this assumption, the encounters would have increased the average velocity of older groups (late dwarfs and red giants) by about a factor of 2, while they would not have had time to affect the velocities of the younger stars (early main sequence).

Even under extreme assumptions the star-cloud encounters are found to be incapable of changing noticeably the velocities of the fast population II stars. This may indicate that all population II stars were formed from the interstellar matter at an early stage, when the velocities of the primeval clouds were still high.

I. INTRODUCTION

If one tries to interpret the observed motions of the stars in our galaxy, one encounters the question whether every star has been following its orbit in the general gravitational field of the galaxy without perturbation for the last three billion years or whether perturbing processes have been effective in changing the stellar orbits. In the first alternative the velocity dispersions now observed would be completely determined by events at the time the galaxy settled to its present state. In the second alternative, at least some of the present velocity characteristics might be determined by perturbation processes which might occur continuously through the life of the stars.

The type of perturbation process that has been fully investigated previously consists of encounters between stars.[1] It has been found that, for regions in our galaxy similar to the neighborhood of the sun, encounters between stars are so ineffective that their results would become appreciable only after a relaxation time of about 10^{14} years; accordingly, the effects of encounters between stars over a time interval of 3×10^9 years should be negligible.

No other perturbation processes seemed apparent as long as it was believed that the interstellar matter, which contains about half the mass in the solar neighborhood, was distributed fairly evenly, so that it would contribute only to the general gravitational field of the galaxy but not to the fluctuating gravitational field. In recent years, however, evidence has been accumulating which shows that the interstellar matter is far from evenly distributed but is rather concentrated into clouds. The uneven distribution of the interstellar matter will produce perturbations on the stellar orbits. Hence the question

* This work was supported in part by funds of the Eugene Higgins Trust allocated to Princeton University.

[1] S. Chandrasekhar, *Principles of Stellar Dynamics* (Chicago: University of Chicago Press, 1942), chap. ii.

arises whether the perturbations by interstellar clouds will affect the stellar velocities noticeably in 3×10^9 years.

To obtain a first estimate of the effectiveness of gravitational perturbations by interstellar clouds, one may approximate the interactions by simple two-body encounters between stars and clouds. For such encounters the relaxation time T—i.e., the time in which the accumulated velocity differences reach the order of magnitude of the original velocities—depends on the average mass of the perturbing clouds, m_c; on the average number of clouds per unit volume, n; and on the average relative velocity, V, according to the relation[2]

$$T \propto \frac{V^3}{m_c^2 n_c}. \tag{1}$$

Since mn is the average density, which is of the same order of magnitude for clouds and stars, the essential change arises from the remaining factor, m_c, which is much larger for clouds than for stars. Since m_c might be 100 solar masses for individual small clouds, the relaxation time would be reduced to 10^{12} years, which is still long compared with the probable age of the galaxy. However, if the large cloud complexes are considered, masses of the order of 10^5 solar masses may be possible. This would bring the relaxation time down to the order of 10^9 years.

What would be the consequences if the relaxation time for star-cloud encounters were actually fairly low? If the relaxation time were much shorter than the age of the galaxy, equipartition of energy should exist between the cloud complexes and the stars. That this is not the case is shown by the velocity measurements for clouds and stars. Nor does it seem likely that the masses of the cloud complexes are great enough to produce so low a relaxation time. If, then, the relaxation time is of the same order as the age of the galaxy, equipartition of energy will not have been established; nevertheless, the star-cloud encounters may already have produced noticeable effects on the stellar velocities. The main effect will have been a steady increase in the stellar velocities, since the encounters work toward equipartition of energy even if the final state is far from being reached.

Under the hypothesis that all stars of population I are formed from interstellar clouds and had, whenever they were formed, an average velocity equal to that of the present clouds, one would conclude that, as a result of star-cloud encounters, the average velocity of any group of population I stars is higher, the older the group. This seems in qualitative agreement with observations: the late-type giants and faint dwarfs, which are expected to be older stars, show fairly big velocity dispersions, whereas the younger early main-sequence stars have low velocities.

The form and amount of this continuous increase in velocity by star-cloud encounters are treated theoretically in the second section. In Section III the theoretically derived effects are related to the observed velocity dispersions.

II. STATISTICS OF STAR-CLOUD ENCOUNTERS

It is well known[3] that, when particles attract one another according to inverse-square forces, the cumulative effect of many small collisions, produced by relatively distant encounters, outweighs the large deflections produced by a few relatively close encounters. Under these conditions the change in velocity of a particle is formally similar to the change of position in Brownian motion, an analogy first pointed out by Chandrasekhar.[4] The change of velocity of a star, interacting with other gravitating centers, is therefore given by a diffusion equation in velocity space. The form of this equation has been de-

[2] *Ibid.*, eq. (2.379).

[3] J. H. Jeans, *Astronomy and Cosmogony* (Cambridge: At the University Press, 1929), p. 319; Chandrasekhar, *op. cit.*, chap. ii.

[4] *Ap. J.*, **97**, 255, 1943; see also *Rev. Mod. Phys.*, **15**, 1, 1943.

rived in a paper by Cohen, Spitzer, and Routly,[5] subsequently referred to as "CSR," for the interaction between electrically charged particles. With obvious modifications, these equations may be utilized for the interaction between gravitating centers.

Let f be the velocity distribution function for some particular type of star; i.e., let $f dv_x dv_y dv_z$ be the number of stars for unit volume in the velocity range $dv_x dv_y dv_z$. We neglect the smoothed gravitational field of the galaxy. This produces galactic rotation and the concentration of the stars to the galactic plane. It is the fluctuations of the field that produce the velocity changes in which we are interested. In this situation, the Boltzmann equation becomes

$$\frac{\partial f}{\partial t} = -K(ff_c), \tag{2}$$

where f_c is the velocity distribution function for the clouds, and $K(ff_c)$ is defined in equation (7) of CSR.

The computation of $K(ff_c)$ for interactions between stars and clouds is much complicated by two considerations. First, the velocity distributions f and f_c are not isotropic. While this fact will alter the detailed variation of f, the resultant change of stellar energy with time should be much the same as for spherical velocity distributions, and we shall accordingly assume that f and f_c are functions only of the total scalar velocities v and v_c and are independent of direction. Second, the velocities of the interstellar clouds are apparently non-Maxwellian.[6] This fact should also have only a secondary influence on the increase of velocity of the stars, especially since the more rapidly moving clouds have apparently less mass than the typical clouds, whose root-mean-square radial velocity is apparently[6, 7] between 7 and 9 km/sec. We shall therefore consider a set of clouds with a Maxwellian velocity distribution and use, accordingly,

$$f_c(v_c) = \frac{n_c}{V_c^3} \frac{1}{(2\pi)^{3/2}} e^{-v_c^2/2V_c^2}, \tag{3}$$

where n_c is the number of clouds per unit volume and V_c denotes the root mean square of one component of the cloud velocities.

On these assumptions, equation (23) of CSR becomes

$$K(ff_c) = \frac{1}{v^2}\frac{\partial}{\partial v}\left[v^2 f\left\{r_0 + \frac{q_0}{v} - \frac{1}{2v^2}\frac{\partial}{\partial v}(v^2 p_0)\right\}\right] - \frac{1}{2v^2}\frac{\partial}{\partial v}\left[v^2 p_0 \frac{\partial f}{\partial v}\right], \tag{4}$$

where r_0, q_0, and p_0 are defined in equation (31) of CSR. From the functional forms of these quantities, given in equation (32) of CSR, we find

$$r_0 + \frac{q_0}{v} - \frac{1}{2v^2}\frac{\partial}{\partial v}(v^2 p_0) = \frac{-3L}{4V_c^2 x^2}\frac{m}{m_c}(\phi - x\phi') \tag{5}$$

and

$$p_0 = \frac{3L}{2^{3/2} V_c x^3}(\phi - x\phi'), \tag{6}$$

where m and m_c are the masses of star and cloud, respectively, and, by definition,

$$x = \frac{v}{\sqrt{2}\, V_c} \tag{7}$$

[5] *Phys. Rev.*, **80**, 230, 1950.

[6] F. L. Whipple, *Centennial Symposia* (Cambridge, Mass.: Harvard College Observatory, 1948).

[7] L. Spitzer, Jr., *Ap. J.*, **108**, 276, 1948.

and $\phi(x)$ is the familiar error function,

$$\phi(x) = \frac{2}{\pi^{1/2}} \int_0^x e^{-u^2} du . \tag{8}$$

The quantity L, defined in the electrostatic case in equation (29) of CSR, here becomes

$$L_c = \frac{8\pi G^2 m_c^2 n_c \ln a}{3} ; \tag{9}$$

the value of a is discussed below.

If these various expressions are combined, equation (2) becomes

$$\frac{\partial f}{\partial t} = \frac{3}{4} \frac{L_c}{2^{3/2} V_c^3} \frac{1}{x^2} \frac{\partial}{\partial x} \left\{ \frac{(\phi - x\phi')}{x} \left(\frac{\partial f}{\partial x} + \frac{2xmf}{m_c} \right) \right\} . \tag{10}$$

As equipartition is approached, $\partial f/\partial x$ approaches $-2xfm/m_c$. However, the situation of interest here is far from equipartition; m_c is so large that we may neglect the term in m/m_c in equation (10). Thus the mass of the stars considered does not enter the following derivations. If we define a dimensionless time by the relationship

$$\theta = t \cdot \frac{3}{2^{7/2}} \frac{L_c}{V_c^3} = t \cdot \frac{\pi}{2^{1/2}} G^2 \frac{m_c^2 n_c}{V_c^3} \ln a , \tag{11}$$

we have, finally,

$$\frac{\partial f}{\partial \theta} = \frac{1}{x^2} \frac{\partial}{\partial x} \left(\frac{\phi - x\phi'}{x} \frac{\partial f}{\partial x} \right) . \tag{12}$$

The value of a in equation (11) still remains to be determined. For interactions between stars, a is a very large quantity, essentially the ratio of the kinetic energy of a star to the gravitational potential energy of two stars at their maximum separation. In the present instance, where interstellar clouds are responsible for the perturbations, a is reduced by the fact that the cloud is diffuse and its gravitational attraction is less than is assumed if the star passes through the cloud. A more detailed consideration of this situation shows that a is essentially the ratio of $b_{\max}$, the largest collision parameter (distance of closest approach), to the radius of the cloud. Since the large clouds considered below have a radius comparable with the thickness of the galaxy, though much smaller than the galactic radius, we shall here assume that a is about 10.

Equation (12) determines a unique solution if the initial velocity distribution, f at $\theta = 0$ for all x, is given. Since equation (12) is to be applied here to population I stars, which are supposedly formed from the clouds, the initial star velocities must be equal to the cloud velocities. Hence, in the present notation,

$$f = e^{-x^2} \qquad \text{at} \qquad \theta = 0 , \tag{13}$$

where, for convenience, f is normalized to 1 at $x = \theta = 0$.

The particular solution of equation (12) corresponding to the initial condition (13) has been derived by numerical integration. To bridge the singularity at $x = 0$ in equation (12), the solution for small x values was represented by an error-curve, with a varying dispersion for increasing θ. Near the origin, $x = \theta = 0$, the step values used were $\Delta x = 0.1$ and $\Delta\theta = 0.01$. For larger x and θ values, 0.2 was used for Δx, while $\Delta\theta$ was several times increased until the value 0.2 was used from $\theta = 1.4$ on. Since these $\Delta\theta$ values were close to the stability limit, the results had to be slightly smoothed after every few steps, to avoid the appearance of spurious oscillations. The solution was carried in 66 steps until $\theta = 10$. The results are shown in Table 1 and Figure 1. The last digits given in Table 1 are not secure for the higher θ values.

TABLE 1

VELOCITY DISTRIBUTION RESULTING FROM STAR-CLOUD ENCOUNTERS*

θ	x										
	0.0	0.2	0.4	0.6	0.8	1.0	1.2	1.4	1.6	1.8	2.0
0.00...	1.000	0.961	0.852	0.698	0.527	0.368	0.237	0.141	0.077	0.039	0.018
0.04...	0.853	.826	.752	.639	.504	.366	.244	.148	.083	.042	.020
0.08...	0.750	.731	.676	.589	.479	.361	.248	.155	.088	.045	.021
0.12...	0.674	.658	.616	.547	.456	.353	.251	.161	.093	.048	.023
0.16...	0.613	.601	.568	.511	.435	.345	.251	.166	.098	.052	.025
0.20...	0.565	.554	.527	.480	.415	.336	.250	.169	.102	.055	.026
0.24...	0.524	.516	.493	.453	.396	.326	.249	.172	.106	.058	.028
0.28...	0.490	.482	.464	.429	.380	.317	.246	.174	.110	.061	.030
0.32...	0.461	.454	.438	.408	.364	.308	.243	.175	.113	.064	.032
0.36...	0.436	.429	.415	.389	.350	.300	.240	.176	.116	.067	.034
0.40...	0.414	.408	.395	.372	.337	.292	.237	.176	.118	.070	.036
0.50...	0.368	.364	.354	.336	.309	.273	.227	.176	.122	.076	.040
0.60...	0.333	.330	.322	.308	.286	.256	.218	.173	.125	.080	.045
0.70...	0.305	.303	.296	.284	.266	.242	.209	.170	.127	.084	.049
0.80...	0.282	.280	.275	.265	.250	.229	.201	.166	.127	.087	.052
0.90...	0.263	.261	.257	.248	.235	.217	.193	.162	.127	.090	.056
1.00...	0.246	.245	.241	.234	.223	.207	.186	.158	.126	.091	.058
1.10...	0.232	.231	.228	.222	.212	.198	.179	.155	.125	.092	.061
1.20...	0.220	.219	.216	.211	.202	.190	.173	.151	.124	.093	.063
1.30...	0.209	.209	.206	.201	.193	.182	.167	.147	.122	.094	.064
1.40...	0.200	.199	.197	.192	.185	.176	.162	.143	.120	.094	.066
1.60...	0.182	.181	.180	.177	.172	.164	.152	.136	.117	.094	.068
1.80...	0.169	.168	.166	.164	.160	.153	.143	.130	.114	.093	.070
2.00...	0.157	.156	.154	.153	.149	.143	.135	.124	.109	.091	.070
2.20...	0.146	.145	.143	.142	.140	.136	.129	.119	.106	.089	.070
2.40...	0.138	.137	.136	.135	.133	.129	.123	.114	.103	.087	.070
2.60...	0.131	.130	.129	.128	.126	.123	.118	.110	.099	.086	.070
2.80...	0.125	.124	.123	.122	.120	.118	.113	.106	.096	.084	.069
3.00...	0.118	.118	.117	.115	.113	.112	.109	.103	.095	.084	.069
3.50...	0.105	.105	.104	.102	.101	.100	.098	.094	.088	.080	.068
4.00...	0.096	.096	.096	.095	.094	.093	.091	.088	.083	.076	.066
5.00...	0.084	.084	.084	.083	.083	.083	.082	.080	.076	.070	.062
6.00...	0.074	.074	.074	.073	.073	.072	.072	.071	.068	.064	.058
7.00...	0.068	.068	.068	.067	.067	.066	.066	.065	.063	.060	.055
8.00...	0.063	.063	.063	.062	.062	.061	.061	.060	.058	.055	.052
9.00...	0.058	.058	.058	.057	.057	.056	.056	.055	.054	.052	.049
10.00...	0.055	0.055	0.055	0.054	0.054	0.054	0.054	0.053	0.052	0.050	0.047
1.00...	0.431	0.424	0.405	0.374	0.331	0.280	0.224	0.168	0.115	0.072	0.040
2.00...	0.312	.309	.298	.280	.256	.226	.191	.154	.116	.082	.053
3.00...	0.254	.252	.243	.231	.214	.193	.168	.140	.111	.084	.058
4.00...	0.217	.215	.208	.199	.186	.170	.150	.129	.106	.083	.061
5.00...	0.192	.190	.185	.177	.166	.154	.138	.120	.100	.081	.061
6.00...	0.173	.172	.167	.160	.152	.141	.128	.112	.096	.078	.061
7.00...	0.158	.157	.153	.148	.140	.131	.119	.106	.091	.076	.060
8.00...	0.147	.146	.142	.137	.131	.122	.112	.101	.088	.074	.060
9.00...	0.137	.136	.133	.129	.123	.115	.106	.096	.084	.072	.059
10.00...	0.129	0.128	0.126	0.121	0.116	0.109	0.101	0.092	0.081	0.070	0.058

* In the upper section, f is tabulated as a function of the normalized velocity, x, and of the normalized time, θ. The lower section gives f_a.

TABLE 1—*Continued*

θ	x									
	2.2	2.4	2.6	2.8	3.0	3.2	3.4	3.6	3.8	4.0
0.00...	0.008	0.003	0.001	0.0004	0.0001	0.0000	0.0000	0.0000	0.0000	0.0000
0.04...	.009	.003	.001	.0004	.0001	.0000	.0000	.0000	.0000	.0000
0.08...	.009	.004	.001	.0004	.0001	.0000	.0000	.0000	.0000	.0000
0.12...	.010	.004	.001	.0005	.0001	.0000	.0000	.0000	.0000	.0000
0.16...	.011	.004	.002	.0005	.0002	.0000	.0000	.0000	.0000	.0000
0.20...	.011	.004	.002	.0005	.0002	.0000	.0000	.0000	.0000	.0000
0.24...	.012	.005	.002	.0006	.0002	.0001	.0000	.0000	.0000	.0000
0.28...	.013	.005	.002	.0006	.0002	.0001	.0000	.0000	.0000	.0000
0.32...	.014	.006	.002	.0006	.0002	.0001	.0000	.0000	.0000	.0000
0.36...	.015	.006	.002	.0007	.0002	.0001	.0000	.0000	.0000	.0000
0.40...	.016	.006	.002	.0007	.0002	.0001	.0000	.0000	.0000	.0000
0.50...	.019	.007	.003	.0009	.0003	.0001	.0000	.0000	.0000	.0000
0.60...	.021	.009	.003	.0010	.0003	.0001	.0000	.0000	.0000	.0000
0.70...	.024	.010	.004	.0012	.0004	.0001	.0000	.0000	.0000	.0000
0.80...	.027	.012	.004	.0014	.0004	.0001	.0000	.0000	.0000	.0000
0.90...	.030	.013	.005	.0017	.0005	.0001	.0000	.0000	.0000	.0000
1.00...	.032	.015	.006	.0020	.0006	.0002	.0000	.0000	.0000	.0000
1.10...	.034	.017	.007	.0023	.0007	.0002	.0000	.0000	.0000	.0000
1.20...	.037	.018	.008	.0027	.0008	.0002	.0001	.0000	.0000	.0000
1.30...	.039	.020	.008	.0031	.0009	.0003	.0001	.0000	.0000	.0000
1.40...	.041	.021	.009	.0035	.0011	.0003	.0001	.0000	.0000	.0000
1.60...	.044	.024	.011	.0044	.0014	.0004	.0001	.0000	.0000	.0000
1.80...	.046	.027	.013	.0054	.0018	.0005	.0001	.0000	.0000	.0000
2.00...	.049	.029	.015	.0065	.0023	.0007	.0002	.0000	.0000	.0000
2.20...	.050	.032	.017	.0076	.0028	.0009	.0002	.0001	.0000	.0000
2.40...	.051	.033	.019	.0088	.0034	.0011	.0003	.0001	.0000	.0000
2.60...	.052	.035	.020	.0100	.0041	.0014	.0004	.0001	.0000	.0000
2.80...	.053	.036	.022	.0111	.0047	.0016	.0005	.0001	.0000	.0000
3.00...	.053	.037	.023	.0122	.0054	.0020	.0006	.0001	.0000	.0000
3.50...	.054	.040	.026	.0148	.0071	.0029	.0009	.0003	.0000	.0000
4.00...	.054	.041	.028	.0170	.0088	.0039	.0014	.0004	.0001	.0000
5.00...	.053	.042	.031	.0206	.0120	.0060	.0025	.0009	.0002	.0001
6.00...	.051	.042	.033	.0231	.0146	.0081	.0038	.0015	.0005	.0001
7.00...	.049	.042	.034	.0248	.0167	.0100	.0052	.0023	.0009	.0003
8.00...	.047	.041	.034	.0259	.0183	.0116	.0065	.0032	.0013	.0005
9.00...	.045	.040	.034	.0265	.0195	.0130	.0078	.0041	.0019	.0009
10.00...	0.043	0.039	0.033	0.0269	0.0204	0.0141	0.0089	0.0050	0.0025	0.0013
1.00...	0.019	0.008	0.003	0.0010	0.0003	0.0001	0.0000	0.0000	0.0000	0.0000
2.00...	.030	.015	.007	.0025	.0008	.0002	.0001	.0000	.0000	.0000
3.00...	.037	.022	.011	.0048	.0018	.0006	.0002	.0000	.0000	.0000
4.00...	.042	.026	.015	.0073	.0031	.0012	.0004	.0001	.0000	.0000
5.00...	.045	.029	.018	.0096	.0046	.0019	.0007	.0002	.0000	.0000
6.00...	.045	.031	.020	.0116	.0061	.0028	.0011	.0004	.0001	.0000
7.00...	.046	.033	.022	.0134	.0074	.0037	.0016	.0006	.0002	.0000
8.00...	.046	.034	.023	.0149	.0087	.0046	.0021	.0009	.0003	.0001
9.00...	.046	.035	.024	.0162	.0098	.0054	.0027	.0012	.0004	.0002
10.00...	0.046	0.035	0.025	0.0172	0.0108	0.0062	0.0032	0.0015	0.0006	0.0002

Any one line in Table 1 gives the velocity distribution for a group of stars, all of the same age, θ. On the other hand, if type I stars have been forming continuously, there will be an appreciable spread of ages in any group of such stars. For example, in a group of low-velocity G dwarfs some stars may be as old as 3×10^9 years, while others may have been formed only very recently. Such an age distribution can be taken into account if one assumes that the rate of star formation has been fairly constant so that the age

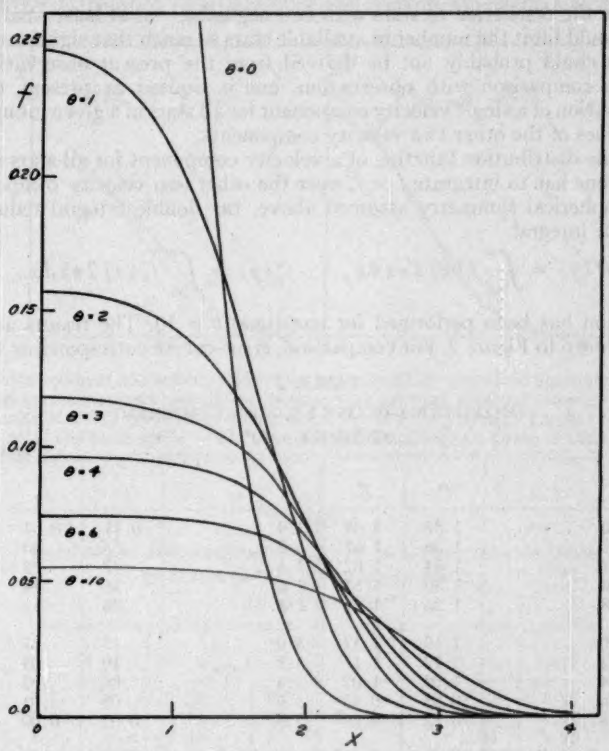

FIG. 1.—Velocity distribution, $f(x)$, resulting from star-cloud encounters, as a function of time, θ

distribution is uniform. The corresponding average velocity distribution, f_a, can then be computed according to the relation

$$f_a = \frac{1}{\theta} \int_0^\theta f \, d\theta . \tag{14}$$

The results of this computation are added at the foot of Table 1.

By definition, $x^2 f(x)$ or $x^2 f_a(x)$ gives the distribution of total velocities for a group of stars at a given time. To compare these theoretical results directly with the observed total velocities would seem of uncertain value, since the ellipsoidal distribution of actual velocities differs appreciably from the spherical distribution assumed in the above derivations. Therefore, it seems safer to compare the theoretical results with observations only in terms of single velocity components. If v_y is a particular velocity component, it may

be normalized in the same way as in equation (7) by

$$y = \frac{v_y}{2^{1/2} V_c}. \tag{15}$$

Again, by definition, $f(x)$ or $f_a(x)$ gives the distribution of the single component y for those stars for which the other two velocity components are negligible, since, under this selection, $y = x$. But here again direct comparison with observations does not seem practical, since the restriction to stars with two negligible—or at least small—velocity components would limit the number of available stars so much that significant distribution functions could probably not be derived from the present observational data. Thus, for the comparison with observation, one is limited at present to the frequency distribution of a single velocity component for all stars of a given group, irrespective of the values of the other two velocity components.

To derive the distribution function of a velocity component for all stars in a group, $f^*(y)$ or $f_a^*(y)$, one has to integrate f or f_a over the other two velocity components. Because of the spherical symmetry assumed above, the double integral reduces to the following single integral

$$f^*(y) = \int_{|y|}^{\infty} f(x)\, 2\pi x\, dx\,, \qquad f_a^*(y) = \int_{|y|}^{\infty} f_a(x)\, 2\pi x\, dx\,. \tag{16}$$

This integration has been performed for one time, $\theta = 10$. The results are given in Table 2 and shown in Figure 2. For comparison, error-curves corresponding to the same

TABLE 2

DISTRIBUTION OF ONE VELOCITY COMPONENT AT TIME $\theta = 10$*

y	f^*	f_a^*	y	f^*	f
0.0	1.37	1.69	2.0	0.71	0.54
0.2	1.36	1.67	2.2	.59	.40
0.4	1.34	1.62	2.4	.47	.28
0.6	1.30	1.55	2.6	.36	.19
0.8	1.26	1.44	2.8	.26	.12
1.0	1.19	1.32	3.0	.17	.07
1.2	1.12	1.17	3.2	.10	.03
1.4	1.03	1.02	3.4	.06	.02
1.6	0.93	0.85	3.6	.03	.01
1.8	0.82	0.69	3.8	0.01	0.00

* The values of f^* refer to a group of stars of the same age, θ. The values of f_a^* apply to a group of stars with a uniform distribution of ages from 0 to θ.

number of stars and to the same root-mean-square velocity have been added in Figure 2. As shown by this figure, the distribution-curves computed from equation (16) differ only slightly from error-curves and could probably not be distinguished from the latter on the basis of the observational material presently available.

Hence the root mean square of a velocity component for a group of stars, V_s, appears to be the only item available at present for comparison with observations. In preparation for such a comparison, the variation of V_s with time, to be expected from the star-cloud encounters, has been computed from the above f functions with the help of the following relation:

$$\frac{V_s^2}{V_c^2} = 2\overline{y^2} = 2\,\frac{\int_{-\infty}^{+\infty} y^2 f^*(y)\, dy}{\int_{-\infty}^{+\infty} f^*(y)\, dy} = \frac{2}{3}\,\frac{\int_0^{\infty} f(x)\, x^4 dx}{\int_0^{\infty} f(x)\, x^2 dx} = \tfrac{2}{3}\overline{x^2}. \tag{17}$$

A corresponding relation holds for the quantities with subscripts a. The results are listed in Table 3. These numerical values can be represented with fair accuracy by the following interpolative relations:

$$V_s \approx V_c \cdot (1+3.2\theta)^{1/5}, \qquad V_{sa} \approx V_c \cdot (1+1.4\theta)^{1/5}. \tag{18}$$

An equation of this general functional form may be derived theoretically[8] if it is assumed that the distribution of stellar velocities remains Maxwellian at all times.

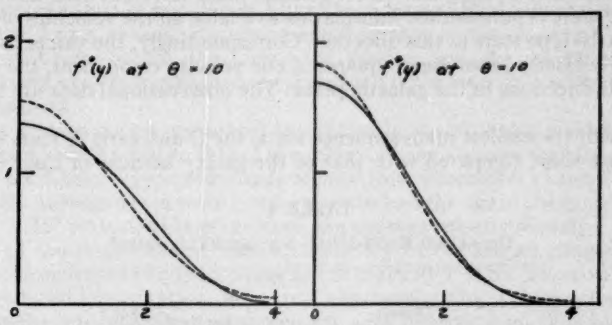

FIG. 2.—Distribution of one velocity component as produced by star-cloud encounters. For comparison, the dashed curves represent normal distributions with the same area and dispersion. The velocities are given in units of $2^{1/2}V_c$ (root-mean-square cloud velocity component). The left figure refers to a group of stars all of the same age, $\theta = 10$. The right figure applies to a group of stars with a uniform distribution of ages, from $\theta = 0$ to $\theta = 10$.

TABLE 3

ROOT-MEAN-SQUARE STAR VELOCITY AS A FUNCTION OF TIME IN UNITS OF THE ROOT-MEAN-SQUARE CLOUD VELOCITY*

θ	V_s/V_c	V_{sa}/V_c	θ	V_s/V_c	V_{sa}/V_c
0	1.00	1.00	6	1.82	1.56
1	1.32	1.18	7	1.88	1.61
2	1.48	1.30	8	1.93	1.65
3	1.59	1.38	9	1.97	1.68
4	1.68	1.45	10	2.01	1.72
5	1.76	1.51			

* The second column refers to a group of stars all of the same age, θ. The third column applies to a group of stars with a uniform distribution of ages from 0 to θ.

Table 3 and equation (18) show that a group of stars reaches twice the average cloud velocity at a time $\theta = 10$ if the stars were all formed simultaneously, and at a time $\theta = 22$ if stars were formed continuously at a steady rate.

In comparing the second and third columns of Table 3, one finds that any entry in the third column for a given θ shows nearly the same value as an entry in the second column for $\frac{1}{2}\theta$. On the other hand, any entry in the third column corresponds to a group of stars with a uniform age distribution from 0 to θ, i.e., an average age of $\frac{1}{2}\theta$. Thus one may conclude that the velocity dispersion shown by a group of stars as a result of star-

[8] L. Spitzer, Jr., *M.N.*, **100**, 396, 1940.

cloud encounters is a function of the average age of the stars in the group, irrespective of the age distribution in the group.

III. APPLICATION TO OBSERVED VELOCITIES

The observed velocity dispersions in relation to the effects of the star-cloud encounters will be discussed in this section consecutively for four types of stars: the early main-sequence stars, the late main-sequence stars, the red giants, and the high-velocity stars. The velocities perpendicular to the galactic plane have not been used in this discussion, since there is only limited information available on the velocities of interstellar clouds and early-type stars in this direction. Correspondingly, the values for V_c and V_s here used correspond to root mean squares of one velocity component, the mean being taken over all directions in the galactic plane. The observational data are summarized in Table 4.

To start with the earliest main-sequence stars, the O and early B stars should have an average age short compared with that of the galaxy because of their high rate of

TABLE 4

OBSERVED ROOT-MEAN-SQUARE VELOCITIES*

Objects	V_c or V_s (Km/Sec)	Ref.†
Interstellar clouds:		
Large clouds	8	1, 2
Small clouds	25	1
Early main-sequence stars:		
Oe5–B5	10	3
B8–B9	12	3
A0–A9	15	4
F0–F9	20	4
Late main-sequence stars:		
F5–G0	23	4
G0–K6	25	4
K8–M5	32	4
Red giant stars:		
K0–K2	25	5
K0–K9	21	4
M0–M9	23	4
High-velocity stars:		
General high-velocity stars	50	6
RR Lyrae variables	120	7
Subdwarfs	150	8

* Mean of two components in galactic plane.

† The following references are cited:

1. F. L. Whipple, *Centennial Symposia* (Cambridge, Mass.: Harvard College Observatory, 1948), p. 118.
2. L. Spitzer, Jr., *Ap. J.*, **108**, 276, 1948.
3. H. Nordstrom, *Lund Obs. Medd.*, Ser. II, No. 79, p. 161, 1936: $[(\frac{1}{2}\sigma_1^2 + \frac{1}{2}\sigma_2^2)^{1/2}]$.
4. E. T. R. Williams and A. N. Vyssotsky, *A.J.*, **53**, 92, 1947 (particularly Table 10.1): $[(\frac{1}{2}\sigma_a^2 + \frac{1}{2}\sigma_b^2)^{1/2}]$.
5. A. N. Vyssotsky, *A.J.*, **56**, 62, 1951 (particularly Table 12.1).
6. J. Oort, *Groningen Pub.*, **40**, 45, 1926: $[2^{-1/2}/0.015]$; also G. Miczaika, *A.N.*, **270**, 258, 1940.
7. J. Oort, *B.A.N.*, **8**, 337, 1939: $[94(\pi/2)^{1/2}]$.
8. A. H. Joy, *Ap. J.*, **105**, 102, 1947: $[121(\pi/2)^{1/2}]$.

energy output. Consequently, one should expect the star-cloud encounters to have had insufficient time to affect the velocities of these stars. Thus the velocities of the O and early B stars should represent the velocities of the clouds from which they were formed. As Table 4 shows, the velocity dispersion of the earliest main-sequence stars is in good agreement with the velocities of the large clouds. The small clouds, with their relatively larger velocities, may have given rise to the formation of rather few stars.

Following down the main sequence, the average age should be increasing because of the slower and slower rate of expenditure of nuclear energy. Under the hypothesis that all main-sequence stars of population I have been formed from interstellar clouds, they all must have had a velocity dispersion equal to that of the clouds at the time they were formed. Consequently, the higher the average age, the greater should be the average velocity as a consequence of the star-cloud encounters, in qualitative agreement with observations.

For early F stars the energy output is sufficiently low so that the oldest stars of this type may have an age equal to that of the galaxy. If one assumes that the normal main-sequence F stars have been continuously formed from interstellar clouds at a fairly constant rate, the average age of early F stars must be half the age of the galaxy, or approximately 1.5×10^9 years. On the other hand, the average velocity of early F stars is about twice that of the larger clouds. Hence, according to the second column of Table 3, $\theta \approx 10$ should correspond to the average age of the early F stars. These values of t and θ may be introduced into equation (11) to test whether the effects of star-cloud encounters can be brought into quantitative agreement with observations. The most uncertain quantity in equation (11) is probably m_c. If one correspondingly solves equation (11) for m_c and uses $V_c = 10$ km/sec, $\log a = 3$, and $m_c n_c = \bar{\rho} = 3 \times 10^{-24}$, one obtains $m_c = 10^6 m_\odot$ by order of magnitude. It is clear that this very large mass cannot be represented by an individual interstellar cloud, but, at best, by a large cloud complex. If one assumes for such a cloud complex ten times the average density of interstellar space, one obtains about 100 parsecs for the diameter of such a cloud complex. This diameter size falls well within the range of the observed diameters of cloud complexes.[9] Bok[10] has deduced a mass of 300 $m_\odot$ for the solid particles within a typical large cloud, with an assumed diameter of 40 parsecs. If the mass of the gas is a hundred times that of the obscuring grains, the total mass of such a cloud becomes $3 \times 10^4 m_\odot$. Whether aggregations with a mass as great as $10^6 m_\odot$ can be moving as a unit through interstellar space with velocities of 5 to 10 km/sec is uncertain, and, as a result, the entire present discussion is necessarily hypothetical. Since no decision in this question seems possible at present, the discussion will here be followed through under the assumption that the masses of the cloud complexes are large enough and their mean velocities high enough to make the star-cloud encounters effective.

Turning, next, to the late main-sequence stars, one finds that the age of a dwarf with spectral type later than F5 may be anywhere between zero and the age of the galaxy. Therefore, if one again assumes that these stars have been formed from interstellar clouds at an essentially constant rate, the average age of any group of dwarfs later than F5 should be equal to half the age of the galaxy, irrespective of spectral type. With the same average age and the same initial velocities, one should expect all the dwarfs later than F5 to have the same velocity dispersions at the present time. Furthermore, this expectation is not affected by the circumstance that the stellar masses decrease with advancing spectral type, since the encounter effects are independent of the stellar masses, as long as the state is far from approaching equipartition of energy with the interstellar clouds.

The above deduction is in disagreement with the observations, which, according to Table 4, show a further increase of the velocity dispersion for the latest main-sequence

[9] J. L. Greenstein, *Harvard Ann.*, 105, 359, 1937.

[10] *Centennial Symposia* (Cambridge, Mass.: Harvard College Observatory, 1948).

stars. However, the later main sequence does not consist purely of population I stars, like the early main sequence, but contains an appreciable fraction of population II stars. Thus the question arises whether the apparent increase in velocity dispersion for the later main-sequence stars may arise solely from an increase in the percentage of population II stars for the later spectral types. To test this possibility, the available velocities of M dwarfs were analyzed.[11] Only the velocity component in the center-anticenter direction was used, to avoid difficulties with asymmetry. It has previously been pointed out that the distribution-curve for this velocity component cannot be represented by one error-curve.[11] Here it was attempted to represent the data by the sum of two error-curves, and it was found that the observations could be fitted if two-thirds of the stars were assumed to belong to an error distribution with a velocity dispersion of 23 km/sec and the remaining third of the stars to an error distribution with a dispersion of 67 km/sec. Such a representation by the sum of two error-curves is, of course, not the only possible representation, but seems to be a possible one. If one assumes the normal ratio for the axes of the velocity ellipsoid in the galactic plane, one can transform the above values for the dispersions in the center-anticenter direction into values of V_s, for which one obtains 20 and 56 km/sec, respectively. Since the latter value is close to that of the high-velocity population II stars in general, one may well assign one-third of the M dwarfs to population II. The remaining two-thirds of the M dwarfs have, then, according to the first of the above V_s values, an average velocity equal to that of the F dwarfs. One may conclude that the later main-sequence stars of pure population I may have a constant average velocity, irrespective of spectral type, in agreement with what one would expect from the effects of star-cloud encounters.

Turning, next, to the red giants, one sees from Table 4 that the average velocities for these stars are somewhat higher than for main-sequence stars of the same brightness. This velocity excess seems to remain even after the small fraction of high-velocity population II giants has been taken account of. (From his material on early K giants Vyssotsky has separated those stars with small velocities perpendicular to the galactic plane; for this group of stars, which should contain hardly any population II stars, he obtained $V_s = 21$ km/sec, a value still higher than the corresponding value for main-sequence A stars.) According to the present hypothesis, all population I stars started out with the low-velocity dispersion of the large interstellar clouds and increased their velocity dispersions by star-cloud encounters according to their age. Because of their higher velocity dispersions, one might conclude, therefore, that the red giants must be somewhat older, on the average, than the bright main-sequence stars—a conclusion which fits well with the current speculations regarding the interior of the red giants.

There remain, finally, the high-velocity population II stars to be discussed. As shown by the bottom part of Table 4, even the general high-velocity stars—not to include the extreme groups like the RR Lyrae variables and the subdwarfs—have velocity dispersions about two and a half times larger than the older stars of pure population I. It seems impossible to explain these high velocities by the effects of star-cloud encounters. On the one hand, since the increase in velocity by encounters rapidly diminishes with increasing velocity (as shown by eq. [1] or more precisely by eq. [18]), the necessary masses for the cloud complexes would have to be even larger than those discussed above. On the other hand, if, contrary to expectation, the relaxation time through star-cloud encounters should be so short that these encounters could produce $V_s = 50$ km/sec, the velocity dispersions of the older main-sequence stars should also have reached high values; but this consequence would disagree with observation.

Thus it seems necessary to conclude that the velocity dispersions of population II stars have not been altered essentially by any encounters and must represent the initial average velocities of these stars at their formation. Other evidence has already indicated that population II stars may all be of about the same age as the galaxy itself. Hence it

[11] A. N. Vyssotsky, *Ap. J.*, **104**, 239, 1946.

seems reasonable to surmise that at the early stage of the development of the galaxy, when presumably the population II stars were formed from interstellar material, the large clouds had average velocities not of 10 km/sec as now, but rather of 50 km/sec—and in part even higher velocities to account for the present extreme high-velocity stars.

IV. CONCLUSIONS

The results of the above discussion may be summarized in the following speculative working hypothesis.

At an early state of the galaxy the interstellar matter had large random velocities, possibly corresponding to violent turbulence with great density fluctuations. At this stage all population II stars were formed out of the interstellar matter.

Subsequently, the velocities of interstellar matter soon decayed to their present average values. Ever since this settling-down process, the population I stars have been forming out of the interstellar clouds at a more or less constant rate.

Only after the settling-down process, was there enough time for interstellar grains to form abundantly. Hence grains did not play a role in the formation of population II stars but did in the formation of population I stars. This accounts for the difference in chemical composition between the two populations.[12]

All stars are continually having encounters with massive cloud complexes. The relaxation time for high-velocity stars, in encounters with large clouds, is too long to have affected appreciably the velocity dispersions of population II stars. This relaxation time is sufficiently short for low-velocity stars, however, so that the star-cloud encounters have speeded up the older groups of population I stars markedly. This accounts for the increased velocity dispersion of the late dwarfs and red giants of population I as compared with the early main-sequence stars.

The above statements are purely hypothetical at present. They seem, however, not to be contradicted by the observational evidence, and they contain a possible, though far from proved, explanation of the velocity dispersions of population I stars. If this working hypothesis should gain substance by future evidence, it would be necessary to expand the theoretical discussion of Section II to take account of the nonsphericity of the actual velocity ellipsoids.

It is a pleasure to acknowledge the carefulness and efficiency with which Mr. Härm carried through the extensive numerical integration described in Section II. To Dr. A. N. Vyssotsky we are most grateful for stimulating discussions regarding the observational basis for this investigation.

[12] Schwarzschild, Spitzer, and Wildt, *Ap. J.*, **114**, 398, 1951.

ON THE DIFFERENCE IN CHEMICAL COMPOSITION BETWEEN HIGH- AND LOW-VELOCITY STARS*

M. SCHWARZSCHILD, L. SPITZER, JR., AND R. WILDT
Princeton University Observatory and Yale University Observatory
Received July 23, 1951

ABSTRACT

The spectroscopic peculiarities of high-velocity stars—strengthening of the *CH* bands and weakening of the *CN* bands and of the metal lines—can tentatively be explained by a general reduction in the abundance of the heavy elements and a somewhat lesser reduction in the abundance of the medium-heavy elements, relative to the abundances for low-velocity stars. As a working hypothesis, it is proposed that such a general difference in chemical composition between stars of populations I and II stems from the preferential accumulation of grains in the denser interstellar clouds from which the stars of population I might be formed.

The astrophysical discussion indicates that the dissociation energy of the molecules N_2 and *CO* should be close to 9.5 e.v.; the considerably lower or higher values still advocated by some spectroscopists are not supported by the astronomical evidence.

I. INTRODUCTION

The high-velocity stars differ from the normal, low-velocity stars in many ways regarding their locations and velocities in our galaxy.[1] This suggests that the stars in these two stellar populations may have evolved in essentially different ways. Such an evolutionary difference would make it plausible that the average chemical composition is not the same in the two stellar populations. Spectroscopic observations do indeed suggest the existence of abundance differences between the two stellar populations.

The first spectroscopic differences were noted in G and K giants, where the bands of *CN* were found weakened in high-velocity stars, while those of *CH* were found strengthened.[2] Furthermore, it was found recently that the lines of the heavier elements in F and G stars seem generally weakened in the high-velocity stars.[3]

The latter observation immediately suggests that the heavier elements are less abundant in population II than in population I. Could such a general abundance difference also explain the peculiar behavior of the *CH* and *CN* bands in giant stars? This is the question examined in the present paper.

II. CHEMICAL EQUILIBRIUM IN GIANT ATMOSPHERES

In order to predict the strength of the *CH* and *CN* bands, the partial pressures of these molecules must be evaluated as functions of the partial pressures of the constituent atoms. A complete analysis of the chemical equilibrium among all possible diatomic molecules, fortunately, proves unnecessary for our purposes. The computation of molecular partial pressures in a stellar atmosphere, though very complex in principle, becomes quite tractable because of the overwhelming abundance of hydrogen in stellar atmospheres and the small binding energies of the hydride molecules.

* This work was supported in part by funds of the Eugene Higgins Trust allocated to Princeton University.

[1] W. Baade, *Ap. J.*, **100**, 137, 1944.

[2] B. Lindblad, *Ap. J.*, **55**, 85, 1922; P. Keenan, *Ap. J.*, **96**, 101, 1942; Morgan, Keenan, and Kellman, *An Atlas of Stellar Spectra* (Chicago: University of Chicago Press, 1943); D. Popper, *Ap. J.*, **105**, 204, 1947; Keenan, Morgan, and Münch, *A.J.*, **53**, 194, 1948; G. Miczaika, *Zs. f. Ap.*, **27**, 1, 1950; and W. Iwanowska, *Spectrophotometric Study of Some High Velocity Stars* (Warsaw, 1950).

[3] M. and B. Schwarzschild, *Ap. J.*, **112**, 248, 1950; N. Roman, *Ap. J.*, **112**, 554, 1950.

Let us write $p(A)$ for the partial pressure of any atomic species and $p(AB)$, or $p(A_2)$, for the partial pressures of the molecules AB, or A_2. Moreover, $P(A)$ will designate the fictitious partial pressure of the atomic species A that would result from complete dissociation, at the same temperature, of all molecules actually present. Finally, let $K(AB)$, or $K(A_2)$, be the equilibrium constants characteristic of the molecules. Although the K's are functions solely of the temperature, their absolute values depend on the pressure unit adopted for specifying the p's. Contrary to standard use in the chemical literature, we shall refer the K's to a pressure scale based on the unit of 1 dyne per square centimeter. The equations defining the chemical equilibrium can now be written as follows:

$$P(H) = p(H)\left[1+\left\{\frac{2p(H)}{K(H_2)}\right\}+\left\{\frac{p(C)}{K(CH)}\right\}+\left\{\frac{p(N)}{K(NH)}\right\}+\left\{\frac{p(O)}{K(OH)}\right\}+\ldots\right], \quad (1a)$$

$$P(C) = p(C)\left[1+\left\{\frac{2p(C)}{K(C_2)}\right\}+\left\{\frac{p(H)}{K(CH)}\right\}+\left\{\frac{p(N)}{K(CN)}\right\}+\frac{p(O)}{K(CO)}+\ldots\right], \quad (1b)$$

$$P(N) = p(N)\left[1+\frac{2p(N)}{K(N_2)}+\left\{\frac{p(H)}{K(NH)}\right\}+\left\{\frac{p(C)}{K(CN)}\right\}+\left\{\frac{p(O)}{K(NO)}\right\}+\ldots\right], \quad (1c)$$

$$P(O) = p(O)\left[1+\left\{\frac{2p(O)}{K(O_2)}\right\}+\left\{\frac{p(H)}{K(OH)}\right\}+\frac{p(C)}{K(CO)}+\left\{\frac{p(N)}{K(ON)}\right\}+\ldots\right]. \quad (1d)$$

The omitted terms in the brackets refer to the partial pressures of the hydrides, etc., of the metals; their contributions are negligible, owing to the low abundance of these atomic species.

A further reduction of this system of equations is accomplished by considering the order of magnitude of the various fractions, p/K, appearing in these equations. At the pressures prevailing in giant atmospheres (see Sec. III, below) and at temperatures higher than 3500° K, all the fractions placed in braces can be neglected compared to 1. For reasons of brevity, no proof of this statement is offered. It may suffice to mention that the maximum error introduced by this procedure amounts to 4 per cent only; this is the value of the fraction $2p(H)/K(H_2)$ at $T = 3500°$ K. Hence we are left with the following simple equations:

$$P(H) = p(H), \quad (2a)$$

$$P(C) = p(C)\left[1+\frac{p(O)}{K(CO)}\right], \quad (2b)$$

$$P(N) = p(N)\left[1+\frac{2p(N)}{K(N_2)}\right], \quad (2c)$$

$$P(O) = p(O)\left[1+\frac{p(C)}{K(CO)}\right]. \quad (2d)$$

These reveal that the fraction of hydrogen existing in molecular combination is too small to affect the chemical equilibrium; that an appreciable fraction of nitrogen may exist in the form of N_2, according to equation (2*c*); and that the depletion of atomic carbon and oxygen is determined by the pair of simultaneous equations (2*b*) and (2*d*).

It would burden the later discussion, which forms the main body of this paper, if we were to analyze in detail the dissociation of N_2 and CO as functions of pressure and temperature. Instead, we shall consider two limiting cases, namely, that of complete dissociation of all molecules, and the opposite situation, in which practically all nitrogen and carbon exists in the form of N_2 and CO, respectively. The question then arises as to the

temperatures at which the equilibrium shifts from N to N_2 and from C to CO, respectively. In the following sections we shall refer to these "critical" temperatures as "transition temperatures." It would be incorrect, however, to think of these transition temperatures as sharply defined. They should be regarded rather as the centers of transition ranges. This point is well illustrated by a diagram[4] showing the dissociation degrees of H_2, N_2, and O_2 as a function of total pressure and temperature.

The dissociation constants, K, of CO and N_2 (see Table 1) have been computed from the following linear expressions valid for temperatures between 3000° and 5000° K:

$$\log K_{CO} = 13.65 - 9.55 \frac{5040}{T} \qquad D_{CO} = 9.14 \text{ e.v.} \tag{3a}$$

$$= 13.65 - 10.01 \frac{5040}{T} \qquad D_{CO} = 9.60 \text{ e.v.} \tag{3b}$$

$$= 13.65 - 11.52 \frac{5040}{T} \qquad D_{CO} = 11.11 \text{ e.v.;} \tag{3c}$$

$$\log K_{N_2} = 13.04 - 7.50 \frac{5040}{T} \qquad D_{N_2} = 7.29 \text{ e.v.} \tag{4a}$$

$$= 13.04 - 9.97 \frac{5040}{T} \qquad D_{N_2} = 9.76 \text{ e.v.} \tag{4b}$$

$$= 13.04 - 12.00 \frac{5040}{T} \qquad D_{N_2} = 11.80 \text{ e.v.} \tag{4c}$$

The accuracy of these equations is probably better than three units in the second decimal of $\log K$. These equilibrium constants contain the rigorous molecular partition functions obtained by numerical summation of all rotation and vibration levels, spaced precisely according to the analysis of the CO and N_2 bands. Instead of citing the widely scattered literature on this subject, we refer to a monograph by E. Justi.[5]

III. DISSOCIATION OF CO AND N_2

The transition temperatures for CO and N_2 may be estimated from the astrophysical evidence in the following way. The maximum of CH strength is observed[6] at about gK0, which corresponds to an effective temperature of 4200° and a temperature in the reversing layer of about 4000°. This maximum is caused by the formation of CO, which takes away the free C and thus reduces the formation of CH. Hence the CH maximum must occur at a temperature fairly close to the transition temperature at which half the C atoms combine to CO. The transition temperature, therefore, should be about 4000°, which is the reversing-layer temperature of a K0 giant.

Regarding the shift from N to N_2, it seems unlikely that the corresponding transition temperature is noticeably higher than that of CO, since this would produce a maximum for CN at an earlier spectral type than the maximum for CH, contrary to observations.[7] On the other hand, if the transition temperature for N_2 were appreciably lower than that

[4] R. Wildt, *Zs. f. Phys.*, **54**, 856, Fig. 1, 1929.

[5] *Spezifische Wärme, Enthalpie, Entropie, Dissoziation technischer Gase* (Berlin: J. Springer, 1938).

[6] W. C. Rufus, *Pub. Obs. U. Michigan*, **3**, 258, 1923; C. Payne, *Stellar Atmospheres* (Cambridge, Mass.: Harvard College Observatory, 1925), p. 194.

[7] P. Keenan, *Ap. J.*, **93**, 475, 1941.

of *CO*, then *CN* should probably show a rather flat maximum at the lower temperatures,[8] while actually a sharp decrease toward later spectral types is observed.[9] It appears that the transition temperatures of N_2 and *CO* cannot differ much.

Let us then assume that the transition temperature for *CO* as well as for N_2 is approximately 4000° and that nitrogen and carbon exist predominantly in the form of free atoms in the reversing layers of giants earlier than K0, but in molecular combination, mainly as *CO* and N_2, in giants later than K0.

This tentative conclusion rests entirely on astronomical evidence. Before it is applied to the problem in hand, it should be checked against the laboratory data on the dissociation energies of *CO* and N_2. Such a check can be made as follows.

At the transition temperature where, by definition, *CO* and *C* are equally abundant, one finds from the dissociation equilibrium that the dissociation constant K_{CO} must be equal to the partial pressure of oxygen. Since the hydrogen pressure in the reversing layer of a red giant[10] is approximately 0.8×10^4 dyne/cm^2 and since the ratio of oxygen to hydrogen, by volume, should normally be about 0.0006, one obtains

$$\log K_{CO} \approx \log (0.0006\times0.8\times10^4) = +0.7\,. \tag{5}$$

Similarly, at the transition temperature for N_2, where half the nitrogen atoms are still free, one finds that the dissociation constant K_{N_2} must be twice the partial pressure of *N*. With a normal ratio of nitrogen to hydrogen of 0.0003, one obtains

$$\log K_{N_2} \approx \log (2\times\tfrac{1}{2}\times0.0003\times0.8\times10^4) = +0.4\,. \tag{6}$$

These *K* values, estimated for the transition temperatures, are to be compared with the *K* values derived from equations (3) and (4) and given in Table 1. Evidently, the

TABLE 1

EQUILIBRIUM CONSTANTS FOR *CO* AND N_2
(Pressure Units = 1 Dyne Cm^{-2})

TEMPERATURE	DISSOCIATION ENERGY IN E.V.					
	log K_{CO}			log K_{N_2}		
	9.14	9.60	11.11	7.29	9.76	11.8
4500°	+2.95	+2.44	+0.75	+4.64	+1.87	−0.40
4000°	+1.62	+1.04	−0.87	+3.59	+0.48	−2.08
3500°	−0.10	−0.76	−2.94	+2.24	−1.32	−4.24

astronomical *K* values are in good agreement with the *K* values derived from laboratory data with a temperature of about 4000° and with the intermediate values for the dissociation energies of *CO* and N_2.

We conclude that the laboratory data in no way disagree with our assumptions regarding the transition temperatures of *CO* and N_2 derived above from astronomical observations. In fact, the spread of the theoretical values of log *K* (see Table 1) is so large as to raise hopes that astrophysical evidence may decide among the rivaling dissociation energies that have been proposed by laboratory spectroscopists. Unless our astrophysical esti-

[8] *Ibid.*, upper half of Fig. 2.

[9] *Ibid.*, lower half of Fig. 2.

[10] Ueno and Matsushima, *Pub. Astr. Soc. Japan*, 2, 32, 1950.

mate of K, based upon a presumable transition temperature close to 4000° K, is much in error, dissociation energies of N_2 as high as 11.8 e.v. or as low as 7.3 e.v. are ruled out. By the same argument, a dissociation energy of 11.11 e.v. for CO seems rather improbable.

IV. STRENGTH OF *CH* AND *CN* IN THE SPECTRA OF GIANTS

The partial pressures of CH and CN, which determine the strength of the CH and CN bands, may now be derived. We utilize the results obtained in equations (2*a*)–(2*d*) above, together with the transition temperature found in the preceding section. If we again use the symbol p to denote the partial pressure of a given atom or molecule, and P for the fictitious partial pressure of a given element that would be obtained if all atoms of this element were free, then the previous results may be summarized approximately in the following set of equations:

$$\text{Earlier than gK0:} \quad P_H = p_H\,, \quad P_O = p_O\,, \quad P_N = p_N\,, \quad P_C = p_C\,; \tag{7a}$$

$$\text{Later than gK0:} \quad P_H = p_H\,, \quad P_O = p_O\,, \quad P_N = 2p_{N_2}\,, \quad P_C = p_{CO}\,, \tag{7b}$$

where we have assumed that P_C/P_O is negligible. Since P_C/P_O may be as great as 0.3 and since in any case the region of transition between equations (7*a*) and (7*b*) is relatively wide, these equations must not be used for precise computations; but they are adequate for the present preliminary and semiquantitative treatment.

Relations (7*a*) and (7*b*) will now be introduced into the equations of dissociative equilibrium of the four molecules in question

$$p_{CH} \propto p_C p_H\,, \quad p_{CN} \propto p_C p_N\,, \quad p_{CO} \propto p_C p_O\,, \quad p_{N_2} \propto p_N^2\,. \tag{8}$$

Here the temperature-dependent factors have been left out, since the equations will be used only for the comparison of stars with equal temperatures.

Furthermore, let us make the basic assumption that carbon, nitrogen, and oxygen do not vary in their abundances relative to one another when normal, low-velocity, and high-velocity stars are compared but that their abundances vary together relative to hydrogen. This assumption can be expressed by a single abundance factor B in the following form:

$$P_H = P\,; \quad P_C \propto P_N \propto P_O \propto B^{-1}P\,. \tag{9}$$

Introducing equations (7) and (9) into equations (8), we obtain

$$\begin{aligned} &\text{Earlier than gK0:} \quad p_{CH} \propto B^{-1}P^2\,, \quad p_{CN} \propto B^{-2}P^2\,; \\ &\text{Later than gK0:} \quad p_{CH} \propto P\,, \quad p_{CN} \propto B^{-1/2}P^{1/2}\,. \end{aligned} \tag{10}$$

Here the partial pressures of CH and CN are expressed in terms of the total pressure P. In comparing high-velocity and low-velocity stars, one cannot assume P to be the same, since a difference in the abundance of the metals which provide the free electrons would produce a difference in the number of H^- ions which provide the opacity; thus the effective depth of the reversing layer and, hence, the representative pressure, P, would vary from star to star. The next step, therefore, is to determine the degree of ionization of the several metals which provide the free electrons.

The degrees of ionization of the most common metals were computed for the temperatures and electron pressures listed in the first three lines of Table 2. The results are given in the last three lines of Table 2. They show that Fe, Mg, and Si are largely ionized only in spectral types earlier than gK0, while the remaining metals are largely ionized in spectral types as late as gK5. Conversely, in spectral types earlier than gK0 the free electrons are produced by all the common metals, all of which are still essentially ionized;

however, in spectral types gK0 to about gK2 the free electrons should result from ionization of the most abundant metals *Fe*, *Mg*, and *Si*, even though these elements are predominantly neutral at the temperatures in question; and, finally, in the latest spectral types here considered the free electrons come from the less abundant metals *Al*, *Ca*, and *Na*, which are almost entirely ionized even at these lower temperatures.

TABLE 2

DEGREE OF IONIZATION OF METALS

	gG2	gK0	gK5
T_e	5000	4230	3580
$T(\tau=0.4)$*	4800	4030	3380
$\log p_e$*	0.0	−0.5	−1.3
$\log n_{II}/n_I$ *Fe, Mg, Si*	+0.9	−0.4	−1.6
$\log n_{II}/n_I$ *Al, Ca*	+2.4	+1.5	+0.7
$\log n_{II}/n_I$ *Na*	+3.4	+2.7	+2.0

* Values taken from Ueno and Matsushima, *Pub. Astr. Soc. Japan*, **8**, 32, 1950.

If M designates the metals which provide most of the free electrons, the ionization equilibrium gives

$$p_{MI} \propto p_{MII} p_e \qquad \text{with} \qquad p_{MII} = p_e . \tag{11}$$

If, further, A is the ratio of hydrogen to metals, by volume, one has

$$P_M \propto A^{-1} P . \tag{12}$$

Together, the last equations give the following relation between p_e and P, depending on the state of ionization of M:

$$\begin{aligned} &M \text{ ionized:} \quad P_M = p_{MII} , \quad p_e = A^{-1} P ; \\ &M \text{ neutral:} \quad P_M = p_{MI} , \quad p_e = A^{-1/2} P^{1/2} . \end{aligned} \tag{13}$$

A second relation between p_e and P is obtained by considering the optical depth of the effective reversing layer, which should be essentially constant. Since the opacity is produced by H^- for the spectral types in question and since the scale height H of an atmosphere is proportional to the reciprocal of the acceleration of gravity, g, for all stars of constant kinetic temperature, one finds

$$\tau = \text{Const.} = \int \kappa \rho dZ \propto \kappa \rho H \propto p_{H^-} g^{-1} \propto P p_e g^{-1} \tag{14}$$

or

$$p_e \propto P^{-1} g . \tag{15}$$

Here, as previously, the atmosphere is assumed to be isothermal. Equations (13) and (15), together, finally give

$$\begin{aligned} &M \text{ ionized:} \quad P \propto A^{1/2} g^{1/2} , \quad p_e \propto A^{-1/2} g^{1/2} , \quad p_{H^-} \propto g ; \\ &M \text{ neutral:} \quad P \propto A^{1/3} g^{2/3} , \quad p_e \propto A^{-1/3} g^{1/3} , \quad p_{H^-} \propto g . \end{aligned} \tag{16}$$

With the help of equations (16), P can be eliminated from equations (10) and the strengths of the *CH* and *CN* bands can be derived. The strength of a line is a function of N, the effective number of oscillators per square centimeter, which is proportional to the partial pressure of the particle producing the line divided by the partial pressure of the

particle producing the general opacity. The final expressions for N_{CH} and N_{CN}, thus derived from equations (10) and (16), are listed in Table 3. In the last line of Table 3 expressions for $N_{Fe\,I}$ are given for comparison, since *Fe* I produces many of the stronger lines in the later spectral types. These expressions follow from equations (16) and from the equations of ionization equilibrium with $P_{Fe} \propto p_{Fe\,II}$ for spectral types earlier than gK0 and $P_{Fe} \propto p_{Fe\,I}$ for spectral types later than gK0.

TABLE 3

DEPENDENCE OF LINE STRENGTHS ON ABUNDANCE FACTORS

Line Strengths	Earlier than gK0	Later than gK0	
	Source of Electrons		
	Fe, etc. (Ionized)	*Fe*, etc. (Neutral)	*Al*, etc. (Ionized)
$N_{CH} \propto p_{CH}/p_{H^-} \propto$	AB^{-1}	$A^{1/3}g^{-1/3}$	$A^{1/2}g^{-1/2}$
$N_{CN} \propto p_{CN}/p_{H^-} \propto$	AB^{-2}	$A^{1/6}B^{-1/2}g^{-2/3}$	$A^{1/4}B^{-1/2}g^{-3/4}$
$N_{Fe\,I} \propto p_{Fe\,I}/p_{H^-} \propto$	A^{-1}	$A^{-2/3}g^{-1/2}$	$A^{-1/2}g^{-1/2}$

V. ABUNDANCE DIFFERENCES

Table 3 shows directly the dependence of the strength of the *CH* and *CN* bands on the abundance of the metals, characterized by A, and on the abundance of the oxygen group, characterized by B. The table indicates that a reduction of the metal abundance (increase in A), while, of course, reducing the strength of the *Fe* I lines, increases the *CH* and *CN* features. This is an immediate consequence of the fact that fewer metals mean lower opacity and therefore higher pressures in the reversing layer, which generally favors molecules. The strengthening of *CH* and *CN* with A should not be so pronounced for spectral types later than gK0, since for these late types increased pressure means increased numbers of *CO* and N_2, which, in turn, reduces the number of free *C* and *N* atoms available for *CH* and *CN*.

On the other hand, a reduction of the abundance of the oxygen group (increase in B) will generally produce a decrease in the strength of *CH* and *CN*. This effect will be stronger for *CN*, which contains two atoms of the oxygen group, than for *CH*, which contains only one atom of the oxygen group. The dependence of *CH* and *CN* on B is again reduced for the spectral types later than gK0 because of the interference by *CO* and N_2.

Table 3 shows that a decrease in the abundance of the metals and a somewhat lesser decrease in the abundance of the oxygen group could result in a strengthening of *CH* (mainly through the increase in A) and, at the same time, a weakening of *CN* (mainly through the increase in B). To give a concrete example, Table 4 shows the percentage increases and decreases in the N values if A increases by a factor of 3 and B simultaneously increases by a factor of 2.

The changes shown by Table 4 are fairly similar for giants earlier than K0 and later than K0; consequently, even an appreciable error in the assumption regarding the transition temperatures discussed in Section III would not have affected the results.

According to Table 3, the gravitational acceleration, g, affects the band and line strengths for the later spectral types. At present, however, it does not seem clear how a change in the abundance factors A and B might affect g.

A quantitative comparison with observations seems at present not possible, since accurate measurements of equivalent widths and curves of growth are not yet available for a direct comparison of high- and low-velocity giants. Furthermore, a detailed discussion of the presently available observational data would be uncertain, since the spectral types of the high-velocity giants are probably affected by the abnormal behavior of *CH*, so that, for the same spectral type, the average temperatures of high- and low-velocity giants may differ slightly.

Qualitatively, however, the data in Table 4 indicate that the strengthening of *CH* and simultaneously the weakening of *CN* in the high-velocity giants may be explained by an increase in *A* and a somewhat lesser increase in *B*.

This tentative result was derived above on the basis of observations on giants. A fairly similar result was previously derived from a spectroscopic comparison of high- and low-velocity dwarfs.[11] Furthermore, the above result is in qualitative agreement with the general weakening of metal lines in F and G high-velocity stars recently observed.[12] Therefore, one may tentatively conclude that the spectroscopic differences between high- and low-velocity stars can be explained throughout by a reduction in the abundance of the heavy elements and a somewhat lesser reduction of the abundance of the medium-heavy elements in the high-velocity stars.

TABLE 4

CHANGES OF LINE STRENGTH FOR AN INCREASE OF *A* BY A FACTOR OF 3 AND A SIMULTANEOUS INCREASE OF *B* BY A FACTOR OF 2

Changes of Line Strengths	Earlier than gK0	Later than gK0	
	Source of Electrons		
	Fe, etc. (Ion.)	*Fe*, etc. (Neutr.)	*Al*, etc. (Ion.)
Change of N_{CH} . . .	+50%	+40%	+70%
Change of N_{CN} . . .	−20%	−20%	−10%
Change of $N_{Fe\,I}$ . . .	−70%	−50%	−30%

VI. ORIGIN OF DIFFERENCES IN CHEMICAL COMPOSITION

If one accepts as a working hypothesis the somewhat greater abundance of the heavier elements in type I stars than in stars of type II, it is natural to inquire as to possible reasons for this difference. According to current physical theory, there is no way in which these differences can result from nuclear processes inside a typical star. One must therefore seek for some process by which more heavy nuclei are brought into a type I star than into a star of type II.

The most natural time to bring material into a star is when the star is being formed. While the details of star formation are naturally very speculative at present, it is worth pointing out that, according to theories already advanced,[13, 14] a star formed from in-

[11] M. and B. Schwarzschild, *op. cit.*

[12] *Op. cit.*

[13] F. L. Whipple, *Ap. J.*, **104**, 1, 1946.

[14] L. Spitzer, Jr., *Centennial Symposia* (Cambridge, Mass.: Harvard College Observatory, 1948).

terstellar clouds should contain an excess of heavy elements, a result of the concentration of the solid particles, or grains, in star-forming clouds. There is good evidence that at least some of the type I stars have formed recently from interstellar clouds, while the type II stars are all old, having been formed by some different process about three billion years ago.[15] If one assumes that all type I stars have condensed from interstellar clouds since the formation of the galaxy—an assumption which is consistent with the evidence from stellar velocities[15, 16]—it appears that this difference in chemical composition between stars of the two population types can be explained.

Let us review briefly the essential steps in star formation which could lead to a concentration of the heavy elements. The distribution of interstellar matter is very spotty, with dense clouds separated by regions in which the density is much lower. Naturally, the denser regions are those most likely to condense gravitationally into new stars. In these dense regions the ratio of heavy elements to hydrogen will exceed that in other regions, since the force of radiation pressure from the general galactic light will push the surrounding grains into these regions. Essentially, a grain in the shadow cast by a dense, opaque cloud will be propelled toward the cloud by radiation coming from the opposite direction and will slowly diffuse through the hydrogen gas. Since the grains contain mostly heavy elements, with relatively little hydrogen, this concentration of grains in the dense clouds will increase the abundance of the heavy elements relative to hydrogen in such clouds. The time required for this process to produce a significant increase in the abundances of the heavy elements is in the neighborhood of 10^7 years.

While a precise quantitative test of this theory is scarcely possible at present, this hypothesis seems at least consistent with the observations. The clouds postulated in recent interstellar studies[17] with a density of 10 hydrogen atoms per cubic centimeter, radii of 5 parsecs, and a spatial density of 10^{-4} clouds per cubic parsec have a total mass equivalent to 0.5 *H* atoms per cubic centimeter, if a smoothed average is taken over the entire volume near the galactic plane, including both clouds and intercloud regions. The density of the intercloud material is estimated by Strömgren[17] as 0.1 *H* atoms per cubic centimeter. On this basis five-sixths of the interstellar material is in the clouds, and, if all the grains were concentrated in these clouds and all the heavy elements were collected in grains, the abundance of the heavy elements would increase by a factor of only $\frac{6}{5}$. Most of these clouds are not sufficiently massive or dense to condense into stars, however, and it is reasonable to assume that in a small fraction of the clouds—containing about one-tenth the mass, for example—the density and opacity are higher, and the concentration of grains may increase the ratio of grains to gas by a factor of perhaps 4. If about half the heavy atoms in the interstellar medium are locked up in grains, on the average, this assumed concentration of grains would result in the observed twofold increase in the abundance of *C*, *N*, and *O* in type I stars as compared to type II objects.

The somewhat greater increase in the abundance of *Fe* in type I stars can be fitted into this picture if it is assumed that a greater fraction of *Fe* atoms is locked up in the grains. In the numerical example just cited, if we assume that two-thirds of the *Fe* atoms are locked up in the grains, then a threefold increase in the number of *Fe* atoms will result. Collisions between grains and selective evaporation of the more volatile constituents might readily lead[18] to such an increase in the fraction of *Fe* and *Mg* atoms in the grains.

Evidently, the concentration of grains into dense clouds, through the action of radiation pressure, might produce differences in chemical composition similar to those discussed in this paper. The suggestion that all type I stars have been formed from interstellar clouds may, perhaps, be taken as a working hypothesis.

[15] L. Spitzer, Jr., *Proc. Phil. Soc. Washington*, in press.

[16] L. Spitzer, Jr., and M. Schwarzschild, *Ap. J.*, **114**, 385, 1951.

[17] B. Strömgren, *Ap. J.*, **108**, 242, 1948; L. Spitzer, Jr., *Ap. J.*, **108**, 276, 1948.

[18] H. C. van de Hulst, *Rech. Astr. Obs. Utrecht*, Vol. 11, Part 2, 1949; L. Spitzer, Jr., and J. W. Tukey, *Ap. J.*, **114**, 187, 1951.

CONTINUOUS EMISSION FROM PLANETARY NEBULAE

LYMAN SPITZER, JR., AND JESSE L. GREENSTEIN
PRINCETON UNIVERSITY OBSERVATORY
and
MOUNT WILSON AND PALOMAR OBSERVATORIES
CARNEGIE INSTITUTION OF WASHINGTON
CALIFORNIA INSTITUTE OF TECHNOLOGY
Received June 15, 1951

ABSTRACT

Simultaneous emission of two photons by an H atom in the metastable 2s level is considered as a source of a continuum in planetary nebulae. Detailed calculations show that the probability of two-photon emission is 8.23 sec^{-1} and that the intensity of radiation emitted by this process increases markedly with increasing frequency. About 32 per cent of electron captures lead directly to the 2s level and then to two-photon emission, since collisional de-excitation proves unimportant. Transitions from the 2p to the 2s level, induced by collisions with free electrons, convert a part of the remaining Lα quanta into this continuous radiation, conversion occurring after a quantum of Lα radiation has been scattered about 10^{10} times, on the average, in a region of ionized H. A neutral hydrogen region may surround the H II region. In such an H I envelope, about 10^{13} scatterings are required for conversion, but the density of neutral H is so much greater that most conversion by collision probably takes place there. The fraction of Lα so converted may vary over a wide range, depending on the physical conditions.

The theory is used to predict the total emission from an ionized hydrogen gas. The Balmer jump is reduced, and the decrement of the continua shortward of the Paschen and Balmer limits is also reduced. A bluish continuum is to be expected in the region from λ 6000 to λ 3646. Our analysis applied to the ultraviolet observations now available results in a reduction of electron temperatures by about 25 per cent. The available wide-slit observations indicate the possibility that a bluish "visual continuum" may exist.

The continuous spectrum of planetary nebulae in the visual region was first measured by Page,[1] and has been analyzed more recently by Aller and Minkowski[2] and by Page.[3] These observations show that longward of the Balmer continuum there exists continuous radiation, with appreciable strength and with a nearly constant intensity per unit wavelength interval between λ 3600 and λ 4800.

Attempts to explain this continuous spectrum have been, so far, uniformly unsuccessful. Previous suggestions have been summarized by Greenstein and Page,[4] who show that emission of radiation in the formation of H^- ions cannot explain the data. The present paper investigates a different source of continuous radiation, based on the simultaneous emission of two quanta from a hydrogen atom in the metastable 2s level. An appreciable fraction of electrons captured by protons will reach the 2s level on their way down to the ground state. In addition, Lα radiation may be converted into two photons of this visual continuum. The absorption of Lα radiation will excite an H atom to the 2p level; and, during the brief interval before the Lα quantum is re-emitted, a collision with a free electron may induce a transition from the 2p to the 2s level. All one-photon transitions from the 2s down to the 1s level are forbidden, and, unless a collision with another free electron induces a transition back to the 2p level, the excited electron will jump down to the 1s level, emitting two photons. Evidently, the sum of the energies of these two photons equals the energy of the Lα photon.

While the probability that an Lα photon will be converted into two photons is relatively small, a single Lα photon is scattered an enormous number of times before it can

[1] *M.N.*, **96**, 604, 1936.
[2] Unpublished.
[3] *Ap. J.*, **96**, 78, 1942.
[4] *Ap. J.*, **114**, 106, 1951.

escape from the planetary nebula. Moreover, the Zanstra process converts most of the stellar energy beyond the Lyman limit into Lα photons. Thus it seems possible that some of the energy emitted by the central star in a planetary nebula can be converted into continuous radiation by two-photon emission.

When this work was nearly complete, it was found that this process had already been considered by Minkowski and Aller,[5] who rejected it because the predicted color distribution was too blue, and, more recently, by A. Y. Kipper;[6] no details of Kipper's work are apparently available in this country.

I. PROBABILITY OF TWO-PHOTON EMISSION

The general theory of two-photon processes has been given by M. Goppert Meyer,[7] and a detailed application of the theory in the case of the 2s−1s transition in H has been given by Breit and Teller.[8] Since Breit and Teller's numerical computations were approximate and did not consider at all the change of intensity with frequency, more detailed computations are required. Let the frequencies of the two photons emitted be $y\nu_{12}$ and $(1-y)\nu_{12}$, where ν_{12} is the frequency of an Lα photon; evidently

$$\nu_{12} = \tfrac{3}{4}\, cR\,, \tag{1}$$

where c is the velocity of light and R is the Rydberg constant for H. Let $A(y)dy$ be the probability that a photon is emitted with a frequency in the range $\nu_{12}dy$. From equation (6.2) in the paper by Breit and Teller, we have

$$A\,(y) = \frac{9\alpha^6 cR}{2^{10}}\,\psi\,(y)\,, \tag{2}$$

where α is the fine-structure constant $2\pi e^2/hc$, and

$$\psi\,(y) = y^3\,(1-y)^3\left|\sum_{m=2}^{\infty} R^{1s}_{mp} R^{2s}_{mp}\left(\frac{3}{1+3y-4/m^2}+\frac{3}{4-3y-4/m^2}\right)\right. \\ \left. +\int_0^{\infty} C_{1s}C_{2s}\,dx\left(\frac{3}{1+3y+4x^2}+\frac{3}{4-3y+4x^2}\right)\right|^2. \tag{3}$$

The quantities R^{ns}_{mp} and C_{ns} are radial quantum integrals defined by Breit and Teller.

Values of $\psi(y)$ have been computed in detail, with R^{ns}_{mp} taken from the tabulation by H. Bethe,[9] and C_{ns} from the paper by M. Stobbe;[10] since Stobbe's tables were not sufficiently complete, new values of these functions were computed from his formulae. The resultant values of $\psi(y)$ are given in Table 1. Since $\psi(1-y)$ equals $\psi(y)$, no values are given for y greater than 0.5. The emissivity j_ν per unit frequency interval is proportional to $h\nu A(y)$, and therefore varies as $y\psi(y)$; values of the relative emissivities are given in the last column.

The familiar Einstein coefficient $A_{2s,\,1s}$ for the two-photon transition is given by

$$A_{2s,\,1s} = \frac{1}{2}\int_0^1 A\,(y)\,dy = \frac{9\alpha^6 cR}{2^{11}}\int_0^1 \psi\,(y)\,dy\,. \tag{4}$$

The factor of ½ is required, since there are two photons, and each pair is counted twice. Numerical integration yields the result

$$\int_0^1 \psi\,(y)\,dy = 3.770\,. \tag{5}$$

[5] Informal communication.
[6] *A.J.U.S.S.R.*, **27**, 321, 1950.
[7] *Ann. d. Phys.*, **9**, 273, 1931.
[8] *Ap. J.*, **91**, 215, 1940.
[9] *Handb. d. Phys.* (Berlin: J. Springer, 1933), **24–1**, 442.
[10] *Ann. d. Phys.*, **7**, 661, 1930.

Inserting numerical values into equation (4), we find

$$A_{2s,\,1s} = 8.227 \text{ sec}^{-1}, \tag{6}$$

a value close to the upper limit found by Breit and Teller; an increase in α above the value used by Breit and Teller is partly responsible for this relatively high value of $A_{2s,\,1s}$.

II. EXCITATION OF 2s LEVEL

We consider, now, the processes by which an electron can reach the 2s state under conditions prevailing in planetary nebulae. The first and simplest process is that in which an electron reaches the 2s state by electron capture, either by direct capture in this state or by capture in a higher state, with subsequent cascading downward to the 2s state.

We first compute the probability $X_{r,\,n}$ that an electron, on recombination with a proton in the level of total quantum number n, passes through the 2s state on its way down. Let $\Gamma_{n'l',\,nl}$ be the number of electrons jumping from the level $n'l'$ to the level nl per second per cubic centimeter; jumps down from and up to the free state will be represented by $\Gamma_{f,\,nl}$ and $\Gamma_{n'l',\,f}$, respectively. Let $\Gamma^*_{n'l',\,nl}$ represent the corresponding quantity in thermodynamic equilibrium with the same density of protons and electrons and at a temperature corresponding to the mean kinetic energy of protons and electrons. Evidently, from the principle of detailed balancing,

TABLE 1

RELATIVE PROBABILITIES AND INTENSITIES OF TWO-PHOTON EMISSION

y	λ(A)	Probability $\psi(y)$	Emissivity $y\psi(y)$	y	λ(A)	Probability $\psi(y)$	Emissivity $y\psi(y)$
0.00	.....	0	0	0.30	4052	4.546	1.363
.05	24,313	1.725	0.0863	.35	3473	4.711	1.649
.10	12,157	2.783	0.2783	.40	3039	4.824	1.929
.15	8105	3.481	0.5222	.45	2702	4.889	2.200
.20	6078	3.961	0.7922	0.50	2431	4.907	2.454
0.25	4862	4.306	1.077				

$$\Gamma^*_{n'l',\,nl} = \Gamma^*_{nl,\,n'l'}. \tag{7}$$

Also, since the electron velocity distribution is Maxwellian, we have

$$\Gamma^*_{f,\,nl} = \Gamma_{f,\,nl}. \tag{8}$$

We wish to compute the fraction of electrons, captured in the level of total quantum number n, which are captured in the level of angular momentum l. From equations (7) and (8) we see that this fraction, y_{nl}, is given by

$$y_{nl} = \frac{\Gamma_{f,\,nl}}{\sum_l \Gamma_{f,\,nl}} = \frac{\Gamma^*_{nl,\,f}}{\sum_l \Gamma^*_{nl,\,f}}. \tag{9}$$

To a first approximation the ratio on the right-hand side of equation (9) is given by the ratio of gf values. The use of an integrated f value for transitions to the continuum neglects the shape of the radiation spectrum and the detailed form of $df/d\nu$ for continuous

absorption, but should give an adequate first approximation. Equation (9) then becomes

$$y_{nl} = \frac{g_{nl} f_{nl,\,f}}{\sum_l g_{nl} f_{nl,\,f}} . \tag{10}$$

Evidently in the case $n = 2$ we have

$$X_{r,\,2} = y_{20} . \tag{11}$$

For captures of electrons in levels of higher n, we must consider subsequent transitions. We may write, in general,

$$X_{r,\,n} = \frac{\sum_l z_{nl} y_{nl}}{\sum_l y_{nl}} , \tag{12}$$

where z_{nl} is the fraction of electrons captured in the level n, l which cascade down to the level 2, 0. For the level $n = 3$ we have

$$z_{3l} = \begin{cases} 0 & \text{for } l = 0 \\ 1 & \text{for } l = 1 \\ 0 & \text{for } l = 2 . \end{cases} \tag{13}$$

Transitions down to the ground level ($n = 1$) are neglected, since any photons emitted in this way will be immediately reabsorbed. For higher levels, more complicated results are obtained. The relative probabilities of two competing downward transitions may be determined directly from the transition probabilities given by Bethe.[9] For $n = 4$, for example, we have

$$z_{4l} = \begin{cases} 0.42 & \text{for } l = 0 \\ 0.74 & \text{for } l = 1 \\ 0.26 & \text{for } l = 2 \\ 0.00 & \text{for } l = 3 . \end{cases} \tag{14}$$

If we now substitute these results for z_{nl} in equation (12) and use in equation (10) the value of $f_{nl,\,f}$ given by Bethe, we find

$$X_{r,\,n} = \begin{cases} 0.38 & \text{for } n = 2 \\ 0.45 & \text{for } n = 3 \\ 0.38 & \text{for } n = 4 . \end{cases} \tag{15}$$

For greater values of n, the value of $X_{r,\,n}$ decreases gradually. However, the number of electron captures on the nth level varies as $1/n^3$ for binding energies less than the kinetic energy of the free electron. In planetary nebulae, where the electron temperature corresponds to a mean kinetic energy of about 1 volt, captures on levels about $n = 5$ may therefore be neglected. The fraction of electrons captured which reach the 2s state should be somewhere between 0.30 and 0.35; we shall assume a mean value of 0.32. Collisional de-excitation may be taken into account in the manner discussed below, with the result that, if T is 10,000°, X_r, the weighted mean of $X_{r,\,n}$, becomes

$$X_r = \frac{0.32}{1 + 8.2 \times 10^{-6} n_e} . \tag{16}$$

A second mechanism for reaching the 2s state is radiative excitation of the 2p state, followed by a collision with a free electron, inducing a transition to the 2s state. The low probability for this collisional process is offset by the very high number of times that a quantum of Lα radiation will be absorbed and re-emitted before it leaves the nebula. On the assumption that all excitation is by radiative absorption of Lα quanta, we now wish to compute the ratio between two-quantum jumps from 2s to 1s and one-quantum jumps from 2p to 1s. This ratio, which we denote by ζ, gives the probability that a quantum of Lα radiation will be converted into two photons when it is absorbed by an H atom.

This ratio clearly depends on the probability of collisionally induced transitions, which has been considered in detail by Breit and Teller.[8] Their computations may readily be modified to include the Lamb shift[11] of the 2s level relative to the $2p_{1/2}$ level; this shift has only a small effect, since the energy of the transition is in any case very small compared to the energy of the incident electron.[12]

With obvious modifications, the equations S' and S'' by Breit and Teller may be combined to yield for the transition probability $C_{2s,\,2p}$

$$C_{2s,\,2p}=\frac{6n_e h^2}{\pi v m^2}\left\{\ln\frac{m v^2}{|E_{2s}-E_{2p_{1/2}}|}+2\ln\frac{m v^2}{|E_{2s}-E_{2p_{3/2}}|}\right\}, \tag{17}$$

where n_e is the electron density per cubic centimeter; m is the electron mass; and v is the velocity of the free electron in centimeters per second. In wave numbers,

$$|E_{2s}-E_{2p_{1/2}}|=0.035\ \text{cm}^{-1}, \tag{18}$$

$$|E_{2s}-E_{2p_{3/2}}|=0.365\ \text{cm}^{-1}. \tag{19}$$

Substituting numerical values and replacing $1/v$ by the harmonic mean at temperature T, we have

$$C_{2s,\,2p}=6.21\times10^{-4}\frac{n_e}{T^{1/2}}\ln(5.7T)\left[1+\frac{0.78}{\ln(5.7T)}\right]\text{sec}^{-1}. \tag{20}$$

The second term in brackets on the right-hand side of this equation is small compared to unity and will be neglected here. Collisional transitions induced by collisions with neutral H atoms may be neglected if n_H does not exceed $10^3 n_e$; the cross-section for such encounters will be several orders of magnitude less than the 10^{-12} cm^2 predicted for electron collisions.

The relative populations of the 2s and 2p levels are readily computed from the condition that statistical equilibrium exists, i.e., that the number of electrons jumping out of each level equals the number jumping in. We neglect stimulated two-quantum emissions. The quantity ζ equals the ratio of populations in the 2s and 2p levels, multiplied by the ratio $A_{2s,\,1s}/A_{2p,\,1s}$. After some analysis we obtain

$$\zeta=\frac{g_{2s}C_{2s,\,2p}}{g_{2p}A_{2p,\,1s}}\frac{1}{1+C_{2s,\,2p}/A_{2s,\,1s}}. \tag{21}$$

The ratio g_{2s}/g_{2p} is $\frac{1}{3}$, and, if we insert numerical values from equation (20), taking the value of $A_{2s,\,1s}$ from equation (6), we have

$$\zeta=\frac{3.31\times10^{-13}n_e\ln 5.7T}{T^{1/2}+7.5\times10^{-5}n_e\ln 5.7T}. \tag{22}$$

[11] *Phys. Rev.*, **72**, 241, 1947.

[12] This situation is in marked contrast to that prevailing in a constant electrical field, where the Lamb shift decreases the radiative transition probability from 2s to 1s by a factor of about 1000, according to G. Luders, *Zs. f. Naturforsch.*, **5a**, 608, 1950.

When T is 10,000° K, a standard value for most planetary nebulae, equation (22) yields

$$\zeta = \frac{3.62 \times 10^{-14} n_e}{1 + 8.2 \times 10^{-6} n_e}. \tag{23}$$

For values of n_e between 10^3 and 10^4 per cubic centimeter—typical values for most planetaries—ζ is about 10^{-10}. Of about 10^{10} Lα quanta absorbed by an H atom, one will give rise to a two-quantum jump. If a region of neutral H surrounds the planetary, n_e in such a region will be less by a factor of 10^3, and ζ will equal about 10^{-13}.

III. MEAN FREE PATH OF Lα QUANTUM

We have seen that some 30–35 per cent of the electrons captured by a proton produce two-quantum emission. The others each produce, among other things, a quantum of Lα radiation; and, if the nebula is sufficiently thick optically, these quanta will also be converted into the visual two-photon continuum. Here we consider the mean free path of an Lα quantum, on the average, before it is converted into two quanta by this process.

The situation is idealized by the assumption that, at some distance from the central star, the density of neutral H is constant in space. With this assumption, the necessity for solving the diffusion equation is eliminated; and the simplified analysis of Brownian motion may be applied. Let s_ν be the mean free path of a photon before absorption and let the absorption coefficient of neutral H for this photon be a_ν. If n_H is the density of neutral H, then we have

$$s_\nu = \frac{1}{n_H a_\nu}. \tag{24}$$

If the probability of conversion into two-quantum radiation is ζ per absorption, then the photon will travel $1/\zeta$ mean free paths, on the average, before it is so converted. The directions of successive paths will be uncorrelated, and the mean square distance l_ν^2 will increase proportionally to the number of paths traveled; hence l_ν^2 will equal s_ν^2 multiplied by $1/\zeta$.

To obtain a realistic picture, we must take into account the Doppler change of ν in successive paths, depending on the thermal motion of the absorbing atom and on the angles between the absorbed and emitted photon. This type of noncoherent scattering has been considered by Henyey[13] and applied to planetary nebulae by Zanstra.[14] The detailed correlation of frequencies between the absorbed and subsequently re-emitted photon will be ignored in this first approximation, and only the statistical distribution of frequencies will be considered; this distribution may be assumed to follow the Maxwellian distributions of H-atom velocities. The mean square distance traveled must be averaged over this distribution of frequencies, and we have the basic equation

$$l^2 = \frac{1}{\zeta n_H^2} \int_0^\infty \frac{\phi(\nu)\, d\nu}{a_\nu^2}, \tag{25}$$

where $\phi(\nu)d\nu$ is the fraction of atoms emitting quanta in the frequency range $d\nu$. From the usual Doppler formula and the Maxwellian velocity distribution we have

$$\phi(\nu) = \frac{1}{\pi^{1/2} b}\, e^{-(\Delta\nu/b)^2}, \tag{26}$$

where $\Delta\nu$ is the difference in frequency from the undisplaced frequency and

$$b^2 = \frac{2kT\nu^2}{m_H c^2}. \tag{27}$$

[13] *Proc. Nat. Acad. Sci.*, **26**, 50, 1940.
[14] *B.A.N.*, Vol. 11, No. 401, 1949.

If a Doppler profile of the line-absorption coefficient were assumed and a_ν therefore varied as $\phi(\nu)$ for all $\Delta\nu$, the integral in equation (25) would diverge; physically the La radiation would leak out of the nebula in the far wings of the profile. Actually, only the center of the line profile is given by the usual Doppler formula, and for large $\Delta\nu$ the resonance wings dominate. To an adequate approximation we may write

$$a_\nu = \frac{\pi e^2 f}{mc} \times \begin{cases} \phi(\nu) & (\Delta\nu \leqslant b) \quad (28a) \\ \phi(\nu) + \dfrac{\gamma}{\pi(\Delta\nu)^2} & (\Delta\nu > b), \quad (28b) \end{cases}$$

where e and m are the electronic charge and mass and γ is the damping constant, numerically equal to $A_{2p,\,1s}/4\pi$.

If equation (28) is substituted in equation (25), we find that the integral comes mostly from values of the integrand for which the Doppler wings and the resonance wings are about equal. If we let w be the value of $(\Delta\nu/b)^2$ at which these two contributions to a_ν are equal, then from equations (26) and (28) we see that w satisfies the equation

$$we^{-w} = \frac{\gamma}{\pi^{1/2} b}. \quad (29)$$

In the present instance γ is several orders of magnitude less than b, and w is moderately large. If we define a new variable, u, by the relation

$$u = \left(\frac{\Delta\nu}{b}\right)^2 - w, \quad (30)$$

then the integral in equation (25) becomes

$$\int_0^\infty \frac{\phi(\nu)\, d\nu}{a_\nu^2} = \frac{m^2 c^2 b^2 e^w}{\pi^{3/2} e^4 f^2 w^{1/2}} \int_{-w}^\infty \frac{e^u (1 + u/w)^{3/2} du}{(1 + e^u + u/w)^2}. \quad (31)$$

In deriving equation (31) we have used equation (28*b*) for all values of $\Delta\nu$; this diminishes somewhat the value of the integral for small $\Delta\nu$, but this region of $\Delta\nu$ contributes a negligible amount to the integrand in any case. When w is infinitely great, the integral in equation (31) equals unity. For $w = 10$, the integral differs from unity by about 10 per cent, a difference which we shall neglect. We have, combining equations (24) and (31),

$$l^2 = \frac{m^2 c^2 b^2 e^w}{\pi^{3/2} e^4 f^2 n_H^2 w^{1/2} \zeta}. \quad (32)$$

For La radiation, f is 0.416, and γ is 4.97×10^7 sec^{-1}. If we set T equal to 10,000° K, b is 1.06×10^{11}. The corresponding value of w found from equation (29) is 10.60. Substituting numerical values in equation (32) and making use of equation (23) for ζ, we obtain

$$l = 2.4 \times 10^3 \frac{(1 + 8.2 \times 10^{-6} n_e)^{1/2}}{n_e^{1/2} n_H} \text{ parsecs}. \quad (33)$$

If l found from equation (33) is small compared to the radius R of the planetary nebula, then all the La radiation will be converted into two-photon emission. If, on the other hand, l much exceeds R, the previous analysis is not strictly applicable. In this case the quanta will escape from the nebula after they have traveled a distance R, on the average, from the point of origin. Since the number of scatterings required to travel a distance R

varies as R^2, the number of scatterings experienced by a photon before escape will be less than the number $1/\zeta$ required for conversion into two-photon radiation by the fraction $(R/l)^2$, where l is the mean free path computed from equation (33) on the assumption that R is effectively infinite. If we denote by X_c the fraction of La radiation so converted by collisions, we have, approximately,

$$X_c = \left(\frac{R}{l}\right)^2. \tag{34}$$

It should be noted that, if the H atoms are distributed in a filamentary system, with regions of high density embedded in regions of lower density, the mean value of $1/n_H^2$ will be increased, and l will exceed the value given in equation (33).

The fraction X_c of La radiation converted into two-photon emission by collisions can be evaluated from a comparison between the size of the planetary and the free path, l, given by equation (33). Observations give only the average n_e in the main body of the nebula; n_H is variable, amounting to about $10^{-3} n_e$ in the main body and increasing at the outer boundary as n_e decreases. The estimate of the mean value of $n_e^{1/2} n_H$ must be based on a definite model for the nebula. Page and Greenstein[15] identify the visible portion of the nebula with the ionized hydrogen region (Strömgren sphere) surrounding the central star. They find that the observed radii R of planetary nebulae agree with those predicted on the basis of Strömgren's theory,[16] using the observed n_e, T_e, and the T_s, R_s of the exciting star. We adopt the model used by Strömgren, that of a homogeneous sphere of pure hydrogen of density n, surrounding a star which radiates as a black body.

First, we consider the fraction of La radiation converted within the H II region; we denote this fraction by $X_{c\text{II}}$. Equation (33) is valid only if n_e and n_H are constant. However, for approximate results we may use this equation for actual nebulae, introducing the following mean value of $n_e^{1/2} n_H$:

$$\overline{n_e^{1/2} n_H} = \frac{n^{3/2}}{R} \int_0^R x^{1/2} (1 - x)\, dr, \tag{35}$$

where x, the fraction of H ionized, is given by the Strömgren theory.[16] We will assume that R equals s_0; since n_e is less than 10^5, we will drop the correction term in the numerator of equation (33). Since R is much smaller than l, we have, from equation (34),

$$X_{c\text{II}}^{1/2} = \frac{R}{l} = \frac{n^{3/2}}{2.4 \times 10^3} \int_0^R x^{1/2} (1 - x)\, dr. \tag{36}$$

The integrand is known as a function of r from Strömgren's differential equation (12) for $1 - x$ less than 1 and from his approximation formula (17) for the region r about equal to s_0. A scale parameter, a, exists which measures both the thickness of the layer in which hydrogen becomes neutral and the fraction of hydrogen neutral near the star. The combination $a s_0$ is independent of the properties of the star:

$$a s_0 = aR = \frac{1}{6.3n}. \tag{37}$$

The unit of length is 1 parsec for R; n is the total number of hydrogen atoms and ions per cubic centimeter. The fraction of neutral hydrogen in the inner part of the sphere is given by

$$1 - x = \frac{a}{1 - (r/R)^3} \left(\frac{r}{R}\right)^2, \qquad (1 - x) < 1. \tag{38}$$

Thus n_H depends mainly on a. The mean $(1 - x)x^{1/2}$ has been obtained by numerical

[15] *Ap. J.*, **114**, 98, 1951. [16] *Ap. J.*, **89**, 526, 1939.

integration; it is $2.7a$ for $a = 10^{-2}$ and 3.8 for $a = 10^{-3}$. At $r/R = 0.7$ the value of $(1 - x)x^{1/2}$ from equation (38) is $0.75a$. The mean ionization determined by integration is seriously influenced by the large value of $1 - x$ in the rim of the ionized region but is not changed in order of magnitude. The maximum value of $(1 - x)x^{1/2}$ is 0.38, but this value is encountered in a shell only $0.007R$ thick. The order of magnitude of the mean free path should be correct, in spite of the large variation of $1 - x$.

Combining equations (36) and (37) and the results of the integrations, we obtain

$$X_{c\,II} = 3.2 \times 10^{-8} n\,, \qquad \text{for} \qquad a = 10^{-2}\,, \tag{39a}$$

$$X_{c\,II} = 6.4 \times 10^{-8} n\,, \qquad \text{for} \qquad a = 10^{-3}\,. \tag{39b}$$

The value of a can be computed from observational data. For a low-temperature and density ($n_e = 750$) nebula, NGC 40, the compilation by Page and Greenstein results in $a = 1.5 \times 10^{-3}$; for NGC 7009, $n_e = 6800$ and $a = 0.7 \times 10^{-3}$. Thus expression (39*b*) is sufficiently good; $X_{c\,II}$ is 4.1×10^{-5} for NGC 40 and 5.0×10^{-4} for NGC 7009. Certain nebulae with apparently large n_e, such as NGC 6790 and IC 4997, would have $X_{c\,II}$ equal to 1.5×10^{-3} and 4.6×10^{-3}, respectively. Thus the known planetaries convert an insignificant fraction of Lα radiation into two-photon emission by means of collisions within the *H* II region.

Page and Greenstein[15] pointed out that, if a planetary nebula has been expanding for a sufficiently long period, the visible disk or shell will be only the ionized core of the gas. The apparent boundary of the *H* emission is then the edge of the Strömgren sphere, and the neutral gas may extend far beyond. Without necessarily adopting the hypothesis of continuous ejection of matter from the star, we may still assume that the gas is expanding radially outward to large distances from the visible boundary at a uniform velocity. Then the density $n(r)$ varies as $1/r^2$, and the total number of atoms per square centimeter outside the visible boundary is $Rn(R)$. Thus in approximate results we can replace this *H* I region by a uniform layer of thickness R. In such a region the free electrons come primarily from *C* and *Mg*, which will be largely ionized. The electron density n_e may be set equal to $n_H/2000$, and we have

$$\overline{n_e^{1/2} n_H} = 2.2 \times 10^{-2} n^{3/2}\,. \tag{40}$$

We let $X_{c\,I}$ be the fraction of Lα radiation converted into two-photon emission in the *H* I shell outside the planetary. Then, by use of equations (33) and (34), we have

$$X_{c\,I}^{1/2} = \frac{R}{l} = 0.9 \times 10^{-5} n^{3/2} R\,. \tag{41}$$

The density of a typical planetary may be taken as $n = 5000$ and $R = 0.1$ parsecs; then $X_{c\,I} = 0.10$, i.e., about one-tenth of Lα is converted into two-photon emission. This is much larger than the $X_{c\,II}$, which would be near 0.001, for these standard conditions. We can expect $X_{c\,I}$ to vary from zero to about $\frac{1}{2}$, depending on physical conditions in this outer envelope. If we take into account the probable fall of temperature in *H* I regions and the consequent increase of ζ and decrease of b, the value of $X_{c\,I}$ is somewhat increased. If we let $X/(1 - X)$ be the ratio of the energy of two-photon radiation to Lα radiation, evidently X may vary from about 0.32 to nearly 1 in planetaries of differing density. A more refined theory of radiative transfer, taking into account the large spatial variations of n_H through the nebula, both in *H* I and *H* II regions, would be required for a more accurate and detailed calculation of X_c.

IV. RELATIVE INTENSITY OF TWO-PHOTON EMISSION

The previous sections give information on the fraction of electron captures that produce two-photon emission, and they also yield information on the distribution of this

emission with wave length. It remains to compare the intensity of this continuous radiation with other features of the hydrogen emission spectrum. We shall here make comparison with the Balmer and Paschen emission continua.

Let j_{2q} be the emissivity per gram in the two-quantum continuum per unit frequency from the planetary nebula, and let j_P and j_B be the corresponding quantities for the Paschen and Balmer continua. The variation of j_{2q} with frequency is given by

$$j_{2q}(\nu) = n_{2q} C_{2q} y \psi(y), \tag{42}$$

where $\psi(y)$ is defined above, n_{2q} is the total number of quanta emitted in two-photon transitions per gram per second, and C_{2q} is a constant to be determined. Similarly, for j_P and j_B we have

$$j_P(\nu) = n_P C_P e^{-h\nu/kT} \qquad (\nu > \nu_P), \tag{43}$$

$$j_B(\nu) = n_B C_B e^{-h\nu/kT} \qquad (\nu > \nu_B), \tag{44}$$

where ν_P and ν_B are the frequencies of the Paschen and Balmer limits, respectively. The functional form of equations (43) and (44) is evident from Kirchhoff's law, since the absorption coefficient for photoionization varies approximately as $(1 - e^{-h\nu/kT})/\nu^3$, when stimulated emission is taken into account.

The constant C_{2q} may be determined from the condition that

$$4\pi\rho \int_0^\infty j_{2q} \frac{d\nu}{h\nu} = n_{2q}, \tag{45}$$

with similar equations for j_P and j_B; in this way we obtain

$$C_{2q} = \frac{h}{4\pi\rho \int_0^\infty \psi(y)\, dy} = \frac{h}{4\pi\rho \times 3.770}, \tag{46}$$

$$C_P = \frac{h}{4\pi\rho Ei(h\nu_P/kT)}, \tag{47}$$

$$C_B = \frac{h}{4\pi\rho Ei(h\nu_B/kT)}, \tag{48}$$

where $Ei(x)$ is the familiar exponential integral.

Lastly, we must determine the ratio of n_{2q}, the number of electrons jumping from 2s to 1s, to n_P, the number of electrons captured on the level $n = 3$. Let n_c be the total number of electrons captured on all levels, excluding the lowest. Then, evidently,

$$\frac{n_{2q}}{n_c} = 2X. \tag{49}$$

The number of electrons captured on the level of total quantum number m may be written, approximately,[17]

$$n_m = \frac{B\beta^2}{m^3} e^{\beta/m^2} Ei \frac{\beta}{m^2}, \tag{50}$$

where β is a constant for all m, and

$$B = \frac{2An_i n_e}{(\pi L)^{1/2}} = \left(\frac{2^{11}k}{3^3\pi m^5}\right)^{1/2} \frac{he^2}{c^3} T^{1/2} n_i n_e, \tag{51}$$

[17] L. Spitzer, Jr., *Ap. J.*, **107**, 6, eq. (14), 1948.

$$\beta = \frac{h\nu_L}{kT} = \frac{158{,}000^\circ}{T}, \tag{52}$$

and ν_L is the frequency at the Lyman limit. For n_e we have

$$n_e = B\beta\phi_2(\beta), \tag{53}$$

where $\phi_2(\beta)$, tabulated by Spitzer,[17] is

$$\phi_2(\beta) = \sum_{m=2}^{\infty} \frac{\beta}{m^3} e^{\beta/m^2} Ei \frac{\beta}{m^2}. \tag{54}$$

The emissivity per gram per unit frequency range in the two-quantum continuum is, if we combine equations (42), (46), (49), and (53),

$$j_{2q} = \frac{Bh\beta^2}{4\pi\rho} \frac{2X\phi_2(\beta)}{3.77\beta} y\psi(y). \tag{55}$$

The recombination emission from captures on level m has emissivity

$$j_m = \frac{Bh\beta^2}{4\pi\rho} \frac{1}{m^3} 10^{-10.169(y-4/3m^2)} \qquad \left(y > \frac{4}{3m^2}\right), \tag{56}$$

where

$$\lambda = \frac{1.216 \times 10^{-5}}{y} \text{ cm}. \tag{57}$$

The quantity θ is the usual reciprocal temperature, $5040^\circ/T$. The ratio j_{2q}/j_3, measuring the relative importance of two-quantum and Paschen emission, is not far from unity at λ 4800 for $X = 0.32$ and $\theta = 0.5$; j_{2q}/j_2 is about 0.03 at the Balmer limit. We define j'_H as the total intensity of the recombination emission continua up to $m = 4$ (eq. [56]). Values of j'_H are given in Table 2; series with $m > 4$ and free-free emission are neglected. The j_{2q} tabulated are obtained for the typical value $X = 0.32$ and can be scaled proportionately. The temperature dependence of the emission is small in units of $Bh\beta^2/4\pi\rho$. (The unit is proportional to $\rho T^{-3/2}$, mass-emission coefficient, and would be proportional to $\rho^2 T^{-3/2}$ per unit volume.) Figure 1 and Table 2 show $\log_{10} j$, the sum of the two sources of emission. Note how the Balmer discontinuity is reduced and how the apparent color temperature varies with frequency. The recombination emission declines quite steeply shortward of each series limit, but the decline is smoothed out by the relatively blue two-quantum continuum. If the electron temperature is derived from the slope just below a series limit, by the use of equations (43) and (44), the resultant value would be higher than the true temperature. Thus, when $\theta = 0.7$, its apparent value from the slope is 0.52 in the range $\lambda\lambda$ 3646–3040 and 0.36 in the range $\lambda\lambda$ 8200–4861; when $\theta = 0.35$ the apparent values are 0.25 and 0.14, respectively. Since the usual determinations of the electron temperature give θ apparently near 0.5, the case of $\theta = 1.00$ is particularly important. Between λ 8200 and λ 6080 the slope corresponds to $\theta = 0.72$; between λ 6080 and λ 4861 the slope corresponds to $\theta = 0.33$, and in the photographic region $\lambda\lambda$ 4861–4050 it corresponds to $\theta = 0.0$; for $\lambda\lambda$ 3646–3040, the usual limit of ultraviolet spectrophotometry, $\theta = 0.74$.

The observational material now available for study is mainly confined to the Balmer emission continuum. T. L. Page[3, 18] finds that the slope of the observed emission for $\lambda < 3646$ corresponds to $7000^\circ < T_e < 10{,}000^\circ$, in general, with only moderate deviations from the older theoretical prediction that j'_ν varies as $\exp(-h\nu/kT)$. This is quite consistent with the results in our Table 2, which show that the two-quantum emission

[18] *M.N.*, 96, 604, 1936.

hardly affects the Balmer emission for $\lambda > 3300$. On the basis of the slight decrease in slope that our results predict, we might suggest that the conventionally deduced electron temperatures are somewhat too high and should be reduced by about 25 per cent. One prediction based on the present analysis is that the electron temperatures deduced from spectrophotometry in the region λλ 6080–4050 should be very much higher than those deduced from either the infrared (Paschen) or ultraviolet (Balmer) emission just shortward of a series limit.

The two-quantum emission reduces the discontinuity at the Balmer limit. From Table 2 we can obtain the predicted ratio of the surface brightness j at λ 4050 to that at λ 3646. This ratio proves rather insensitive to temperature and is equal to 0.23 and 0.09 for $\theta = 0.35$ and $\theta = 1.0$, respectively. Without the two-quantum emission, the ratio would be 0.10–0.01.

It is tempting to interpret the so-called V_c observed by Page[3] in the region λλ 4800–

TABLE 2

THE INTENSITY* OF THE RECOMBINATION EMISSION (j'_H), THE TWO-QUANTUM EMISSION (j_{2q} FOR $X = 0.32$), AND THE TOTAL EMISSION (j)

λ (A)	y	$\theta=0.35$			$\theta=0.50$			$\theta=0.70$			$\theta=1.00$		
		$\log_{10} j'_H$	$\log_{10} j_{2q}$	$\log_{10} j$	$\log_{10} j'_H$	$\log_{10} j_{2q}$	$\log_{10} j$	$\log_{10} j'_H$	$\log_{10} j_{2q}$	$\log_{10} j$	$\log_{10} j'_H$	$\log_{10} j_{2q}$	$\log_{10} j$
8202..	0.148	−1.34	−2.04	−1.26	−1.35	−2.15	−1.29	−1.37	−2.25	−1.32	−1.39	−2.36	−1.35
6080..	.20	−1.52	−1.85	−1.35	−1.61	−1.96	−1.45	−1.74	−2.06	−1.57	−1.92	−2.17	−1.73
4861..	.25	−1.70	−1.72	−1.41	−1.87	−1.82	−1.55	−2.10	−1.92	−1.70	−2.43	−2.04	−1.89
4050..	.30	−1.88	−1.62	−1.43	−2.12	−1.72	−1.58	−2.37	−1.82	−1.71	−2.94	−1.94	−1.89
3646..	.333	−0.88	−1.56	−0.79	−0.88	−1.66	−0.82	−0.90	−1.76	−0.84	−0.90	−1.88	−0.86
3470..	.35	−0.94	−1.53	−0.84	−0.97	−1.64	−0.89	−1.02	−1.74	−0.94	−1.07	−1.85	−1.00
3040..	.40	−1.11	−1.47	−0.95	−1.22	−1.57	−1.06	−1.38	−1.67	−1.20	−1.58	−1.79	−1.37
2700..	.45	−1.31	−1.41	−1.05	−1.48	−1.51	−1.19	−1.73	−1.61	−1.37	−2.09	−1.73	−1.57
2430..	.50	−1.47	−1.36	−1.11	−1.75	−1.47	−1.28	−2.09	−1.57	−1.45	−2.59	−1.68	−1.63
2210..	.55	−1.65	−1.31	−1.15	−2.00	−1.43	−1.32	−2.44	−1.53	−1.47	−3.11	−1.64	−1.63
2020..	0.60	−1.85	−1.29	−1.18	−2.26	−1.39	−1.34	−2.80	−1.49	−1.47	−3.61	−1.61	−1.61

* Emissivities are given in units of $Bh\theta^2/4\pi\rho$.

3900 as the two-quantum emission essentially unaffected by the ordinary Paschen continuum. Unfortunately, his observations were made with a very wide slit and were uncorrected for unresolved weak emission lines. They give a V_c from one-half to one-quarter the Balmer emission. This ratio is very high compared to that predicted for ordinary recombination emission but is consistent with the present theory if $X = 1$. His observations indicate, however, that the V_c is approximately constant per wave-length interval, i.e., slightly decreasing shortward, per $d\nu$, while the Paschen continuum decreases rapidly and the two-quantum emission increases slowly shortward.

P. Swings and O. Struve[19] reproduce spectra showing a strong continuous spectrum in the Orion nebula and in IC 418. The great strength found for the continuum in IC 418, λλ 4900–3700, is quite remarkable. One peculiarity of IC 418 is the relatively low temperature and high corresponding photographic brightness of the central star. The Balmer discontinuity is very small. The Balmer discontinuity is also quite small in the Orion nebula, possibly because of the starlight scattered by interstellar dust grains.[20] The Crab nebula has a strong continuous spectrum, certainly unaffected by scattered starlight.

[19] *Ap. J.*, **96**, 310, 1942.

[20] J. L. Greenstein, *Ap. J.*, **104**, 414, 1946.

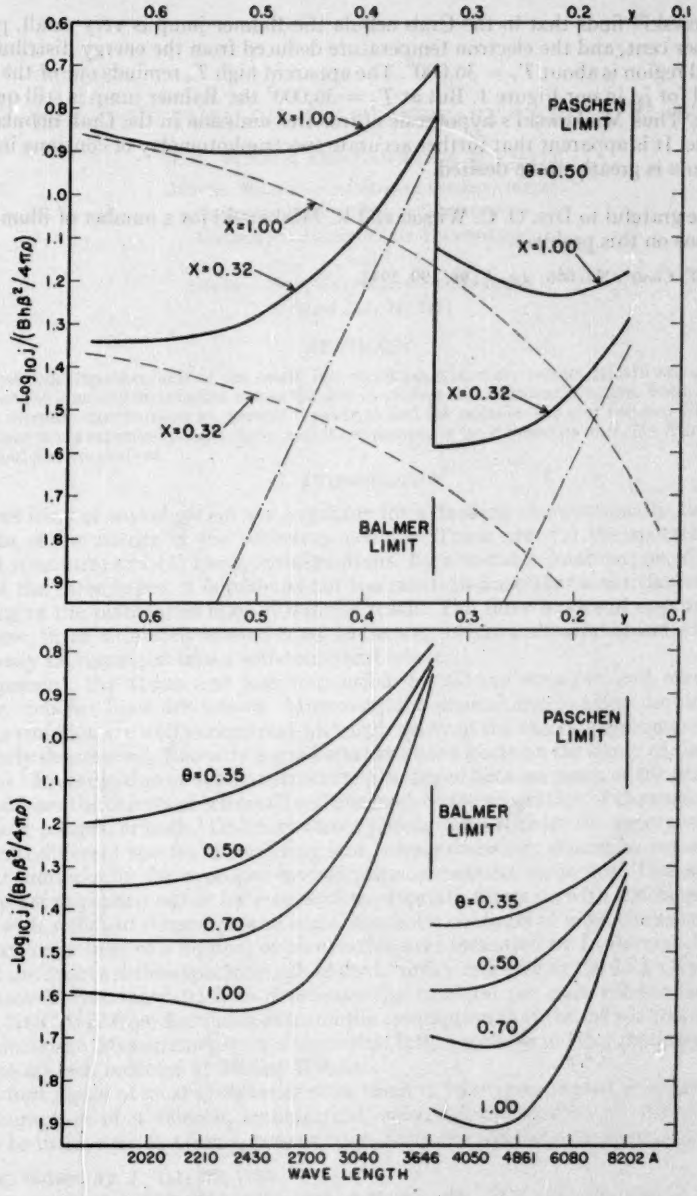

FIG. 1.—*a*, Upper section. Plotted are: the straight lines (*dots and dashes*), representing the hydrogen recombination emission, j'_H; dashed-line curves for the two-quantum emission, j_{2q} when $X = 0.32$ and 1.00; solid-line curves, showing their sum, j, the total hydrogen emission. All are given for electron temperature 10,000°, $\theta = 0.5$. *b*, Lower section. The total emission, j, including two-quantum radiation for $X = 0.32$ at various electron temperatures.

R. Minkowski[21] finds that in the Crab nebula the Balmer jump is very small, perhaps only 15 per cent, and the electron temperature deduced from the energy distribution in the visual region is about $T_e = 36{,}000°$. The apparent high T_e reminds one of the results predicted for j_{2q} in our Figure 1. But at $T_e = 36{,}000°$ the Balmer jump is still quite appreciable. Thus Minkowski's hypothesis of free-free emission in the Crab nebula seems preferable. It is apparent that further accurate spectrophotometry of continua in planetary nebula is greatly to be desired.

We are grateful to Drs. O. C. Wilson and R. Minkowski for a number of illuminating discussions on this problem.

[21] *Mt. W. Contr.*, No. 666; *Ap. J.*, 96, 199, 1942.

THE STRUCTURE OF THE PLANETARY NEBULA IC 418

O. C. WILSON AND LAWRENCE H. ALLER
MOUNT WILSON AND PALOMAR OBSERVATORIES
CARNEGIE INSTITUTION OF WASHINGTON
CALIFORNIA INSTITUTE OF TECHNOLOGY
and
OBSERVATORY, UNIVERSITY OF MICHIGAN
Received July 12, 1951

ABSTRACT

Slitless coudé spectrograms of the small, low-excitation, planetary nebula IC 418 are analyzed to determine the intensity distribution across the disk in various monochromatic images. From an analysis of these intensity distributions an attempt is made to find the emission per unit volume. The emission in ergs/cm³/sec is expressed in c.g.s. units, and the approximate ionic densities of *H*, *He*, *N* II, *O* II, *O* III, *Ne* III, and *S* II are derived.

I. INTRODUCTION

Three lines of investigation are available for attacking observationally the general problem of the nature of the planetary nebulae. These are: (1) the spectra; (2) the spatial structure; and (3) the internal motions. By a suitable combination of sufficient data of the three types, it is perhaps not too much to hope that a satisfactory understanding of the planetaries may ultimately result. The three modes of approach yield, in a sense, three intimately related cross-sections of the same physical object which must eventually be combined into a self-consistent whole.

At present, the atoms and ions responsible for all the stronger, and many of the weaker, nebular lines are known. Moreover, the general mechanisms leading to the nebular emission are well understood, although many of the atomic parameters involved are poorly determined. Recently a good start has been made on the study of the internal motions.[1] Investigation of nebular structure has lagged because much of the earlier work suffered from the defects of too small scale or inadequate separation of the various monochromatic images, or both.[2] Ordinary direct photographs register the superposed effects of several different species of radiating ions, whose emissions should be separated and studied individually for a proper investigation of nebular structure. This separation may be accomplished either by means of appropriate filters or with a slitless spectrograph with sufficient dispersion and scale. Isophotic contours of monochromatic images of the stronger lines of a number of planetaries were measured by L. Berman,[3] who employed the quartz slitless spectrograph of the Crossley reflector at the Lick Observatory. Vorontsov-Velyaminov[4] tried to determine the emission per unit volume for various ions in NGC 6572 from Berman's data, on the assumption that the nebula was spherically symmetrical. Measurements on a somewhat larger scale were later made by Seyfert[5] with the 60-inch reflector at Mount Wilson.

The best plates of most planetaries show them to have complicated structures; hence the assumption of a smooth, symmetrical, spherical distribution of radiating gases cannot be valid, even as a first approximation. Since the nebulae are necessarily observed

[1] O. C. Wilson, *Ap. J.*, **111**, 279, 1950.

[2] H. D. Curtis, *Pub. Lick Obs.*, **13**, 55, 1918; J. H. Reynolds, *M.N.*, **80**, 200, 1919; B. Vorontsov-Velyaminov, *Russ. Astr. J.*, **14**, 194, 1937; B. Vorontsov-Velyaminov and Mrs. O. Cramer, *Russ. Astr. J.*, **14**, 301, 1937; and H. Bucerius, *A.N.*, **244**, 59, 1931.

[3] *Lick Obs. Bull.*, **15**, 86, 1930.

[4] *Zs. f. Ap.*, **12**, 247, 1936.

[5] *Pub. A.S.P.*, **55**, 32, 1943.

in plan, only those which are spherically symmetrical can be utilized to derive true spatial distributions of the radiating matter. Actually, none of the objects is truly symmetrical, and the only recourse is to select the most uniform-appearing and derive the intensity as a function of distance from the center. The method is to make microphotometer tracings across the center, average the two sides, and attempt to obtain the average emission per unit volume for various monochromatic images. Only qualitative results may be expected from this procedure, but they should, nevertheless, provide a more realistic approach to the interpretation of the nebulae than does the assumption of a uniform sphere or shell in which all the radiating atoms are evenly mixed.

For the purpose of deriving radial structure, one of the best prospects is the small, bright, low-excitation planetary IC 418. Although this object is somewhat oval in shape, it appears otherwise very uniform and smooth, with no disturbing fine structure visible in even the best photographs. We have therefore chosen it as a suitable nebula in which to attempt the determination of the distribution of the radiating atoms.

II. THE OBSERVATIONAL DATA

In this paper, and others, our intention is to carry the study of the structural features of the planetaries as far as possible with the best modern equipment and methods. A motor-driven image-rotating prism of fused quartz has recently been added to the coudé spectrograph at Mount Wilson to counteract the normal image rotation during exposure. Slitless spectrograms of a number of planetary nebulae have been obtained with this equipment, and detailed photometric measures are in progress. Some results for NGC 7662 and 6572 have already been briefly reported.[6]

The slitless spectrograms on which this study is based were obtained with the 32-inch camera of the coudé spectrograph at the 100-inch telescope, with the image rotator adjusted to make the major axis of the nebula perpendicular to the dispersion.[7] Five exposures, ranging from 4 to 120 minutes, were made on a single plate during a period of good seeing. Guiding was accomplished by means of a hinged mirror, as previously described,[1] and photometric standards were impressed on another plate from the same box by means of the same spectrograph equipped with step slits.

Figure 1 shows a number of monochromatic images of IC 418, with comparable densities, chosen from the various exposures. Note the inner condensation in [*O* III] and the outer ring present in all the images except those of [*Ne* III] and probably [*O* III]. The ring is prominent in *H*, [*S* II], [*O* II], and [*N* II], while the [*Ne* III] image appears comparable in size to the inner condensation of [*O* III].

Microphotometer tracings were made across the nebular images perpendicular to the dispersion and also across the star spectrum close to the images. The tracings were reduced in the usual manner, and the intensity distribution in the nebular images was corrected for the contribution from the nucleus. Finally, it is necessary to correct for guiding error, seeing, and turbidity in the photographic emulsion, all three of which may be combined for the purpose. It is the blurring influence of these effects that causes the star image on the spectrogram to have a finite width. Let $K(s)$ be the relative intensity distribution across the nuclear spectrum, where s is the distance from the center of the image. If $I_0(x)$ is the observed intensity distribution in a nebular image after subtraction of the light of the central star and $I(x)$ is the true distribution, then I_0 and I are related by the integral equation

$$I_0(x) = \int_{-\infty}^{\infty} K(y-x)\, I(y)\, dy, \tag{1}$$

[6] L. H. Aller and O. C. Wilson, *A.J.*, **55**, 70, 1950.

[7] As pointed out to us by R. Minkowski, nonspecular reflection at the grating reduces the image size in the direction of dispersion compared to that in the perpendicular direction. In the Mount Wilson coudé this reduction is about 25 per cent; hence the nebula is considerably less elliptical in shape than it appears in the reproductions.

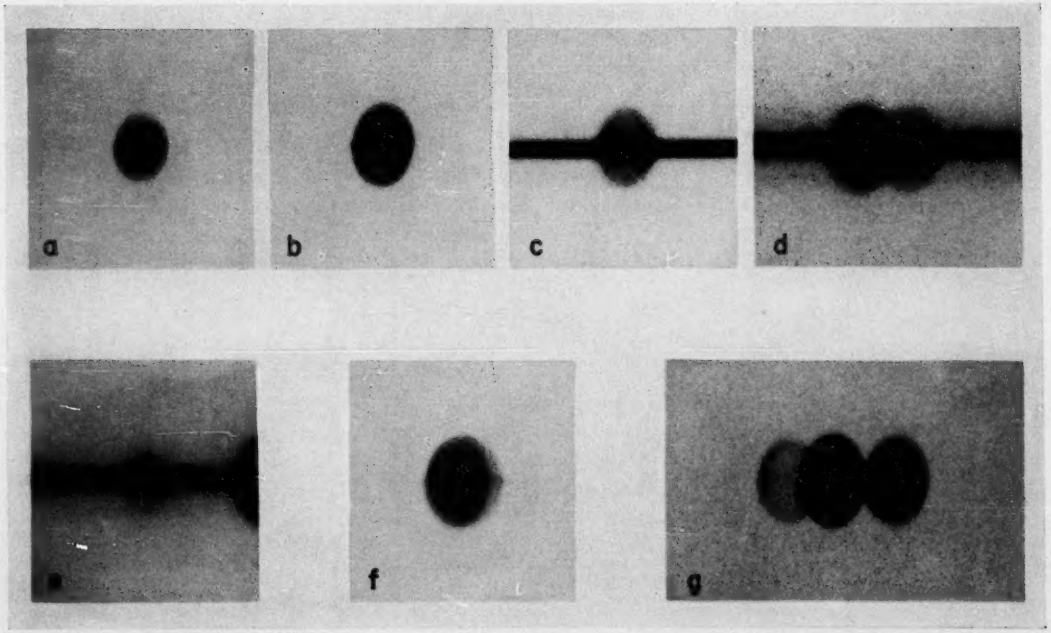

FIG. 1.—Monochromatic images of IC 418. *a*, λ 5007 [*O* III]; *b*, *Hβ*; *c*, λ 4471 *He* I; *d*, λλ 4068–4076 [*S* II]; *e*, λ 3868 [*Ne* III]; *f*, λλ 3726–3728 [*O* II]; *g*, λλ 6543, 6584 [*N* II], with *Hα* in center.

where K is so normalized that

$$\int_{-\infty}^{\infty} I_0(x)\,dx = \int_{-\infty}^{\infty} I(y)\,dy\,. \qquad (2)$$

Equation (1) must be solved by successive approximations, and, if $K(s)$ is narrow compared with $I(y)$, the first approximation is sufficient. This first approximation is obtained by substituting I_0 for I under the integral in equation (1), solving the equation for a new I_0 (call it I_0'), and then adding to the original $I_0(x)$ the amount $I_0 - I_0'$. The result is, of course, that the steep parts of the curve become steeper and the fluctuations are enhanced.

As an example, Figure 2 shows for $H\beta$ the initial cross-section $I_0(x)$, the "diffusing kernel" $K(s)$, and the resulting $I(x)$. The solution is checked by inserting the derived $I(y)$ into equation (1) and comparing the calculated $I_0(x)$ with the observed $I_0(x)$. In

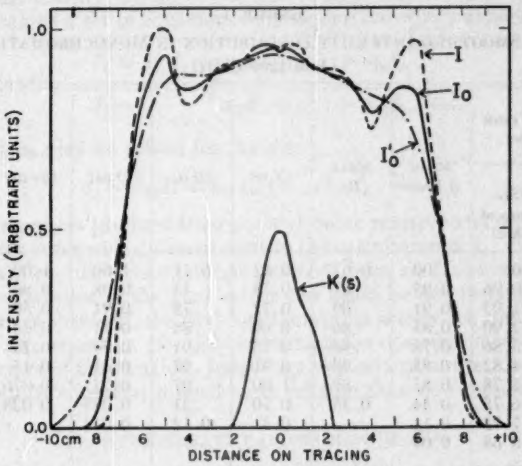

FIG. 2.—Example of correction for seeing, guiding, and turbidity errors. Curves described in text

most instances the agreement is good—better, in fact, than the agreement between successive lines of the Balmer series.

The nebula does not possess perfect spherical symmetry; hence $I(x) \neq I(-x)$, where $x = 0$ is the position of the central star. The two sides are sufficiently similar, however, to justify drawing a mean curve for most images to represent the average radial intensity distribution. Nebular images selected for analysis are: λ 6584, λ 6548 [*N* II]; λ 5007, λ 4959 [*O* III]; λλ 4861, 4340, 4101, 3889, 3835, 3797, 3770 *H;* λ 4471, λ 4026 *He* I; λ 4068 [*S* II]; λ 3868 [*Ne* III]; and λ 3727 [*O* II]. For each of these a mean $I(x)$, corrected for the contribution from the central star and for the effects of seeing and guiding, has been derived. Resultant values of $I(x)$ are given in Table 1, where in each instance the maximum has been arbitrarily set equal to 1.0. It must be emphasized that these results are not of high accuracy. This is especially true of the weaker images, in which the correction for the central star is much larger than the final derived nebular intensity. In this respect a nebula with a relatively fainter nucleus would be more advantageous.

III. THE EMISSION FUNCTION

After the mean intensity distribution $I(x)$ for the various images has been found, the next step is to derive the emission per cubic centimeter, $E(r)$. Theories of nebular line

intensities[8] give the emission per cubic centimeter, and, if $E(r)$ is known, the corresponding densities, $N(r)$, of the various ions may be calculated. For a spherically symmetrical distribution of emitting material, $I(x)$ and $E(r)$ are related by the well-known integral equation,

$$I(x) = 2\int_0^\infty \frac{E(r)\,dr}{\sqrt{r^2 - x^2}}, \tag{3}$$

whose formal solution involves a differentiation of the observed $I(x)$. Since $I(x)$ is subject to observational errors as well as to deviations from the exact values, because of the necessity of averaging both sides of the nebula, such a procedure can introduce large systematic errors. Hence the range in solution of $E(r)$ is such that fairly large variations in this quantity will permit representation of $I(x)$ within the errors of observation. The accuracy with which $E(r)$ may be derived is thus much lower even than the already

TABLE 1

ADOPTED SMOOTHED INTENSITY DISTRIBUTION IN MONOCHROMATIC IMAGES
(Arbitrary Units)

Distance from Nucleus		Mean *H* Lines	Mean *He*	[*N* II]	[*O* II]	[*O* III]	[*Ne* III]	[*S* II]
(Cm on Trace)	(Seconds of Arc)							
0	0	1.00	0.67	0.82	0.71	1.00	1.00	0.72
1	0.96	0.95	.67	0.78	.73	0.98	0.80	.72
2	1.93	0.91	.69	0.72	.78	0.91	0.50	.71
3	2.90	0.83	.86	0.69	.84	0.71	0.34	.71
4	3.86	0.78	.98	0.73	.91	0.54	0.23	.77
5	4.82	0.85	.98	0.91	.97	0.41	0.15	.87
6	5.78	0.85	.87	1.00	.97	0.25	0.076	.99
7	6.75	0.44	0.35	0.70	.51	0.085	0.038	.87
8	7.72	0.14	.....	0.31	0.12	0.034	.....	0.12
9	8.68	0.04	.....	.....	.....	.....	.....	.....

rather low accuracy of the $I(x)$ values from which it is determined. This difficulty is inherent in any process depending upon the solution of equation (3).

In connection with an analogous problem, Chandrasekhar and Münch[9] have proposed the assumption of some plausible analytic form with adjustable parameters for functions of the type $E(r)$, and the determination of the parameters from the moments of $I(x)$. To apply this suggestion, we have assumed a ring structure of the form

$$E(r) = A\,r^a e^{-br}, \tag{4}$$

where A, a, and b are constants to be evaluated and a must be positive for $E(r)$ to remain finite at the center. The nth moment of x is, by definition,

$$\overline{x^n} = \frac{\int_0^\infty I(x)\,x^n dx}{\int_0^\infty I(x)\,dx}. \tag{5}$$

[8] See, e.g., the series of papers entitled "Physical Processes in Gaseous Nebulae," by D. H. Menzel and colleagues. The last paper, *Ap. J.*, **102**, 239, 1945, contains references to the others.

[9] *Ap. J.*, **111**, 142, 1950.

From equations (3) and (4) it may be shown that

$$\overline{x^n}\int_0^\infty I(x)\,dx = A\sqrt{\pi}\,\frac{\Gamma(n+a+2)\,\Gamma([n+1]/2)}{b^{n+a+2}\Gamma([n/2]+1)}. \tag{6}$$

Here A is found from the condition that $\overline{x^0} = 1$, and the constants a and b are evaluated by means of the first and higher moments. Detailed calculation shows the values of A and b to be unstable in most instances, and it appears doubtful that significant results could be obtained by choosing a more complicated functional form for $E(r)$, since the higher moments are poorly defined by the observations.

The method finally used to determine $E(r)$ is that employed by A. Wallenquist[10] for the analogous problem of finding the space distribution of stars in a spherical cluster from star counts made in concentric rings about the center. Consider the nebula as made up of n shells of constant density, $d_1, d_2, \ldots d_n$ and radii $x_1, x_2, \ldots, x_n$. From purely geometrical considerations a set of equations may be derived which express $I(x)$ as a function of the d's:

$$I_1 = a_{11}d_1 + a_{12}d_2 + \ldots + a_{1n}d_n,$$

$$I_2 = \qquad a_{22}d_2 + \ldots + a_{2n}d_n, \text{ etc.}$$

This set of equations may be solved for the d's:

$$d_1 = b_{11}I_1 + b_{12}I_2 + \ldots b_{1n}I_n, \text{ etc.},$$

where the b's are numbers (derived from the a's), some positive and some negative, and thus the various I_k's enter with different signs in the calculation of d_j. Thus in the derivation of $E(r)$ by Wallenquist's method, one proceeds from an $I(x)$-curve to a histogram for $E(r)$, and uncertainties in the $I(x)$ values can again be accentuated in the derived $E(r)$ values. However obtained, the $E(r)$ functions must satisfy the condition that, when they are inserted into equation (3), they reproduce the observed intensity distribution $I(x)$ within the errors of observation. Judged by this criterion, the $E(r)$ histograms obtained by Wallenquist's method proved more reliable than do functions of the form of equation (4).

IV. APPROXIMATE CALIBRATION OF $E(r)$

The derived $E(r)$ values have been placed on a relative scale by the condition that

$$\int E(r)\, r^2 dr$$

for each image be proportional to the intensity of the line integrated over the whole nebula. We have adopted the relative total intensities of the emission lines in IC 418 given in Table 2, basing these values upon visual estimates by Wyse[11] and photometric studies by L. H. Aller.[12] The quantity of physical interest is the emission per unit volume in ergs per second, which could be computed if the distance and total emission of the nebula were known. Since neither of these quantities is known accurately, we must proceed by approximate methods.

There are two methods by which the electron density in a planetary nebula may be estimated. The first is that given by Menzel and Aller,[13] which requires a knowledge of the surface brightness in the Balmer continuum, the apparent size of the nebula and its distance, and the electron temperature, T_e. The electron temperature is derived by comparing the intensity of λ 4363 of [O III] with that of the green nebular lines, and it is further assumed that the nebula is of uniform density and constant T_e throughout. On the other hand, no knowledge of, or assumptions concerning, any properties of the nuclear star are necessary.

[10] *Upsala Medd.*, No. 65, 1936.
[11] *Ap. J.*, **95**, 356, 1942.
[12] *Ap. J.*, **93**, 236, 1941.
[13] *Ap. J.*, **93**, 195, 1941.

A second means for estimating the electron density is provided by applying the methods developed by B. Strömgren[14] for the study of interstellar hydrogen. Here it is assumed that the relatively sharp outer boundary of a nebula such as IC 418 represents the zone where the ionization of hydrogen falls rapidly toward zero because of exhaustion of the ionizing radiation from the nucleus. This method, which has recently been utilized in a study of the planetary nebulae by Page and Greenstein,[15] also requires, in its simplest form, the assumption that density and electron temperature are uniform throughout the nebula. As in the procedure of Menzel and Aller, a knowledge of the apparent size and distance of the nebula is required, but, in addition, the surface temperature and radius of the central star must also be known. Strömgren has shown that the outer boundary,

TABLE 2

ADOPTED TOTAL RELATIVE INTENSITIES

λ	El.	Int.	λ	El.	Int.
6584	[*N* II]	24.0	4101.....	*Hδ*	2.4
6548.....		11.0	4068.....	[*S* II]	0.21
5007	[O III]	13.9	4026.....	*He* I	0.11
4959.....		5.0	3889.....	*H*	1.26
4861.....	*Hβ*	10.0	3869.....	[*Ne* III]	0.3
4471.....	*He* I	0.4	3835.....	*H*	0.64
4340.....	*Hγ*	4.5	3727.....	[*O* II]	15.7

S_0, of the ionized region in a mass of hydrogen of uniform density is given by the expression,

$$1 = 3.08 \times 10^{18} \frac{a_\nu}{C_1} \int_0^{S_0} N_e^2 S^2 d\,s\,,$$

where S is the distance from the central star in parsecs, N_e is the number of electrons per cubic centimeter, and a_ν is the absorption coefficient at the limit of the Lyman series, 6.3×10^{-18}. The quantity C_1 is defined by

$$\log C_1 = \left(-0.51 - \frac{5040\,I}{T}\right) + \log\sqrt{\frac{T_e}{T}} + \tfrac{3}{2}\log T + 2\log\frac{R}{R_\odot},$$

where T and R are temperature and radius of the central star, $R_\odot$ is the solar radius, and I is the ionization potential of hydrogen.

It is unlikely that, in a nebula derived from a central star, either of the basic assumptions underlying both the foregoing methods of estimating N_e is correct. Thus the location of the boundary of the Strömgren sphere may depend critically on the run of density and ionization with radius. Moreover, it seems possible to account for bright rings, such as those in IC 418 and many other nebulae, only by supposing that the ring represents either a region of higher total density or one of lowered electron temperature. Nevertheless, for lack of a better means of proceeding, we have applied both methods to IC 418 and find that the resultant estimates of N_e agree within the observational errors.

For both calculations we have taken the distance of IC 418 to be 1800 parsecs, from Berman's[16] results. In applying the Menzel-Aller method, we have used the earlier determinations of intensity in the Balmer continuum,[13] and have followed Page and Greenstein in assuming the radius and temperature of the nucleus to be 3 solar radii and 30,000°, respectively, in making the computation based on Strömgren's theory. Finally,

[14] *Ap. J.*, **89**, 526, 1939.

[15] *Ap. J.*, **114**, 98, 1951.

[16] *Lick Obs. Bull.*, **18**, 57, 1937.

with the general value of N_e established, we can transform our measured $E(r)$ into the density function $N_i(r)$ for hydrogen ions (since it is assumed that $N_i = N_e$) by means of the equation,[17] valid for the intensity of $H\beta$,

$$E(r) = N_i N_e \frac{KZ^4}{T_e^{3/2}} b_4 \frac{g}{2^3} \frac{2hrZ^2}{4^3} e^{X_4}, \tag{7}$$

where $K = 3.26 \times 10^{-6}$, $g = 0.822$, $T_e = 9700°$ K, $b_4 = 0.15$, and

$$X_4 = \frac{1.570 \times 10^5}{16T_e}.$$

The adopted density distribution of hydrogen ions is given in Table 3.

Since all the $E(r)$ functions are known relatively and $E(r)$ for hydrogen is expressible

TABLE 3

ADOPTED DENSITY DISTRIBUTION OF HYDROGEN IONS

Distance from Nucleus		N_i	Distance from Nucleus		N_i
r (Cm on Trace)	r (Seconds of Arc)		r (Cm on Trace)	r (Seconds of Arc)	
0	0	5.9×10^3	5	4.82	3.8×10^3
1	0.96	5.5	6	5.78	6.4
2	1.93	5.1	7	6.75	5.3
3	2.90	4.5	8	7.72	2.8
4	3.86	3.7	9	8.68	0

on an absolute scale, it follows that all the emission functions may now be expressed on an approximate absolute scale also.

V. APPROXIMATE DENSITIES OF VARIOUS IONS

From the $E(r)$ values on an absolute scale given in Table 4, the densities of the various radiating ions in the upper levels of the transitions involved may now be estimated. To derive from these numbers the total densities of the different ions requires, however, additional information. For instance, to estimate the total number of ionized nitrogen atoms from the emission per unit volume of the forbidden lines, we must know the target area for collisional excitation of the $^1D_2$ level. Likewise, to estimate the density of neutral helium from the observed intensity of λ 4471, we must know how the population of the upper level deviates from its value for thermodynamic equilibrium at the given electron temperature. Unfortunately, the basic atomic parameters are poorly determined, and the $E(r)$ values are of only qualitative significance at best; our results, therefore, are highly schematic.

The reductions from $E(r)$ to the concentrations of N II, O II, O III, Ne III, and S II are made with the aid of appropriate formulae[8] for the collisional excitation of forbidden lines. We have assumed the target area parameters, Ω,[18] to be reduced by a factor of 3 for p^2 or p^4 configurations,[19] although the previously adopted Ω values for S II and O II

[17] See, e.g., D.H. Menzel, *Ap. J.*, 85, 333, eq. (9), 1937. For a literal definition of K, see eq. (6).

[18] See M. H. Hebb and D. H. Menzel, *Ap. J.*, 92, 408, 1940, for definition of Ω.

[19] *Ap. J.*, 111, 609, 1950.

have been retained. Since the latter Ω values represent upper limits, the derived densities of singly ionized sulphur and oxygen are lower limits.

Final results are shown in Figure 3, where slight irregularities have been smoothed in drawing the curves. Only the general trends are significant; the details cannot be considered trustworthy. Any revision of the over-all electron density will change the scale of ordinates but not the shapes of the distributions. If, for example, N_e is too large by a factor y, all the $E(r)$ values in Table 4 should be multiplied by $1/y^2$ and the ionic densities of Figure 3 diminished by a factor y, except for *O* II, where the factor appears to be closer to y^2.

The concentrations of *N* II, *S* II, and *O* II in the outer part of the nebula are conspicuous, whereas *Ne* III and *O* III have maximum concentrations at the center. Although

TABLE 4

APPROXIMATE EMISSION IN ERGS/CM³/SEC IN MONOCHROMATIC IMAGES

DISTANCE FROM NUCLEUS							
r (Cm on Trace)	r (Seconds of Arc)	*He* I λ 4026	[*N* II]	[*O* II]	[*O* III]	[*Ne* III]	[*S* II]
0	0	0	2.7×10^{-18}	0	13.8×10^{-18}	2.4×10^{-18}	0.18×10^{-19}
1.0	0.96	0	2.0	0.16×10^{-18}	13.2	1.2	.19
2.0	1.93	0	1.4	0.8	11.3	0.45	.16
3.0	2.90	0.67×10^{-20}	0.7	1.4	9.0	0.24	.11
4.0	3.86	2.2	0.29	2.0	7.2	0.12	.10
5.0	4.82	3.4	1.2	2.7	5.6	0.08	.24
6.0	5.78	5.1	3.8	6.5	4.3	0.06	.50
7.0	6.75	3.6	3.3	4.6	2.9	0.03	.92
8.0	7.72	0	1.6	1.3	1.3	0.01	0.29
9.0	8.68	0	0	0	0	0	0

both *S* II and *N* II are shown to coexist to some extent with *O* III and *Ne* III in the central regions, we do not regard this result as certain. Probably the distributions of *H*, *O* II, *N* II, and *S* II are very similar in the outer shell, and the small differences in our $N(r)$ curves represent the influence of errors of observation. Data on the distribution of *O* I would be of great interest, but these images were rather weak on our series of exposures.

The outer edges of the luminous shells may be sharper than we have pictured them. In any case, they are sharp enough to suggest the rapid decrease of ionization to zero as predicted by Strömgren's theory. This fact, together with the concentration of *O* III toward the center of the nebula, recalls the characteristics of certain interstellar gas clouds observed by Struve and his co-workers. Our results are not inconsistent with the concept of IC 418 as an extensive gas mass, only the inner portion of which is excited and rendered visible by radiation from the nucleus.

VI. DISCUSSION

Have we obtained any real information as to the distribution of mass with radius in IC 418? In our opinion the answer to this question is by no means an unqualified Yes. In the first place, the whole procedure, from original spectrogram to final $N(r)$-curves, is of a type in which errors tend to accumulate and propagate with great fertility. This difficulty is inherent in the problem, and we know of no means of improving the situation other than to strive for increased accuracy at each step. In spite of all this, we

feel that our final results are probably schematically correct in major outline—after all, they resemble closely what is visible to the eye on the original plate. But we are up against a much more formidable difficulty than accumulated errors. Looking at the curves of Figure 3, as they stand, one is forced to the conclusion that hydrogen, which doubtless comprises the bulk of the nebular matter, has a most peculiar radial-density distribution. The curves for the other lines are understandable in terms of a smooth real-density distribution on which are superposed the effect of gradual outward depletion of exciting radiation; hence the particles of higher excitation are observed in the central regions, while the low-excitation particles become more abundant near the periphery. But for hydrogen no such explanation is available; and we must conclude either that the density does indeed vary with distance, as shown in Figure 3, *a*, or that the observed curve represents the combined effects of variable density and variable electron temperature or that the deviations of the distribution from spherical symmetry are seri-

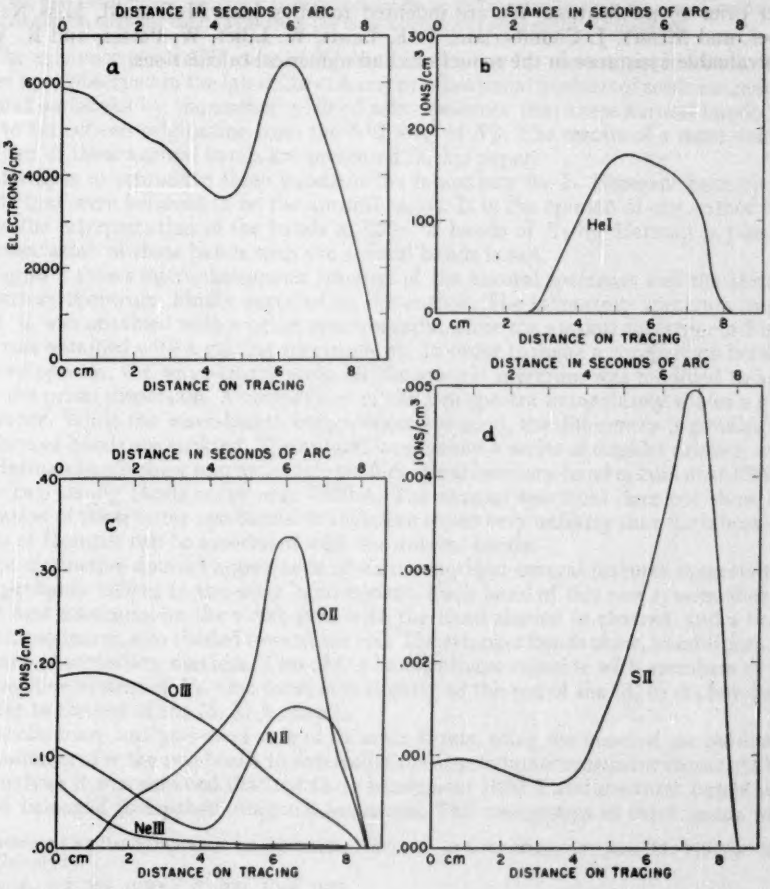

FIG. 3.—Derived mean radial-density distributions. Curve *a* also represents the distribution of hydrogen.

ous. If the electron temperature is variable, its distribution must be known before we can deduce the true mass structure of the nebula, while, if the nebular matter does not have spherical symmetry, no unique solution for $E(r)$ is possible.

Finally, it should be recalled that, of the nebular lines studied in this paper, only those of [*S* II] show a measurable expansion velocity.[1] All the others, including the lines of [*O* II] and [*N* II], are single. This probably means that the [*S* II] lines are produced farther out than those of [*O* II] and [*N* II] and may provide a measure of the hydrogen velocity on the extreme outer fringes of the luminous region. There is some slight evidence from Figure 3 that the [*S* II] maximum occurs a trifle farther out from the nucleus than do the maxima of [*O* II] and [*N* II]. The differences are so small, however, that they may well be due entirely to observational error. Further theoretical discussion will be reserved for a later paper.

Thanks are due Drs. T. L. Page and J. L. Greenstein for allowing us to read their paper prior to publication. We are indebted to Miss Jean McDonald, Miss Nancy Weber, and Messrs. J. Chamberlain, T. E. Lewis, W. Liller, W. Potter, and K. Yoss for invaluable assistance in the reductions and numerical calculations.

THE ANALYSIS OF AURORAL EMISSION BANDS FROM THE $A^2\Pi$ STATE OF N_2^+*

A. B. MEINEL
Yerkes Observatory
Received June 22, 1951

ABSTRACT

A study of the derived molecular constants, possible constituents, band profiles, relative band intensities, and isoelectronic sequence correlations leads to the conclusion that the strong unidentified infrared auroral emission bands arise from the long-missing $A^2\Pi$ level of the N_2^+ molecule.

The existence of an $A^2\Pi$ state of N_2^+ has been known for some time; however, it has never been observed in the laboratory. A recent vibrational analysis of some unidentified auroral emissions by the author[1] yielded some evidence that these auroral bands were due to transitions originating from the $A^2\Pi$ level of N_2^+. The results of a more detailed analysis of these auroral bands are presented in this paper.

Attempts to reproduce these bands in the laboratory by L. Herman[2] have yielded bands that were believed to be the auroral bands. It is the opinion of the author that, while the interpretation of the bands as $^5\Sigma - {}^5\Sigma$ bands of N_2 by Herman is possible, his association of these bands with the auroral bands is not.

Figure 1 shows microphotometer tracings of the auroral spectrum and the Herman laboratory spectrum, kindly supplied to the author. The laboratory spectrum in Figure 1, *a*, was obtained with a prism spectrograph, while the auroral spectrum in Figure 1, *b*, was obtained with a grating spectrograph. In order to make a comparison between the two spectra, the wave-length scale for the auroral spectrum was modified to agree with the prism dispersion. A comparison of the two spectra immediately shows a great difference. While the wave-length coincidences are good, the differences in profiles and numbers of bands are striking. The auroral bands show a series of doublet profiles, while the Herman bands show narrow, single profiles. No laboratory band occurs near 8300 A, while two strong bands occur near 7500 A. The auroral spectrum does not show any indication of these latter two bands. It therefore seems very unlikely that the laboratory bands of Herman can be associated with the auroral bands.

The distinctive doublet appearance of six unidentified auroral features suggests that they probably belong to the same band system. Each band of this new system shows a sharp first maximum on the violet side, with the band shaded to the red, and a broad second maximum, also shaded toward the red. The stronger bands show, in addition, the presence of secondary maxima. Two of the bands almost coincide with members of the first positive system of N_2. One band falls slightly to the red of the (3, 0) N_2 band and another to the red of the (5, 2) N_2 band.

A preliminary analysis was made of these six bands, using the mean of the published wave numbers for the two heads to determine the approximate molecular constants.[3] In this analysis it was assumed that the three bands near 7000 A and the three bands near 8000 A belonged to separate diagonal sequences. The two groups of three bands were

* Presented at the Symposium on Molecular Structure and Spectroscopy, June 11, 1951, at Ohio State University.

[1] *Ap. J.*, **112**, 562, 1950; *C.R.*, **231**, 1049, 1950.

[2] *Proc. Conference on Auroral Physics, London, Ontario*, 1951.

[3] A. B. Meinel, *Ap. J.*, **113**, 583, 1951.

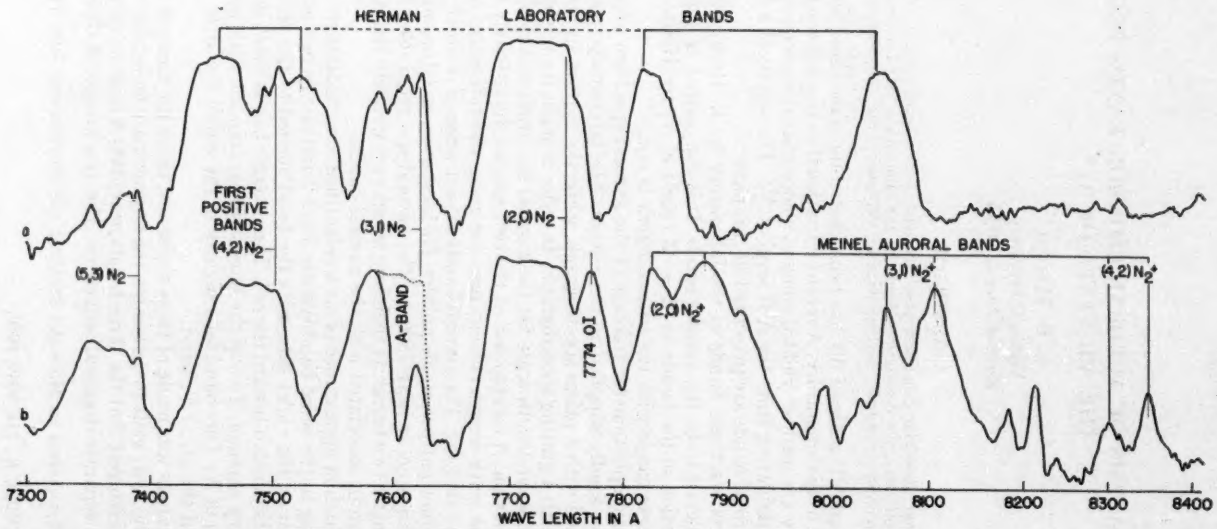

FIG. 1.—Spectrum *a* is a laboratory spectrum by L. Herman (prismatic dispersion). Spectrum *b* is an auroral spectrum by A. B. Meinel (grating dispersion modified to prismatic dispersion).

combined in all possible ways. This procedure provided a large number of values for ω_e' and ω_e'', from which it was necessary to find the real values.

When the manifold of possible ω_e values was obtained, a search was made for coincidences with the numerous molecular constants tabulated by Herzberg.[4] Since there were several cases of coincidences with a known state for a particular molecule, it was necessary to consider what molecules would conceivably be present in the aurora. As a consequence, coincidences with one of the known states of molecules like *GeTe* or *GdO* could be eliminated. After applying this elimination process, one outstanding coincidence remained—a coincidence between a measured ω_e'' of 2205 cm^{-1} and the tabulated value of $\omega_e = 2207$ cm^{-1} for the $X^2\Sigma$ level of N_2^+.

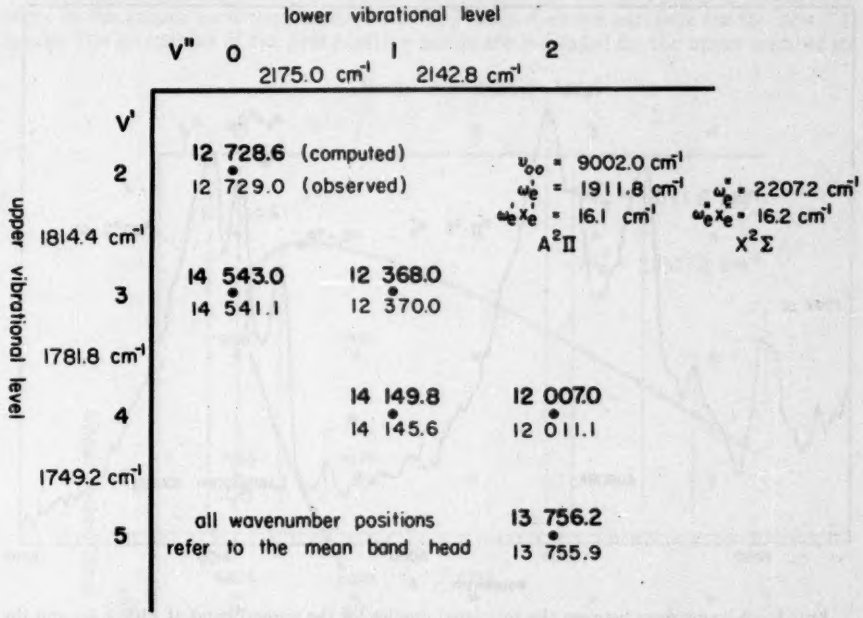

FIG. 2.—A comparison between the observed and the predicted auroral bands and the corresponding vibrational constants. A distance of 10 μ on the photographic plate corresponds to an interval of 4.2 cm^{-1} in this spectral region.

The association of the new band system with N_2^+ is immediately appealing. In the first case, N_2^+ is well known in aurorae, and, secondly, there should exist a low-lying $^2\Pi$ state for this molecule. Assuming that the $X^2\Sigma$ state is the ground state for these auroral bands, the constants for the $^2\Pi$ state were determined to give the best fit to the observed bands. The resulting molecular constants and the comparison of the predicted and observed positions are shown in Figure 2. There appears to be a systematic difference between the observed bands and the computed bands; however, the magnitude of this difference is small enough to be accounted for by the changes in the detailed rotational structure from band to band. It should be emphasized that the molecular constants for the $A^2\Pi$ level are subject to the degree of fit that is desired between the bands at the top and bottom of Figure 2. As a consequence, the value for the position of the (0, 0)

[4] *Spectra of Diatomic Molecules* (2d ed.; New York: D. Van Nostrand Co., Inc., 1950).

band may be in error by as much as 10 cm^{-1}. The assignment of vibrational numbers to the v' levels will be discussed later.

A laboratory study of the $A^2\Pi - X^2\Sigma$ transition of *CN* has provided a third line of evidence for the correctness of the N_2^+ identification. The $A^2\Pi - X^2\Sigma$ bands of *CN* arise from equivalent states in a molecule that is isoelectronic to N_2^+. The (3, 1) *CN* band at 8100 A was observed in the laboratory with the auroral spectrograph and compared directly with the auroral band at 8100 A. Microphotometer tracings of these two bands are shown in Figure 3. Figure 3, *a*, shows the auroral band with the characteristic two strong maxima and two weaker maxima. Comparison with Figure 3, *b*, shows, aside from differences in relative intensity, that the auroral band structure is identical to the *CN*

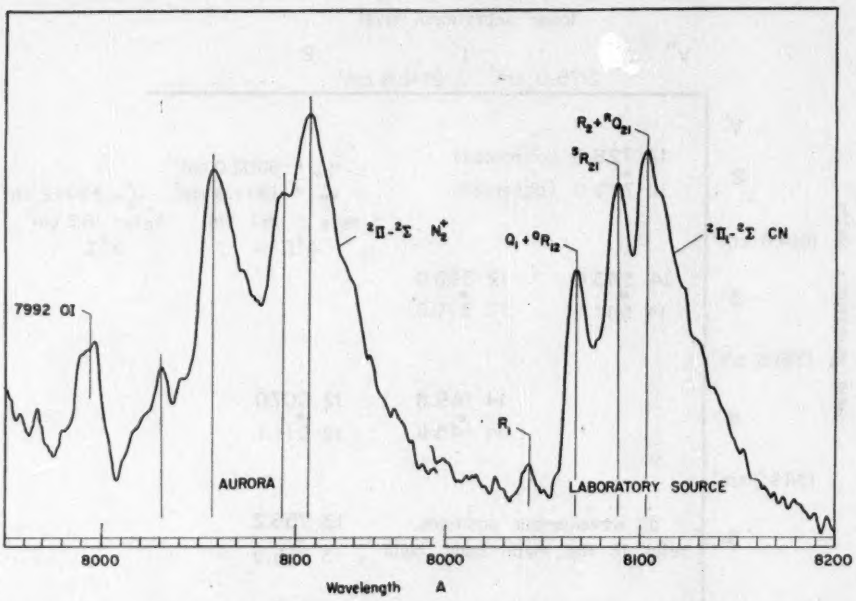

FIG. 3.—A comparison between the rotational profiles for the auroral band at 8100 A (*a*) and the 8100 A *CN* band observed in the laboratory (*b*).

band structure and, therefore, completely compatible with the proposed $A^2\Pi - X^2\Sigma$ transition.

Another important piece of evidence for the N_2^+ identification is provided by the splitting of each auroral band into two distinct heads, which would be associated with the $^2\Pi$ electronic doublet separation. Although the electronic doublet separation cannot be obtained accurately until a complete rotational analysis has been made, a rough estimate can be obtained from the separation of the main or the secondary heads. According to Mulliken,[5] the doublet separation for any $^2\Pi$ state is exactly A; likewise, the over-all triplet separation for a $^3\Pi$ state is A. As a consequence, one would predict about the same A value for the N_2^+ $^2\Pi$ level as for the $^3\Pi$ level in N_2, similar to the case for CO^+ and CO.[6] For N_2 the observed A value from the $^3\Pi$ states is 80 cm^{-1}, while the observed splitting for the auroral bands is 75 cm^{-1}. The value of 75 cm^{-1} should be reasonably

[5] *Rev. Mod. Phys.*, **4**, 1, 1932.

[6] R. S. Mulliken, private communication.

near the true A value, since the observed splitting for CN in Figure 3 is 52 cm^{-1}, which agrees with the true electronic splitting of 52 cm^{-1}.

A fifth independent set of evidence for the N^+ identification is presented by the relative band intensities. Figure 4 shows the table of the observed auroral bands and their intensities when arranged according to the relative positions appropriate to the set of constants that coincide with N_2^+. Using the intensities previously published by the author,[4] it is possible to draw the Franck-Condon parabola with reasonable accuracy. This procedure immediately indicates the most likely vibrational numbering of the v' states and the position of the (0, 0) band. It should be noted that the v' number is now increased by one unit over the numbering originally proposed by the author.

The Franck-Condon parabola was also determined for the first positive bands that occur in the aurora for a comparison with the Franck-Condon parabola for the new N_2^+ bands. The intensities of the first positive bands are indicated by the upper number in

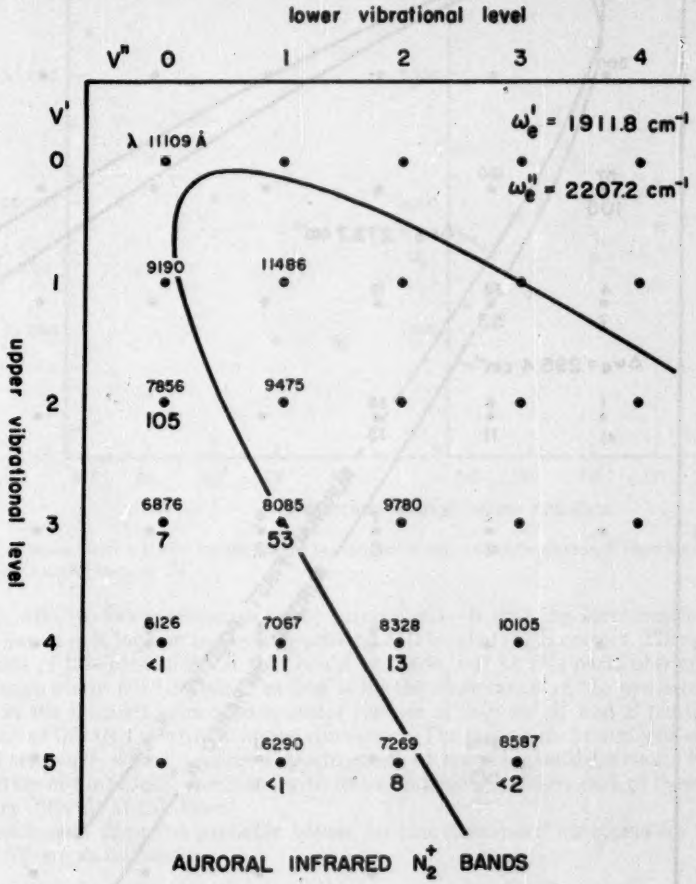

FIG. 4.—Positions and intensities of the infrared auroral N_2^+ bands, showing the most probable numbering for the upper vibrational levels.

Figure 5, and the N_2^+ bands by the lower number. Since the degree of "openness" of the parabola is directly proportional to the difference between the vibrational constants for the upper and lower states, we can again check the N_2^+ identification. For the first positive bands the quantity $\omega_e'' - \omega_e' = 273.7$ cm^{-1}, while the difference between the values obtained from the vibrational analysis of the auroral bands is 295.4 cm^{-1}. As a

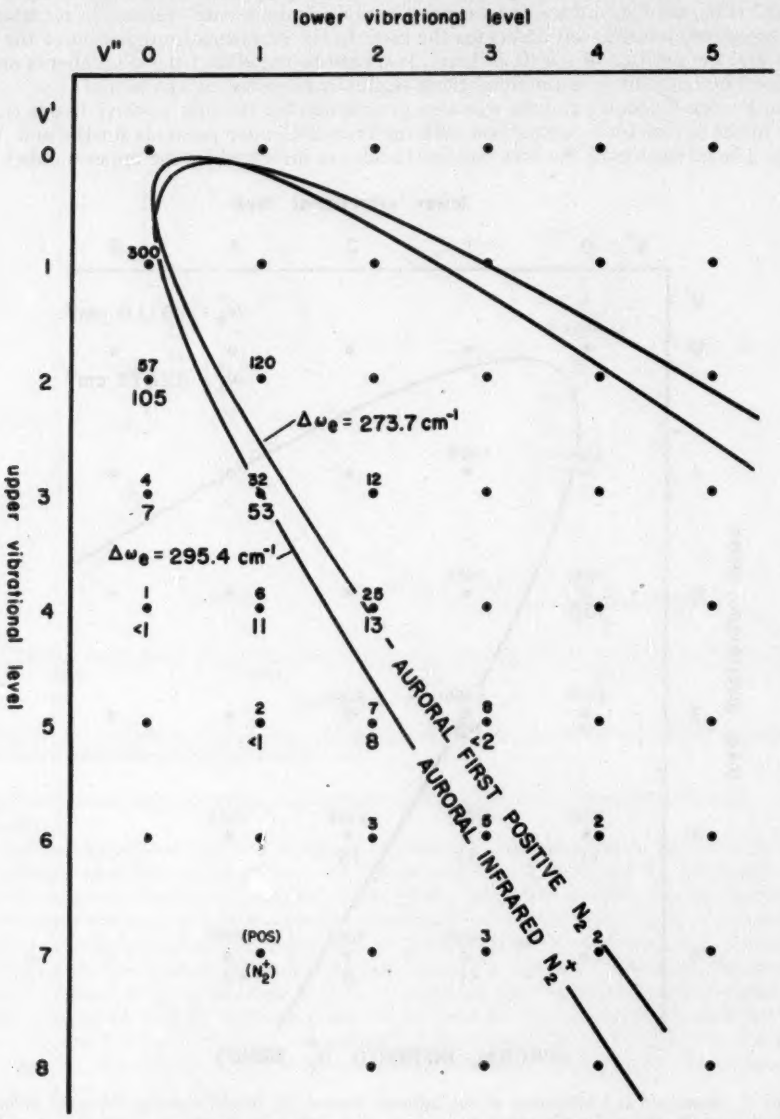

FIG. 5.—A comparison of the Franck-Condon parabolas based on the observed intensities for the first positive bands of N_2 and $A^3\Pi - X^2\Sigma$ bands of N_2^+.

consequence, the N_2^+ Franck-Condon parabola should be more "open" than for the first positive bands, which is in complete agreement with Figure 5.

A sixth and final independent set of evidence for the N_2^+ identification is presented by considering the derived constants for the $A^2\Pi$ state of N_2^+ with the constants for the other isoelectronic molecules. The values of ω_e and $\nu_{0,0}$ for the 13-electron molecules *BeF*, *BO*, CO^+, *CN*, and N_2^+ are plotted in Figure 6 for the $A^2\Pi$ level and ω_e for the $B^2\Sigma$ level. The derived values for N_2^+ are shown by the encircled dots. It is quite apparent that the derived values fit well into the isoelectronic sequence.

The conclusion that is rendered by each of the six considerations—(1) molecular constants, (2) possible constituents, (3) band profiles, (4) doublet splitting, (5) band intensities, and (6) isoelectronic sequence correlations—is that the identification of the auroral bands as being due to the long-missing $A^2\Pi$ level of N_2^+ is correct. There are two more tests of this identification that could be made; but at this particular time both are instrumentally not feasible. The first is by the observation of the predicted bands farther in the infrared, which necessitates the use of infrared *M* and *Z* photographic emulsions or infrared electronic image converters. The second is the analysis of the rotational structure, which requires a spectrograph of much higher dispersion. The transient nature of the aurora, combined with its low intensity, renders each of these further tests very difficult at this time.

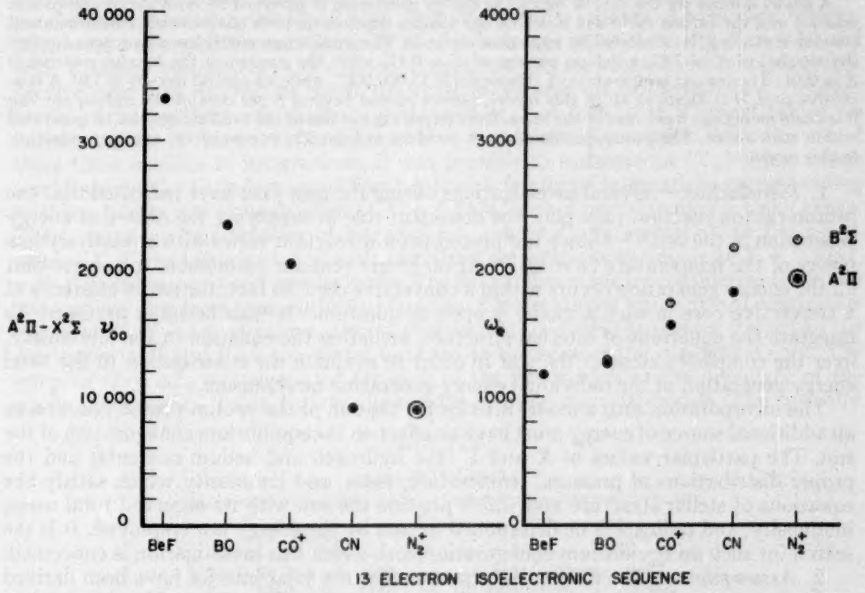

FIG. 6.—Molecular constants for the 13-electron isoelectronic molecular sequence, showing the values derived for the $A^2\Pi$ state of N_2^+.

In conclusion, the most probable values for the vibrational constants for the $A^2\Pi$ level of N_2^+ are as follows:

$$\omega_e = 1911.8 \text{ cm}^{-1}, \qquad \omega_e\chi_e = 16.1 \text{ cm}^{-1},$$
$$\nu_{0,0} = 9002 \text{ cm}^{-1} \pm 10 \text{ cm}^{-1}, \qquad A = -75 \text{ cm}^{-1}.$$

A TWO-ENERGY SOURCE SOLAR MODEL

I. EPSTEIN
Rutherfurd Observatory, Columbia University
Received April 11, 1951

ABSTRACT

A model interior for the sun, in which the energy generation is governed by both the proton-proton reaction and the carbon cycle and in which the opacity depends on both photoelectric ionizations and electron scattering, is calculated by numerical methods. The equilibrium model has a hydrogen content (by weight) of $X = 0.82$, a helium content of $Y = 0.17$, while the content of the heavier material is $Z = 0.01$. The central temperature of this model is 15,000,000°, while its central density is 150. A convective core, if it exists at all in this model, cannot extend beyond 8 per cent of the radius, nor can it include more than 5 per cent of the mass. Only 30 per cent or less of the total energy can be generated within such a core. The proton-proton reaction provides at least 95 per cent of the energy production in this model.

1. *Introduction.*—Several investigations during the past year have indicated that the proton-proton reaction may play the dominant role in supplying the source of energy generation in the sun.[1, 2, 3] Since the proton-proton reaction varies with a relatively low power of the temperature ($\epsilon = \epsilon_0 \rho T^4$), it no longer remains permissible to assume that all the energy generation occurs within a convective core. In fact, the entire existence of a convective core in such a model is open to question.[4] It thus becomes necessary to integrate the equations of internal structure, including the equation in the luminosity, over the complete extent of the star in order to evaluate the contribution to the total energy generation of the individual energy-generating mechanisms.

The incorporation into a model interior for the sun of the proton-proton reaction as an additional source of energy must have an effect on the equilibrium configuration of the sun. The particular values of X and Y (the hydrogen and helium contents) and the proper distributions of pressure, temperature, mass, and luminosity which satisfy the equations of stellar structure and which provide the sun with its observed total mass, luminosity, and radius will be determined in part by the energy law employed. It is the search for such an equilibrium configuration with which this investigation is concerned.

2. *Assumptions.*—The differential equations for the solar interior have been derived under the assumptions that the material is homogeneous (of constant molecular weight), that the perfect gas laws are valid throughout, and that the contribution of radiation pressure to the total pressure is negligible. Further, it was assumed that elements of the carbon-nitrogen group constitute one-quarter of the total heavy material by weight; that is, that $\alpha = \frac{1}{4}(1 - X - Y)$.

Energy-generation rates ϵ_p and ϵ_c for the proton-proton and carbon cycle were taken from previous investigations.[1, 2] In the proton-proton reaction it was assumed that all He^3 nuclei combine with alpha particles rather than with other He^3 nuclei. It appears, however, that the $He^3 + He^3$ reaction is actually the correct one.[5] This would require a reduction in the value of ϵ_p by a factor of 2. This latest modification in the proton-proton reaction has not been included in this investigation.

For the opacity arising from photoelectric ionizations, guillotine factors correspond-

[1] L. H. Aller, *Ap. J.*, **111**, 173, 1950.
[2] I. Epstein, *Ap. J.*, **112**, 207, 1950.
[3] J. B. Oke, *J.R.A.S. Canada*, **44**, 135, 1950.
[4] T. G. Cowling, *M.N.*, **98**, 528, 1938.
[5] W. A. Fowler, *Phys. Rev.*, **81**, 655, 1951 (Paper G5), and unpublished note by D. E. Osterbrock.

ing to a heavy composition of 60 per cent oxygen and 40 per cent Russell mixture were taken from Mrs. M. H. Harrison's tables.[6] Three empirical formulas were used to represent the guillotine factor over three ranges of temperature. Electron scattering was also included in the total opacity, which was taken to equal the sum of the larger contributor (photoelectric ionizations) plus 1.5 times that of the smaller (electron scattering).[7]

The differential equations for the solar interior are given in the appendix, along with the necessary definitions and the expressions used for the energy generation and opacity.

3. *Method of investigation.*—With the differential equations given in the appendix and the observed mass, luminosity, and radius of the sun, starting values of the dependent variables were developed near the surface, and a number of numerical integrations were performed inward. A family of solutions was integrated with $X = 0.80$ and with Y taking on various values. Each integration was terminated either when a convective core was reached or when the solution became an isothermal one. Another family of integrations was similarly performed at $X = 0.88$, with Y again taking on various values. A third set was done at $Y = 0$ and with X variable. With the use of these three families of integrations, it was possible to estimate an (X, Y)-pair which would satisfy the boundary conditions. A fourth family of integrations corresponding to this estimate was accomplished at $X = 0.8474$, with Y variable over a small range. Then, using all four families of integrations, a second approximation to the eigenvalues (X, Y) was obtained, and a fifth family of integrations was made at $X = 0.8231$, with Y variable over a still smaller range. The final fit was made by considering those five integrations (one from each of the five families of integrations) which gave a continuous march of $M(r)$—and, of course, also of $P(r)$ and $T(r)$—from the surface inward to the convective core and from the center outward to the edge of the convective core. The jump in $L(r)$, ΔL, was computed for each of the five models at the boundary of the convective core, r_f. Table 1 gives the results of these mass-fit models. The quantity

TABLE 1

MASS-FIT MODELS

(X, Y)-Pair	ΔL	$\log r_f$
$X=0.9979$ $Y=0.0000$	-1.640×10^{33}	9.87
$X=.8800$ $Y=.1146$	-1.002×10^{33}	9.83
$X=.8474$ $Y=.1453$	-0.565×10^{33}	9.78
$X=.8231$ $Y=.1675$	-0.078×10^{33}	9.68
$X=0.8000$ $Y=0.1875$	$+0.789\times10^{33}$	9.47

ΔL was then plotted against X and Y separately to give the eigen-values X_0 and Y_0 for which ΔM and ΔL both vanished at the boundary of the convective core. These values were $X_0 = 0.8201$ and $Y_0 = 0.1702$ and represent the hydrogen and helium contents, respectively.

This procedure was also reversed, and the solutions characterized by $\Delta L = 0$ were used to compute corresponding ΔM values, which were plotted against X and Y. The eigen-parameters of the composition X_0 and Y_0 corresponding to $\Delta M = 0$ were in complete agreement with those values derived in the alternative method described above.

The logarithms of the distributions of P, T, M_r, L_r, and ρ, corresponding to the eigen-

[6] *Ap. J.*, **108**, 310, 1948.

[7] S. Chandrasekhar, *An Introduction to the Study of Stellar Structure* (Chicago: University of Chicago Press, 1939), p. 271.

compositions $X_0 = 0.82$, $Y_0 = 0.17$, and $Z_0 = 0.01$, were then obtained by interpolation and are given in Table 2, in which

$$U = \frac{d\,(\log M_r)}{d\,(\log r)}, \qquad V = -\frac{d\,(\log P)}{d\,(\log r)}, \qquad (n+1) = \frac{d\,(\log P)}{d\,(\log T)}.$$

4. *Solution.*—The adopted solution (Table 2) is an interpolated one, corresponding to a hydrogen and helium abundance of $X = 0.8231$ and $Y = 0.1674$, and not to the equilibrium values $X_0 = 0.8201$ and $Y_0 = 0.1702$. It is therefore not surprising that all continuity conditions are not precisely met. The best compromise can be made by introducing a convective core, not when $(n + 1)$ drops to 2.50, but at $(n + 1) = 2.91$. This discrepancy would presumably disappear if an actual integration were to be performed with the eigen-values X_0 and Y_0. However, for present purposes, the approximations made in the assumptions do not warrant such a refinement.

TABLE 2

A. ADOPTED SOLUTION FOR THE RADIATIVE ENVELOPE OF THE SUN

log r	log P	log T	log M_r	log L_r	log ρ	U	V	$(n+1)$	log ϵ_p/ϵ_c	log κ_i/κ_e*
10.78.....	11.24	5.68	33.30	33.58	−2.61	0.00	31.16	4.12	.....	1.26
10.74.....	12.22	5.92	33.30	33.58	−1.87	0.01	19.78	4.14	.....	1.23
10.70.....	12.90	6.08	33.30	33.58	−1.35	0.04	14.82	4.13	.....	1.20
10.66.....	13.43	6.21	33.30	33.58	−0.95	0.07	12.02	4.13	.....	1.18
10.62.....	13.87	6.32	33.29	33.58	−0.61	0.11	10.22	4.13	.....	1.16
10.58.....	14.26	6.41	33.28	33.58	−0.32	0.17	8.92	4.11	.....	1.15
10.54.....	14.59	6.49	33.28	33.58	−0.07	0.24	7.95	4.09	.....	1.13
10.50.....	14.89	6.57	33.27	33.58	0.16	0.31	7.17	4.06	.....	1.12
10.46.....	15.17	6.64	33.25	33.58	0.37	0.39	6.52	9.49	.....	1.10
10.42.....	15.42	6.67	33.23	33.58	0.59	0.52	6.35	6.56	.....	0.70
10.38.....	15.67	6.71	33.21	33.58	0.80	0.67	5.99	5.45	.....	0.67
10.34.....	15.90	6.76	33.18	33.58	0.98	0.83	5.53	4.97	.....	0.62
10.30.....	16.12	6.80	33.14	33.58	1.15	1.01	5.04	4.71	.....	0.56
10.26.....	16.31	6.84	33.10	33.58	1.30	1.20	4.53	4.51	.....	0.49
10.22.....	16.48	6.88	33.05	33.57	1.43	1.39	4.03	4.33	.....	0.43
10.18.....	16.63	6.92	32.99	33.57	1.55	1.58	3.55	4.16	.....	0.36
10.14.....	16.76	6.95	32.92	33.56	1.65	1.77	3.10	3.99	.....	0.30
10.10.....	16.88	6.98	32.85	33.54	1.73	1.94	2.67	3.83	.....	0.24
10.06.....	16.98	7.00	32.77	33.52	1.81	2.09	2.29	3.67	>4.00	0.19
10.02.....	17.06	7.03	32.68	33.49	1.87	2.23	1.95	3.53	3.69	0.13
9.98.....	17.13	7.05	32.59	33.46	1.92	2.35	1.65	3.69	3.35	0.08
9.94.....	17.19	7.06	32.49	33.41	1.96	2.46	1.40	3.46	3.08	−0.01
9.90.....	17.24	7.08	32.39	33.36	2.00	2.55	1.17	3.29	2.84	−0.04
9.86.....	17.29	7.09	32.29	33.29	2.03	2.64	0.98	3.15	2.63	−0.06
9.82.....	17.32	7.10	32.18	33.22	2.05	2.70	0.82	3.06	2.44	−0.09
9.78.....	17.35	7.11	32.07	33.14	2.07	2.76	0.68	2.97	2.28	−0.11
9.74.....	17.38	7.12	31.96	33.05	2.09	2.81	0.57	2.91	2.15	−0.12

* In the column headed "log κ_i/κ_e," κ_e is not the electron scattering itself but 1.5 times this value, which is the quantity used in computing the total opacity. Thus κ_i (the opacity arising from photoelectric ionizations) exceeds the electron-scattering opacity (two-thirds of κ_e) throughout the entire radiative envelope.

B. VALUES AT CENTER OF CONVECTIVE CORE ATTACHED TO RADIATIVE ENVELOPE AT log r_f = 9.74

log P_c	log T_c	log ρ_c	U	V	$(n+1)$	log ϵ_p/ϵ_c	log κ_i/κ_e
17.50	7.17	2.16	3.00	0.00	2.50	1.37	−0.23

The exact extent of the convective core is rather indeterminate; however, definite upper limits may be given for it. From the analysis of all integrations performed, it appears that a convective core could not extend beyond $\log r_f = 9.74$, corresponding to 8 per cent of the sun's radius. Such a core could not contain more than 5 per cent of the sun's mass or generate more than 30 per cent of its energy.

A discontinuity occurs in the polytropic index at $\log r = 10.46$. This is due to the analytic approximations used for the guillotine factor. The first two expressions, κ_i(I) and κ_i(II) in the appendix were forced to be continuous at an assumed (P, T)-pair. In actual practice it is more feasible to change the opacity formula at a fixed $\log r$ rather than at a fixed (P, T)-pair. The $\log r$ value chosen here for the change did, however, not turn out to lie close the (P, T)-pair at which κ_i(I) and κ_i(II) are continuous, and thus the jump in the polytropic index was caused. It would be necessary, in principle, to know the pressure and temperature distributions beforehand in order to get a perfectly continuous variation of the guillotine factor across the place where the switch in formulas is made. There is no appreciable discontinuity in the polytropic index on changing from κ_i(II) to κ_i(III) at $\log r = 9.98$.

5. *Summary.*—Under the assumptions made above, the model of the solar interior derived in this investigation differs in several important details from earlier models. First, incorporation of the proton-proton reaction as an energy-producing mechanism serves to lower the central temperature of the sun to about 14.9 million degrees as compared with 19.8 million degrees in M. Schwarzschild's Russell mixture model[8] and with 18.9 million degrees in G. Keller's intermediate model.[9]

Furthermore, it is found that the proton-proton reaction is responsible for well over 95 per cent of the total energy generation. Even at the solar center, the proton-proton reaction outweighs the carbon cycle in its energy-producing properties by a factor of 23. Also, because of the much lower temperature dependence of the energy generation, the convective core is reduced to negligible size.

On the other hand, the central density and the density distribution as a whole may be fairly well represented by a polytrope of index $n = 3.3$, not differing greatly from the density distributions of the Russell mixture model ($n = 3.5$) or of the intermediate model ($n = 3.7$).

The incorporation of electron scattering in the present model has proved to be of some importance. Within the regions in radiative equilibrium near the center of the sun, the opacity arising from electron scattering is approximately equal to that arising from photoelectric ionizations.

Finally, the ratio of the hydrogen to helium abundances (by weight) has increased from a value of 47:41 in the Russell mixture model and a value of 67:29 in the intermediate model to the value 82:17 in the present two-energy source model.

The author again takes pleasure in expressing his gratitude to Professor Martin Schwarzschild for many helpful discussions concerning this investigation. Also, it is a pleasure to thank Professor Bengt Strömgren for his interest in this investigation. Finally, I wish to record my indebtedness to the Princeton University Observatory for a research grant given to me during the summer of 1950, during which time much of this investigation was carried out.

APPENDIX

1. Definitions:

$$x = \log r$$

$$\sigma = \log P\,, \qquad \tau = \log T\,, \qquad \nu = \log M_r\,, \qquad \lambda = \log L_r\,:$$

$$\eta = \log \epsilon = \log (\epsilon_p + \epsilon_c)\,; \qquad \theta = \log \kappa = \log (\kappa_i + \kappa_e)\,.$$

[8] *Ap. J.*, **104**, 203, 1946.

[9] *Ap. J.*, **108**, 347, 1948.

2. Differential equations for radiative regions: $(d\sigma/d\tau) > 2.5$

$$\log\left(-\frac{d\sigma}{dx}\right) = \log\left(\frac{G\mu H}{k}\right) - \tau + \nu - x;$$

$$\log\left(-\frac{d\tau}{dx}\right) = \log\left(\frac{3}{16\pi a c}\frac{\mu H}{k}\right) + \sigma - 5\tau + \lambda + \theta - x;$$

$$\log\left(\frac{d\nu}{dx}\right) = \log\left(\frac{4\pi\mu H}{k}\right) + \sigma - \tau - \nu + 3x;$$

$$\log\left(\frac{d\lambda}{dx}\right) = \log\left(\frac{4\pi\mu H}{k}\right) + \sigma - \tau - \lambda + \eta + 3x.$$

3. Expressions for the energy generation:

$$\log \epsilon_p = \log\left\{\frac{1.91}{100}\left(\frac{X}{0.316}\right)^2\left(\frac{1}{15\times 10^6}\right)^4\left(\frac{\mu H}{k}\right)\right\} + \sigma + 3\tau;$$

$$\log \epsilon_c = \log\left\{1.0\times 10^{-143}\left(\frac{\mu H}{k}\right) X\mathfrak{a}\right\} + \sigma + 19\tau;$$

$\eta = \log(\epsilon_p + \epsilon_c)$ by addition logarithms;

$\mathfrak{a} = \frac{1}{4}(1 - X - Y) = \frac{1}{4}Z$.

4. Expressions for the opacity:

(I) $x \geqslant 10.46$:

$$\log \kappa_i = 23.8061 + (0.988)\sigma - (4.241)\tau + (0.988)\times\log\left\{\left(\frac{\mu H}{k}\right)(1+X)\right\} + \log(1 - X - Y);$$

(II) $10.46 > x \geqslant 9.98$:

$$\log \kappa_i = 28.5950 + (0.680)\sigma - (4.689)\tau + (0.680)\times\log\left\{\left(\frac{\mu H}{k}\right)(1+X)\right\} + \log(1 - X - Y);$$

(III) $x < 9.98$:

$$\log \kappa_i = 21.3011 + (0.490)\sigma - (3.415)\tau + (0.490)\times\log\left\{\left(\frac{\mu H}{k}\right)(1+X)\right\} + \log(1 - X - Y).$$

In all cases,

$$\log \kappa_e = \log\{(1.5)(0.19)(1+X)\};$$

$\theta = \log(\kappa_i + \kappa_e)$ by addition logarithms.

5. Test for radiative equilibrium:

$$\frac{d(\log P)}{d(\log T)} = \frac{d\sigma}{d\tau} > 2.5;$$

$$\log\frac{d\sigma}{d\tau} = -9.5959 + 4\tau + \nu - \lambda - \sigma - \theta.$$

ON THE INTENSITY OF *Ti* LINES AT DIFFERENT POINTS OF THE SUN'S RADIUS

V. BAROCAS AND G. RIGHINI
Astrophysical Observatory, Arcetri, Florence, Italy
Received March 27, 1951

ABSTRACT

The equivalent width of eighteen medium-intensity *Ti* lines in the region λλ 5210–4512 is measured at five different points of the sun's radius. A comparison between *Fe* and *Ti* lines shows that, whereas the *Fe* lines appear to decrease from the center to the limb, the *Ti* lines reach a maximum at a point $\cos\theta = 0.4$ approximately.

The theory of Fraunhofer lines in its complete form, as elaborated by Houtgast,[1] gives a satisfactory explanation of the variation of the form of the profile of strong lines which are observed in the spectra that are obtained at different points of the radius of the solar disk. Similarly, Minnaert's[2] recent theory explains the behavior of weak lines. At present, a theory explaining the behavior of medium-intensity lines is not available. By "medium-intensity lines" we mean those lines which lie in the flat part of the curve of growth.

For this reason, we have studied in this work the eighteen lines of medium intensity of *Ti* given in Table 1 with the intention of contributing toward the knowledge of the behavior of their variation of intensity between the center and the limb of the sun. The value W (equivalent width) given in the last column of the table was determined by us. The method adopted will be described farther on. It can be noted that all the lines lie in the flat part of the curve of growth.

OBSERVATIONS

A set of plates was taken with the spectrograph of the Arcetri solar tower, which has a plane grating of 600 lines/mm and a ruled surface of 10 × 11 cm. The photographic camera has a focal length of 4 meters, giving a dispersion, in the first order, of 3.3 A/mm. The spectrograms were obtained with the first order. A strong ghost exists very close to the lines, and, in order to suppress it, a strip of the grating 2 cm wide had to be covered. The width of the slit used was 0.010 mm. Under these conditions the resolving power determined by measuring the instrumental profile taken by a sharp *Cd* line, is 34,000. This is 0.64 of the maximum theoretical resolving power of the grating.

Ten spectra (two for each point of the sun's radius) and a calibration spectrum, taken with a Zeiss step filter, were recorded on each plate. To equalize the exposures of all the spectra and of the calibration, we used a set of suitable neutral filters. The diameter of the sun's image given by the Arcetri solar tower was 169 mm. The spectra were taken with a tangential slit at the following points: $\cos\theta = 1.00$ (center), 0.76, 0.59, and 0.32, while at the limb they were taken with a radial slit in order to select a point at $\cos\theta = 0.10$. Ilford Rapid Process Panchromatic Plates were used.

Of the set of plates obtained, we chose four in all. Two containing the same nine lines for the blue region λλ 4512–4681 and also two containing the same nine lines for the green region λλ 4999–5210. In every plate we selected for each of the five positions on the solar disk the spectrum which had a suitable density for photometric work. Micro-

[1] "The Variations in the Profiles of Strong Fraunhofer Lines along a Radius of the Solar Disc" (Diss., Utrecht, 1942).

[2] *B.A.N.*, **10**, 339, 1948; also p. 399.

photometric tracings of selected parts of each spectra were obtained with the Arcetri microphotometer with a magnification ratio of 1/50. The microphotograms were reduced in the usual way, using the calibration curves obtained from the step-filter spectra. The profile of each line was plotted on a large scale, and the area was measured by means of a planimeter. In this way we obtained for every line, at every position, two independent values of the equivalent width. As these values were in good agreement, we adopted the mean value corrected for the ghosts of the grating.

RESULTS AND DISCUSSION

Table 1 contains the equivalent width W for the lines measured in the spectrum of the center of the disk ($\cos\theta = 1.00$) as determined by us at Arcetri. When we compare our

TABLE 1

LINES OF *Ti*

No. of Line	λ	Multiplet	J	Rowland Intensity	Equivalent Width W (Center) (mA)
1.....	5210.39	$a^3F - z^3F^0$	4–4	3	103
2.....	5192.98	$a^3F - z^3F^0$	3–3	2	75
3.....	5173.74	$a^3F - z^3F^0$	2–2	2	77
4.....	5064.66	$a^3F - z^3D^0$	4–3	3	71
5.....	5039.96	$a^3F - z^3D^0$	3–2	3	82
6.....	5024.85	$a^5F - y^5G^0$	2–2	3	86
7.....	5022.87	$a^5F - y^5G^0$	3–3	2	88
8.....	5020.04	$a^5F - y^5G^0$	4–4	2	96
9.....	4999.51	$a^5F - y^5G^0$	3–4	3	130
10.....	4681.91	$a^3F - z^3G^0$	4–5	3	100
11.....	4656.47	$a^3F - z^3G^0$	2–3	3	98
12.....	4555.50	$a^5F - y^5F^0$	5–4	3	74
13.....	4548.72	$a^5F - y^5F^0$	3–2	2	91
14.....	4534.78	$a^5F - y^5F^0$	4–4	4	121
15.....	4533.25	$a^5F - y^5F^0$	5–5	4	98
16.....	4527.32	$a^5F - y^5F^0$	1–2	3	143
17.....	4518.03	$a^5F - y^5F^0$	3–4	3	88
18.....	4512.74	$a^5F - y^5F^0$	4–5	3	85

values with those obtained by Allen,[3] we find that the Arcetri values of the equivalent width are greater; the average ratio being

$$\frac{W\,(\text{Arcetri})}{W\,(\text{Allen})} = 1.13 \pm 0.04\,.$$

It is interesting to note that Mulders,[4] comparing the results of Righini,[5] with his own, has already found a ratio,

$$\frac{W\,(\text{Righini})}{W\,(\text{Mulders})} = 1.11\,.$$

The fact that the instrumental equipment used by Righini in his earlier work was the same as the present one seems to suggest that this discrepancy is due to some sort of in-

[3] *Mem. Comm. Solar Obs. Canberra*, Vol. 1, No. 5, Part 2, 1934.

[4] Diss., Utrecht, 1934.

[5] *Pub. Oss. Arcetri*, 51, 59, 1935.

strumental effect. However, these systematic differences have no importance for us, as we are interested only in the variations of W and not in its absolute values. In order to study the variations of W, we have taken for each line the ratios r between the equivalent width $W(\cos\theta)$ at each different point and $W(\cos\theta = 1)$ corresponding to the center of the disk. Taking the mean of the values of r for all the lines belonging to the same spectral region for each position, we obtain the results given in Table 2, from which we

TABLE 2

VALUES OF r FOR SAME SPECTRAL REGION

λ_m	cos θ			
	0.76	0.59	0.32	0.10
5070.....	1.06	1.15	1.22	1.13
4570.....	1.12	1.18	1.23	1.13

see that there is no substantial difference in the behavior of the lines as regards the wave length. If, on the other hand, we group the lines according to the lower term of the multiplet and again take the mean of r for each of the five positions observed, we obtain the results given in Table 3. It is easy to see that the differences are negligible.

TABLE 3

VALUES OF r ACCORDING TO LOWER MULTIPLET TERM

Lower Term	cos θ			
	0.76	0.59	0.32	0.10
a^3F.....	1.02±0.05	1.13±0.05	1.11±0.06	1.13±0.04
a^5F.....	1.13±0.03	1.15±0.05	1.30±0.07	1.12±0.08

We have thus shown that neither the different wave length nor the small difference (0.8 volt) in the excitation potential of the lines has any decisive influence on the variation of r from the center to the limb of the sun, at least within the limits of accuracy of our measurements. We think, therefore, that we are justified in taking the general mean of the ratios r for all the lines which we have measured. The mean is given in Table 4.

TABLE 4

MEAN VALUES OF r

cos θ....	0.76	0.59	0.32	0.10
r.....	1.07±0.06	1.18±0.06	1.22±0.06	1.12±0.05

Except for the four lines of the multiplet $a^3F - y^3F$ of *Ti* for which Thackeray[6] has measured the ratio r for the position cos $\theta = 0.14$, there are no other measurements similar to ours for this element. On the other hand, there is quite a large number of measure-

[6] *Ap. J.*, **84**, 438, 1936.

ments for the *Fe* lines, generally at one, or at most two, points of the solar radius. These measurements, when suitably grouped, can offer a useful comparison with our measurements.

Table 5 gives the mean of r for the positions ($\cos\theta$) and for the number of lines used. Only lines having an equivalent width W greater than 80 mA have been selected among

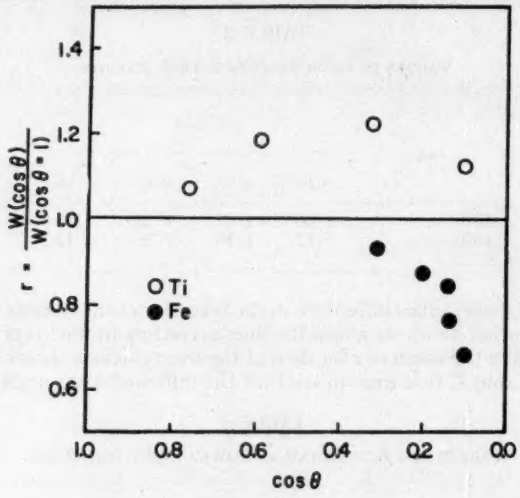

FIG. 1.—Behavior of lines of *Ti* and *Fe*

TABLE 5

MEAN VALUES OF r FOR VARIOUS OBSERVERS

λ Mean	cos θ	r Mean	No. of Lines	Observer
Fe lines:				
5130 A.....	0.31	0.935	11	Adam (*M.N.*, **98**, 115, 1938)
5200.....	.20	.865	24	Bruggencate and Houtgast (*Zs. f. Ap.*, **19**, 154, 1941)
5200.....	.14	.840	24	Bruggencate and Houtgast (*ibid.*)
3900.....	.14	.760	30	Thackeray (*Ap. J.*, **84**, 438, 1936)
5330.....	.10	.68	39	Righini (*Pub. Oss. Arcetri*, **51**, 62, 1933)
Ti lines:				
3900.....	0.14	0.90	4	Thackeray (*Ap. J.*, **84**, 438, 1936)

those measured by different observers. With the data from Tables 4 and 5 we have drawn Figure 1, which shows the different behavior of *Ti* and *Fe* lines. While the *Ti* lines seem to reach a maximum at $\cos\theta = 0.4$ approximately, the *Fe* lines appear to decrease from the center to the limb. The single point obtained by Thackeray for the *Ti* is not in good agreement with our measurements.

Recently Allen[7] has made a new set of measurements of the variations of some lines of medium intensity between the center and the limb of the sun. Among these there are three medium-intensity lines of *Fe* which behave more like the *Ti* lines than do the other

[7] *M.N.*, **109**, 349, 1949.

Fe lines. The equivalent width of these lines, however, has been determined by approximating the profile of the line by means of a Voigt function[8] and measuring only the width instead of the area of the profile. It is interesting to note that the excitation temperature of the solar atmosphere, as determined by many authors, differs systematically when the *Ti* lines are used rather than the *Fe* lines. The *Ti* lines give a systematically lower excitation temperature.

If we take the mean for the values of T determined by Prouse,[9] Menzel,[10] King,[11] and Wright[12] for the *Ti*, and the mean for the values of T determined by Gottschalk[13] and Wright[12] for the *Fe*, we have:

$$Ti: \; T = 4400^\circ \text{ K},$$

$$Fe: \; T = 4850^\circ \text{ K}.$$

Similar results are obtained by Bruggencate[14] and by Bruggencate and Houtgast[15] for the same elements; they give

$$Ti: \; T = 5040^\circ \text{ K},$$

$$Fe: \; T = 5800^\circ \text{ K}.$$

In both cases the temperature given by *Ti* is lower than the one given by *Fe*. This difference, like the difference in behavior of the variation center limb, could be attributed to a different effective optical depth of formation of the lines.

V. Barocas, of the Jeremiah Horrocks Observatory, Preston (England), wishes to acknowledge the help of a grant from UNESCO through the I.A.U. which enabled him to carry out his part of this work. He also wishes to thank Professor G. Abetti, director of the Arcetri Observatory, for his kindness in allowing him to work there and to use the necessary instruments.

[8] H. C. van de Hulst and J. J. M. Reesinck, *Ap. J.*, **106**, 121, 1947.
[9] *Ap. J.*, **95**, 323, 1942.
[10] *Ap. J.*, **87**, 81, 1938.
[11] *Ap. J.*, **87**, 40, 1938.
[12] *Ap. J.*, **99**, 249, 1944.
[13] *Ap. J.*, **108**, 326, 1948.
[14] *Zs. f. Ap.*, **18**, 301, 1939.
[15] *Zs. f. Ap.*, **19**, 154, 1941.

THE PHYSICAL THEORY OF METEORS. II. ASTROBALLISTIC HEAT TRANSFER*

RICHARD N. THOMAS AND FRED L. WHIPPLE
University of Utah and Harvard University
Received July 10, 1951

ABSTRACT

Previous difficulty in formulating a quantitative physical theory of meteors has in large part originated from the wide gap between terrestrial experiments and meteor observations. The physical theory of meteors falls into three aspects: air resistance, heat transfer, and radiation. This paper summarizes an attempt to analyze the heat-transfer aspect from the standpoint of the available meteor data and of some recent laboratory experiments. The section that relates to the laboratory experiments represents the first published attempt to measure heat transfer to bodies in free flight when the velocity is so high that ablation occurs—thus defining the astroballistic region. The free-flight heat transfer in the astroballistic region appears from these experiments to vary with velocity and air density according to the meteor formula rather than according to the conventional aerodynamic formulae established at lower velocities. The heat-transfer efficiency, expressed in terms of that to a Newtonian putty ball, is about 1 per cent in the region near 1–2 km/sec. The meteor results show considerable scatter in values of the heat-transfer efficiency, with no obvious dependence upon velocity or air density and with a favored estimate lying near 5 per cent. A possible interpretation of the scatter of meteor values lies in the fragmenting and flaring of meteors; and the great importance of further study on this point is emphasized. Some considerations on the maximum-sized meteorite capable of surviving intact lead to an independent gross estimate of the heat-transfer efficiency. An attempt is made to interpret the deep pitting observed in some meteorites in terms of enhanced ablation on an initially irregular surface, in accordance with some additional free-flight experiments.

I. INTRODUCTION

Early reports[1] by one of the authors and by L. G. Jacchia contain a presentation of the theory underlying the translation of meteor observations into data on the interaction of meteoroid and atmosphere. As was indicated in these reports, the theory definitely needs improvement, but attempts to improve it have been severely handicapped by the small advance in our fundamental knowledge of the physical processes involved—from either experimental or theoretical work—since the summary[2] presented by one of us at the beginning of the Harvard meteor studies prior to the war. A recent, more comprehensive investigation[3] by one of us into the air-resistance aspect contained only a few results that could not have been predicted on the basis of our state of knowledge at the time of the earlier report.

Stimuli from at least four sources, however, have prompted us to enter afresh into an investigation of the meteor theory. First, several recent results from the Harvard meteor program have indicated small departures from the functional relations of the earlier theory. Second, the laboratory production and investigation of particles of higher velocity is just now reaching the point of quantitative, experimental study in the region of velocity and air density relevant to the meteor problem. Third, some recent work[4] by one of us, in conjunction with M. A. Cook and H. Eyring, of the University of Utah, has pre-

* An investigation partially carried out under NOrd Contract No. 10449 of the U.S. Naval Bureau of Ordnance.

[1] F. L. Whipple, *Proc. Amer. Phil. Soc.*, **79**, 499, 1938; L. G. Jacchia, *Harvard Repr. Ser.*, II-26 (Tech. Rept. No. 2 [1948]), *ibid.*, II-31 (Tech. Rept. No. 3 [1949]), and *ibid.*, II-32 (Tech. Rept. No. 4 [1949]).

[2] F. L. Whipple, *Rev. Mod. Phys.*, **15**, 246, 1943.

[3] R. N. Thomas, *Harvard Repr. Ser.* II-34 (Tech. Rept. No. 5 [1950]).

[4] M. A. Cook, H. Eyring, and R. N. Thomas, *Ap. J.*, **113**, 475, 1951.

sented a theoretical approach to the surface temperature of the meteor on the basis of the generalized reaction-rate theory. Fourth, the Aeroballistics Division of the U.S. Naval Ordnance Laboratory, under the direction of R. J. Seeger, has made available to us the facilities of its controlled-pressure ballistics free-flight range for a study of heat transfer in the conventional ballistic-velocity region.

The meteor theory falls rather naturally into three parts: the problem of air resistance; the problem of heat transfer to the meteoroid; and the problem of radiation from the meteoroid. In the air-resistance summary cited, it was indicated that the effect of heat transfer on drag was the least understood aspect of the drag problem. Theoretical work on the radiation aspect—a problem in classical quantum mechanics—is almost nonexistent.[5] In order to define the amount of radiating material, any experimental approach to the radiation aspect must be based upon a complete, quantitative understanding of the heat-transfer problem. Consequently, we have commenced our reanalysis of the meteor theory with an investigation of the heat-transfer problem.

a) METEOR HEAT-TRANSFER THEORY

The spread in velocity and air density encountered in the meteor problem far exceeds that readily accessible in the laboratory. The velocity range is from about 8 to 73 km/sec; and the air density varies from the sea-level value of 10^{-3} to 10^{-10} gm/cm^3 at the 120-km level. We note that the lowest meteor velocity observed is still high enough that vigorous melting or vaporization of the meteor surface occurs (necessarily, of course, if we are to see the meteor!). Thus we consider that loss of mass by melting or vaporization defines the fundamental characteristic of the range of physical conditions under which we wish to study heat transfer in meteors. We have adopted the term "astroballistic" to designate this region.[6]

We wish, then, an approach to heat transfer in the astroballistic region—and a satisfactory approach must clearly be general enough to cover the whole region. At present there exists no satisfactory theoretical approach to the problem in any part of the relevant range of density or velocity. The hydrodynamic theories of heat transfer do not include the case of mass loss from the body. There is no satisfactory theoretical treatment of the accommodation coefficient for discrete molecules, in the case either of melting or of nonmelting. In the present investigation we proceed empirically, trying first to obtain an over-all estimate of the heat-transfer efficiency across the relevant region. We study the variation of the heat-transfer coefficient, defined—by analogy with the drag coefficient—as a measure of the efficiency of heat transfer in the actual case relative to that in the Newtonian putty-ball case. That is, for the air resistance, we have

$$\text{Drag} = -\Gamma \rho v^2 \mathfrak{A} \tag{1}$$

and, for the heat transfer,

$$\text{Heat transfer} = -\Lambda \frac{\rho v^3}{2} \mathfrak{A}\,, \tag{2}$$

where ρ, v, and $\mathfrak{A}$ are air density, velocity, and cross-sectional area of the moving object,

[5] One theoretical paper exists—E. Öpik, "Atomic Collisions and Radiation of Meteors," *Harvard Reprints*, No. 100, 1933. This calculation is a rough approximation, failing in several theoretical details.

[6] In a recent discussion over the precise meaning of the terms "hyperballistic" and "hypervelocity" between one of us and J. S. Rinehart, of the Naval Ordance Test Station, particularly in reference to shaped-charge phenomena, Rinehart suggested that the term "hyperballistic" be given precise meaning by applying it to the range to which we have applied the term "astroballistic." "Hyperballistic" and "hypervelocity" seem, however, to have been adopted to designate the region above Mach 10. Since the Mach number is hardly the basic similarity parameter relevant to heat-transfer problems—particularly those involving melting and vaporization—we feel that our introduction of the term "astroballistics" should be useful.

respectively. For the meteor analysis, the further assumption,

$$\mathfrak{A} = m^{2/3} A \,, \tag{3}$$

is introduced, where A is a constant.

b) THE OBSERVATIONAL MATERIAL AVAILABLE

We have four sources of empirical data on Λ, if we exclude data on the accommodation coefficient.

1. From the meteor observations themselves it is possible to infer values of the quantity

$$\sigma = \frac{\Lambda}{2\Gamma\zeta}, \tag{4}$$

where ζ is the energy necessary to separate 1 gm of material from the solid meteoroid. The observed acceleration measures Γ; but the mass and dimensions of the meteoroid are unknown. The observed luminosity measures Λ, under the assumption that the luminosity measures the mass loss from the meteoroid; and the mass loss, in turn, measures the heat transfer. The uncertainty as to mass and dimension—and air density, if one assumes this quantity unknown—then restricts the direct observational data to values of the quantity σ.

2. Values of Γ and Λ may be obtained independently from photographic studies of bodies in free flight. Since the mass and dimensions of the bodies are known, the measured decelerations give Γ directly. Heat-transfer values are inferred from observations of the mass loss from the body; hence the experimental conditions mimic the meteor case closely.

3. A limited amount of wind-tunnel data on a carbon dioxide sphere provides a comparison with the free-flight results. Again, the data on heat transfer are derived from an observation of the mass loss, so the experiment is closely related to the meteor case.

4. Some indirect evidence on the details of the heat-transfer process is obtained from phenomena in meteorites and from some free-flight measures on magnesium projectiles. Long, narrow holes have been found in several meteorites. The question arises as to how such holes or "pits" could be produced. An observation that offers a possible explanation results from a study of ignition as a function of surface contour on the flat front of a magnesium projectile.

c) CONVENTIONAL AERODYNAMIC HEAT-TRANSFER THEORY

In the foregoing, we have expressed the heat transfer in terms of that to be expected for the Newtonian "putty-ball" model, in which the incident air molecules are absorbed by the surface. The laboratory experiments with which this paper deals have, however, been performed in the hydrodynamic-flow region, for which a certain amount of theory exists. The unique feature of the present experiments is the melting of the surface. The conventional aerodynamic theory of heat transfer deals with bodies that do not melt. The physical point of interest is the alteration in the rate of heat transfer to the body when melting occurs.

We note that the conventional aerodynamic theory of heat transfer does not involve any physical characteristic of the body except its surface temperature. That is, the theory specifies the existence of a thermal boundary layer, across which the temperature changes from the free-stream value to that of the body surface. Because of this temperature gradient, there is a heat flow from air to body, given by

$$q = h\,(t_s - t_b)\,, \tag{5}$$

where q is the heat flow; t_b the body surface temperature; t_s the gas temperature outside the thermal boundary layer; and h the heat-transfer coefficient. An expression for h re-

sults from solving the steady-state heat-flow equation. For a flat plate, the solution[7] is expressed in the form (for the laminar-flow region)

$$N_u = 0.331 P_r^{1/3} R_e^{1/2}, \tag{6}$$

where

$$N_u = \frac{h\chi}{k}, \qquad P_r = \frac{\nu}{a} = \frac{\mu c_p}{k}, \qquad R_e = \frac{u_s \chi}{\nu}, \tag{7}$$

and k is the thermal conductivity, c_p the specific heat at constant pressure, μ the viscosity, ν the kinematic viscosity, and a the thermal diffusivity of the gas, u_s the flow velocity at the edge of the boundary layer, and χ the length of the plate. The quantities N_u, P_r, and R_e are the Nusselt, Prandtl, and Reynolds numbers of the flow. Thus we see that the heat flow should be the same and independent of the composition of the body, so long as l_b remains the same.

Furthermore, in the case where the temperature of the body is held fixed, the theory gives no difference in the heat flow to a solid and to a liquid, so long as the liquid has zero velocity with respect to the solid surface. If the liquid flows over the surface, the hydrodynamics of this liquid motion must be included in the analysis. The problem does not appear to have been treated. Thus it seems difficult to estimate the direction of the correction (to eq. [6]) that would make the solution applicable to situations where melting occurs.

We might, however, inquire whether a formula of type (6) or one of type (2) might be expected to represent the general behavior of the heat transfer, and hence the melting rate. That is, we have two parameters to vary—air density and air speed. Air-speed variation corresponds to a variation of the air temperature near the body. With the exception of a possible—and unknown—dependence of Λ on ρ and v, equation (2) shows that heat transfer varies as ρv^3. On the other hand, equations (5) and (6) lead to a velocity variation through the velocity-temperature dependence of the product

$$k\,(t_s - t_b)\sqrt{\frac{u_s}{\nu}}, \tag{8}$$

since P_r is essentially temperature-independent in the temperature range of astroballistic interest. The density dependence enters only through the term ν, which varies inversely as ρ. Thus, while the quantitative difference in velocity-temperature dependence between equations (2) and (6) is not immediately obvious, the contrast in density dependence is apparent. The meteor expression (2) varies as ρ, while equation (6) varies as $\rho^{1/2}$. Since a characteristic feature of the free-flight tests reported in a later section is an air-density variation, some discrimination between equations (2) and (6) should be possible. The same discriminating criterion should, of course, hold for the meteor moving in the lower atmosphere where the conditions for the hydrodynamic-flow region should hold. The experiments reported in Section III involve this density discrimination.

We note that the Reynolds number corresponding to the meteor observations is about 10^4 or less for both fast and slow meteors (since the fast meteors occur higher in the atmosphere). Hence we have quoted the laminar heat-transfer result in equation (6). For turbulent flow, we have[7] a smaller numerical coefficient in equation (6) and the exponent of R_e becomes 0.8. The experiments reported in Section III were conducted in the normal ballistic regime, at velocities of $2000 < v < 6000$ feet/sec, and at a range of air densities from $\frac{1}{10}$ to 2 standard atmospheres. Thus the free-stream values of R_e lie near and above the transition region of about 5×10^5 for R_e. We note, however, that for these heat-transfer computations we are interested in R_e computed behind the shock wave near the sur-

[7] E. R. G. Eckert, *Introduction to the Transfer of Heat and Mass* (New York: McGraw-Hill Book Co., Inc., 1950).

face. With the blunt bodies we have used, the relevant R_e then falls below the critical value, and we would expect to be in the laminar-flow region.

d) SUMMARY OF INFORMATION ON Γ

As already mentioned, the meteor data appear as a combination of Γ and Λ. To estimate Λ, we require an estimate of Γ. A summary of the problem outside the specific astroballistic effects has been presented elsewhere.[3] The summary indicates that Γ approaches a constant asymptotic value as velocity increases, so long as the rise in velocity does not activate additional degrees of freedom of the atmosphere and meteor. Such activation obviously causes a decrease in the asymptotic value. Consequently, if we commence our analysis with a highly rarefied gas moving at relatively low velocity and progress both to higher gas densities and to higher velocities, the asymptotic value of Γ decreases. The situation is illustrated in regions *I*, *II*, and *III* of Figure 1, where we have indicated

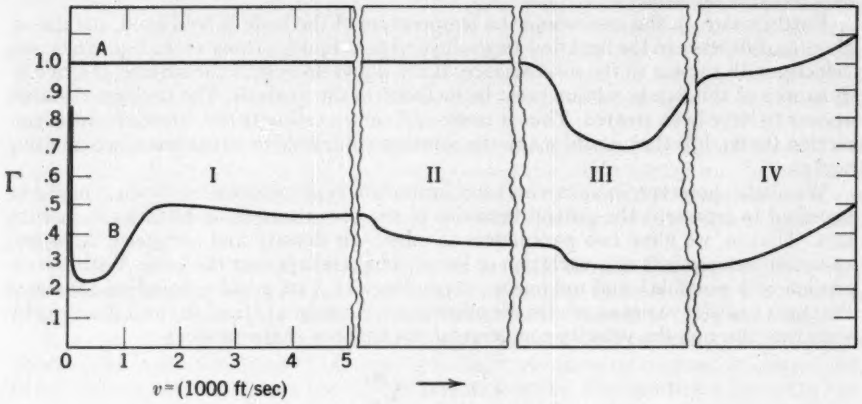

FIG. 1.—The drag coefficient Γ

semiquantitatively the value of Γ for a sphere. Curve *A* represents the situation for a highly rarefied gas; curve *B*, for the hydrodynamic case.[8] The decrease in curve *A* in region *III* results from the onset of inelastic collisions between gas and solid, but the reflection is still specular. The rise of Γ to 1 corresponds to the complete absorption of the incident atoms and re-emission with zero velocity. That Γ before and after the drop has the same value is, of course, peculiar to the sphere, for which $\overline{\sin^2\theta} = \frac{1}{2}$ over the surface. Region *I* of curve *B* is quantitative, taken from some work by one of us and A. C. Charters.[9] The decrease of Γ in regions *II* and *III* reflects, respectively, the activation of additional degrees of freedom of the gas and of the solid; the numerical values are schematic. On this basis, we see that Γ for a sphere lies between about $\frac{1}{4}$ and 1, with the former value applying to (hydrodynamic regime) all degrees of freedom of gas and solid activated, and the latter applying to no degrees of freedom excited other than the original unidirectional translation of the gas. Since, at the highest meteor velocities and lowest air densities, we expect most of the air molecules to be absorbed by the meteor surface, a value of Γ between $\frac{1}{2}$ and 1 would seem the most reasonable.

[8] H. S. Tsien, *J. Aer. Sci.*, **13**, 653, 1946, has presented a more refined treatment of the very low air-density region, obtaining the velocity dependence of our curve *A*. For our schematic interest, however, curve *A* is sufficient, particularly since a really quantitative discussion requires a knowledge of accommodation coefficient and per cent specular reflection, which are unknown.

[9] A. C. Charters and R. N. Thomas, *J. Aer. Sci.*, **12**, 468, 1945.

We note the possibility of an overdrag term in the astroballistic regime.[4] For a low rate of heat transfer to the meteor—i.e., for the meteor just entering the atmosphere or for a low-velocity object at sea-level—the body dissipates the heat by conduction inward and radiation outward. For a high rate of heat transfer, however, the outer, heated layers are shed faster than conduction can carry the heat inward. After the body reaches a surface temperature much over 2000° K, the energy dissipation by radiation is trivial compared with that by melting and vaporization.[4] For air densities such that the free path of the vaporized meteor atoms exceeds the meteor dimension, the momentum transfer to the solid from the vaporizing material is readily calculated.[4] One obtains a Γ varying with s as $(1 + 0.16s)$, where s is the meteor velocity in units of 10 km/sec. Thus the fastest meteoroids (probably invisible), in the high upper atmosphere, might double their Γ value from this effect. At greater air densities, more refined calculations are needed to establish whether the effect is nontrivial. At present, we can only acknowledge the possibility of this overdrag term and include it as an uncertainty in Γ. Region *IV* of Figure 1 exhibits the effect schematically.

In summary, for a spherically shaped meteor, we expect Γ to be about $\frac{1}{2}$, with an uncertainty factor of about 2, depending on air density and speed. We might also expect some decrease in Γ as we go from the faster meteors in the upper atmosphere to the slower meteors in the lower.

Finally, we should comment on the uncertainty in Γ because of the meteor shape. Most meteors are probably highly irregular in shape, and possibly they are rotating, although this point is uncertain. So long as the meteor simply serves as a "trap"[2] for the incident air molecules—i.e., so long as incident air molecules penetrate the meteor surface—this shape factor is not critical. And it would seem that this picture is the most likely one. At worst, in the purely hydrodynamic regime, Γ cannot have a value more than twice that for the sphere, but it may have a value considerably less than that for a sphere in the case of elongated bodies (the values are roughly in the ratio $[\frac{1}{2}] : \overline{\sin^2 \theta}$, where θ is the inclination of the surface to the direction of motion). As mentioned, however, this shape factor should be of significance only at the very lowest velocities; so we favor the value $\Gamma = (\frac{1}{2}) \pm$ a factor of 2.

II. METEOR DATA—DISCUSSION AND RESULTS

a) PHOTOGRAPHIC OBSERVATIONS OF METEORS

A theory of the luminosity and deceleration of photographic meteors as developed by one of the authors[10] has operated with good success in the determination of upper-atmospheric densities. The various observed data for the photographic meteors led independently to various methods of determining upper-atmospheric density, pressure, and temperature. The comparison of these various methods showed, however, that only one quantity of astroballistic interest could be obtained: $\sigma = \Lambda/(2\Gamma\zeta)$. From all the doubly photographed meteor data available from the Harvard Meteor Program, Jacchia evaluated this quantity for each meteor and, in some cases, at several points along the trail of a single meteor[11] from the following equation (in which I is the observed luminous intensity of the meteor and t is the time measured along the meteor trail and the subscript e denotes the end of the trail):

$$\sigma = \frac{I}{v^3}\left[\int_t^{t_e} \frac{I}{v^3}\, dt\right]^{-1} \left(v \frac{dv}{dt}\right)^{-1}. \tag{9}$$

Thus σ is determined by the relative mass loss divided by the velocity times the deceleration—or, essentially, from the relative persistence of the meteor divided by its decelera-

[10] F. L. Whipple, "Photographic Meteor Studies. I," *Proc. Amer. Phil. Soc.*, **79**, 499, 1938. Cf. also n. 2.

[11] L. G. Jacchia, *Harvard Repr. Ser.* II-31 (Tech. Rept. No. 3 [1949]).

tion in the atmosphere. Three assumptions specifically enter the analysis: the intensity is proportional to the rate of mass loss; the proportionality factor varies as some power of the velocity; and the drag coefficient remains constant. However, a considerable variation in these assumptions will not greatly affect the derived values of σ. From data on thirty-six meteors, whose velocities exceed 20 km/sec and which provide 55 independent determinations of σ, Jacchia finds a mean value of $\log_{10} \sigma = -11.75$.

A considerable search for correlations of individual values of σ with velocity, atmospheric height, atmospheric density, or residuals from the mean of the density determinations has proved unsuccessful. Figure 2 exhibits plots of $\log \sigma$ against $\log v$ and $\log \rho$. As seen from the figures, there is a considerable range in the observed values, nearly one order of magnitude in σ. On the other hand, the range for a single meteor, where more than one determination of deceleration and hence of σ is possible, amounts to very much

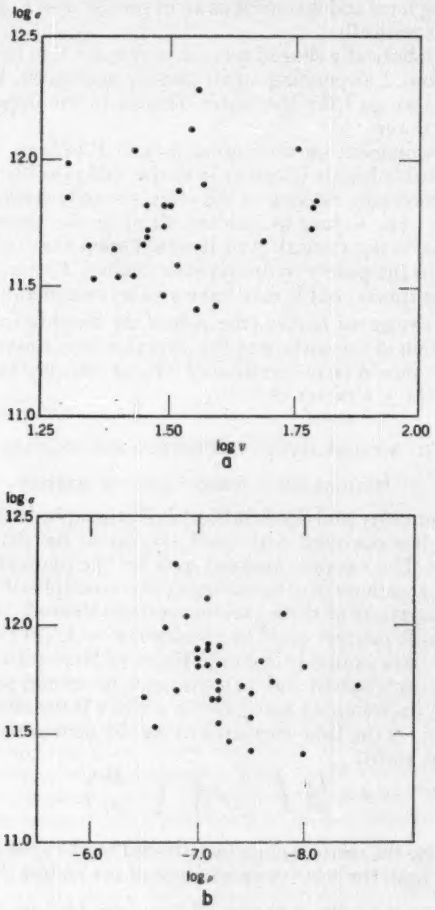

FIG. 2.—*a*, correlation of σ with v; *b*, correlation of σ with ρ

less than this quantity. The maximum range is approximately 0.4 in the logarithm but is usually very much smaller.

There seems to be no escape from the conclusion that the value of σ is a near-constant characteristic for a single meteor but varies widely from one meteor to another. In addition, among the meteors with velocities greater than 20 km/sec, there appears to be no systematic variation of σ along the path for a single meteor.

For ten slower meteors (seven included in the above general average) with velocities ranging from initial velocity about 30 km/sec to end-velocities as low as 8 km/sec, Jacchia finds a mean value of $\log_{10}\sigma = -11.61$, with a median value of -11.53. There is some suggestion of an increase in the value of σ with decreasing velocity at the low-velocity range. Jacchia, from unpublished data, has found additional evidence for this effect among single meteors of low velocity, although it is not clearly marked among the faster meteors.

The quantity σ is of great interest with regard to the passage of meteorites through the atmosphere, particularly in reference to the loss of matter. The theory of Hoppe,[12] as used by one of the present writers,[2, 10] leads immediately to a relationship between the mass of the meteor at any time, its velocity v, and its original velocity v_∞ before entering the earth's atmosphere. The relation is

$$m = m_\infty \exp\left[\sigma \frac{v^2 - v_\infty^2}{2}\right]. \tag{10}$$

If the mean observed value $\log \sigma = -11.75$ is adopted, we find that, for initial velocities of 12, 20, and 70 km/sec, the ratios of the final to initial masses are, respectively, 0.3, 0.03, and 1.2×10^{-19}. Hence one should not expect appreciable residual particles remaining from any but the slowest meteors. These results are of the greatest importance in evaluating the initial masses of meteorites found on the surface of the earth.

The interpretation of σ in terms of the heat-transfer coefficient demands a knowledge of the drag coefficient Γ and the heat of fusion or vaporization. In Section *Id* we found that there does not seem to be too great a leeway for the choice of a value for Γ; hence we have adopted the value $\Gamma = \frac{1}{2}$.

There is a greater uncertainty in the quantity ζ and its interpretation. The heat of fusion from 20° C. for common metals found in meteors is of the order of 10^{10} erg/gm; and the heat of vaporization is of the order of 10^{11} erg/gm. The values suitable for stone are not greatly different. Hence we see that much depends on whether the meteoric material is assumed to be immediately fused or immediately vaporized. If fusion is the principal process, we see that the value of Λ is of the order of 0.016; while if vaporization is the principal process, the value becomes 0.16. E. Öpik[13] concludes that solid metallic meteorites, because of their high conductivity and low viscosity just above the melting point, should generally spray material in droplets—so that the heat of fusion should be applicable for such bodies. On the other hand, he concludes that, for stones or silicate-type meteoroids, the low heat conductivity and the high viscosity just above the melting point makes spraying unlikely—so that the heat of vaporization should be used in the equations. We have no certain knowledge as to the physical structure or precise chemical composition of the observed photographic meteors. One of the writers has amassed some evidence to indicate that they are of a rather fragile character, probably consisting of a poorly sintered mass of typical material from interstellar space.[14] If such is the case and we are dealing with an inappreciable percentage of meteoritic irons or their equivalent,

[12] J. Hoppe, *A.N.*, **262**, 169, 1937.

[13] "Researches on the Physical Theory of Meteor Phenomena. III. Basis of the Physical Theory of Meteor Phenomena," *Tartu Obs. Pub.*, Vol. **29**, 1937.

[14] F. L. Whipple, *Ap. J.*, **111**, 375, 1950.

as is suggested by the cometary character of the orbits under consideration,[15] then the heat conductivity of the material should be very small and a considerable amount of silicates should probably be present in the complicated conglomerate. Spectroscopic data as yet do not distinguish among these hypotheses. In any case, it is probably better to assume that the heat required in the ordinary photographic meteor process is the heat of vaporization. Hence we are led to a value $\Lambda \cong 0.1$.

It is necessary, however, to account in some rational fashion for the large intrinsic variation of σ and hence of Λ or ζ among the individual meteors. We must attribute the major source of the variation to ζ or else to unconsidered factors in the problem. One such factor is fragmentation. Jacchia has shown[11] that flares among the photographic meteors must almost certainly arise from fragmentation. It is not at all impossible that fragmentation of a minor character occurs fairly regularly.[4] In terms of the equation for σ, the process of fragmentation would be equivalent to the introduction of a smaller value of ζ, leading to a value of σ greater than one would expect, were fragmentation absent. In turn, our derived value of Λ would be correspondingly increased. If we assume that for the faster meteors the minimum observed value of σ ($\log \sigma = -12.3$) corresponds to the case of zero fragmentation and that ζ corresponds to the heat of vaporization, approximately 10^{11} erg/gm, the value of Λ is 0.05.

The possible, but not definitely proved, increase of σ for very low meteoric velocities does not fit well with the above discussion of fragmentation, since flaring is most frequent among the high-velocity meteors. It is conceivable that in the slower meteors we are dealing with bodies that are like the meteorites rather than the conglomerate[14] of cometary origin. Orbital considerations in four examples support such a view.[16] If so, we might expect that the fragmentation factor would become negligible but that the heat of fusion, instead of the heat of vaporization, would become more applicable because of the increased percentage of metallic material; but we are probably not justified in pressing these interpretations.

b) CONSIDERATIONS BASED ON THE MAXIMUM-SIZE METEORITE CAPABLE OF SURVIVING IMPACT

1. *Basic assumptions and calculations.*—It is evident a priori that there must be a limit to the maximum size of a meteorite falling as a single body. Factors determining the limiting size must include the drag coefficient, the density distribution in the atmosphere, the heat-transfer coefficient, the nature and shape of the meteoritic mass, the gravitational attraction of the earth, the velocity of the body at great distances from the earth, and the detailed circumstances of fall. The largest known meteorite probably represents an optimum or nearly optimum situation with regard to these various factors. Since either precise or optimum conditions are known or can be assumed for all the foregoing factors except the heat-transfer coefficient, it seemed likely that some knowledge of this quantity should be acquired by a careful study of the problem of the maximum meteorite size.

The largest known single body certainly identified as a meteorite is the Hoba-West meteorite found near Grootfontein, Southwest Africa.[17] According to L. J. Spencer and M. H. Hey,[18] the present mass weighs about 6×10^7 gm and is a nickel-rich ataxite of specific density 7.96, composed of iron 83 per cent, nickel 16 per cent, and other substances about 1 per cent. "The metal is comparatively soft and quite malleable," an important characteristic in preventing fracture on landing.[19] An estimate by C. C. Wylie[20] places the original terminal mass at approximately 1.5×10^8 gm.

[15] F. L. Whipple, *A. J.*, **54**, 53, 1948.

[16] Current work in progress on the Harvard Meteor Project.

[17] The Ahnighito of the Cape York meteorites is probably a very close second.

[18] *Mineral. Mag.*, **23**, 1, 1932.

[19] See, e.g., a discussion of terminal ballistics in solids by J. S. Rinehart, *Pop. Astr.*, **58**, 458, 1950.

[20] *Sky and Tel.*, **10**, 3, 1950.

In order to determine the resistance of the atmosphere to such a body entering under the optimum geometrical conditions, we found it necessary to integrate the equations of motion for several sets of geometrical circumstances. These integrations were carried out numerically

If the earth is assumed to be spherically symmetrical throughout, the change in radial distance, r, from the center can be neglected through the relatively thin atmosphere, as can the variation in the acceleration of gravity, g. We choose time, t, as the independent variable and introduce v, the total velocity, and v_h, the radial or vertical velocity.

From the meteor theory[1] the initial mass of the meteorite, m_∞, and the final mass, m_f, are related to the mass m at velocity v by the equations

$$m = m_\infty \exp\left(\sigma \frac{v^2 - v_\infty^2}{2}\right) = m_f \exp\left(\sigma \frac{v^2}{2}\right). \tag{11}$$

We may define an auxiliary quantity, $f(m)$, given by

$$f(m) = \Gamma A m^{-1/3} = \Gamma A m_f^{-1/3} \exp\left(-\sigma \frac{v^2}{6}\right). \tag{12}$$

The equations of motion, as used, then take the forms

$$\frac{dv}{dt} = -g \frac{v_h}{v} - f(m)\, \rho v^2 \tag{13}$$

and

$$\frac{dv_h}{dt} = \frac{v^2 - v_h^2}{r} - g - f(m)\, \rho v v_h, \tag{14}$$

where the air density, ρ, is determined by the height, h, above sea-level.

Numerical values of ρ were smoothed from the N.A.C.A. Tentative Atmosphere[21] in the range above $h = 22$ km and from the mean values given in the *Handbook of Chemistry and Physics*[22] below this height.

Starting values of v_0, v_{h0}, and h_0 were adopted at a point in the trajectory where the velocity had been reduced by 1 per cent. The loss of mass above this height was neglected. Above this point the orbit was assumed to deviate negligibly from the conic section (parabola or hyperbola) determined by the velocity, v_ϱ, at very great distances from the earth and by the height, h_p, of the perigee point to which the body would come, were there no atmosphere.

The eccentricity, e, of an orbit with perigee at $r = r_p$ is given by

$$e = \frac{r_p v_\varrho^2}{GM} + 1, \tag{15}$$

where G is the constant of gravity and M the mass of the earth.

Near perigee, the projected distance, l, along the earth's surface from the projected perigee point closely approximates the actual orbital arc length. If this approximation is made, the change in height, Δh, above perigee is given closely by

$$\Delta h = r - r_p = e l^2 [2(1+e) r_p]^{-1}. \tag{16}$$

If, in addition, the variation of ρ with height is assumed to be of the form

$$\rho = \rho_p \exp(-b \Delta h), \tag{17}$$

[21] C. A. Warfield, Nat. Adv. Comm. for Aer., Tech. Rept. No. 1200, 1947.

[22] (31st ed.; Cleveland: Chemical Rubber Pub. Co., 1949), p. 2678.

the deceleration equation (13) at and before the initial point of the numerical integrations becomes (since $v_h \ll v \cong v_\infty$)

$$\frac{dv}{v} = -\Gamma A\, m_\infty^{-1/3} \rho_p \exp\left[-\frac{b e l^2}{2(1+e)\, r_p}\right] dl. \tag{18}$$

This equation integrates, for a small decrease in v to $v(1-\epsilon)$, to the form

$$I(y) = 1 - \epsilon\left\{\frac{\pi^{1/2}}{2}\Gamma A\, m_\infty^{-1/3}\rho_p\left[\frac{2(1+e)\, r_p}{be}\right]^{1/2}\right\}^{-1}, \tag{19}$$

where $I(y)$ is the probability integral of y and $\Delta h = y^2/b$.

To determine initial values of v_0, v_{h0}, and h_0 for the numerical integration of an orbit determined by h_p or r_p and v_g, the value of e is given by equation (15), $h_0 = h_p + \Delta h$ by equation (19),

$$v_0 = (1-\epsilon)\left(v_g^2 + \frac{2GM}{r_p}\right)^{1/2},$$

$$v_{h0} = -\, v_0 e l_0 \left[\, r_p (1+e)\,\right]^{-1}, \tag{20}$$

and

$$l_0^2 = 2\Delta h\, r_p \frac{1+e}{e}.$$

In the actual calculations the values $\epsilon = 0.01$ and $b = 10^{-6}$ cm^{-1} were adopted.

The fundamental data for six numerical integrations are given in section *a* of Table 1

TABLE 1

HOBA-WEST INTEGRATIONS

	a) Assumed and Starting Data					
Trial number	1	2	3	4	5	6
Geocentric vel., v_g(km/sec)	0	0	0	0	12	12
Height of perigee, h_p(km)	13.5	18.1	22.2	33.7	13.3	17.8
$\rho(0)/\rho(h_p)$	5	10	20	100	5	10
ΓA(gm$^{-2/3}$cm^2)	0.225	0.225	0.225	0.225	0.225	0.225
$\log_{10}\sigma$ (cm^{-2}sec^2)	−11.75	−11.75	−11.75	−11.75	−11.28	−11.28
m_∞ (gm×10^{-8})	4.58	4.58	4.58	4.58	1240	1240
h_0 (km)	59.1	57.6	55.2	52.8	38.9	37.5
v_0 (km sec^{-1})	11.10	11.10	11.10	11.10	15.82	15.82
v_{h0} (km sec^{-1})	−0.926	−0.871	−0.797	−0.606	−1.230	−1.078
	b) Results of Integrations					
Total time (sec.)	141.3	148.8	162.5	265.*	112.8	155.6
h of max., v_h(km)	11.1	15.5	19.9	40.4	11.6	17
Max. v_h(km sec^{-1})	−0.235	−0.230	−0.198	+0.130	−0.108	+0.028
$\int \rho v dt$ (gm cm^{-2}×10^{-3})	7.5	7.5	7.4	1.2	13.2	13.1
$\int v dt$ (km)	876	916	1002	2330	753	1025
v at h=0 (km sec^{-1})	0.63	0.67	0.61	7.59*	0.59	0.62
v_h at h=0 (km sec^{-1})	−0.28	−0.28	−0.29	+0.07*	−0.27	−0.29
Zenith A of fall	64°	66°	62°	.....	63°	62°
h of max. pressure (km)	19.6	20.5	22.3	32.7	15.1	18.0
Max. pressure (atm.)	24	22	18	6	153	111

* At the end of the calculation, t = 265 sec., h = 52.1 km.

and the numerical results in section *b*. The first four integrations were carried out for parabolic orbits ($v_g = 0$) representing the minimum velocity of fall; the height of perigee (h_p, if no atmospheric resistance) was varied to determine the range of the earth's effective target area for an ideally tangential approach.

The important numerical product, $\Gamma A = 0.225\ \mathrm{gm}^{-2/3}\ \mathrm{cm}^2$, was adopted from $\Gamma = 0.5$ and $A = 0.45\ \mathrm{gm}^{-2/3}\ \mathrm{cm}^2$. The "shape-density" factor, A, takes the value 0.306 for a steel sphere and $0.385\ \mathrm{gm}^{-2/3}\ \mathrm{cm}^2$ for a steel cube, following the observational result by J. S. Rinehart and G. E. Hanshe[23] that, ballistically, the effective cross-sectional area of steel cubes is $1.50\ d^2$, where d is the length of an edge.

Table 1, section *a*, also lists the adopted values of σ, the initial mass m_∞ of the meteorite, the starting height h_0, total velocity v_0, and vertical velocity v_{h0}, for the six integrations.

2. *Results of the integrations.*—The first four integrations of parabolic orbits were carried out under nearly "ideal" conditions of meteorite fall. The value $\log \sigma = -11.75$ ($\mathrm{cm}^{-2}\ \mathrm{sec}^2$) as adopted is the mean value observed for meteors and leads to a total mass loss by ablation of 67 per cent for the parabolic case.

An inspection of Table 1, section *b*, shows that in the fourth trial (the greatest perigee distance) the body fails to strike the earth. In the first three trials the vertical velocity reaches a maximum algebraically (second line) a short distance below the nonatmospheric height of perigee with a small negative velocity (third line). The total amount of air encountered is nearly constant (fourth line) for the first three trials (a surprising result), roughly eight times the amount for vertical fall, while the body traverses about 1000 km (fifth line) of horizontal motion. In addition, the final velocity at impact (sixth line) is nearly constant, at only about 2000 feet/sec, while the vertical component (seventh line) and consequent zenith angle of impact (eighth line) are also nearly constant.

If we limit ourselves to theoretical impacts in which v_h always remains negative, the results of the first four integrations indicate that a parabolic fall for a meteorite like Hoba-West is fairly likely. The target area for such an encounter (measured by the height of perigee) corresponds to more than 30 km of the peripheral radius of the earth. The velocity of impact is not excessive, possibly leading to breakage under adverse circumstances but not providing energy for appreciable melting. It is clear that the limiting conditions might be much more extreme than those postulated, i.e., greater final masses, greater initial velocities, or greater percentages of mass loss (σ).

Trials 5 and 6 were therefore integrated to study the effects of increasing the velocity and percentage mass loss. A study of the asteroids with perihelion distance less than 1 A.U. showed that the minimum velocity of encounter with the earth would be slightly over 12 km/sec (2 cases out of 7), corresponding to a perigee velocity, v_∞, slightly greater than 16 km/sec. Hence v_∞ was adopted as 16 km/sec for trials 5 and 6. At the same time, a maximum value of σ was adopted from the meteor data, $\log_{10} \sigma = -11.28$. The resultant mass loss becomes m (final)/m (original) = 1/826.

An inspection of Table 1, section *b*, shows that the much more extreme conditions of trials 5 and 6 do not greatly alter the calculated conditions of air flight or impact from those for trials 1, 2, and 3. The *minimum* value of the assumed (nonatmospheric) perigee distance which will provide enough atmospheric retardation to reduce the velocity below 1 km/sec can be based roughly on the hyperbolic path alone if we require that $\int \rho dl \cong 1.5 \times 10^4\ \mathrm{gm\ cm}^{-2}$. We find that $h_p = -10$ km appears to give a reasonable lower limit. Thus the Hoba-West meteorite might have landed with a velocity less than 1 km/sec within a perigee range of $-10\ \mathrm{km} < h_p < 20\ \mathrm{km}$.

The probability, then, that a given meteorite of $v_\infty = 16$ km/sec struck the earth in the range $-10\ \mathrm{km} < h_p < 20\ \mathrm{km}$ can be calculated to be about 0.007, allowing for the increased target area of the earth, produced by gravity. Since the statistics of the space frequencies of such large bodies are practically unknown, it is difficult to interpret the

[23] *Pop. Astr.*, **58**, 467, 1950.

probability of 0.007 in terms of time intervals, geological deterioration, and probability of discovery.

Thus we find that the calculations of trajectories for the maximum-sized meteorites give us only a crude suggestion of an upper limit on the value of σ, perhaps 10^{-11} gm erg^{-1}. On the other hand, the integrations lead us to predict that *very much larger meteorites* than the Hoba-West or the Ahnighito *could* reach the surface of the earth with terminal velocities below 1 km/sec. The questions as to whether they have done so, have survived burial and weathering, and will be found are not easily answered.

Eventually, other observational and theoretical approaches to the value of σ for meteorites should become useful. Particularly, more direct methods of determining actual surface losses by ablation should be developed. Perhaps a detailed theory of pitting (see Sec. V) will throw light on this question. Also the suggestions and calculations by C. A. Bauer[24] of cosmic-ray activity in meteorites based on *He* content bear directly on our problem. His results indicate that the ratio m (final)/m (initial) is probably not less than $\frac{1}{10}$ *if* we accept his interpretation of the observed *He* content in meteorites. Otherwise, the penetration of cosmic rays into the meteorites would be too small to support his proposed mechanism of *He* production.

III. FREE-FLIGHT MEASURES ON WOODS-METAL PROJECTILES

a) EXPERIMENTAL DETAILS

The Naval Ordnance Laboratory made available to us the facilities of their controlled-pressure free-flight range. The equipment is the standard spark-photographic instrumentation[25] that provides a shadow photograph of the moving body in each of two orthogonal aspects transverse to the direction of motion and thus hydrodynamic flow pattern and time-distance records of the motion.

The various low-melting-point alloys provide good material for this study of melting phenomena[26] at velocities that are easily reached. We have used Woods metal (*Bi*, 0.50; *Pb*, 0.25; *Sn*, 0.125; *Cd*, 0.125). Figure 3 shows a sketch of the model. The highest muzzle velocities reached some 6000 feet/sec. The first photograph was taken some 15 feet from the muzzle, and the observations were continued over the next 122-foot base line. Experiments were conducted at velocities of approximately 5000, 4300, 3700, and 2500 feet/sec and at pressures ranging from $\frac{1}{10}$ to 2 atm.

b) EXPERIMENTAL RESULTS

Melting is clearly visible at all the experimental velocities except the lowest, 2500 feet/sec. By comparing measures of the body on the first and last photographs, we could estimate the mass melted. The nose does not lose material symmetrically but tends to change from cylindrical toward hemispherical shape. Presumably, this change of shape results from the greater air velocity at the corners, the melted material being more easily removed there.[27]

Table 2 contains the experimental data relating to the heat transfer. The accuracy in measurement of length changes depends on the pressure, as the optical distortion by the shock wave is the chief limiting factor. Thus the sixth entry in the table shows the results of two sets of measures under poorest conditions. The other cases are much better, and it would appear that $\pm 0''.01$ is about the limit of measuring accuracy. This value is rather poor, in view of the small melting over the observed base line.

[24] "On the Age and Origin of Meteorites" (doctoral diss., Harvard, 1949); *Phys. Rev.*, **74**, 225, 1948.

[25] For a description of similar apparatus, see n. 9.

[26] One of us (cf. n. 3) had carried out experiments with paraffin projectiles that demonstrated the feasibility of such studies.

[27] The question of the equilibrium shape under such melting is an interesting one. The present experiments do not contain sufficient material to solve the problem.

The last column of Table 2 contains Λ, computed from equation (2) with 0.47×10^9 erg/gm as the energy to melt Woods metal from an initial temperature of 75° F.[28] The cross-sectional area of the Woods-metal cylinder is used for the area factor. The Λ values do not show too great a scatter, in view of the measuring accuracy, and we conclude that Λ is about $1\times10^{-2}\pm50$ per cent uncertainty.

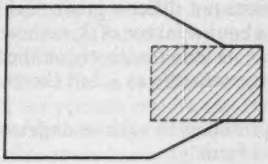

FIG. 3.—Sketch of projectile

TABLE 2

FREE-FLIGHT RESULTS

Rd.	$\bar{v}$ (Feet/Sec)	$\bar{M}$	Air-Density Ratio in Range (to 1.19 $\times10^{-3}$ Gm/Cm^3)	Pressure in Range (Atm.)	Reynolds No. *behind* Shock	$-\Delta l$ (Cm)	$\Lambda\times10^2$
95	4540	4.00	0.093	0.10	4.7×10^3	− 0.013	.....
101	4300	3.79	0.94	1.0	5.1×10^4	+ .101	1.3
102	4460	3.93	0.45	0.49	2.4×10^4	+ .030	0.74
104	3725	3.28	0.93	1.0	6.2×10^4	+ .089	1.5
105	3605	3.18	1.91	2.1	1.3×10^5	+ (.076) (.152)	(1.1) (2.1)
106	4025	3.54	0.46	0.50	2.9×10^4	0.053	1.5
109	2215	1.95	.....	2.0	.....	0	.....
110	2555	2.25	.....	0.50	.....	0	.....

c) DISCUSSION OF RESULTS

We have three items of interest in the present data. First, we inquire whether the results cast any light on the discussion in Section I*c* on the variation of heat transfer with air density. Second, we ask about the numerical value of the heat transfer relative to the value obtained from the meteor results. Finally, we note the value of Λ itself, simply as a measure of the fraction of the energy actually going into heating the moving body. We can offer no comment on the last point other than that the 1 per cent heat transfer at these velocities is indeed quite small. We then consider the first two points of interest.

The physical problem here differs considerably from the flat plate lying parallel to the air stream that was considered in Section I*c*. Indeed, the Woods-metal nose more closely resembles a flat plate held perpendicular to the stream. We can, however, ask whether the general form of the heat-transfer dependence on air density follows the direct or the square-root relation.

1. *The variation of heat transfer with air density.*—The second, third, and fourth entries in Table 1 correspond essentially to the same velocity and the same time of flight and

[28] The melting point of Woods metal is 65°.5 C. The heat of fusion is taken to be 0.4×10^9 erg/gm; and the specific heat to be 0.15×10^7 erg/° C gm.

cover a density range of a factor of 10. While the considerable uncertainty in the experimental values has already been remarked, it seems that the data are sufficiently good to cast doubt on $\sqrt{\rho}$ rather than ρ dependence. The first and second entries differ by a factor of 10 in ρ; if the $\sqrt{\rho}$ dependence were correct, one should have a reduction only by a factor of 3 in the melting from the second entry. No appreciable melting can be detected in the first entry because the measured negative length change reflects the measuring accuracy. The sixth entry does not differ a great deal in velocity; and the third and sixth entries together indicate about a factor of 2, rather than $\sqrt{2}$, reduction at $\frac{1}{2}$ atm. pressure. One cannot, of course, conclude positively on the basis of these rather uncertain results that the heat transfer varies exactly as ρ, but the variation seems to follow ρ more closely than it does $\sqrt{\rho}$.

We note that heat-transfer problems in various engineering applications[7, 29] are often approached in the more general form

$$\frac{h\chi}{\kappa} = \text{Constant}\, P_r^{\alpha} R_e^{\beta} . \tag{21}$$

As we have already noted, $\beta = 0.5$ for laminar and 0.8 for turbulent flow on the basis of calculations for a flat plate ($\alpha = \frac{1}{3}$). A least-squares solution for β from our results, involving the shock-wave relations to obtain $(t_b - t_s)$, gives $\beta = 1.06 \pm 0.15$ (m.e.). This result only emphasizes the need for more experiments in the *air-velocity* range here considered (i.e., free-flight rather than wind-tunnel experiments).

2. *Comparison of the results with meteoric values.*—As has been discussed, the meteor observations give values of

$$\sigma = \frac{\Lambda}{2\Gamma\zeta} .$$

The free-flight observations give directly Λ/ζ and Γ. We note, however, that the measured Γ value applies to the body as a whole, and not just to the Woods-metal nose. Thus, to make the comparison with the meteor results valid, we must use the Γ which the cylindrical Woods-metal nose would have, were it the whole projectile. Some experiments have been performed on the drag of cylindrical-headed projectiles, but the complete variation of Γ with Mach number is not so completely known as that for spheres, for example. From the material on hand, however, we estimate Γ for cylinders to be about 0.60 for the average value applying to the present experiments. We do not expect the value to be in error by as much as 10 per cent. From the data of Table 2 we see that Λ/ζ ranges in value from 1.5×10^{-11} to 4.2×10^{-11}, with no obvious dependence on velocity or air density. Thus, from the present experiments, we have the range in σ values:

$$1.25\times10^{-11} < \sigma < 3.6\times10^{-11} .$$

From the meteor results discussed in Section II, we have the following range in σ:

$$5\times10^{-13} < \sigma < 4\times10^{-12} .$$

Again, as we have stated, there appears to be no obvious dependence on velocity or air density of the σ values.

We note that there probably is not much difference between the Γ value for an average meteor and that for the cylinder considered in the present experiments. On the other hand, the meteoric material most probably vaporizes, rather than melts, from the surface; and the material—either stone or iron—has a higher value for ζ for either melting or vaporizing than does the Woods metal. For vaporization, ζ has been taken as 9×10^{10} in the earlier meteor work; and, for melting, ζ becomes 1.2×10^{10}. Thus we should expect

[29] Cf. H. W. McAdams, *Heat Transmission* (2d ed.; New York: McGraw-Hill Book Co., Inc., 1942).

σ to decrease in the meteor results, as compared with the Woods-metal results, by a factor of 200 for vaporization or a factor of 30 for melting, from the ζ factor alone. If the meteoric material does indeed vaporize, then we must conclude that Λ rises by a factor of 10 or greater in the meteor range of velocity and density over the value inferred from the Woods-metal experiments. If, on the other hand, the meteoric material melts, the necessity of concluding that Λ rises probably remains, but the rise is small. Certainly some kind of rise in efficiency of heating is to be expected; for the accommodation coefficient certainly exceeds 0.01 in the meteor velocity range. Probably the best estimate is a rise in Λ by a factor of 5 from these experiments to meteor results.

It would be extremely worth while to extend the present work to higher velocities. We can predict, on the basis of the present results and the knowledge that the value of Λ will rise at the higher velocities, that we should be able to observe melting phenomena in iron projectiles for a factor of 50 increase in v^3. Melting in Woods metal began in the range 2500–3500 feet/sec under normal atmospheric pressure. Hence, at a velocity of somewhere between 9000 and 13,000 feet/sec, we should be able to observe significant melting in iron projectiles. These velocity values are *upper limits*, since Λ is expected to increase.

IV. WIND-TUNNEL RESULTS

Our results in this section come through the kindness of the Naval Ordnance Laboratory group under Dr. H. H. Kurzweg. We are particularly indebted to Mr. J. M. Kendall.

TABLE 3

WIND-TUNNEL EXPERIMENTS ON SOLID CO_2

Mach No.	Velocity (w Sec^{-1})	Air Density (Gm Cm^{-3})	Mass Loss (Gm Sec^{-1}Cm^{-2})	Λ
1.87.....	483	3.28×10^{-4}	4.3×10^{-2}	1.35×10^{-2}
4.25.....	673	2.66×10^{-5}	1.0×10^{-2}	1.42×10^{-2}

One of us suggested the possibility of rate-of-mass-loss measures on a dry-ice model in the Naval Ordnance Laboratory supersonic wind tunnels (because of the low air speed in such tunnels, one is forced to use very low-boiling-point substances). Table 3 contains the data from these experiments.

We see that the results on Λ are in excellent agreement with those from the free flight experiments on Woods metal and that they further support the linear dependence of heat transfer upon air density. The wind-tunnel experiments are, of course, inherently limited with respect to the free-flight experiments if we wish to test any great range of materials.

V. PITTING ON METEORS AND THE IGNITION POINT OF MAGNESIUM

a) PITTING ON METEORS

A glance at a few of the larger museum meteorite specimens shows that their surfaces are covered to a great extent by depressions, pits, and holes, with diameters of the order of inches. An unpublished study of the Goose Lake meteorite by E. P. Henderson and S. H. Perry indicates almost conclusively in this case that weathering could not have been responsible for the pitting in this large iron meteorite weighing 2573 pounds. The striking characteristic of many of the pits in the Goose Lake meteorite is the fact that the internal cross-section is larger than the cross-section near the surface of the body.

Because of ablation, we believe that the major portions of the pits on such a meteorite could not directly represent holes that were already present when the meteor struck the atmosphere. On the other hand, there is every reason to believe that meteoroids in space are frequently struck by smaller meteoroids, which would produce a large array of or-

dinary-shaped crater pits, ranging in size from microscopic dimensions to dimensions comparable with the meteoroid. One would not expect these "crater" pits to penetrate so deeply into the meteor as the "worm-hole" pits on which we seek to comment. We need, then, a mechanism to extend such crater pits deeply into the meteor. Some additional experiments performed by us with the facilities of the Naval Ordnance Laboratory cast a suggestive light on such a mechanism.

b) THE IGNITION POINT OF MAGNESIUM

In the course of the Woods-metal experiments it became evident that melting does not occur below Mach numbers somewhat higher than those at which the stagnation temperature reaches the melting point. We have already seen, however, that the whole phenomenon of heat transfer in this astroballistic region may possibly be better approached by ignoring the concept of temperature difference between gas and solid and by considering heat-transfer efficiency *as though* the gas atoms collided individually with the solid (even though such a naïve picture is certainly incorrect in its details). Then the value of Λ may be regarded as measuring a combination of this degree of inelasticity of collision between one gas atom and the surface and the likelihood of collision with the surface rather than with other atoms alone. Hence one way to raise the effective Λ value is to alter the geometry of the surface to increase these preceding two processes. We note here, of course, that the same idea may be presented from the thermal viewpoint. We recognize that stagnation temperature in the gas occurs only in a limited region at the very center of the cylindrical head. Thus, in order to raise a significant fraction of the surface to the melting point, one must either go to higher Mach numbers or alter the geometry of the surface in some such way that stagnation temperature holds over a greater area.

A straightforward method of increasing the "contact" area, or area over which stagnation conditions hold, is simply to make the front surface of the cylinder concave. Drag measures on such a body show a considerable increase as compared with such measures on a body with a flat face. One might also ask whether the results cannot be accomplished by roughening the front surface. We have studied such a method briefly. As a more sensitive indicator than the melting phenomenon, the flare point of magnesium was used. The flare point occurs at some 750° C, corresponding to stagnation conditions at Mach 3.7 and standard atmospheric temperature, or about 4200 feet/sec. The projectiles used in the study had a muzzle velocity of about 6000 feet/sec. Those projectiles whose flat front surface was nicely polished before firing did not flare. The same negative result occurred when the front of the surface was defaced, no indentation being much more than 1 mm or so in depth. However, when a circular "moat" was cut into a front surface (which was otherwise highly polished), flaring occurred. The phenomenon is reproducible. The distance of travel before flaring appears to vary with the diameter of the "moat," but, owing to lack of time allowed for the use of the experimental facilities, no detailed measures were made.

We interpret the results in the same manner as those for the drag on a body with a concave front. Stagnation conditions hold in the concavity, and the flare point occurs there (spreading out, of course). Now, if the flow pattern were such as to empty the cavity of molten material continuously, we should expect the cavity to propagate into the body at a more rapid rate than the outer surface melts. Thus we suggest the likelihood that the deep holes in meteorites may well represent the enlargement of initial, shallow "crater" pits according to the same mechanism as our magnesium flaring results.

The suggestion is difficult to check experimentally unless some method can be devised to recover the projectiles without damaging their front surfaces or to photograph them end-on in flight. One should probably prefer experiments with iron projectiles. Thus again we point out the desirability of carrying out experiments at velocities above 10^4 feet/sec if the proper launching device can be made available.

VI. SUMMARY

The results on the heat-transfer coefficient, Λ, from the various sources have been discussed in detail in the separate sections. In summary, we conclude that a value of Λ (see eq. [2] for definition) between 1×10^{-2} and 1.5×10^{-2} seems a reasonable estimate for velocities between 0.5 and 1.5 km/sec and in a range of air densities from 3×10^{-5} to 4×10^{-3} gm cm^{-3}. Moreover, the use of the formula

$$\text{Heat transfer} = \Lambda \frac{\rho v^3}{2}$$

seems to give a fair representation of the results over a factor of 200 range in ρ and of 3 in v. When we reach the meteor range of ρ and v—lying between 10^{-6} and 10^{-9} gm cm^{-3} and 8–65 km/sec, respectively—the value of Λ is not so well settled. On the basis of the present meteor observations, we can find no conspicuous correlation of Λ with ρ or v over the meteoric range. We can, however, conclude definitely that Λ increases by at least a factor of 3 when we pass from the ballistic region to the meteoric, since probably the best estimate we can make on the basis of our meteor data gives $\Lambda \sim 5\times10^{-2}$ in the meteor range. We must leave largely unexplained a variation by a factor of nearly 10 in the quantity $\sigma = \Lambda/(2\Gamma\zeta)$ for meteors, although we have presented several quasi-interpretations of the variation. We believe that further laboratory experimental investigation must be carried out in the velocity range 1.5–10 km/sec, at a variety of air densities. With these results and the meteor data now on hand and currently being obtained, the question of heat transfer in the astroballistic regime may be finally settled. We see no fundamental difficulty in the path of such a program.

We call attention to the great simplification in the computations of the heat transfer to rapidly moving bodies in the ballistic and aerodynamic regions that the above work implies. Use of the meteor formula,

$$\text{Heat transfer} = \frac{\Lambda}{2} \rho v^3 ,$$

rather than of the aerodynamic-ballistic formula,

$$\text{Heat transfer} = h\,(t_s - t_b) ,$$

eliminates the need of knowing the body temperature, t_b, or the stagnation temperature, t_s. We need know only air speed and air density, the two quantities that are always available. The implication of the result for aerodynamic and ballistic research is obvious.

We are deeply indebted to a number of people who have contributed to our thinking and aided in obtaining the results here presented. From the meteor standpoint we are indebted to L. Jacchia for his analysis of the extensive meteor data, and to E. Öpik for extended discussion over the physical theory of meteors. From the same sense, extended to the more general case of the general high-speed reaction between solid and medium, we are especially indebted to M. A. Cook, H. Eyring, and J. S. Rinehart. We are extremely grateful for the use of the Naval Ordnance Laboratory facilities, made possible by R. J. Seeger, and the co-operation in the research there of H. H. Kurzweg, H. Polachek, J. M. Kendall, D. Shanks, G. R. Eber, B. M. Shepard, C. E. Patton, and W. T. Whelen. In our early work in high-velocity ballistics we have been particularly aided by A. C. Charters and members of the Aerodynamics Free-Flight group at Aberdeen. E. P. Henderson has shown great consideration in providing us with the results of his extensive investigations and unpublished manuscripts on meteor pitting.

LABORATORY STUDIES OF THE λ 4050 GROUP OF COMETARY SPECTRA*

A. E. DOUGLAS
Division of Physics, National Research Council, Ottawa, Canada
Received April 16, 1951

ABSTRACT

The group of bands occurring in the spectra of comets near 4050 A has been produced in the laboratory and photographed under high resolution. By using deuterium in the source, it has been verified that the molecule emitting the bands does not contain hydrogen; by using the C^{13} isotope, it has been indicated that the emitter does contain more than one carbon atom. Although the exact composition of the emitting molecule has not been unambiguously determined, evidence from the fine structure of the 4050 A band and the isotope effect indicate that it may be a linear triatomic carbon molecule, C_3.

A group of emission bands which appears to be identical with that occurring near λ 4050 in the spectrum of comets was first produced in the laboratory by Herzberg.[1] He suggested that they might be due to the CH_2 molecule. Later, by the use of deuterium, Monfils and Rosen showed that the CH_2 molecule could not be the emitter, but they suggested no other.[2] The work described below was initiated in order to determine the emitter of these bands. Though this objective has not yet been reached, the importance of these bands in the study of cometary and possibly stellar spectra[3] seems to warrant publication of the results obtained up to this time.

The λ 4050 bands have been excited in a discharge through a mixture of xenon and hydrogen between carbon electrodes. This method of excitation (first described by Herman[4]) produces the bands relatively free from overlapping. The bands were photographed in the third order of a 6-meter concave grating, and the plates show a resolving power of about 200,000.

The strongest of the bands is shown in Figure 1, *A*. This band appears to consist of a *P*, a *Q*, and an *R* branch. The wave numbers of the lines, together with a possible *J* numbering, are given in Table 1. The lines of the *P* and *Q* branches are regularly spaced and with few exceptions have a regular intensity distribution, but the lines of the *R* branch are not quite so regularly spaced and have a rather irregular intensity distribution. While this effect may be due to an overlapping of lines, it is not certain that all the *R* branch lines listed in Table 1 are true members of the branch.

A tentative analysis of the band has been made, assuming that the band is emitted by a $\Sigma - \Pi$ transition of a linear triatomic carbon molecule. The fact that the nuclear spin of C^{12} is zero causes every other level of the Σ state, and thus every other line of the band, to be missing. These assumptions seem to lead to the most regular arrangement of energy levels. The analysis gives the following rotational constants:

$$B' = 0.412\ \text{cm}^{-1}, \qquad B'' = 0.430\ \text{cm}^{-1},$$
$$D' = 0.26 \times 10^{-6}\ \text{cm}^{-1}, \qquad D'' = 0.87 \times 10^{-6}\ \text{cm}^{-1}.$$

Though the correct numbering of the lines is not definitely known, it appears unlikely that it can be shifted by more than one unit from the numbering given in Table 1. The analysis appears reasonably satisfactory, but two unusual points should be noted. First,

* *Contributions from the National Research Council*, No. 2503.
[1] *Ap. J.*, **96**, 314, 1942.
[2] *Nature*, **164**, 713, 1949.
[3] A. McKellar, *Ap. J.*, **108**, 453, 1948.
[4] *C.R.*, **223**, 280, 1946.

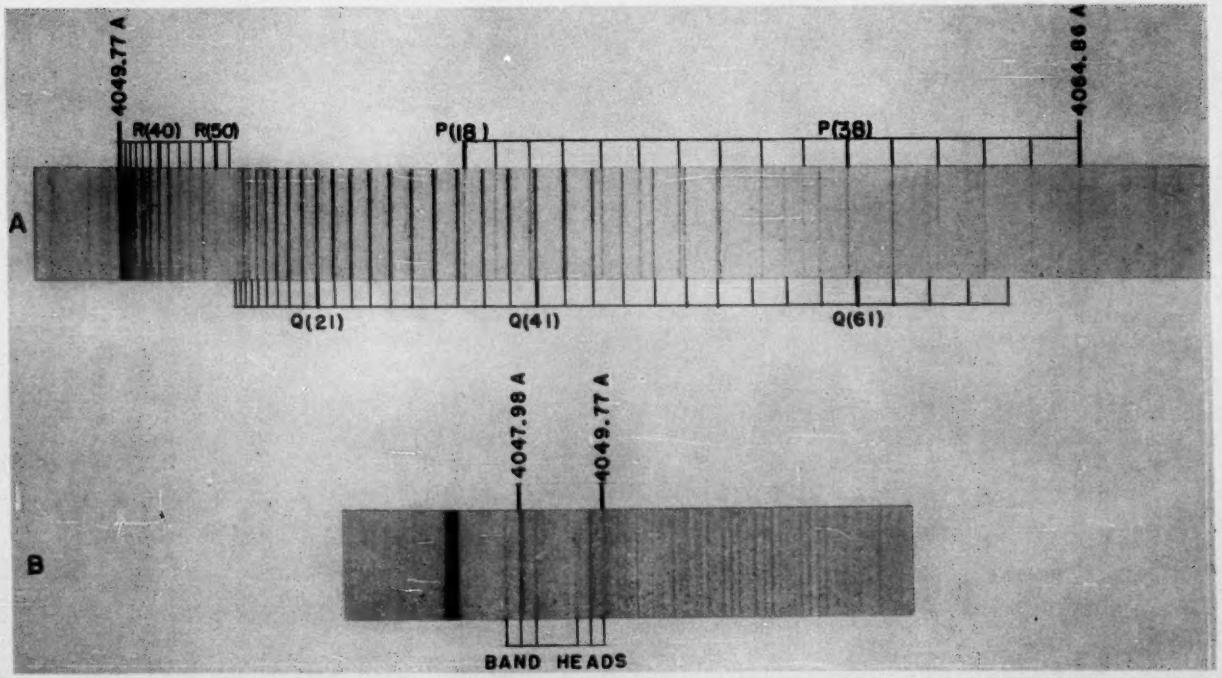

FIG. 1.—The spectrum of the strongest band of the λ 4050 group. *A* shows the band from a source containing natural carbon. *B* shows the same band from a source containing carbon enriched in the C^{13} isotope.

the D values are from two to four times larger than one would expect, and, second, the Λ-type doubling of the $^2\Pi$ state does not vary as $J(J+1)$ and is large even for $J = 0$. The fact that a large D value must exist for at least one of the states can be deduced from the spacing of the lines of the P and Q branches. The large Λ doubling may not be real and may result from an incorrect numbering of the lines.

The bands have also been excited by using carbon in which the C^{13} isotope concentration had been enriched up to 50 per cent. The spectrum that one obtains from this mixture is very complex, and none of the fine structure can be analyzed. A portion of the spectrum is shown in Figure 1, B. On the basis of this complexity alone, one can be al-

TABLE 1

J	$Q(J)$	J	$P(J)$	$R(J)$
3	24675.54(?)	16	24657.35	.....
5	75.20	18	54.59	.....
7	74.75	20	51.77	.....
9	74.22	22	48.68	.....
11	73.52	24	45.46	.....
13	72.68	26	42.09	24685.78
15	71.72	28	38.61	85.57
17	70.61	30	35.05	85.27
19	69.38	32	31.37	84.93
21	68.02	34	27.59	84.44
23	66.54	36	23.77	83.85
25	64.92	38	19.75	83.18
27	63.21	40	15.73	82.38
29	61.37	42	11.57	81.51
31	59.42	44	07.33	80.57
33	57.35	46	03.04	79.53
35	55.20	48	598.66	78.41
37	52.94	50	94.17	77.23
39	50.59	52	89.64	75.97
41	48.15			
43	45.58			
45	42.97			
47	40.25			
49	37.45			
51	34.57			
53	31.63			
55	28.59			
57	25.49			
59	22.32			
61	19.06			

most certain that the molecule emitting the bands contains more than one carbon atom. Still more convincing is the fact that with the mixture of isotopes the band head at 4049 A obtained using C^{12} is replaced by six heads, at least two of which are more intense than the C^{12} head. The displacements of the six heads from the C^{12} head are 0, 1.9, 3.6(?), 9.0, 11.0, and 12.9 cm^{-1}. These band heads can be interpreted as being the six heads that one would expect from a linear C_3 molecule. If one assumes that the band is a (000, 000) band, then one is forced to accept the fact that the symmetric stretching frequencies of the C_3 molecule in the upper and lower states are nearly equal but that the sum of the antisymmetric stretching frequency plus twice the bending frequency is about 650 cm^{-1} greater in the lower state than in the upper state.

The work of Monfils and Rosen has been repeated by using deuterium in place of hydrogen along with xenon in the discharge tube. The spectra so obtained confirm their result, in that this isotopic substitution does not change the position of the bands. Also,

it was found that the lines of the Q branch measured on plates taken with deuterium in the discharge tube show no shift with respect to those taken with hydrogen in the tube. Since the accuracy of measurement is better than 0.05 cm^{-1}, it appears certain that there is no hydrogen in the molecule that emits the bands.

All the other bands of the system appear to be more complex than the band discussed above. A number of series of lines can be found in these bands, but no analysis has been possible. Also all the other band heads, except for one at 4038.4 A, are not sharp, so that high-dispersion plates give no better measurements than those obtained with medium dispersion. This diffuseness of the band heads makes it impossible to measure the C^{13} isotope shift on bands other than the band at 4049 A.

The problem of determining the emitter of the bands is still a difficult one. The assumption that the molecule is a linear C_3 molecule has some merit. The presence of a relatively simple band seems to point to a linear molecule. The rotational constant B'', which corresponds to an internuclear distance of 1.28 A, is a reasonable one for a C_3 molecule. The carbon isotope experiment tends to support the idea. Also, from a wide variety of experimental conditions, it appears that carbon and hydrogen are the only two elements necessary for the excitation of the bands, and it is known that hydrogen is not present in the emitting molecule. On the other hand, it can be pointed out that the B values have been obtained from a rather uncertain analysis, in which it has been assumed that every other line is missing. If this assumption had not been made, B values of about 0.8 cm^{-1} would have been obtained. The D values are high, and the relationship $\omega^2 = 4B^3/D$ gives $\omega'' = 600$ cm^{-1} and $\omega' = 1000$ cm^{-1} for the vibrational constants of the symmetric stretching frequency in the upper and lower states. The results of the carbon isotope experiment indicate that these two values should be the same. At present there is no satisfactory vibrational analysis to account for all the bands. One also has to recognize that past experience has shown that the conditions of excitation do not always lead to reliable conclusions regarding the nature of the emitter of a band system. All that can be stated definitely is that here we are dealing with a molecule that contains no hydrogen and does contain more than one carbon atom. Of all molecules that have been considered, the C_3 molecule leads to the fewest difficulties.

Two experiments, either of which might definitely determine the emitter of the bands, have been considered. First, it may be possible to excite the bands at a low temperature. This should increase the intensity of the lines of low rotational quantum number and thus make possible an unequivocal analysis of some of the bands. A more definite experiment would be that of using nearly pure C^{13} in a source. If the molecule is a linear C_3 molecule, then C^{13} will give bands with twice as many lines as C^{12}. Up to the present, however, I have been unable to find a suitable low-temperature source and have been unable to secure a sample of C^{13} of sufficient purity.

I wish to thank Dr. G. Herzberg for suggesting this problem and for helpful advice during the course of the work.

TRANSITION PROBABILITIES OF FORBIDDEN LINES

DONALD E. OSTERBROCK*
Yerkes Observatory
Received June 29, 1951

ABSTRACT

Transition probabilities are given for a number of forbidden lines of astrophysical interest. Also, from the computed transition probabilities, expected equivalent widths of [*Ca* II] and [*S* I] forbidden absorption lines in the solar spectrum are calculated.

I. INTRODUCTION

A knowledge of the transition probabilities of forbidden lines is important not only for making identifications but also for discussing the physical conditions in the objects which emit these lines. In this paper the transition probabilities are given for a number of forbidden lines of astrophysical interest. Besides the transition probabilities of the observed lines, probabilities are computed for the other transitions which compete with them in removing atoms from the excited levels. In each case the computations have been carried out by the methods of Shortley,[1] calculating the line strengths first and then, from them, the transition probabilities.

II. THE *Ca* II 4^2S-3^2D DOUBLET

The *Ca* II 4^2S-3^2D doublet has been identified and studied in υ Sagittarii by Merrill[2] and by Greenstein and Merrill.[3] These lines occur only by quadrupole transitions, and, from the simple formulae for the case of one electron outside a closed shell, the line strengths are found to be

$$S_q(3^2S_{1/2},\ 4^2D_{5/2}) = 36\, s_q^2(4d,\ 3s),$$

$$S_q(3^2S_{1/2},\ 4^2D_{3/2}) = 24\, s_q^2(4d,\ 3s),$$

in terms of the radial integral

$$s_q(4d,\ 3s) = -\frac{1}{3\sqrt{5}} \int_0^\infty r^2 R(4d) R(3s)\, dr.$$

This integral was evaluated numerically from the Hartree wave functions with exchange[4] for *Ca* II and was found to have the value $s_q = 10.83/3\sqrt{5} = 1.61$ atomic units. The cancellation between positive and negative portions of the integral, the importance of which for judging the reliability of the results has been emphasized by Bates,[5] is negligible, for the last 4s loop contributes 10.896, while the second-last loop contributes -0.068, and the first two loops do not affect the result at all. Transition probabilities, computed using the observed energy difference, are given in Table 1.

* Atomic Energy Commission Pre-doctoral Fellow in Astrophysics.

[1] *Phys. Rev.*, **57**, 225, 1940. Definitions of line strengths and all other quantities used are given in Shortley's paper and therefore are not repeated here.

[2] *Pub. A.S.P.*, **55**, 242, 1943.

[3] *Ap. J.*, **104**, 177, 1946.

[4] D. R. Hartree and W. Hartree, *Proc. R. Soc. London, A*, **164**, 167, 1938.

[5] *Proc. R. Soc. London, A*, **188**, 350, 1947.

The magnetic dipole strength of the transition $4^2D_{3/2} \leftarrow 4^2D_{5/2}$ is $\frac{1}{5}^2$, and the corresponding transition probability is given in Table 1. This transition can also occur by quadrupole radiation, but the probability is smaller by a factor of about 10^{-5} and has therefore not been calculated. The smallness of the $^2D_{3/2} \leftarrow {}^2D_{5/2}$ transition probability shows that the $^2D_{5/2}$ level is not drained by this transition.

TABLE 1

TRANSITION PROBABILITIES OF FORBIDDEN LINES*

Ion	Transition	Coupling Parameter x	Wave Length	Transition Probability (Sec^{-1})	
				Electric Quadrupole	Magnetic Dipole
Ca II.....	4s–3d $^2S_{1/2}-{}^2D_{5/2}$	.....	7291.46	1.3	.....
	$^2S_{1/2}-{}^2D_{3/2}$	.....	7323.88	1.3	.....
	3d $^2D_{3/2}-{}^2D_{5/2}$	.....	.....	—	2.4×10^{-6}
Fe XV.....	3s3p $^3P_0^0-{}^3P_2^0$	.....	7059.62	1.6×10^{-3}	38
	$^3P_1^0-{}^3P_0^0$	.....	.....	1.8×10^{-3}	.....
A XI.....	$2p^4$ $^3P_2-{}^3P_1$	0.270	6919	3.0×10^{-4}	67
	$^3P_2-{}^3P_0$	.....	5414	1.5×10^{-3}	.....
	$^3P_1-{}^3P_0$	.....	.....	.....	3.4
K VI.....	$3p^2$ $^1D_2-{}^1S_0$	0.1369	4097?	8.1	.....
	$^3P_2-{}^1S_0$	.....	.....	0.30	.....
	$^3P_1-{}^1S_0$	.....	.....	.....	15
Ca VII....	$3p^2$ $^1D_2-{}^1S_0$	0.1701	3688	8.9	.....
	$^3P_2-{}^1S_0$	.....	.....	0.53	.....
	$^3P_1-{}^1S_0$	.....	.....	.....	33
S I.....	$3p^4$ $^1D_2-{}^1S_0$	0.0517	7724.7	4.1	.....
	$^3P_1-{}^1S_0$	.....	4589.0	.....	0.34
	$^3P_2-{}^1S_0$	.....	4506.9	0.015	.....
Cl II.....	$3p^4$ $^1D_2-{}^1S_0$	0.0719	6152.9	5.2	.....
	$^3P_1-{}^1S_0$	.....	3675.0	.....	1.3
	$^3P_2-{}^1S_0$	.....	3583.0	0.044	.....
A III.....	$3p^4$ $^1D_2-{}^1S_0$	0.0959	5191.4	6.2	.....
	$^3P_1-{}^1S_0$	.....	3109.0	.....	3.2
	$^3P_2-{}^1S_0$	.....	3005.1	0.090	.....
K IV.....	$3p^4$ $^1D_2-{}^1S_0$	0.1239	4511.0	7.0	.....
	$^3P_1-{}^1S_0$	.....	.....	.....	10
	$^3P_2-{}^1S_0$	.....	.....	0.17	.....
Kr III....	$4p^4$ $^3P_2-{}^1D_2$	0.4148	6826.9	—	4.7
	$^3P_1-{}^1D_2$	.....	9902.2	—	0.53
Xe III....	$5p^4$ $^3P_2-{}^1D_2$	1.014	5846.3	—	21
	$^3P_1-{}^1D_2$	.....	.....	—	0.62
	$^3P_2-{}^3P_1$	.....	10206.5	—	19

* Wave lengths from the *RMT* are given for lines in the observable regions.

III. THE [*Fe* XV] 3s3p $^3P_1^0-{}^3P_2^0$ TRANSITION

The [*Fe* XV] 3s3p $^3P_1^0-{}^3P_2^0$ transition is the only coronal line identified by Edlén[6] as arising from a highly excited state (E.P. = 31.9 volts) and not from a transition within the ground configuration. In pure LS coupling the magnetic dipole line strength of a $^3P_1-{}^3P_2$ transition is $S_m = \frac{5}{2}$; but, if the breakdown of coupling is taken into account, the $^3P_1^0$ and $^1P_1^0$ levels are mixed. If we write $\psi(^3P_1^{0\prime})$ and $\psi(^1P_1^{0\prime})$ as the actual eigenfunctions, and $\psi(^3P_1^0)$ and $\psi(^1P_1^0)$ as the LS eigenfunctions, then

$$\psi(^3P_1^{0\prime}) = a\psi(^3P_1^0) + b\psi(^1P_1^0),$$

$$\psi(^1P_1^{0\prime}) = -b\psi(^3P_1^0) + a\psi(^1P_1^0),$$

[6] *Zs. f. Ap.*, 22, 30, 1943.

and the magnetic dipole line strength is $S_m(^3P_1^{0\prime}, {}^3P_2^0) = \frac{5}{2}a^2$. The sp configuration is a special case of the sl configuration, which has been worked out completely,[7] and in which all results can be expressed in terms of the single coupling parameter $\chi = 3\zeta/4G_0$. In terms of this parameter,

$$a = 1 - \tfrac{1}{9}\chi^2 + \tfrac{2}{27}\chi^3 + \tfrac{5}{164}\chi^4 + \ldots .$$

Only the asymptotic expansion for small χ is given here, because all the experimental data fall in this range. For evaluating χ, only the ^3P splitting is available in the case of *Fe* XV, and the ratio[8] $(^3P_2^0 - {}^3P_1^0)/(^3P_1^0 - {}^3P_0^0) = 2.43$ gives $\chi = 0.202$, which, in turn, gives $a = 0.996$ and $S_m = 2.48$. The resulting transition probability, calculated with the observed coronal wave number, is given in Table 1.

Similarly, the quadrupole line strengths of the transitions from the $^3P_2^0$ level are found to be

$$S_q(^3P_2^0, {}^3P_1^{0\prime}) = \tfrac{15}{16}a^2 s_q^2(3p, 3p),$$

$$S_q(^3P_2^0, {}^3P_0^0) = \tfrac{15}{81}s_q^2(3p, 3p),$$

from the formulae applying for the two-electron case. Here

$$s_q(3p, 3p) = -\frac{2}{5}\int_0^\infty r^2 R(3p) R(3p)\, dr .$$

The value of this radial integral has been estimated by taking the effective charge acting on the 3p electron to be $10\frac{1}{2}$ atomic units and using the hydrogen-like approximation. This procedure gives a value $s_q(3p, 3p) = 0.30$ atomic units. The wave number for the $^3P_0^0 - {}^3P_2^0$ transition was obtained by using the laboratory value of the ratio $(^3P_2^0 - {}^3P_1^0)/(^3P_1^0 - {}^3P_0^0)$ and the coronal wave number of the $^3P_2^0 - {}^3P_1^0$ transition; and the resulting transition probabilities are tabulated in Table 1. The extreme smallness of the quadrupole transition probabilities in comparison with the magnetic dipole transition probabilities has been emphasized many times in previous work on forbidden lines.

IV. THE p^n FORBIDDEN TRANSITIONS

Fairly recently a number of forbidden lines whose transition probabilities were not given either by Pasternack[9] or by Edlén[6] have been identified.[10] These transition probabilities may easily be calculated from the tables published by Shortley, Aller, Baker, and Menzel,[11] but it has seemed worth while to give the final numerical results here. Transition probabilities are given only for the p^2 and p^4 configurations, and in these cases the effects of the spin-spin and spin–other-orbit matrix elements[12] on the transition probabilities are small and can safely be neglected. The estimates of the radial integrals as given by Pasternack[9] have been used in calculating the quadrupole probabilities, and for *A* XI the value $s_2 = \frac{5}{2}s_q = 0.124$ was estimated from the extrapolated F_2 by his method. In the $4p^4$ and $5p^4$ configurations the quadrupole moments can hardly be found

[7] See E. U. Condon and G. H. Shortley, *The Theory of Atomic Spectra* (Cambridge: At the University Press, 1935), p. 271, and references given there.

[8] B. Edlén, *Zs. f. Phys.*, **103**, 536, 1936.

[9] *Ap. J.*, **92**, 129, 1940.

[10] See P. Swings, *J. Opt. Soc. America*, **41**, 153, 1951, and references given there.

[11] *Ap. J.*, **93**, 178, 1941.

[12] L. H. Aller, C. W. Ufford, and J. H. Van Vleck, *Ap. J.*, **109**, 42, 1949.

in this way, because of the different regions in the ion effective in determining F_2 and s_q, and so only the magnetic dipole transition probabilities are given for these cases. The quadrupole transition probabilities are very low anyhow, in comparison with the magnetic dipole probabilities, except for the $^1D_2-{}^1S_0$ transition, which is not likely to be observed because of the high excitation energy required. In all cases the value of the coupling parameter χ was calculated from the ratio $(^3P_2-{}^3P_0)/(^1D_2-{}^3P_2)$, and the line strengths were obtained either from the tables[11] or, for low χ, from their asymptotic expressions. In the $3p^4$ configurations the energies of the $^1S_0$ levels, as located by Edlén[13] and given in the table of atomic energy levels[14] were used, while in the $3p^2$ configuration the extrapolated positions as given in the *RMT*[15] were used. For *A* XI, the extrapolated values of χ and $^3P_2-{}^3P_1$ (which has been confirmed by the identification[16] of this line in the post-maximum spectrum of RS Ophiuchi) given by Edlén[6] have been used. The numerical results are collected in Table 1.

V. FORBIDDEN LINES IN ABSORPTION

As Bowen[17] has pointed out, forbidden transitions may be observed in absorption as weak lines. Using the transition probabilities computed above, expected equivalent widths in the solar spectrum of the [*Ca* II] and [*S* I] lines have been calculated by Minnaert's[18] detailed theory of weak lines. The abundances assumed, together with the calculated widths, are given in Table 2. If the [*S* I] 7725 line could be observed in a star,[17]

TABLE 2

CALCULATED EQUIVALENT WIDTHS OF FORBIDDEN LINES IN THE SOLAR SPECTRUM

Ion	Assumed Abundance Relative to Hydrogen	Wave Length (A)	Equivalent Width (mA)
Ca II.....	1.6×10^{-6}	7291.46	10.5
		7323.88	7.2
S I.....	2×10^{-5}	7724.7	1.9
		4589.0	0.5

say HD 45677, so that an accurate wave length could be determined, it might be possible to observe this line in absorption in the sun and determine a value for the solar abundance of sulphur. There are atmospheric O_2 lines[19] at λ 7724.59 and λ 7724.88.

I wish to thank Professor S. Chandrasekhar for reading the manuscript and discussing it with me, and Professor B. Strömgren for discussing the problem of weak solar lines. Also I wish to thank the Atomic Energy Commission for fellowship support during the time this work was done.

[13] *Phys. Rev.*, **62**, 434, 1942.

[14] C. E. Moore, *Atomic Energy Levels as Derived from the Analyses of Optical Spectra*, Vol. 1 (Circ. No. 467 of the National Bureau of Standards [1949]).

[15] C. E. Moore, *A Multiplet Table of Astrophysical Interest* (rev. ed.) (*Contr. Princeton U. Obs.*, No. 20 [1945]).

[16] A. H. Joy and P. Swings, *Ap. J.*, **102**, 353, 1945.

[17] *Rev. Mod. Phys.*, **20**, 109, 1948.

[18] *B.A.N.*, **10**, 339, 399, 1948.

[19] H. D. Babcock and C. E. Moore *The Solar Spectrum, λ 6600 to λ 13495* (*Carnegie Institution of Washington Publications*, No. 579 [1947]).

THE *Ba* II STARS*

WILLIAM P. BIDELMAN AND PHILIP C. KEENAN
Yerkes, McDonald, and Perkins Observatories
Received July 16, 1951

ABSTRACT

The spectroscopic characteristics of a newly discovered group of peculiar G- and K-type stars are described. All the stars discussed show abnormally strong lines of ionized barium, as well as *CH*, C_2, and probably also *CN* bands of anomalous intensity. The strength of the lines of *Ba* II is not due to high luminosity but appears rather to be associated with an atmospheric carbon abundance intermediate between that of normal stars and that of members of the presently accepted carbon-star group. The possible connection between the *Ba* II stars and the stars of type S is briefly discussed.

INTRODUCTION

The extraordinary strength of one of the resonance lines of ionized barium, λ 4554, has long been known as one of the distinctive characteristics of the spectra of stars of type S.[1] This line is also well marked in the cooler carbon stars, being very strong indeed in some objects such as HD 59643, class $C6_2$, and the star V CrB, class $C6_3$. Furthermore, it has been noted to be somewhat enhanced in the *CH* stars.[2] Among the normal stars of earlier type, the line λ 4554 was shown by Morgan[3] to increase greatly in strength with increasing luminosity after spectral type F5, while Miss Burwell stated that it was stronger in the spectra of δ CMa and ρ Cas, both type F8 I*a*, than in any other star of known absolute magnitude, aside from stars of classes S and N.[4] Since the neutral barium atom has an ionization potential of only 5.2 e.v., a positive absolute-magnitude effect of the resonance lines of the ionized atom in the late-type stars is to be expected. It is conceivable that the great enhancement of the λ 4554 line in the spectra of the S-type stars and in some of the carbon stars is a natural consequence of the low temperatures and low pressures in these stellar atmospheres.

The stars to be discussed in this paper are a group of G- and K-type stars which show very strong lines of *Ba* II but which, however, do not appear to be supergiant stars. These stars appear to be related to the carbon stars. The existence of this heretofore unstudied group of stars casts considerable doubt on the hypothesis that the strength of λ 4554 in the stars of classes S and N is purely a consequence of ionization and excitation processes taking place in stellar atmospheres in thermodynamic equilibrium.

THE *Ba* II STARS

The objects which we now consider as members of the *Ba* II star group are given in Table 1. Low-dispersion spectra (76 A/mm at $H\gamma$) of the photographic region of these stars are reproduced in Figure 1, together with spectra of a G5 II star, β Scuti, and a K0 III star, ν Ophiuchi. All the *Ba* II stars show, in addition to an abnormally strong line at λ 4554, a definite enhancement of the G band (due to *CH*) and also, probably, of the violet bands of *CN* as well. The lines of *Sr* II at λ 4077 and at λ 4215 [the latter blended with the head of the (0, 1) *CN* band] are also strengthened, the case of ζ Capri-

* *Contributions from the McDonald Observatory, University of Texas*, No. 203.

[1] P. W. Merrill, *Mt. W. Contr.*, No. 306; *Ap. J.*, **63**, 13, 1926.

[2] P. C. Keenan, *Ap. J.*, **96**, 101, 1942.

[3] *Ap. J.*, **77**, 291, 1933.

[4] *Mt. W. Contr.*, No. 598; *Ap. J.*, **88**, 278, 1938.

corni being notable. In normal stars the increased intensities of the lines of *Ba* II, of *Sr* II, and of the *CN* band would indicate a very high luminosity for these objects; however, the hydrogen lines are not strong enough to permit us to consider these stars as normal supergiants. It is significant in this connection that HR 5058 was classified as a subgiant at the Mount Wilson Observatory.[5] This conclusion concerning the weakness of the hydrogen lines is not quite so certain in the case of ζ Capricorni, which, to judge by the weakness of *Ca* I λ 4226, is the earliest in type; but the correct spectral type of ζ Capricorni is in any case difficult to assess. In short, the stars of this group cannot be fitted into the spectral-class–luminosity-class array defined by the normal stars.

We have obtained higher-dispersion spectra (27 A/mm at $H\gamma$) of the photographic and visual region of all the stars of Table 1 except HD 211594. In their peculiarities these spectra are closely similar. An inspection reveals the following facts in all cases:

A. The lines of ionized barium arising from the first excited levels (e.p. 0.7 and 0.6

TABLE 1

NAME	m_v	(1900) α	(1900) δ	λ	β	μ	RV (KM/SEC)	TRIG. π	REMARKS
HR 774.....	5.92	2^h33^m4	+81° 1′	95°	+20°	0".070	+24	.....	1
HR 2392.....	6.38	6 28.1	−11 6	188	− 8	.009	.....	.....	2
HR 5058.....	5.25	13 20.3	−39 14	278	+22	.193	+68	0".007	3
ζ Cap.....	3.86	21 21.0	−22 51	355	−45	.024	+ 3	−0.015	4
HD 211594...	8.3	22 13.1	− 6 21	25	−49	0.024	.....	.....	5

NOTES TO TABLE 1

1. Strong λ 4554 was noted at the David Dunlap Observatory (*Pub. David Dunlap Obs.*, 1, 311, 1945).
2. The *Henry Draper Catalogue* suggests that this star may be intermediate between classes K and R.
3. Strong λ 4554 was noted at the Mount Wilson Observatory (*Mt. W. Contr.*, No. 511; *Ap. J.*, 81, 187, 1935).
4. Strong lines of *Sr* II and *Ba* II were noted by Miss Maury (*Harvard Ann.*, 28, 97, remark 111, 1897).
5. The *Henry Draper Catalogue* suggests that the *CN* absorption is abnormally strong.

volts) are greatly enhanced, as well as those from the ground level; consequently, we are not dealing with a mechanism affecting only the resonance lines.

B. The head of the (0, 0) band of the Swan system of C_2 at λ 5165 shows clearly in the *Ba* II stars, whereas it does not appear at all on similar spectrograms of the many normal stars investigated in this region. The star ζ Capricorni is thus the star of greatest apparent brightness known to show the C_2 bands in appreciable strength.

C. The abnormal strength of the bands of *CH* is very apparent on the higher-dispersion spectrograms. This strengthening is most clearly shown by the increased intensity of a linelike feature at $\lambda\lambda$ 4323–4324, which is almost entirely due to the closely packed heads of the *Q* branches of the (2, 2) band of the $^2\Delta-{}^2\Pi$ system of *CH*.[6] A great many differences between the spectra of the *Ba* II stars and normal stars can be accounted for by the increased *CH* absorption in these objects. Also noteworthy is the weakening of many atomic lines in the violet region of the spectra of the *Ba* II stars, though the effect is not so conspicuous as in the *CH* stars.[2]

In Figure 2 we have reproduced portions of the higher-dispersion spectra of the *Ba* II star HR 774 and of a normal K0 giant, λ Hydrae. In the reproduction of the region of the *CH* bands, the upper spectrum is that of the peculiar star HR 885, in which

[5] *Mt. W. Contr.*, No. 511; *Ap. J.*, 81, 187, 1935.

[6] L. Gerö, *Zs. f. Phys.*, 118, 27, 1941.

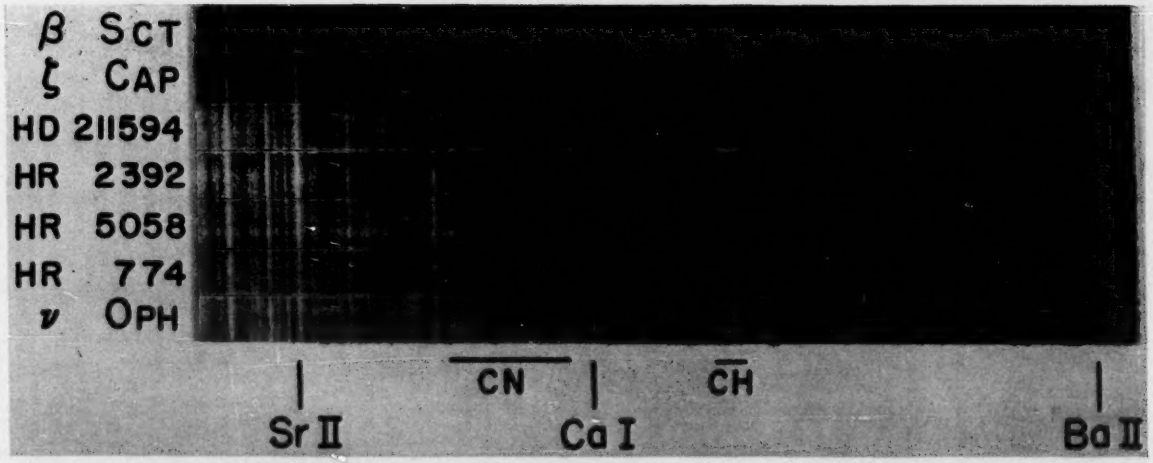

FIG. 1.—The photographic region of the spectra of the *Ba* II stars and of the normal stars, β Scuti, G5 II, and ν Ophiuchi, K0 III

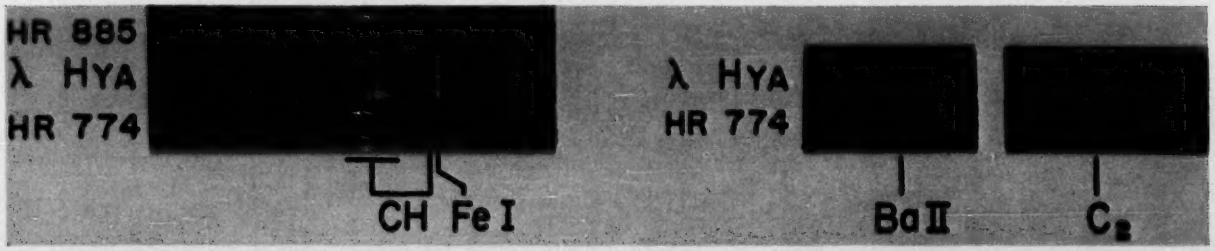

FIG. 2.—Details in the spectrum of the *Ba* II star HR 774. The spectrum of the normal K0 giant star λ Hydrae is shown for comparison, as is also that of the peculiar star showing no *CH* absorption, HR 885. The *Ba* II line reproduced is λ 4554, the C_2 absorption is that of the (0, 0) band at λ 5165.

no *CH* or *CN* absorption is evident, although the other spectral features would indicate a spectral type of about G5 III.[7] The remarkable absence of *CH* in HR 885 thus represents a departure from a normal spectrum in the opposite sense from that shown by the *Ba* II and the *CH* stars.

For one of the *Ba* II stars, HR 774, the region from λ 7000 to λ 8600 has been photographed with grating dispersion of 48 A/mm. In this part of the spectrum the intensity distribution is about that of a normal G8 or K0 giant, in agreement with the appearance of the blue and yellow regions. The infrared *CN* bands, which belong to the $^2\Pi-^2\Sigma$ system, are strengthened to about the same degree as the blue bands.

The atomic lines in the infrared which are most sensitive to luminosity are the *Fe* I lines and the ultimate doublet of *K* I.[8] In HR 774 the strength of these features is not great and suggests a luminosity not exceeding that of an ordinary giant. Actually, the *Fe* lines may be a little weak even for a giant, for the type assigned on the basis of their absolute intensity would be one or two subdivisions earlier than that given by the *Ti* I lines. A few other infrared lines appear slightly stronger in HR 774 than in a typical K0 giant. Their approximate wave lengths are as follows:

λ		λ	
7484	*La* II ?	7909	Possibly atmospheric H_2O
7895	.....	8511–8512	Blend

THE GENERAL PROBLEM OF THE *Ba* II STARS

1. Two other stars are known which are probably related to the *Ba* II group. The eighth-magnitude high-velocity star HD 26, recently discussed by Keenan and Kellar,[9] is rather similar to the *Ba* II stars. The C_2 and *CH* bands are stronger in HD 26, however, and the suppression of the metallic lines in the violet region of the spectrum is somewhat greater. These facts led to the suggestion that HD 26 may be intermediate in character between the stars of the *Ba* II and *CH* groups. In any case, the resemblance of HD 26 to the *Ba* II stars is of considerable importance, since the very high proper motion of HD 26 ($\mu = 0''.258$ per year) suggests an upper limit of its luminosity near visual absolute magnitude zero. This fact offers rather conclusive proof that the enhancement of the *Sr* II and *Ba* II lines in that star is not due to normal ionization effects, and it strengthens our similar conclusion in the case of the *Ba* II stars. On the other hand, it must be kept in mind that HD 26 is a star of very high velocity, while the data of Table 1 suggest that the space motions of the *Ba* II stars are more moderate.

Another related star is the cooler object, HD 121447, which has generally been considered an S-type star, although the *ZrO* bands do not appear on recent spectrograms of low dispersion. HD 121447 does show *CH* and *CN* bands which are abnormally strong for its equivalent spectral type, which may be estimated at about M0. The line λ 4554 of *Ba* II is extremely intense in this star. Thus HD 121447 could be considered a cooler member of the *Ba* II group and perhaps a connecting link between these and the S-type stars.

2. The abnormal strength of the bands of C_2, *CH*, and *CN* in the *Ba* II stars appears to imply a carbon abundance in their atmospheres intermediate between that of the normal stars and that of the carbon-star group. Because the C_2 sequence starting at λ 4737 is not strong in the *Ba* II stars, it is not surprising that objects of this sort have not hitherto been found. The reason why an abnormal strength of the lines of *Sr* II and *Ba* II should be associated with an intermediate carbon abundance is obscure. This relationship may be connected with the properties of the *BaO* and *SrO* molecules, the

[7] W. P. Bidelman, *Ap. J.*, **113**, 304, 1951.

[8] P. C. Keenan and J. A. Hynek, *Ap. J.*, **101**, 265, 1945.

[9] *Ap. J.*, **113**, 700, 1951.

formation of which would certainly be affected by an abnormal carbon abundance. In any case the connection between the *Ba* II stars and the carbon stars is a direct inference from observation. Reasons for thinking that the S-type stars may also be cases of intermediate carbon abundance have been sketched previously by one of us.[10] If this be correct, it would follow that the *Ba* II stars and the S-type stars could be regarded as manifestations of the same abundance anomaly at considerably different temperatures. The essential question is whether the same relative abundances could give the observed *Ba* II star features at the temperature of early K-type stars and also the observed S-type star features at the temperature of the M-type stars. On the theoretical side this question requires further computations of the dissociation equilibria in late-type stars with varying atomic abundances, while on the observational side the next step is the comparative study of the spectra of the *Ba* II stars and the S stars with the highest practicable dispersion.

[10] W. P. Bidelman, *Ap. J.*, **112**, 219, 1950.

THE Of-TYPE SPECTROSCOPIC BINARY BD+40°4220

O. C. WILSON AND ARTHUR ABT
MOUNT WILSON AND PALOMAR OBSERVATORIES
CARNEGIE INSTITUTION OF WASHINGTON
CALIFORNIA INSTITUTE OF TECHNOLOGY
Received August 8, 1951

ABSTRACT

The components of the spectroscopic binary BD+40°4220 are of spectral types Of and O9 and the period is 6.600 ± 0.002 days. The mass of the O9 star (probably a giant or supergiant) is about four times that of the Of. Rather pronounced periodic variations in visibility of some of the spectral features are briefly discussed.

I. OBSERVATIONS

A total of 48 spectrograms of BD+40°4220[1] was obtained by Wilson during the observing seasons of 1946–1949. The one-prism spectrograph of the 60-inch telescope was used throughout, for the most part with a camera of 9-inch focus. Dispersion at $H\gamma$ was 80 A/mm on 43 of the plates and 35 A/mm on the remainder. Baked Eastman 103-O emulsion was used for the majority of the exposures, and the spectra were widened as much as practicable, to increase the visibility of faint detail. In 1948 a preliminary note[2] gave estimates of the period and amplitudes and called attention to the variable visibility of the lines.

The spectrum contains narrow emission bands of λ 4686 *He* II and λ 4634, λ 4640 *N* III (not resolved on many of the plates); it also shows emission components on the longward sides of the absorption lines of $H\beta$, $H\gamma$, and occasionally $H\delta$. Absorption lines, all shallow and usually somewhat widened, include the Balmer series, $H\beta$ through $H8$; the Pickering series of *He* II (λ 4541, λ 4199); λλ 4471, 4387, and 4026 of *He* I; and λ 4097 of *N* III. Of these absorption lines, only $H\gamma$ is visible on most of the plates. Part of the difficulty in seeing more lines on a given exposure is caused by the extreme redness of the object. When the λ 4686 region is exposed to optimum density, the spectrum is already very weak at λ 4100. The reddening is undoubtedly due, for the most part, to selective interstellar absorption; a strong interstellar absorption band is present at λ 4430, H and K are strong, and some of the interstellar molecular lines can occasionally be seen even on the small-dispersion plates.

The spectral type of the absorption-line star cannot be estimated as accurately as we should like, partly because of the unknown contribution of the Of component to the continuum. Also the quality of the spectrograms is not sufficient to justify an attempt to measure accurate equivalent widths. Eye estimates yield the somewhat uncertain mean intensity ratios of 2.4 for λ 4471/λ 4541 and of 9 for λ 4340/λ 4541, which indicate the spectral type to be about O9. Since λ 4387 *He* I is very weak, the star is probably a supergiant.[3]

Measured radial velocities for λ 4686 and for $H\gamma$ are given in Table 1. About half the plates were measured by both authors, with satisfactory agreement, and were given double weight in forming the normal points. Of the emission lines, only λ 4686 gave a well-defined velocity-curve. Velocities from λ 4634, λ 4640 *N* III are, however, similar to

[1] 1950 R.A., $20^h30^m.7$; Decl., +41°8′; mag., 9.1.

[2] O. C. Wilson, *Pub. A.S.P.*, **60**, 385, 1948.

[3] W. W. Morgan, P. C. Keenan, and E. Kellman, *An Atlas of Stellar Spectra* (Chicago: University of Chicago Press, 1943).

TABLE 1

RADIAL VELOCITIES AND PHASES

PLATE	JD	PHASE*	RADIAL VELOCITY (KM/SEC)	
			He II 4686	$H\gamma$
γ 27900	2432049.868	0.348	+210	− 23
908	050.878	.502	+ 27	− 86
931	070.847	.527	+ 18	− 43
935	071.795	.671	− 91	+ 70
943	072.757	.817	− 88	+ 21
958	074.726	.115	+150	− 62
967	075.793	.277	+232	− 27
28034	101.785	.215	+216	.....
038	102.686	.351	+207	.....
042	103.698	.505	+ 14	.....
746	397.963	.090	+115	− 57
749	398.882	.229	+200	−157
755	399.949	.391	+196	− 68
762	401.975	.698	−215	+ 50
877	430.836	.071	+114	− 61
882	431.832	.222	+239	− 93
888	432.788	.367	+199	− 53
894	433.840	.526	− 9	− 42
898	434.715	.659	−107	+ 70
921	452.816	.401	+172	− 26
926	453.767	.545	+ 9	− 10
932	454.727	.691	−136	+ 68
29722	747.864	.105	+ 87	− 76
730	749.839	.405	+198	− 55
734	750.885	.563	− 33	−104
825	777.880	.653	−121	− 25
921	789.832	.464	− 28	− 60
927	790.845	.618	−127	+ 25
933	791.811	.764	−169	− 56
974	810.836	.647	− 82	.....
979	811.732	.782	−150	.....
985	812.713	.931	− 75	−142
993	813.727	.085	+ 40	− 78
30777	2433080.941	.572	−101	− 29
779	081.878	.714	−149	+ 58
782	082.868	.864	− 60	− 23
882	115.809	.855	−125	− 29
887	116.924	.024	+ 76	− 35
890	117.805	.157	+212	+ 62
893	132.798	.429	− 63	− 82
896	133.793	.580	−125	.....
999	161.885	.836	.....	− 63
31002	162.771	.970	+ 10	− 79
006	163.767	.121	+173	− 58
115	191.760	.362	+145	− 76
120	192.736	.510	− 11	− 76
201	220.644	.739	−138	− 26
206	221.630	0.888	− 36	− 75

* Fraction of period since time of crossing the γ-axis on rising branch of velocity-curve.

those from λ 4686, and there is no possibility of a difference in γ velocity greater than 40 km/sec between *He* II and *N* III. Measures of the emission line at *Hβ* scatter too much to permit its positive identification with either component of the system. On the other hand, while only *Hγ* proved suitable for determining the velocity-curve of the O9 star, measures of the other absorption lines show a scatter consistent with the smaller amplitude of this component, and none of them can be attributed to the Of star.

Intercomparison of the λ 4686 velocities for the four observing seasons yielded a period of 6.600 days, with an estimated uncertainty of ±0.002 day. When the measured *He* II velocities were assembled with this period, it was apparent that there was no appreciable eccentricity. Accordingly, normal points (Table 2) were formed and a least-squares solution made for the remaining elements. Velocities from *Hγ* were handled in

TABLE 2

NORMAL POINTS

Line	Phase	Vel. (Km/Sec)	Weight	Line	Phase	Vel. (Km/Sec)	Weight
λ 4686....	0.062	+ 72.6	7	*Hγ*.....	0.096	−51.7	12
	.127	+171.2	4		.245	−79.4	5
	.239	+211.7	8		.388	−53.2	11
	.372	+193.0	13		.524	−56.8	14
	.515	− 4.9	16		.670	+48.1	11
	.630	−107.9	10		.813	−22.1	7
	.731	−164.1	9		0.930	−98.7	3
	0.862	− 78.7	6				

TABLE 3

ORBITAL ELEMENTS OF BD+40°4220

$P = 6.600 \pm 0.002$ (est. error)	$\gamma_{O9} = -34.8 \pm 2.9$ km/sec
$e = 0.0$ (assumed)	$(a \sin i)_{Of} = 1.77 \times 10^7$ km
$K_{Of} = 194.9 \pm 2.8$ km/sec	$(a \sin i)_{O9} = 4.30 \times 10^6$ km
$K_{O9} = 47.3 \pm 4.6$ km/sec	$m_{Of} \sin^3 i = 1.90\odot$
$\gamma_{Of} = +29.0 \pm 2.4$ km/sec	$m_{O9} \sin^3 i = 7.83\odot$

Time of crossing γ-axis on rising branch of velocity-curve =

JD $2432747.167 \pm 0.018 + (6.600 \pm 0.002)E$.

similar fashion, with the additional assumption of a 180° phase difference from the Of star. Moreover, because of the large observed intensity ratio of λ 4340/λ 4541, no wavelength correction was made for blending with λ 4339 *He* II. Final orbital elements are in Table 3, and the velocity-curves are shown, with the normal points, in Figure 1.

The variable visibility of the absorption lines is a function of the phase which remains the same from one cycle to another. In the phase interval from 0.95 to 0.55, the absorption lines are constant at maximum strength. At about phase 0.55, as the O9 star is beginning to recede from the observer, its lines become indistinct and attain their most washed-out appearance near phase 0.75, returning again to maximum at phase 0.95. It is not possible to state whether the lines really change in intensity or whether they merely become broader and shallower without variation in equivalent width. In any event, the effect is probably the same as that which has been observed in a number of other binaries and which still does not have a satisfactory explanation.[4]

[4] See, e.g., O. Struve, *Stellar Evolution* (Princeton: Princeton University Press, 1950), p. 182.

The emission lines do not vary greatly in visibility except for the emission component of $H\beta$, the strongest of the Balmer emissions, which occurs only between phases 0.20 and 0.70, while the Of star is passing behind its companion.

II. DISCUSSION

A problem of long standing has been the relationship, if any, of the Of stars to the Wolf-Rayet stars, and the importance of BD+40°4220 lies in the assistance it may give

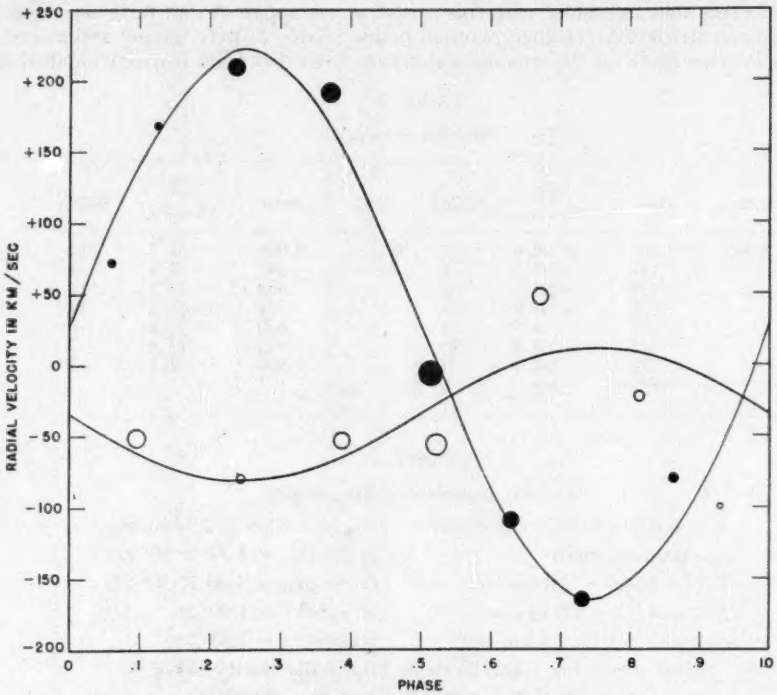

FIG. 1.—Radial-velocity-curves of BD+40°4220. Solid and open circles are normal points for the Of and O9 components, respectively.

in resolving this question. This system is remarkable in that it seems to be the only binary known in which one member is an Of star and in which two spectra are visible. The nearest approach to it in the literature is 29 Canis Majoris, also a spectroscopic binary containing an Of star but one in which all the emission and absorption lines originate in the same object. Earlier work on 29 CMa had indicated the presence of a faint secondary spectrum and had led to a mass ratio of 0.75. However, a careful investigation by Struve and Sherman[5] failed to produce any evidence of a secondary spectrum; hence the mass ratio quoted above must be considered doubtful.

a) ***Mass and luminosity.***—Since the spectra of both components of the system are visible, the two stars cannot differ greatly in brightness, although the absence of absorption lines due to the Of star may indicate that it is somewhat fainter than the O9. On

[5] *Ap. J.*, 93, 84, 1941.

the other hand, the mass ratio of 4 would lead to the expectation of a difference in bolometric magnitude of about 5 mag., provided that both stars followed the empirical mass-luminosity relationship for the O-type stars.[6] If both stars had identical surface temperatures, the photographic magnitudes would, of course, differ by the same amount, and both spectra could not possibly be observed. Since, in view of the lines observed in the two spectra, there is no evidence for appreciable differences in surface temperature, the proper conclusion would appear to be that the Of star is considerably more luminous for its mass than it would be if it obeyed the same mass-luminosity relationship as do the absorption O's. As to the absolute magnitude of the Of star, not much can be said beyond the fact that its luminosity must be fairly close to that of the absorption O-type star with which it is associated. From this one example, therefore, there is no support for the view expressed by Miss N. Roman[7] that the Of stars in general are the most luminous of the O stars; but neither is one example adequate to negative the suggestion.

b) *The* γ *velocities.*—The γ velocity of the Of star is shifted with respect to that of the O9 by +64 km/sec. This is of the same order as, but somewhat less than, the mean red shift of λ 4686 observed for six Wolf-Rayet binaries and tabulated by W. A. Hiltner.[8] Whether the cause is the same in the Of star as in the others we cannot yet say. In 29 CMa, Struve and Sherman[5] observed a similar displacement between the emission and absorption lines and attributed it to P Cygni type absorption components, which they observed on the violet sides of the emission lines during part of the cycle. In BD+40°4220 we have not observed such absorption components, but they could probably be masked by the small scale and coarse grain of our plates, together with the influence of the overlying continuum of the O9 star.

c) *Summary.*—Comparing the system of BD+40°4220 to those in which one component is a Wolf-Rayet star, we find a number of striking resemblances:

1. The companion of the emission-line star lies within the rather narrow spectral range O7–B0. In so far as their spectra can be determined, the companions of Wolf-Rayet stars also all seem to be included within this interval.

2. The emission band of λ 4686 *He* II in the Of star is shifted longward by an amount quite comparable to that which has been observed in a number of Wolf-Rayet binaries.

3. Although the Of star is only about a fourth as massive as its companion, the two stars have comparable luminosities; much the same situation is found in all the Wolf-Rayet binaries thus far investigated.

The foregoing comparisons seem to point to a general similarity between the physical characteristics of the Of and the W stars. Beyond this it is not at present feasible to go. In any case, it appears highly desirable to study BD+40°4220 with higher dispersion, and the authors hope to apply more powerful equipment to the problem in the future. The star should also be investigated photometrically, although the small values of $m \sin^3 i$ do not appear favorable for the existence of eclipses.

[6] G. E. Kron and K. C. Gordon, *Ap. J.*, 111, 454, Fig. 8, 1950.

[7] *A.J.*, 56, 46, 1951 (abstr.).

[8] *Ap. J.*, 113, 317, Table 2, 1951.

A FINDING LIST OF HIGH-LUMINOSITY STARS. II

LUIS MÜNCH
Observatorio Astrofisico Nacional, Tonanzintla, Puebla, Mexico
Received July 19, 1951

ABSTRACT

A catalogue is given of 141 stars classified on objective-prism plates as belonging to the group OB or to the supergiant classes earlier than G0.

This list is of the nature of a supplement to the one recently published by the author,[1] and it has been arranged in a manner entirely similar to this earlier one. Following a suggestion of Dr. W. W. Morgan after List I had been prepared, it was decided to extend the limits of the survey of high-luminosity objects in the Southern Milky Way to galactic latitude $\pm 10^{\circ}$. The observational material which is the basis of the present list was obtained by the writer in the winter of 1950–1951 with the 26–30-inch Schmidt telescope and the 4° objective prism of the Tonanzintla Observatory. The centers of the plates were so chosen as to obtain some overlapping with the regions covered by the plates from which List I was prepared. This overlap insures completeness of the survey and also uniformity in the definition of the system of classification.

The stars found in the plates as belonging to the OB group or to the c classes earlier than G0 are listed in Tables 1 and 2. The identifications have been made, as before, by reference to the *Durchmusterung* catalogues.[2] For the identification of the few stars not contained in these catalogues, we have prepared the charts given in Figure 1. From this listing we have omitted those stars already given in List I or in the list of Nassau and Morgan.[3]

It should be emphasized, again, that among the stars listed there may be some peculiar objects which, in the small dispersion used, show some of the spectral features characteristic of higher-luminosity objects, i.e., certain types of Be stars and peculiar A–F stars of the γ Equ type.

[1] *Ap. J.*, 113, 309, 1951; this paper will be referred to hereafter as "List I."

[2] The writer is indebted to Misses Guillermina and Graciela Gonzalez for their valuable help in the identification of the stars.

[3] *Ap. J.*, 113, 141, 1951.

TABLE 1

STARS REFERRED TO THE BD

No.	BD	HD	α_{1855}	δ_{1855}	m	Sp.	HD Type
1	1304	.....	$6^h20^m.6$	− 0° 21′	9.0	OB	.....
2	.....	.....	31.8	− 4 15	.....	OB	.....
3	1314	.....	31.9	− 1 22	9.5	OB	.....
4	.....	.....	34.0	− 1 38	.....	OB	.....
5	.....	.....	37.3	− 2 05	.....	OB	.....
6	.....	.....	39.9	− 6 00	.....	OB	.....
7	1405	.....	40.1	+ 3 57	9.3	OB	.....
8	1451	.....	44.8	+ 5 19	9.0	OB	.....
9	1684	.....	47.2	−12 57	9.8	OB	.....
10	1700	.....	49.2	−12 49	9.9	OBe	.....
11	1622	51956	52.0	+ 1 06	8.3	cF9	K0
12	1770	53456	57.9	−11 18	7.9	OB	B5
13	1971	.....	7 0.0	− 5 00	9.5	OBe	.....
14	1699	54167	0.4	+ 1 56	9.3	OB	B
15	1773	.....	2.4	− 7 28	9.3	OB	.....
16	1751	.....	4.3	−14 07	9.5	OB	.....
17	1823	.....	4.3	−17 21	9.8	OB	.....
18	.....	.....	4.5	−17 56	.....	OB	.....
19	.....	.....	5.5	−14 15	.....	OB	.....
20	1712	55885	7.7	−15 08	9.4	OB	B
21	2037	56037	8.1	− 5 46	8.3	cF9	G5
22	1798	.....	8.2	−20 51	8.9	OB	.....
23	1724	.....	8.5	−15 06	9.5	OB	.....
24	1960	56670	10.6	− 9 10	9.3	OB	B
25	1767	56727	11.0	−18 27	8.8	OB	B5
26	1834	.....	11.2	−20 48	9.4	OB	.....
27	1769	56806	11.4	−18 33	9.2	OB	B
28	1838	.....	11.6	−20 09	10.0	OB	.....
29	1786	57258	13.3	−18 25	8.7	OB	B8
30	1874	57236	13.3	−21 44	8.7	OB	B0
31	1874	57613	14.9	−20 30	9.2	OB	B8
32	2015	57775	15.5	−10 33	9.0	OB	B
33	.....	.....	16.0	− 6 17	.....	OB	.....
34	1944	.....	16.5	−17 40	10.0	OB	.....
35	1896	.....	16.6	−20 36	9.4	OB	.....
36	1906	58321	18.1	−20 49	9.1	OB	B8
37	2018	58902	20.4	−13 05	9.5	OB	B
38	2072	.....	23.1	−10 57	8.6	OBe	.....
39	.....	.....	25.6	−14 15	.....	OB	.....
40	2021	.....	26.3	−12 44	9.3	OB	.....
41	2025	60307	26.5	−12 48	8.8	OB	B
42	1966	60325	26.7	−14 00	6.8	OB	B5
43	1975	.....	27.4	−14 25	9.4	OB	.....
44	2133	.....	30.8	−10 39	9.4	OB	.....
45	2143	61347	31.5	−13 31	8.3	OB	B2
46	2043	.....	32.9	−11 56	9.6	OBe	.....
47	2173	.....	36.2	−14 58	9.7	OB	.....
48	.....	.....	37.5	−12 20	.....	cF9	.....
49	2159	62866	38.9	−20 28	8.5	OB	B
50	2183	.....	40.6	−20 48	9.3	OBe	.....
51	2163	64058	44.9	−16 39	8.5	cF0	F5
52	.....	.....	53.9	−20 03	.....	OB	.....

TABLE 2

STARS REFERRED TO THE CD

No.	CD	HD	α_{1875}	δ_{1875}	m	Sp.	HD Type
53.....	5139	56808	$7^h12^m.4$	−24° 34′	8.7	OB	B8
54.....	4439	58011	17.6	−25 46	7.5	OBe	B1p
55.....	4310	58200	18.4	−29 50	8.8	OB	B9
56.....	5395	58256	18.6	−23 41	8.9	OB	B3
57.....	5500	.....	22.1	−23 41	9.3	OB	.....
58.....	4081	59756	25.3	−32 05	9.0	OB	B5
59.....	4634	60017	26.4	−30 15	8.3	cF0	F2
60.....	4485	60196	27.2	−28 27	8.9	OB	B
61.....	4197	.....	27.3	−27 51	8.6	OB	.....
62.....	4205	60284	27.6	−27 35	9.0	OB	B
63.....	4502	60369	28.0	−28 03	7.9	OB	B3
64.....	4140	.....	28.2	−32 16	9.8	OB	.....
65.....	4229	60479	28.5	−27 42	8.6	OB	B
66.....	4664	.....	32.1	−29 45	9.4	OB	.....
67.....	4864	61709	34.4	−31 01	8.0	OB	B1
68.....	4870	61778	34.8	−25 16	9.0	OB	B5
69.....	4266	61827	35.0	−32 17	7.5	OB	Oe5
70.....	4879	61851	35.1	−31 13	9.3	OB	B5
71.....	4908	.....	36.0	−31 38	9.3	OB	.....
72.....	4287	62150	36.4	−32 21	7.8	OB	Oe5
73.....	4043	.....	36.9	−33 32	9.8	OB	.....
74.....	3814	.....	37.0	−34 30	9.5	OB	.....
75.....	4348	.....	39.7	−32 55	9.0	OB	.....
76.....	4998	62844	39.7	−31 56	8.3	OB	B0
77.....	3865	63150	41.3	−36 11	8.4	OBe	Oe5
78.....	4186	63804	44.5	−33 00	8.0	OB	B
79.....	3669	64012	45.7	−39 53	8.9	cF5	F8
80.....	6495	64993	50.2	−23 44	8.2	OB	B0
81.....	4743	.....	50.7	−27 49	9.7	OBe	.....
82.....	5218	.....	53.9	−28 02	9.7	OB	.....
83.....	5235	.....	54.3	−28 34	9.7	OB	.....
84.....	3859	.....	54.8	−39 43	9.5	OB	.....
85.....	.....	.....	56.0	−27 56	.....	OB	.....
86.....	4114	66334	56.9	−36 50	8.5	OB	B
87.....	.....	.....	57.1	−27 27	.....	OBe	.....
88.....	5369	.....	58.4	−28 18	9.5	OE	.....
89.....	5453	66695	58.6	−26 42	9.4	OB	B
90.....	3933	.....	58.7	−39 58	9.3	OB	.....
91.....	2142	66929	58.7	−22 01	7.8	cF9	G0
92.....	5565	.....	59.6	−30 40	9.9	OBe	.....
93.....	5090	68026	8 4.5	−27 04	8.9	OB	B5
94.....	4967	.....	7.2	−32 11	8.9	OB	.....
95.....	5181	.....	8.9	−27 56	9.8	OBe	.....
96.....	3636	.....	11.6	−48 50	9.9	OBe	.....
97.....	4113	69648	11.9	−43 46	8.3	OB	B2
98.....	5838	.....	12.0	−25 38	9.8	OBe	.....
99.....	5843	69756	12.2	−25 55	7.5	cF2	F5
100.....	4090	69882	13.0	−42 08	7.1	OB	B2
101.....	4156	70122	14.3	−43 52	9.2	OB	B8
102.....	4950	.....	15.7	−34 06	9.0	OB	.....
103.....	4858	71913	23.8	−34 19	8.0	OB	B5
104.....	3572	71934	24.1	−49 41	8.3	OB	B8
105.....	4887	72063	24.7	−34 30	8.6	OB	B8

TABLE 2—*Continued*

No.	CD	HD	α_{1875}	δ_{1875}	m	Sp.	HD Type
106	4219	72554	8^h27^m6	−45°42′	8.6	OB	B0
107	3621	72754	28.5	−49 10	7.5	OBe	Bp
108	4631	.....	34.6	−39 58	8.1	OB	.....
109	3761	74753	39.7	−49 22	5.8	OB	B2
110	4569	74804	40.1	−40 49	7.3	OB	B5
111	4593	74979	41.2	−40 10	7.2	OB	B8
112	5030	75222	42.6	−36 17	7.6	OB	B3
113	4691	75860	46.4	−43 17	7.6	OB	B0
114	4762	76341	49.5	−42 00	7.4	OB	B2
115	4637	.....	50.8	−41 06	9.4	OBe	.....
116	4786	.....	52.6	−46 33	9.3	OB	.....
117	3710	76968	53.5	−50 16	7.5	OB	B0
118	4551	.....	53.7	−47 15	8.5	OB	.....
119	5049	.....	55.4	−39 03	9.4	OB	.....
120	4838	77581	57.4	−40 03	7.1	OB	B0
121	4855	77718	58.1	−46 04	8.9	OB	B2
122	4382	77959	59.6	−48 03	9.3	OB	B
123	2772	.....	9 1.4	−52 43	8.4	OB	.....
124	4650	78344	1.6	−47 16	9.0	OB	B
125	4889	78785	3.9	−45 45	8.7	OB	B2
126	2811	.....	4.5	−52 04	9.1	OBe	.....
127	5017	78927	4.8	−42 47	8.9	OB	B2
128	4989	78958	5.0	−43 22	9.0	OB	B
129	5206	79186	6.5	−44 21	5.6	OB	B5
130	4264	80077	11.7	−49 27	8.1	OB	B
131	5006	80834	15.9	−41 39	9.1	OBe	B
132	4643	.....	18.4	−48 58	9.3	OB	.....
133	5140	82415	25.7	−41 36	8.3	cF8	G0
134	5274	82830	28.5	−46 12	9.4	OBe	B
135	4602	.....	36.8	−49 26	10.0	OB	.....
136	4902	84136	36.9	−48 02	9.1	OB	B3
137	4982	.....	41.5	−48 06	10.0	OBe	.....
138	5287	85356	45.2	−47 21	8.0	OB	B0
139	4561	.....	45.4	−50 13	10.8	OB	.....
140	5089	.....	47.9	−48 14	9.8	OB	.....
141	.....	.....	49.9	−47 12	.....	OB	.....

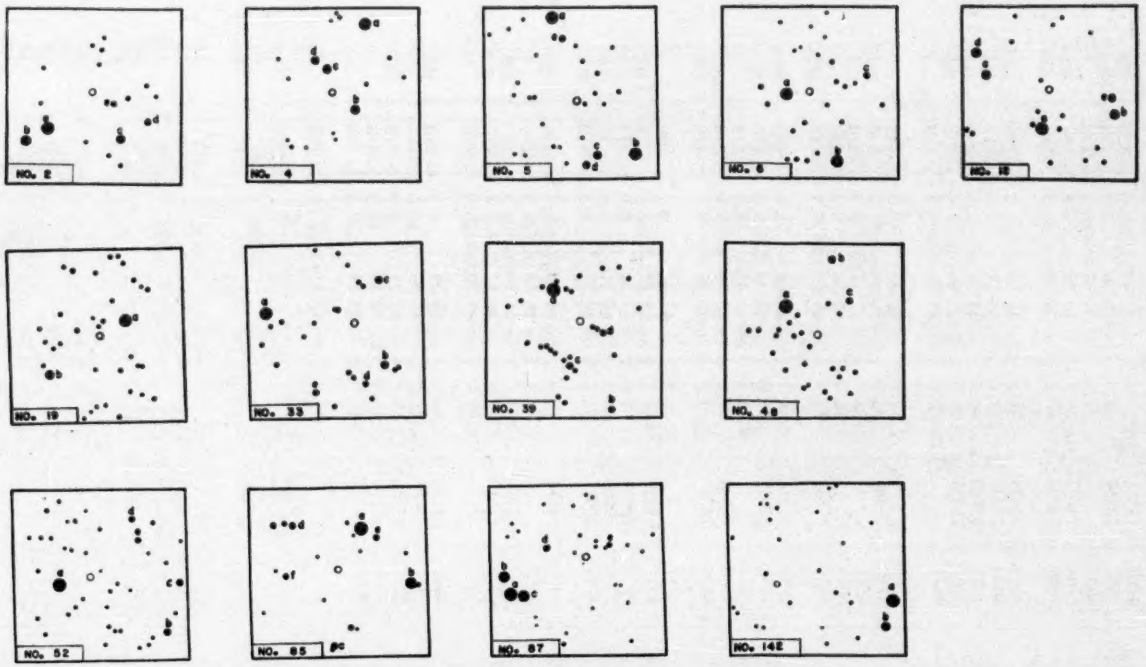

FIG. 1.—Identification charts for stars not contained in the *Durchmusterung* catalogues. The stars to be identified have been indicated by a circle and the field stars by dots of varying sizes according to their brightness. In all cases, south is at the top and west to the left. The angular dimensions of the squares drawn are $28' \times 28'$. *For* No. 142 *read* No. 141.

TABLE 3

IDENTIFICATION OF THE REFERENCE STARS MARKED IN FIGURE 1

No. 2			No. 4			No. 5			No. 6		
	BD	m		BD	m		BD	m		BD	m
a	−4° 1597	8.5	a	−1° 1335	8.8	a	−2° 1741	8.5	a	−5° 1897	8.0
b	−4 1595	9.0	b	−1 1334	9.2	b	−1 1362	8.8	b	−5 1803	8.8
c	−4 1601	9.2	c	−1 1331	9.3	c	−1 1360	9.3	c	−6 1737	9.5
d	−4 1603	9.7	d	−1 1329	9.3	d	−1 1357	9.4			
e	−4 1599	9.8				e	−2 1742	9.5			
No. 18			**No. 19**			**No. 33**			**No. 39**		
	BD	m		BD	m		BD	m		BD	m
a	−17° 1824	8.0	a	−14° 1768	8.2	a	−6° 2084	8.8	a	−14° 1950	8.5
b	−17 1830	9.0	b	−14 1761	9.0	b	−6 2097	9.2	b	−14 1956	9.4
c	−17 1819	9.0				c	−6 2095	9.3	c	−14 1951	9.5
d	−17 1815	9.0				d	−6 2093	9.5	d	−14 1955	9.5
e	−17 1829	9.1				e	−6 2088	9.5			
No. 48			**No. 52**			**No. 85**			**No. 87**		
	BD	m		BD	m		CD	m		CD	m
a	−12° 2111	8.5	a	−20° 2324	8.7	a	−28° 5316	8.5	a	−27° 4871	8.6
b	−12 2118	9.2	b	−19 2193	9.2	b	−27 4889	8.9	b	−27 4868	8.8
c	−12 2119	9.3	c	−20 2336	9.3	c	−27 4872	9.3	c	−27 4873	8.8
			d	−20 2331	9.7	d	−28 5288	9.3	d	−27 4879	9.3
			e	−20 2332	9.8	e	−28 5321	9.4	e	−27 4891	9.4
						f	−27 4857	9.5			
No. 141											
	CD	m									
a	−47° 5381	7.3									
b	−47 5378	9.2									

PROPER MOTIONS FOR THIRTY-THREE BLUE STARS IN HIGH GALACTIC LATITUDE

WILLEM J. LUYTEN AND WILLIAM C. MILLER
UNIVERSITY OF MINNESOTA
and
MOUNT WILSON AND PALOMAR OBSERVATORIES
CARNEGIE INSTITUTION OF WASHINGTON
CALIFORNIA INSTITUTE OF TECHNOLOGY
Received July 20, 1951

ABSTRACT

The proper motions of all thirty-three blue stars found by Humason and Zwicky near the north galactic pole have been measured. Three of the stars are found to have motions larger than 0".1 annually; at least one of these appears to be a normal white dwarf. Five more stars seem to have motions which may be individually real and may be population II high-velocity stars, though perhaps somewhat less luminous than the average. The motions of the remaining twenty-five stars are so small as to have only statistical significance; these may also be population II stars at a distance of around 5000 parsecs. There is a faint indication that their average motion reflects the revolution of the sun around the galactic center.

Preliminary measures of the proper motions of all thirty-three of the faint blue stars found by Humason and Zwicky[1] in high galactic latitude have been made. The first-epoch plates were kindly supplied by the Harvard Observatory and consisted mainly of plates taken with the 16-inch Metcalf telescope (scale 1 mm = 98".6) and a few taken with the 24-inch Bruce refractor (1 mm = 59".2). The second-epoch plates were mostly taken by Miller during May, 1949, with the 60-inch telescope (1 mm = 27".1); a few additional plates were taken by Luyten with the 36-inch reflector of the Steward Observatory (1 mm = 44".5). While we realize that such heterogeneous plate material—the old plates all taken with refractors, the new plates all with reflectors—is not conducive to high accuracy in the measures, we feel that the importance of deciding even approximately whether these stars are genuine white dwarfs, high-velocity stars of population II, or extremely distant normal blue stars is great enough to justify even this attempt.

All plates were measured by Luyten; from four to six comparison stars were used in each case. The measures on all plates were reduced to the scale of the 16-inch Metcalf plates by multiplication with the proper factor (0.277 for the 60-inch plates; 0.459 for the 36-inch plates; and 0.609 for the 24-inch plates); beyond this, reductions were carried out by using a linear formula only, allowing for orientation and a remnant of scale difference, but no second-order terms were used. In three instances one of the comparison stars chosen proved to have a measurable motion; this star was then rejected, another chosen to replace it, and new measures and reductions made.

The results are shown in Table 1, where the first five columns give the H-Z designation of the star, its 1950 position, and its apparent photographic magnitude and spectral class as determined by Humason and Zwicky. The next three columns show the measured, annual, relative proper motion and the mean magnitude of the comparison stars used (estimated differentially against that of the proper-motion star). The last three columns give the number of old and new plates used and the interval in years between them, respectively. From a discussion of the internal disagreements and residuals, we find for the mean error of each component of the proper motion a value of $\pm 0''.011$, on the average.

[1] *Ap. J.*, **105**, 85, 1947.

In each individual case the motion finally accepted was immediately judged in relation to the residuals in the measures, and, on the basis of this comparison, the thirty-three stars whose motions are here presented were arranged in three different groups: (*a*) those for which the motions are so large and definite as to leave no doubt as to their reality—viz., the stars H-Z Nos. 21, 28, and 43; (*b*) those for which the motions found are large enough to suggest that they may be individually real, although leaving considerable uncertainty as to the actual amounts and directions (this group comprises H-Z Nos. 22, 33, 34, 44, and 46); and (*c*) those stars for which the motions found are so small as to possess no individual reality.

It should be emphasized that, while the decision as to which group each star belongs is somewhat arbitrary and subjective, this decision was made immediately after the

TABLE 1

THIRTY-THREE BLUE STARS IN HIGH GALACTIC LATITUDE

H-Z No.	1950 R.A.	1950 Dec.	m_{pg}	Sp.	μ_α	μ_δ	m	n	ΔE (YEARS)
16.....	11h55m5	+30° 14′	14.4	A0	−0″.004	−0″.009	14.5	2,2	29.1
17.....	12 02.7	+40 25	14.4	B2	+ .006	− .009	13.8	1,2	28.4
18.....	12 06.5	+37 19	15.1	B2	+ .002	− .002	14.2	1,1	44.4
19.....	12 10.3	+34 10	12.8	B5	+ .006	− .008	13.5	1,2	41.9
20.....	12 10.2	+42 57	14.9	B3	− .003	+ .003	14.5	1,1	27.1
21.....	12 11.4	+33 12	14.2	B0	− .076	+ .073	14.0	2,2	25.5
22.....	12 12.3	+36 57	12.7	B3	+ .030	− .021	12.8	1,1	44.4
23.....	12 14.9	+32 27	14.2	A0	− .015	− .006	13.5	1,2	39.8
24.....	12 22.3	+39 26	11.4	B8	+ .029	+ .004	13.5	1,1	27.4
25.....	12 23.0	+36 16	10.0	B5	+ .003	− .009	12.3	1,1	44.4
26.....	12 26.3	+28 38	13.7	B5	+ .010	− .005	14.0	2,1	27.8
27.....	12 29.4	+39 17	12.5	A0	+ .005	− .018	14.5	1,1	27.4
28.....	12 30.0	+41 46	15.2	B3	− .117	+ .018	14.5	2,2	27.2
29.....	12 32.4	+37 55	13.6	B0	+ .017	+ .033	13.5	1,1	27.4
30.....	12 34.8	+38 52	13.4	B5	+ .032	+ .011	14.0	1,1	27.4
31.....	12 40.5	+32 21	12.8	A0	− .012	+ .004	13.5	2,1	24.5
32.....	12 48.7	+37 27	15.2	B1	+ .010	− .010	15.0	1,1	30.1
33.....	12 48.7	+33 54	14.6	A0	− .034	− .026	14.0	1,1	22.9
34.....	12 53.0	+37 49	14.7	B0	− .029	− .049	15.0	1,1	30.1
35.....	12 50.9	+30 23	15.0	B2	+ .005	− .011	15.2	1,1	15.3
36.....	12 54.0	+32 42	14.3	A0	− .026	+ .004	14.5	1,2	22.9
37.....	13 00.3	+38 43	12.0	B8	− .004	− .022	13.0	2,1	27.4
38.....	12 57.0	+27 49	13.9	B0	− .015	.000	14.8	1,2	15.3
39.....	13 02.4	+28 23	14.8	B0	+ .012	− .005	14.5	3,2	36.9
40.....	13 11.2	+37 14	13.8	B2	− .009	− .002	12.5	2,1	22.0
41.....	13 14.9	+39 19	13.3	F0	+ .025	− .004	14.0	2,2	27.2
42.....	13 10.8	+31 38	14.2	B5	+ .008	+ .008	13 2	1,2	26.2
43.....	13 14.0	+29 22	12.5	DB0	− .138	− .079	13.5	2,3	26.2
44.....	13 21.3	+36 23	11.0	B2	− .052	+ .035	13.0	1,1	28.3
45.....	13 23.5	+40 23	12.4	B5	+ .005	− .022	13.0	1,1	26.3
46.....	12 54.6	+32 42	14.7	F	− .077	.000	14.0	1,2	22.9
47.....	12 57.1	+27 37	14.7	B5	− .004	− .002	14.8	2,2	40.0
48.....	12 57.4	+41 17	13.6	A0	+0.020	−0.005	13.5	1,1	25.4

motions had been measured and reduced and before any statistical discussion was undertaken.

The stars in these groups may now be discussed separately.

For H-Z No. 21 a pair of 24-inch Bruce plates was available; this pair was blinked, and the motion was easily seen. Measures on this pair of plates gave $-0''.078$ and $+0''.065$ for the motion, while those on the 16–60-inch combination yielded $-0''.074$ and $+0''.080$. The spectral class of this star was found by Humason and Zwicky to be B0, without typical white-dwarf characteristics; a very preliminary determination of the color by Luyten at Tucson gave $m_{pg} = 13.8$, $m_{pv} = 14.8$, and I.C. $= -1.0$ mag. Since with a total motion of $0''.1$ annually the star is not likely to have a parallax less than $0''.001$—and, in fact, the direction of its motion would suggest that the parallax is very much larger than this—the star would appear to be fainter than +4 absolute or fainter than a typical cluster-type high-velocity star or a typical B star of population II.

The motion of H-Z No. 28 was found to be $-0''.123$ and $+0''.028$ from an old Harvard plate and a new plate taken with the 36-inch reflector at Tucson, and $-0''.111$ and $+0''.008$ from a pair of 16–60-inch plates. The spectral class is given as B3 by Humason and Zwicky, its magnitude was determined by Luyten at Tucson as 15.37 pg and 15.50 pv.[2] Humason and Zwicky remarked that the absorption lines of this star are wide and shallow, and they provisionally designated it as a white dwarf; this prediction is fully substantiated by the present data.

The motion of H-Z No. 43 was found by Luyten while blinking a pair of Harvard 24-inch plates but was not measured at the time, as it did not appear very large. When subsequently measured on these plates, it gave the values $-0''.143$ and $-0''.072$, whereas the 16–60-inch combination yields $-0''.134$ and $-0''.086$, resulting in the average shown in Table 1. Luyten finds the magnitude to be 11.90 pg and 12.86 pv,[2] indicating the unusual color index of -0.96 mag. While this value will probably need considerable reduction when referred to the usual International System, there can be no doubt that this is an extremely blue star.

Humason and Zwicky classified the spectrum as DB0 and remarked on the fact that it appears nearly continuous. Several spectrograms obtained with the Q $f/1$ spectrograph of the McDonald Observatory confirm this and show no lines at all. It is a puzzling object, its total proper motion of only $0''.16$ suggesting that its absolute magnitude is not so faint as that of a typical white dwarf and almost certainly brighter than that of most continuous-spectrum white dwarfs, whose absolute magnitudes appear to be around +14. The proper motion alone would perhaps indicate a luminosity comparable to that of the sun.

For the five stars H-Z Nos. 22, 33, 34, 44, and 46, the measured motions are large enough to suggest that they are individually real. However, the measures for Z No. 46 are especially uncertain, owing to the fact that this star's image lies imbedded in that of a small extragalactic nebula. The straight mean of the five motions comes out as $-0''.032$ and $-0''.015$ or, when corrected for the mean drift of the comparison stars, $-0''.042$ and $-0''.021$, which accords well enough in general direction with their expected motion toward the antapex to lend further support to the supposition that the motions may be real. While final judgment should be withheld until such time as more accurate measures become available, a parallax of around $0''.005$ is suggested by these data, further indicating an absolute magnitude around +7 or so—again a little too faint to consider them typical population II stars.

While the motions of the remaining twenty-five stars are so small, averaging only $0''.010$ in either co-ordinate when taken without regard to sign, that they do not possess any individual reality, the case might be different statistically. The algebraic averages are $+0''.0043$ and $-0''.0033$, respectively, with expected mean errors of around $0''.0022$.

[2] *Ap. J.*, **112**, 212, 1950.

One star among this group, H-Z No. 25, is nearly 4 mag. brighter than the average of the others; its rejection, however, would result in only a trifling change in the average motions. For the star H-Z No. 41 Humason and Zwicky found a spectral class of F0, and they comment on the fact that the color of this star is much bluer than its spectrum would indicate; they suggest that the discrepancy may be due to defective spots on the Schmidt photographs. Preliminary estimates of the color made by Luyten at Tucson indicate $m_{pg} = 12.6$, $m_{pr} = 13.2$, and I.C. $= -0.6$, thus substantiating the blueness. The star may thus be similar to L 1491-27, where likewise the color appears to be much bluer than the spectrum indicates. We have therefore felt no need to reject this star from the further discussion.

Since the mean magnitude of all the comparison stars used is 13.8, the average drift for these stars in this part of the sky may be adopted as $-0''.0104$ and $-0''.0060$, respectively (total secular parallax $0''.012$). Correction therefor yields, for the mean absolute motion of our twenty-five blue stars, $-0''.0061$ in R.A. and $-0''.0093$ in Dec., or $0''.011$ in 213°. At this point in the sky the direction toward the galactic center is in position angle 126°, and the direction of the sun's motion around this center in position angle 36° is almost exactly opposite to that of the twenty-five stars just mentioned.

As Humason and Zwicky concluded, it would clearly be erroneous to identify these stars as ordinary B stars of mean absolute magnitudes between -2 and -2.5, as this would place them at extragalactic distances. If they are considered to be similar to Baade's population II blue stars, with absolute magnitudes similar to those of the cluster variables, i.e., around 0 to $+0.5$, then their distance, derived from their mean apparent magnitude of 13.8, comes out slightly greater than 5000 parsecs. At this distance a proper motion of $0''.011$ annually corresponds to a linear tangential speed of 260–300 km/sec, closely enough equal to the accepted value of the solar galactic-rotational velocity to suggest this as an explanation.

While it would thus be tempting to suggest that the present investigation foreshadows for the first time the possibility of determining the galactic rotation from such distant, galactically peripheral stars belonging to population II, which themselves may possess only a small rotational motion—if any—around the galactic center, it should be borne in mind that the motions listed here are extremely provisional in character and that any conclusions drawn from them for so small a number of stars may well be completely fortuitous.

Data for the three comparison stars for which appreciable motions were indicated by the measures are given in Table 2, the different columns of which are self-explanatory.

TABLE 2

COMPARISON STARS

In Field of:	1950		m_{pg}	μ	p
	R.A.	Dec.			
H-Z No. 22	12^h11^m8	+37°01′	12.9	$0''.06$	211°
H-Z No. 30	12 34.4	+38 51	12.9	0.15	16
H-Z No. 48	12 57.1	+41 15	13.4	0.12	216

In conclusion we should like to express our thanks to Dr. Harlow Shapley for his kindness in lending us the early Harvard plates, without which the present measures could not have been made.

A STUDY OF THE CONCENTRATION OF EARLY-TYPE STARS IN CYGNUS

NANCY G. ROMAN
Yerkes Observatory
Received June 30, 1951

ABSTRACT

The area of 14 square degrees centered on P Cygni contains nine Wolf-Rayet stars, three Of stars, seven early, absorption O stars, and numerous other early-type objects. Slit spectra have been obtained for seventy-three of these stars, and photoelectric magnitudes and colors have been determined for most of them. The spectroscopic parallaxes indicate that there is a strong concentration of these objects at a distance of 1600 parsecs. The use of the known absolute magnitudes of the B-type stars permits the following calibration for the absolute magnitudes of the earlier objects: Wolf-Rayet stars, −4.9; Of, −6.0; O5, −5.3; O7, −4.7; and O8, −4.4.

As is well known, the very early-type stars not only are concentrated toward the galactic plane but are far from uniformly distributed, even in low galactic latitudes. Some of the apparent nonuniformity arises from the irregular distribution of interstellar matter, but much of it results from a real tendency of these objects to occur in groups. One of the most striking of these groups is in Cygnus, just south of γ Cygni. Here in an area of 14 square degrees are seven Wolf-Rayet stars brighter than 8.2 mag., three Of stars,[1] and seven other stars earlier than O9. Since the scatter in the distances of these objects is relatively small, the known absolute magnitudes of the B stars provide a calibration for the absolute magnitudes of the O and Wolf-Rayet stars.

Although this region has been studied extensively on objective-prism plates, a more detailed study seemed worth while. The area selected for this investigation is centered approximately on P Cygni and has the galactic co-ordinates $l = 39°$–$45°$, $b = -1°$ to $+3°$. It is illustrated in Figure 1. The choice of the region was based on the distribution of the Wolf-Rayet stars, although, as the photograph shows, the area also contains an unusually large number of stars brighter than the ninth magnitude. The majority of these are early-type stars; a plot of the stars in the *Henry Draper Catalogue* later than B5 shows no appreciable concentration in this area. This is in accord with the results of star-count analyses, which show no abrupt increase of density in this region except for the early-type stars.[2]

Originally, it was intended to obtain slit spectra of the stars in the *Henry Draper Catalogue* earlier than type B3. Later, most of the stars in the region from the "Finding List of O and B Stars of High Luminosity"[3] were added to the program. The spectra were obtained with the small spectrograph attached to the 40-inch refractor and have a dispersion of 125 A/mm at $H\gamma$. The majority are well widened, although a few are somewhat narrower, either because the stars are unusually faint or because they are situated in an unusually crowded field.

The stars cover a sufficiently large area that it is impractical to assume that the same amount of absorption affects the light of each one. This is particularly true in the negative galactic latitudes, which are affected by the extremely heavy absorption in the

[1] In keeping with the classification introduced at Victoria, we shall use the letter "f" to denote the presence of the blend *N* III 4634–4640 and *He* II 4686 in emission in an O-type star with no other Wolf-Rayet characteristics.

[2] See Bart J. Bok, *The Distribution of the Stars in Space* (Chicago: University of Chicago Press, 1937), p. 119.

[3] J. J. Nassau and W. W. Morgan, *Ap. J.*, 113, 141, 1951.

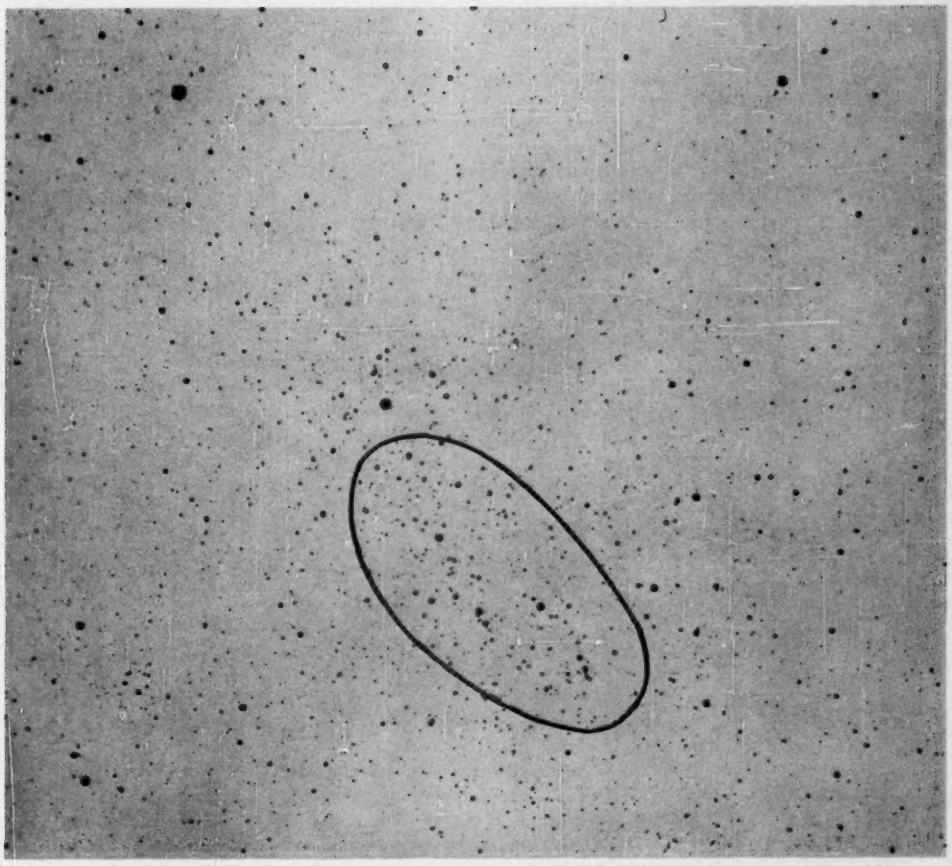

FIG. 1.—A portion of Cygnus, showing the region included in this investigation. North is up. α Cygni, δ Cygni, η Cygni, and ϵ Cygni are near the corners of the print, which is centered slightly west of γ Cygni. The photograph is enlarged about 10× from a Leica negative.

Cygnus rift. A few of the stars are in the list of colors of 1332 B stars,[4] but it seemed advisable to obtain the colors of as many of the stars as possible. Also, except for the brightest stars, only rough magnitudes were available. For these reasons, the colors and magnitudes of eighty-eight stars were determined photoelectrically with a photometer designed by W. A. Hiltner attached to the 12-inch refractor of the Yerkes Observatory. The average number of observations for each star is 2.4, which corresponds to an internal mean error of 0.008 mag. in the color and 0.011 in the magnitude. Only four stars have less than two observations. Since the faintest stars observed are near the limit of the equipment, the results for these stars are less accurate than those for the brighter stars. This is particularly true of the colors of the faint, highly reddened stars for which the blue deflections were comparable with those from the sky background.

Twenty-one of the stars observed have published colors on the C_1 system.[4] This per-

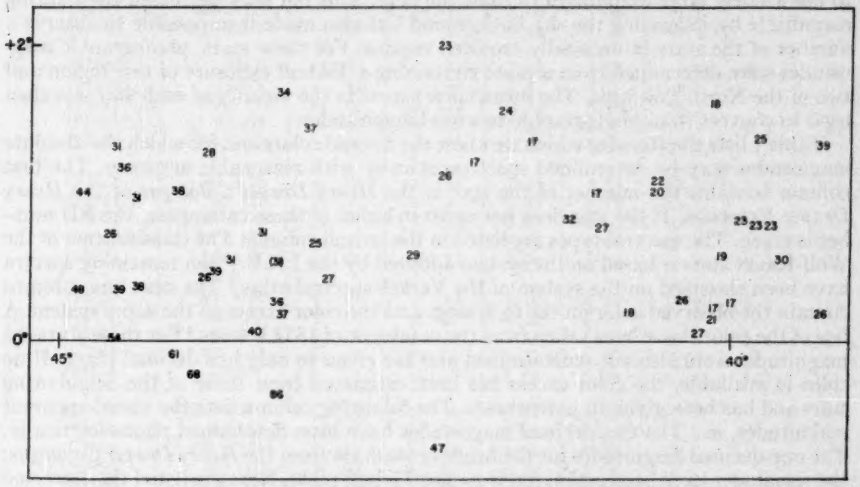

FIG. 2.—A map of the color excesses in the region. The value in parentheses is that for P Cygni

mitted a transfer of the measured colors to this system without a significant loss of accuracy. Several additional stars near, but not in, the region were measured to strengthen the red portion of the transfer; but a large extrapolation was necessary from the reddest star with a C_1 color, $C_1 = +0.34$ mag., to the reddest star measured, $C_1 = +0.61$ mag. Only reddened B stars were used to define the relation between the two systems. Although the base line of the measured colors is about twice that of the C_1 colors, there was no indication of a deviation from a linear relation. A partial check on the extrapolation may be found in the fact that Code and Whitford have found a similar color for the reddest star measured.[5]

The color on the C_1 system and the spectral type were used to compute the color excess for each star. These were based on the normal colors currently in use by W. W. Morgan.[6] Figure 2 gives a map of these color excesses. Two stars which are obviously foreground objects have been omitted. The remaining stars are certainly all behind the predominant absorbing matter in this region. The increase of the absorption in the

[4] Stebbins, Huffer, and Whitford, *Ap. J.*, 91, 20, 1940.

[5] Private communication.

[6] Unpublished.

higher galactic longitudes and, particularly, in the negative latitudes, i.e., in the region of the Cygnus rift, is quite noticeable. This indicates that the boundaries of the cloud on the north and east may be due to absorption; there is no indication that the southern and western boundaries are not intrinsic properties of the stellar distribution.

The magnitude of each star measured was referred to that of HD 191495. Later, this star was compared with seven stars in the North Polar Sequence with visual magnitudes in the range 6.5–9.1 mag.[7] The comparisons were made on two nights when the Cygnus region was at nearly the same altitude as the North Pole. It was assumed that the color term, which is 0.21 C_1, is the same for the intrinsically red standards as for the space-reddened, early-type stars. Thus it was possible to place the observed yellow magnitudes on the International photovisual system.

Because of the color-curve of the refractor used for the photometry, it was necessary to use a fairly large diaphragm to limit the field. This not only decreased the limiting magnitude by increasing the sky background but also made it impossible to observe a number of the stars in unusually crowded regions. For these stars, photographic magnitudes were determined from a plate containing a Tikhoff exposure of this region and two of the North Pole area. The mean color excess in the vicinity of each star was then used to convert from photographic to visual magnitudes.

Table 1 lists the stars for which we know the normal colors and for which the absolute magnitudes may be determined spectroscopically with reasonable accuracy. The first column contains the number of the star in the *Henry Draper Catalogue* or the *Henry Draper Extension*. If the star does not occur in either of these catalogues, the BD number is given. The spectral types are listed in the second column. The classification of the Wolf-Rayet stars is based on the system adopted by the I.A.U.;[8] the remaining spectra have been classified on the system of the Yerkes spectral atlas.[9] The next two columns contain the observed color on the C_1 system and the color excess on the same system. A few of the colors have been taken from the catalogue of 1332 B stars.[4] For these stars the magnitudes were also not redetermined and are given to only one decimal place. If no color is available, the color excess has been estimated from those of the neighboring stars and has been given in parentheses. The following column lists the visual apparent magnitudes, m_v. The two-decimal magnitudes have been determined photoelectrically. The one-decimal magnitudes for the brighter stars are from the *Henry Draper Catalogue;* the remainder have been estimated from the Tikhoff plate. Next are listed the corrected apparent magnitude, computed from the relation

$$m_0 = m_v - 7E_1 ,$$

and the corrected distance modulus based on the spectroscopic absolute magnitude. Finally, the last two columns contain the data available on the polarization of the light from these stars. These have been taken from lists by Hall and Mikesell[10] and by Hiltner.[11] For stars contained in both lists, mean values have been taken. The position angle

[7] The stars measured, together with their visual magnitudes and colors, are as follows:

NPS	m_v	C	NPS	m_v	C
7.....	7.55	−0.10	10.....	9.07	+0.16
3r.....	7.54	+1.44	2r.....	6.50	+1.49
8.....	8.16	+0.26	4r.....	8.24	+1.07
9.....	8.86	+0.21			

[8] *Trans. I.A.U.*, 6, 248, 1938.

[9] Morgan, Keenan, and Kellman, *An Atlas of Stellar Spectra* (Chicago: University of Chicago Press, 1943).

[10] *Pub. U.S. Naval Obs.*, Vol. 17, Part I, 1950.

[11] *Ap. J.*, 114, 241, 1951.

TABLE 1

NORMAL STARS LATER THAN O8

STAR	SP. TYPE	C_1	E_1	m_g	m_0	$m_0 - M$	POLARIZATION	
							Per Cent	θ
HD 190429 ft..	O9 III	.....	(+0.25)	7.2	5.4	10.8	.....	.....
190467....	B3 III	−0.05	+ .18	8.20	6.94	10.6	0.4	62°
190919....	B1 II	− .03	+ .22	7.36	5.82	10.9	0.7	107
190967....	B1 Ib	+ .05	+ .30	8.61	6.51	12.5	1.0	14
191139....	B0.5 III	− .04	+ .22	8.02	6.48	10.9	.....	.....
191201....	O9.5 III	− .07	+ .19	7.30	5.97	11.7*	0.4	150
191396....	B0.5 Ib	− .03	+ .23	8.17	6.56	12.6	.....	.....
191456....	B0.5 IV	− .09	+ .17	7.42	6.23	10.2	.....	.....
191473....	B0.5 III	− .09	+ .17	8.64	7.45	11.8	.....	.....
191495....	B0 V	− .09	+ .17	8.44	7.25	11.1	.....	.....
191566....	B0 V	− .05	+ .21	7.39	5.92	9.8	0.6	62
191610†...	B3 V	− .20	+ .03	4.8	4.6	6.6	.....	.....
191611....	B0.5 IV	+ .01	+ .27	8.59	6.70	10.7	‡	‡
191917....	B1 III	− .07	+ .18	7.83	6.57	10.9	0.2	84
192079....	B0.5 IV	.00	+ .26	8.76	6.94	10.9	.....	.....
192422....	B0.5 Ib	+ .08	+ .34	7.21	4.83	10.8	1.6	101
192444....	B1 III	+ .12	+ .37	8.38	5.79	10.1	.....	.....
193007....	B0.5 IV	.....	(+ .27)	7.9:	6.0:	10.0:	.....	.....
193032....	B0.5 III	+ .02	+ .28	8.41	6.45	10.8	1.6	128
193076....	B0.5 II	+ .01	+ .27	7.70	5.81	11.0	0.5	6
193183....	B1.5 Ib	+ .07	+ .31	7.10	4.93	10.9	0.5	125
193427....	B1 III	+ .06	+ .31	9.16	6.99	11.3	.....	.....
193443....	O9 III	+ .04	+ .31	7.33	5.16	10.6	1.4	143
193444....	B0.5 V	+ .10	+ .36	8.52	6.00	9.6	.....	.....
193516....	B1 III	+ .12	+ .37	8.68	6.09	10.4	1.3	131
193611....	O9.5 V n:	+ .13	+ .39	8.74	6.01	10.1:	.....	.....
193634....	B2 III	+ .02	+ .26	7.47	5.65	9.7	.....	.....
193794....	O9.5 IV	+ .18	+ .44	9.09	6.01	10.5	.....	.....
193855....	B2 III	+ .02	+ .26	7.78	5.96	10.1	.....	.....
194009....	B3 II	+ .15	+ .38	8.79	6.13	10.6	.....	.....
194094....	O9.5 IV	+ .13	+ .39	9.13	6.40	10.9	.....	.....
194153....	B1 Iab	+ .36	+ .61	8.66	4.39	11.0	.....	.....
194280....	B0 Ib	+ .22	+ .48	8.50	5.14	11.1	.....	.....
HDE 227634....	B0 II	− .03	+ .23	8.1	6.5	11.7	.....	.....
227696....	B0.5 V	− .04	+ .22	8.6	7.1	10.7	.....	.....
227704....	B0 III	.00	+ .26	8.68	6.86	11.4	.....	.....
227757....	O9.5 V	− .06	+ .20	9.27	7.87	12.0	.....	.....
227877....	B2 V	− .07	+ .17	9.05	7.86	10.5	.....	.....
227902....	B2 IV	.00	+ .24	9.30	7.62	11.0	.....	.....
228053....	B1 Ib	+ .07	+ .32	8.93	6.69	12.7	0.8	41
228101....	B1 IV	− .08	+ .17	8.47	7.28	11.1	.....	.....
228690....	B0.5 V	− .01	+ .25	9.33	7.58	11.2	.....	.....
229227....	B0 III	.....	(+ .54)	8.6	4.8	9.3	0.9	153
229234....	O9 II	.....	(+ .54)	8.6:	4.8:	10.5:	1.2	3
229238....	B0.5 II	.....	(+ .54)	8.5:	4.7:	9.9:	1.4	176
BD+35°3955...	B0.5 II	−0.04	+ .22	7.8	6.3	11.5	.....	.....
+37°3859...	B1 III	.....	(+ .27)	9.8::	7.9::	12.2::	.....	.....
+37°3862...	B0 V	.....	(+0.27)	9.7:	7.8:	11.7:	.....	.....

* The distance modulus includes a correction of 0.7 mag. to allow for the fact that this star is a two-line spectroscopic binary.

† 28 Cygni. This star is definitely a foreground object.

‡ No observable polarization.

given is that of the magnetic vector of the polarized light in an equatorial system of co-ordinates.

It may be seen from Table 1 that there is a strong concentration of stars with distance moduli near 11.0 mag. Unfortunately, the observational errors are such that it is difficult to estimate the true spread in distance of these objects. The standard deviation of the distance moduli is 0.7 mag. If the mean error of the spectroscopic absolute magnitudes were 0.6 mag. and the mean error of the corrected apparent magnitudes were 0.2 mag., a dispersion of about 0.3 mag. would still remain to be accounted for as a spread in distance. This corresponds to a line-of-sight diameter of 450 parsecs for the group. In contrast, the dimensions of the group perpendicular to the line of sight are about 170 by 110 parsecs. The suggestion has frequently been made that in Cygnus we are looking along a spiral arm. It seems impossible on the basis of the present data to decide whether the explanation for the apparent spread in distance lies in the fact that we are observing a knot in a spiral arm or whether it lies in the inaccuracy of our observations.

The group is certainly not the usual type of cluster. It is far bigger than the Pleiades or even the Orion concentration of B stars. As the star-count analyses confirm, the region is not one of unusually high stellar density. Nevertheless, the concentration of early-type objects is certainly real. In Table 1 the mean apparent magnitudes of the stars of luminosity classes I, III, and V are 8.07, 8.34, and 8.63, respectively. (The near-by dwarf, 28 Cygni, has been omitted in forming the means.) If the stars were uniformly distributed in distance, we would expect the three groups to have the same mean apparent magnitude. On the other hand, the difference between the apparent magnitudes for the three groups is not so large as we would expect if all the stars were at the same distance. This can be explained by the fact that, in the portions of the region covered by the denser absorbing matter, we are not reaching the dwarf or even all the giant stars. Support for this interpretation may be found in the fact that the mean of the corrected distance moduli for stars with color excesses less than 0.30 mag. is almost identical with that for stars with distance moduli between 0.30 and 0.50 mag. If the stars were uniformly distributed, the redder stars should be nearer, on the average, since the heavier absorption would keep us from observing the more distant ones. The smoothness of the change of color excess with position in the sky also supports a limited range in distance for these stars. If the range in distance were very great, we would expect the more distant objects to be redder.

Radial velocities have been published for only a few of the stars in the region. Most of these are uncertain, either because the star has poor lines or because its velocity is variable, and the observational errors are comparable with the expected dispersion in the velocities of a random selection of early-type stars. The measures of the interstellar lines given by Adams[12] for ten stars in the region do not even permit the distinction in an unambiguous way between the stars nearer and more distant than the main absorbing medium.

Figure 3 shows a map of the polarization measures in this region. No stars which are definitely nearer than the absorbing cloud were measured by either Hall or Hiltner. Even behind this cloud, the polarization of the stars is not large, and the position angles are not well determined. Nevertheless, the large range from no polarization to more than 2 per cent and the great range in the position angles are certainly real. There is some correlation between the percentage polarization and color excess in this region, but most of the scatter remains unexplained. The widely different results found for the small cluster, NGC 6913 (on the galactic equator near longitude 44°.5), are particularly difficult to interpret.

The stars in NGC 6913 seem to be nearer than most of the others. Their color excess, 0.54 mag., is based on a C_1 color for one member of the group. Although this member is a Be star, the derived color excess is almost exactly that estimated independently from

[12] *Ap. J.*, **109**, 354, 1949.

the position of the cluster. However, the magnitudes in this group are also uncertain because of overlapping images, and it was difficult to obtain spectra of the highest quality for these stars.

Fortunately, the dispersion in the distance moduli in Table 1 is small enough to permit a good calibration of the absolute magnitudes of the earlier O-type and Wolf-Rayet stars. These and the other emission-line objects are shown in Table 2. The arrangement of the data is the same as in Table 1 except that, in the seventh column, the distance modulus is replaced by the absolute magnitude which results from a distance modulus of 11.0 mag. The normal color of each Wolf-Rayet star in the region appears to be very near −0.24 mag., and this value has been used in the computation of the color excesses. For the re-

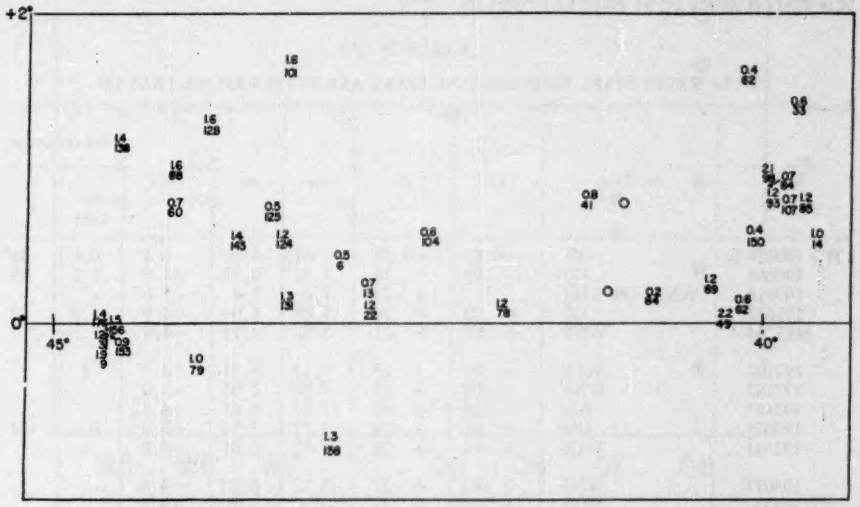

FIG. 3.—A map of the polarization measures in the region. The circles denote stars for which no polarization was observed. For the remaining stars, the upper figure gives the percentage polarization and the lower one the position angle of the magnetic vector.

maining emission-line objects, the colors of normal stars of the same spectral types were used. In no case did these assumptions lead to color excesses appreciably different from those for the other stars in the region.

A plot of the absolute magnitudes of the Wolf-Rayet and early O stars is given in Figure 4. Three results are apparent. The Of stars are brighter than the absorption O stars and have an absolute magnitude near −6.0. Although the scatter is large for the O8 stars, the following absolute magnitudes may be adopted for the absorption O stars: O5, −5.3; O7, −4.7; O8, −4.4. The luminosity of the Wolf-Rayet stars resembles that of the absorption O stars rather than that of the Of stars. A value of −4.9 seems reasonable for their absolute magnitude. Although the correlation between absolute magnitude and spectral type (i.e., excitation) appears suggestive, it should not be taken too seriously in view of the scatter in Table 1.

Three other stars in Table 2 deserve some comment. One of these is the well-known "permanent nova," P Cygni. If this star has a distance modulus of 11.0 mag., its visual absolute magnitude must be −8.3, making it as bright as S Doradus. However, in view of the dispersion in the distance moduli in Table 1, an absolute magnitude of −7.5 cannot be completely ruled out. The luminosity must be of this order. A rough lower limit

may be found from the fact that P Cygni is behind the absorbing cloud covering the entire area. Several lines of evidence indicate this. The color excess, computed on the assumption that the unreddened color for the star is the same as for a normal B1 star, agrees with the color excesses of the other stars in the vicinity. The polarization and the intensity of the interstellar K line also agree well with those for neighboring stars. In addition, Duke[13] has found that the central intensity of the interstellar feature at λ 4430 is of the same order of magnitude in P Cygni as in fourteen other stars in Tables 1 and 2. It is much less in the foreground star, 28 Cygni. From the small color excess, HD 192445 appears to be nearer than much of the absorbing material in this region. If we assume that this star has an absolute magnitude of −2.6, corresponding to that of a B2 dwarf, its distance modulus is 9.3 mag. Since P Cygni is certainly more distant than this star, it must be at least as bright as $-6^{M}.6$.

TABLE 2

WOLF-RAYET STARS, EMISSION-LINE STARS, AND STARS EARLIER THAN O9

STAR	SP. TYPE	C_1	E_1	m_v	m_0	M	POLARIZATION	
							Per Cent	θ
HD 190429 br.	O5f	−0.06	+0.25	6.64	4.89	−6.1	0.6	33°
190864...	O7	− .06	+ .23	7.83	6.22	−4.8	1.2	85
190918...	WN5+O9.5 III	.....	(+ .23)	7.0	5.4	−5.6*	.....	.....
191612...	O8	− .02	+ .26	7.88	6.06	−4.9	1.2	69
191765...	WN6	+ .03	+ .27	8.05	6.16	−4.8	.....	.....
192103...	WC7	− .01	+ .23	8.12	6.51	−4.5	†	†
192163...	WN6	− .02	+ .22	7.50	5.96	−5.0	.....	.....
192445...	B2e	− .16	+ .08	7.23	6.67	−4.3‡	.....	.....
192639...	O8f	+ .01	+ .29	7.17	5.14	−5.9	0.6	104
192641...	WC6	+ .04	+ .28	7.97	6.01	−5.0	.....	.....
193077...	WN5	+ .03	+ .27	8.12	6.23	−4.8	.....	.....
193237...	B1p§	+ .06	+ .31	4.9	2.7	−8.3	.....	.....
193514...	O7f	+ .07	+ .36	7.48	4.96	−6.0	1.4	138
193576...	WN5	+ .11	+ .33	8.10	5.65	−5.3	.....	.....
193595...	O8	+ .03	+ .31	8.79	6.62	−4.4	.....	.....
193682...	O5	+ .09	+ .40	8.52	5.72	−5.3	.....	.....
193928...	WN6	+ .30	+ .54	9.93	6.15	−4.8	.....	.....
HDE 227611...	Bep‖	+ .01	(+ .23)	8.86	7.25	−3.8	.....	.....
227245...	O8	+ .11	+ .39	9.91	7.18	−3.8	.....	.....
228041...	B0.5 V: e	+ .01	+ .27	9.11	7.22	−3.8	2.2	49
228766...	WN7	+ .15	+ .39	9.28	6.55	−4.4	1.2	22
228841...	O7	+ .09	+ .38	9.07	6.41	−4.6	1.6	88
228854...	O8	+ .19	+ .47	8.72	5.43	−5.6	.....	.....
229059...	B1.5 Ibe	+ .61	+ .86	8.88	2.86	−8.1	.....	.....
229221...	B0 II: e	+0.28	+ .54	8.8	5.0	−6.0	1.5	156
229239...	B0.5 IIe	.....	(+0.54)	8.6:	4.8:	−6.2:	1.9	9

* If we assume that the light in this system is contributed equally by the two components, we obtain an absolute magnitude of −4.9 for each. This is in good agreement with the expected values.

† No observable polarization.

‡ Since, according to the color, this is a foreground object, no weight should be given the absolute magnitude derived on the assumption of membership in the group. The star is almost certainly a dwarf.

§ P Cygni.

‖ This star has strong lines of *Fe* II. The only absorption features visible on the dispersion used are λ 4387, the wings of $H\gamma$ and $H\delta$, and the interstellar band at λ 4430.

[13] *Ap. J.*, **113**, 100, 1951.

The spectral type assigned to HDE 228766 merits some comment. Hiltner[14] announced that this star is a Wolf-Rayet spectroscopic binary; but, on plates of the dispersion used in this study, the spectrum of this star cannot be distinguished from that of an Of star. The emission features near λ 4640 and λ 4686 are very strong but not unusually broad. No other emission features are observed with certainty. Since Hiltner found that *N* IV 4058 is also in emission, his classification, WN7, has been retained. On the basis of the width of the emission features, this star would certainly be called an Of

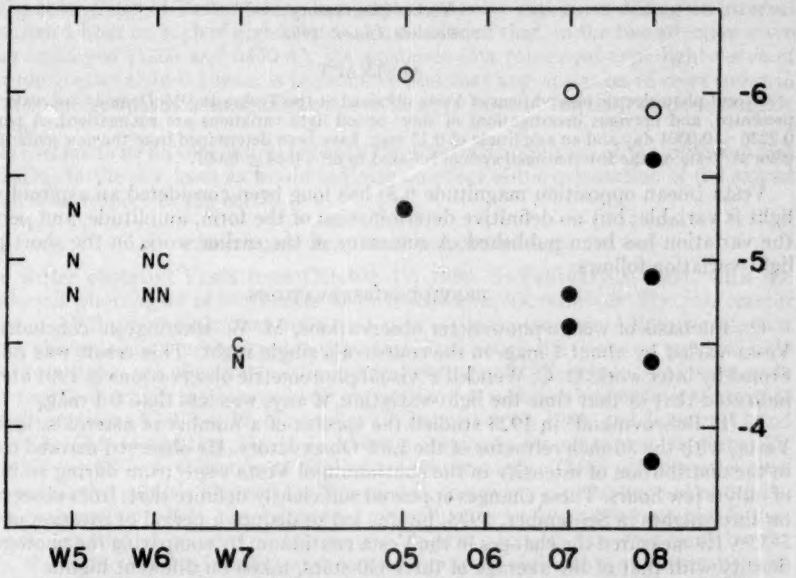

FIG. 4.—The absolute magnitudes of the earliest stars based on a distance modulus of 11.0 mag. The letters *N* and *C* denote Wolf-Rayet stars of the nitrogen and carbon sequences, respectively. The open circles denote Of stars, the filled circles, absorption O stars.

star. Since the Of stars are at least 1 mag. brighter than the Wolf-Rayets, the problem of a clear distinction between the two types becomes an important one. In this case, both the apparent magnitude and the color support the classification as a Wolf-Rayet, unless the star is appreciably more distant and more reddened than the other stars in the vicinity.

About twelve years ago, Morgan[15] called attention to the very red B star, HDE 229059. The color given in Table 2 corresponds to that of an early K giant. $H\beta$ is in very weak emission in this star, but it is unlikely that $H\alpha$ emission contributes appreciably to the color. The star is situated in the very heavily absorbed region of the Cygnus rift. It is unlikely that the star is as bright as $-8^{M}1$; it is almost certainly no brighter than a I*b* supergiant, and it may not be that bright. Not only may the star not be a member of the concentration, but the corrected apparent magnitude may be in serious error. If the ratio of total absorption to E_1 is 6 instead of 7, as has been used here, the corrected apparent magnitude should be reduced by 0.9 mag.

I wish to thank Drs. Nassau and Morgan for the use of the list of high-luminosity O- and B-type stars, and Dr. Hiltner for the use of his polarization results, both before publication. I am also grateful to Dr. Morgan for the use of a number of plates, for access to a great deal of unpublished data, and for the suggestion from which this investigation developed.

[14] *Ap. J.*, **113**, 317, 1951.

[15] *Pub. A.A.S.*, **9**, 301, 1939.

THE LIGHT-CURVE AND THE COLOR OF VESTA

C. BRUCE STEPHENSON
Yerkes Observatory
Received June 2, 1951

ABSTRACT

Recent photoelectric observations of Vesta obtained at the Yerkes and McDonald Observatories are presented, and previous investigations of short-period light-variations are summarized. A period of 0.2226 ± 0.0001 day and an amplitude of 0.12 mag. have been determined from the new material. The color of Vesta on the International system is found to be +0.64 ± 0.007.

Vesta (mean opposition magnitude 6.5) has long been considered an asteroid whose light is variable; but no definitive determination of the form, amplitude, and period of the variation has been published. A summary of the earlier work on the short-period light-variation follows.

PREVIOUS OBSERVATIONS

On the basis of wedge-photometer observations, M. W. Harrington[1] concluded that Vesta varied by about 1 mag. in the course of a single night. This result was not confirmed by later work. O. C. Wendell's[2] visual photometric observations in 1901 and 1904 indicated that at that time the light-variation, if any, was less than 0.1 mag.

N. T. Bobrovnikoff[3] in 1928 studied the spectra of a number of asteroids, including Vesta, with the 36-inch refractor of the Lick Observatory. He observed marked changes in the distribution of intensity in the continuum of Vesta's spectrum during an interval of only a few hours. These changes appeared sufficiently definite that, from observations on three nights in September, 1928, he was led to deduce a period of rotation of about 5^h55^m. He measured the changes in the Vesta continuum by comparing the photographic density with that of the average of three G0 stars, taken on different nights.

T. Kanamori,[4] making visual-magnitude estimates with a small telescope on three nights in December, 1932, believed that a variation of about 0.5 mag. existed, with a period of 3 hours. W. K. Green[5] observed Vesta photographically at Amherst and found that his observations could be represented by a period of 0.31304 day, an amplitude of 0.21 mag., and a probable error of one observation of ±0.04 mag. The asteroid was also observed in 1934 by W. A. Calder[6] and by W. A. Johnson.[7] The former found no variation photoelectrically in May, 1934, but he observed in dusty skies. Johnson compared spectra of Vesta and several G0 stars taken by F. G. Watson and derived a variation in the color index of Vesta of more than 1 mag. From subsequent unpublished photometric observations made in March and April, 1934, he concluded that the asteroid had been reddest at maximum light.

F. G. Watson[8] took a number of photographs of Vesta for color index during an interval of about 1 hour (Dec. 15–16, 1936). During this interval he found no evidence for variation either of light or of color.

On October 16 and December 16, 1939, W. K. Green and J. S. Hall[9] obtained photographic and photoelectric observations of Vesta simultaneously, finding that it varied

[1] *Amer. J. Sci.*, third ser., **26**, 462, 1883.
[2] *Harvard Ann.*, **69**, 200, 1913.
[3] *Lick Obs. Bull.*, **14**, 18, 1929.
[4] *Bull. Kwasan Obs.*, No. 248, 1933.
[5] *Pub. A.A.S.* **8**, 113, 1935.
[6] *Harvard Bull.*, No. 904, p. 11, 1936.
[7] *Harvard Bull.*, No. 911, p. 13, 1939.
[8] *Harvard Bull.*, No. 913, p. 3, 1940.
[9] *Pub. A.A.S.*, **10**, 13, 1940.

systematically in brightness by more than 0.1 mag. but not in color. Photoelectric observations made at 8100 A and photographic observations made at 4300 A agreed in amplitude within 0.01 mag. The two nights mentioned gave accordant results, but on a third night, October 17, the photoelectric observations indicated no appreciable change in brightness over a period of more than 3 hours. No photographic observations were made on this date.

From January to March, 1941, H. Fischer[10] made a photographic study of the brightness and color index of Vesta, taking from eight to twelve exposures during an interval of less than 1 hour on each of eight nights. He concluded that, in the two effective wave lengths employed (4200 and 6450 A), the existence of a rotational-type light-curve of amplitude greater than 0.1 mag. is improbable and that any variation of color index in the Göttingen system is so insignificant as to be at or beyond the limit of photographic detection.[11]

There seems to be no correlation between the observed amplitude of the variation and the position in the sky, such as would indicate an effect of the orientation of the axis of rotation with respect to the earth.

YERKES AND McDONALD OBSERVATIONS

The writer observed Vesta from October 19, 1950, to February 8, 1951, with the photoelectric photometer of the Yerkes 12-inch photographic refractor. The photometer contains a 1P21 photomultiplier tube and uses a Brown recorder. Because of poor weather, observations were confined to a few nights, although the telescope was available two to three nights per week during the interval mentioned. Altogether, runs were made on five nights on which the atmospheric extinction was sufficiently constant to provide usable observations: October 19, November 14, December 10, 1950, and January 11 and February 8, 1951. In addition, Dr. H. L. Johnson obtained a 6-hour run on December 22, 1950, with the 82-inch telescope at McDonald Observatory. These observations were kindly put at the writer's disposal for inclusion in this paper. In the hope of obtaining runs on consecutive nights, the writer took observations on five additional nights that gave some promise of being of "photometric" quality, but, as was confirmed by the records, the extinction was insufficiently constant on these nights; hence the results were not used.

In general, each "observation" consisted of a set of three 30- to 50-second exposures of the photocell to the comparison star with the yellow filter and three with the blue, followed by a measurement of the yellow and blue sky intensity and by one or two sets of three measurements of Vesta in both colors. The effective wave lengths are approximately 5350 A for the yellow filter and, near spectral type G, around 4100 A for the blue filter. The mean of a set of three measurements of Vesta as compared with the average of the preceding and following set for the comparison star was taken as a single observation and is plotted as a single point in the light-curves given here. At fairly large zenith distances, only one set of three measurements of Vesta was made for each set of three for the comparison star, to minimize errors caused by rapid variation in the extinction. In order to reduce extinction errors, the comparison stars were never more than 1° from Vesta, except for the 82-inch run (in which the extinction was known with good accuracy), and were nearly always within 40′ of the asteroid. On the longest run Vesta and the comparison star were only about 10′ apart. For the same reason the comparison stars were selected to be stars with spectral types as close as possible to G0. On most nights the comparison star was periodically compared with a second star to check possible variability.

[10] *A.N.*, **273**, 124, 1942–1943.

[11] Some of the above work has been re-examined by H. Auzinger and H. Haupt, *Mitt. Wiener Sternw.*, Vol. 4, No. 13, 1950. This paper was received after the present paper was written.

In applying the correction for differential extinction between asteroid and comparison star, the secant law of extinction was employed. The coefficients used were those derived by the writer for yellow stars: 0.24 mag. for $\lambda = 5350$ A and 0.45 mag. for $\lambda = 4100$ A. A separate determination for each night was not made but was not warranted in view of the proximity of the comparison stars. Except in the reduction of the 82-inch run, no term allowing for the color difference with the comparison star was included in the extinction coefficient, for lack of data. However, it is not believed that this correction was ever appreciable. The color term was quite insignificant in the reduction of the 82-inch run except for zenith distances in excess of 63°. The Yerkes runs were usually not made beyond a zenith distance of about 60°, but the exclusion of a color term from the extinction correction may contribute slightly to the scatter in the observations shown in the light-curves, six different comparison stars having been used. The coefficient of differential extinction used in correcting the color observations was also a mean value derived from previous data; but the coefficient was adjusted in some instances so as to satisfy the condition that the extinction-corrected color of the comparison star remain constant.

The following method was used in determining the period of light-variation of Vesta. Since the phase coefficient of Vesta is not known with precision, little use could be made of the absolute values of the magnitudes, which varied by more than 1 mag. from October to February. Furthermore, this would have required the magnitudes of the six comparison stars to be known with accuracy. Therefore, only the phase and the shape of the light-curves were employed. The different runs were superimposed in pairs, so as to give the best possible fit, and the times of observation of corresponding points at an arbitrary point on the composite curve were noted. The interval between these two times of observation, when corrected for light-time according to the known change in distance between Vesta and the earth, represents an integral number of periods. Making use, as it does, of the whole of each run, this method should be better than measuring the interval between, say, maxima or minima. A great many such intervals could be derived, and the period of variation was determined by the requirement that it be an integral factor of these intervals, as well as of any linear combinations of them. Two runs of the six apparently covered more than one entire period: Johnson's run of December 22, 6 hours in length, and the Yerkes run of October 19, 7^h48^m in length. These two runs indicate a period of about 5^h27^m, with a maximum uncertainty of about 15 minutes; but, in order to be safe, any period between 5 and 6 hours was considered possible. Only one such period was found to satisfy all the observations: $5^h20^m53 \pm 0^m02 = 0.2226 \pm 0.0001$ day.

In Figure 1 the observations in yellow light are combined on the basis of this period, each night's run being represented by a different symbol; the closed circles represent the 82-inch run, and the others, Yerkes runs. The vertical position of each run has been adjusted, as has been explained. There is no evidence of appreciable systematic difference between the various runs. It is, of course, conceivable that the true period is precisely double the period given. For this reason Figure 2 shows the observations combined on this assumption. There is no reason to adopt the longer period, on the basis of decreased scatter or unequal shape of the two halves of the curve. In either case the amplitude is 0.12 mag. The amplitude underwent no definite variation as Vesta moved between 2^h26^m and 3^h15^m, and between $+6°3'$ and $+11°33'$.

No definite color variation of Vesta was found at Yerkes, but the 82-inch observations indicate a variation of about 0.03 mag. on the McDonald system, with a period of roughly 5^h30^m. The fact that the color repeats itself during the short period lends weight to the probability that the short period rather than the long one is correct. On the basis of this one run, Vesta is reddest about 1 hour before mid-maximum and bluest about $1\frac{1}{2}$ hours after mid-maximum.

A least-squares solution was made for the relation between the Yerkes system of colors and the International system, on the basis of data for forty-seven stars having Yerkes

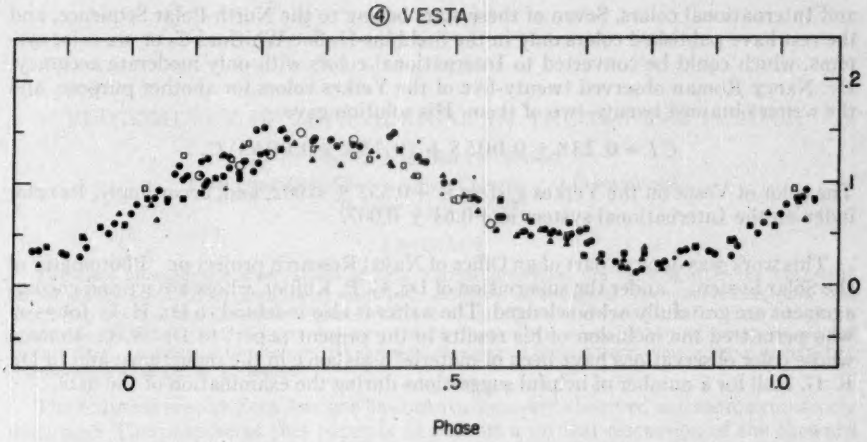

FIG. 1.—Light-curve of Vesta. Closed triangles represent October 19, 1950; closed squares, November 13; open triangles, December 10; closed circles (82-inch run), December 21; open squares, January 11, 1951; open circles, February 8. In each run the weight of an observation is proportional to the size of its symbol. Zero phase is 6^h54^m U.T. October 20, 1950. Period = 0.2226 day.

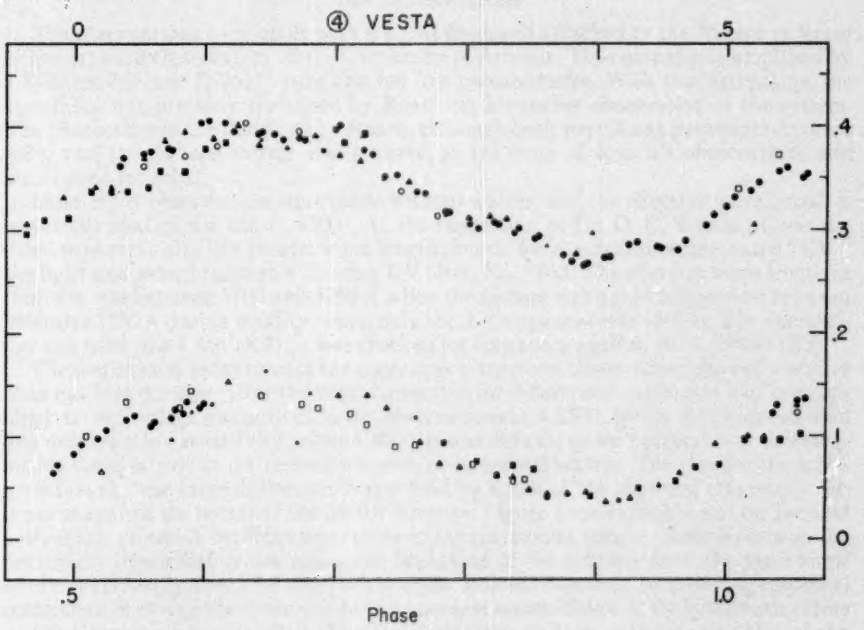

FIG. 2.—The observations of Figure 1 combined on the basis of the double period =0.4452 day

and International colors. Seven of these stars belong to the North Polar Sequence, and the rest have published colors only in the Stebbins-Huffer-Whitford C_1 or six-color systems, which could be converted to International colors with only moderate accuracy. Dr. Nancy Roman observed twenty-five of the Yerkes colors for another purpose, and the writer obtained twenty-two of them. His solution gave

$$CI = 0.238 \pm 0.0055 + (0.753 \pm 0.0063) C_y .$$

The color of Vesta on the Yerkes system is $+0.532 \pm 0.002$, and, accordingly, its color index on the International system is $+0.64 \pm 0.007$.

This work was done as part of an Office of Naval Research project on "Photometry of the Solar System," under the supervision of Dr. G. P. Kuiper, whose advice and encouragement are gratefully acknowledged. The writer is also indebted to Dr. H. L. Johnson, who permitted the inclusion of his results in the present paper; to Dr. N. G. Roman, whose color observations have been of material assistance in the reductions; and to Dr. R. G. Hall for a number of helpful suggestions during the examination of the data.

PHOTOMETRY OF ZETA AURIGAE IN THE 1947–1948 ECLIPSE

FRANK BRADSHAW WOOD
Flower and Cook Observatories, University of Pennsylvania
Received April 18, 1951

ABSTRACT

Two-color photoelectric observations of Zeta Aurigae preceding, during, and after the 1947–1948 eclipse are discussed. Observations were made both at ingress and at egress. The observations show that the eclipse began in the ultraviolet region, well before any effect was detectable in the blue, and that a systematic difference exists between the two sets of observations when fraction of eclipse is plotted against time. An attempt to interpret the physical meaning of these observations is being prepared in collaboration with Dr. F. E. Roach.

The eclipsing system Zeta Aurigae has been extensively observed and more extensively discussed. The purpose of this paper is to present a critical discussion of the Steward Observatory observations made preceding, during, and after the 1947–1948 eclipse and to point out the effects which certain features of this discussion may have in the interpretation of some of the earlier photometric investigations.

THE OBSERVATIONS

The observations were made with a Kunz photocell attached to the 36-inch reflector of the Steward Observatory of the University of Arizona. The current was amplified by a Western Electric D-96475 tube and fed to a galvanometer. With two exceptions, the apparatus was precisely that used by Roach[1] in his earlier observation of the system. The photocell was not that used by Roach, although both were Kunz potassium-hydride cells, and the 36-inch mirror was silvered at the time of Roach's observations and aluminized for mine.

Most of the observations were made without a filter, and the effective wave length is essentially that of the cell (λ 4500). At the suggestion of Dr. O. C. Wilson, it was decided to observe also in a shorter wave length; hence, for observations designated "UV," the light was passed through a Corning UV filter, No. 9863. The effective wave length in this case was between 3700 and 3750 A when the system was not in eclipse and between 3800 and 3850 A during totality, when only the K component was visible. The comparison star used was 2 Aur (K2); it was checked for constancy against BD+35°930 (B2).

The preliminary reductions of the noneclipse ultraviolet observations showed a scatter of as much as 0.2 mag. after the usual correction for differential extinction had been applied; no such effect was noticed in the observations at λ 4500. While the photocell used had relatively low sensitivity below λ 4000, it was difficult to see how errors of this magnitude could be due to instrumental causes or to normal scatter. The clue for the interpretation of these large differences is provided by a plot of the observed magnitude differences against the secant of the zenith distance. Figure 1 shows such a plot for the first two nights, on which readings were made in the ultraviolet region. Observations on the next night (immediately preceding the beginning of the eclipse) show the same slope but lie consistently about 0.1 mag. below these. It is obvious that, by applying empirical corrections to reduce the observations to a common zenith distance, the systematic errors will be removed; however, it is rather unsatisfactory to do so without some idea of the physical cause of this effect. It can scarcely be explained by a change in the coefficient used in computing the differential extinction, since such an explanation requires that the

[1] *Ap. J.*, 93, 1, 1941.

extinction coefficient be increased by a factor of at least 30. The proper explanation seems to lie in the great color difference between the comparison star and the B component of the variable. Below λ 4000, the light of the B component strongly predominates, and hence we here effectively compare an early-type variable with a late-type comparison star. While the effective wave length of the cell-filter combination lies about 3800 A, light shorter than 3500 A still has an appreciable effect; the B star, of course, produces a much greater fraction of its radiation in this region than does the K star. It is thus in this region that the rapid increase of atmospheric extinction will tend to dim the B star more rapidly than the K star and to decrease the measured difference of magnitude between them. It is important to see whether this increased extinction will be great enough to explain the observed correlation between difference of magnitude and zenith distance.

A computation, making use of the transmission-curve of the filter, the spectral sensitivity of the photosensitive surface, and the transmission of the atmosphere at Tucson

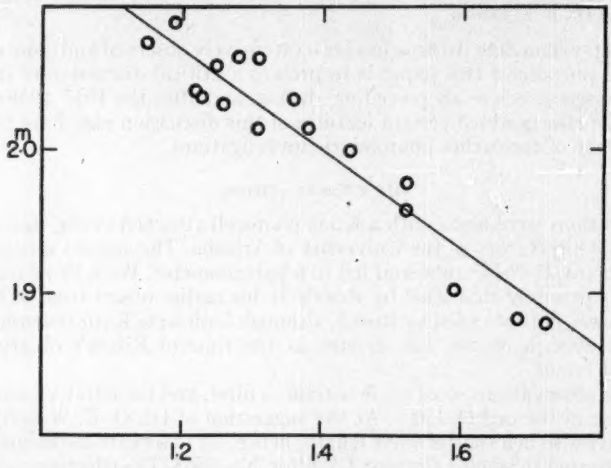

FIG. 1.—Individual UV observations outside eclipse. *Ordinate:* observed magnitude difference; *abscissa:* secant of zenith distance.

in various wave lengths as determined by Pettit[2] and checked by photoelectric measures at a few selected wave lengths and, for a first approximation, black-body energy distribution of the stellar radiation from each star indicates that, in these wave lengths, the B star should lose approximately 0.2 mag. more light than the K star as the two pass from the zenith to altitude 30°. The value found from an empirical plot of the observations is 0.35 mag.; this agreement is perhaps as good as can be expected, in view of the various uncertainties involved.

If the above idea is correct, the same effect should appear in the comparison-check star measures. In the choice of a comparison star, it was realized that it was impossible to match the color of both components of the variable; therefore, the check star was deliberately chosen of early spectral type so that any troubles arising from color difference would also be present in the comparison-check measures. This is well borne out by the measures available; unfortunately, these are few in number and were taken at rather small hour angles, so that the confirmation is not strong.

In the observations made without the filter, we should expect the same result but by

[2] *Ap. J.*, 75, 185, 1932.

a less noticeable amount. Nevertheless, the effect is easily detectable in the comparison-check star measures; the measured magnitude difference between the two varies from 0.25 near the zenith to 0.36 at 45° zenith distance. In the variable-comparison star measures, the effect should be much smaller because of the contribution of the K component of the variable. This again is found; the difference of extinction for air-mass unity is 0.028 mag. It should be pointed out that this effect becomes noticeable only when observations are made over a considerable range of altitude on nights when the system is not in eclipse and is scarcely detectable in wave lengths above 4000 A. Even in the ultraviolet, if filters were used which cut off the radiation below 3500 A or which permitted radiation only in a band of 300–500 A width, it is doubtful whether it would be noticeable.

The observations are listed in Table 1. The first column gives heliocentric time in Julian days and fraction of a day measured from Greenwich mean noon. The second column gives the observations corrected only for differential extinction in the usual manner. The third column gives a correction which, in the noneclipse observation, in the ultraviolet is given by $+0^m.35$ (sec $z - 1$) and in the blue by $+0^m.028$ (sec $z - 1$). During totality no correction is applied, and during the partial phases a fraction of the above, proportional to the noneclipsed fraction of the light of the blue component. The fourth column lists the corrected observations. Individual observations made out of eclipse have been combined chronologically in groups of two or three to form normals; when this has been done, the number of observations so combined is given in parentheses following the normal. During eclipse, the use of normals tends to mask the scatter of the observations. In any discussion of the light-changes, it is important, especially at these critical times, that the accuracy of the observations be neither over- nor underestimated; hence the observations during eclipse are the individual observations. In every case this consists of three measures of the comparison star, six of the variable, and three of the comparison star, with such measures of sky background as seemed appropriate under the existing conditions.

In the blue, the probable error of an individual observation is ± 0.008 mag. This is unusually large for a star of this brightness and is caused chiefly by small fluctuations from night to night. The fluctuations are larger during totality, suggesting that they are caused by the K component. Roach[3] also found irregular fluctuations during totality; and Kron[4] has announced that his observations, especially during totality, show fluctuations larger than random errors, and he suggested that the K component varies in brightness. Similar suggestions have been made by many of the earlier observers.

The time of the center of minimum from these observations is JD 2432553.666. New light-elements are suggested as Primary min. = JD $2432553.666 + 972^d.162E$.

DISCUSSION

One of the reasons for attempting the ultraviolet observations was to determine whether the light of the system was dimmed in these wave lengths sooner than in the longer ones. The evidence indicates that this is the case. The corrected observations the night before eclipse show an average difference between variable and comparison star of 2.031 mag.; the two preceding nights gave values of 2.138 and 2.144 mag. The system was thus 0.11 mag. fainter on the night before eclipse than on the two preceding ones; in the blue, however, the measures gave a magnitude difference of 1.166 on the night preceding eclipse and 1.173 and 1.166 on the two earlier nights; any loss was less than the errors of the observations. Weather prevented a repetition of such measures on the night after emergence.

The difference in behavior for the two colors is shown clearly by Figure 2, which is

[3] *Harvard Announcement Card* No. 518, 1939.

[4] *Pub. A.S.P.*, **52**, 124, 1940.

TABLE 1

ZETA AURIGAE

OBSERVATIONS AT 4500 A

JD 243	(a−v)	Cor.	(Δm) Cor.	n
2473.7556	1m157	0m023	1m180	(2)
.7881	1.161	.014	1.175	(2)
2478.7500	1.140	.020	1.160	(2)
.7660	1.142	.016	1.158	(3)
2494.7039	1.137	.021	1.158	(2)
.7420	1.145	.012	1.157	(2)
2499.6782	1.164	.024	1.188	(2)
2513.7231	1.148	.007	1.155	(3)
.7400	1.157	.004	1.161	(2)
2527.6879	1.163	.006	1.169	(2)
.7087	1.158	.004	1.162	(3)
2531.7275	1.164	.002	1.166	(3)
.7334	1.166	.001	1.167	(2)
2532.7337	1.165	.002	1.167	(2)
.7515	1.178	.001	1.179	(3)
2533.6643	1.161	.007	1.168	(2)
.7227	1.164	.001	1.165	(3)
2534.5981	0.883	.009	0.892	.....
.6041	0.910	.008	0.918	.....
.6099	0.854	.008	0.862	.....
.6168	0.877	.006	0.883	.....
.6228	0.870	.006	0.876	.....
.6285	0.850	.006	0.856	.....
.6349	0.830	.005	0.835	.....
.6404	0.832	.004	0.836	.....
.6474	0.823	.004	0.827	.....
.6533	0.849	.003	0.852	.....
.6896	0.807	.001	0.808	.....
.6963	0.828	.001	0.829	.....
.7031	0.839	.001	0.840	.....
.7122	0.811	.001	0.812	.....
.7191	0.786	.001	0.787	.....
.7392	0.822	.000	0.822	.....
.7451	0.809	.000	0.809	.....
.7516	0.806	.000	0.806	.....
.7591	0.775	.000	0.775	.....
.8012	0.758	.000	0.758	.....
.8097	0.782	.000	0.782	.....
.8209	0.757	.000	0.757	.....
.8417	0.724	.000	0.724	.....
.8497	0.734	.000	0.734	.....
.8569	0.732	.000	0.732	.....
.8646	0.713	.000	0.713	.....
.8710	0.729	.000	0.729	.....
.8783	0.727	.001	0.728	.....
.8854	0.722	.001	0.723	.....
.9372	0.673	.001	0.674	.....
.9442	0.693	.001	0.694	.....
2536.6816	0.636	.000	0.636	.....
2547.6421	0.653	.000	0.653	.....
.6636	0.656	.000	0.656	.....
2552.5967	0.630	.000	0.630	.....
.6048	0.611	.000	0.611	.....
.6118	0.608	.000	0.608	.....
.6189	0.616	.000	0.616	.....
.6255	0.619	.000	0.619	.....
2553.6061	0.622	.000	0.622	.....
.6161	0.621	.000	0.621	.....
.6207	0.621	.000	0.621	.....
.6315	0.608	0.000	0.608	.....

TABLE 1—*Continued*

JD 243	(a−v)	Cor.	(Δm) Cor.	n
2554.5962	0m646	0m000	0m646	.....
.6096	0.612	.000	0.612	.....
.6161	0.635	.000	0.635	.....
2570.6076	0.629	.000	0.629	.....
.6136	0.629	.000	0.629	.....
.6200	0.640	.000	0.640	.....
.6269	0.626	.000	0.626	.....
.6333	0.613	.000	0.613	.....
2572.5840	0.804	.001	0.805	.....
.5907	0.771	.001	0.772	.....
.5973	0.816	.001	0.817	.....
.6148	0.826	.001	0.827	.....
.6173	0.806	.001	0.807	.....
.6451	0.842	.000	0.842	.....
.6515	0.868	.000	0.868	.....
.6581	0.839	.000	0.839	.....
.6662	0.845	.000	0.845	.....
.6962	0.898	.000	0.898	.....
.7025	0.897	.000	0.897	.....
.7089	0.883	.000	0.883	.....
.7290	0.900	.001	0.901	.....
.7352	0.897	.001	0.898	.....
.7421	0.905	.001	0.906	.....
.7487	0.918	.001	0.919	.....
.7555	0.925	.001	0.926	.....
.7625	0.934	.002	0.936	.....
.7694	0.915	.002	0.917	.....
.8067	0.899	.003	0.902	.....
.8172	0.917	.004	0.921	.....
.8233	0.900	.005	0.905	.....
.8301	0.928	.005	0.933	.....
.8368	0.919	.006	0.925	.....
.8436	0.913	.007	0.920	.....
.8514	0 926	.008	0.934	.....
2615.6464	1.155	.003	1.158	(3)
2618.6151	1.159	.001	1.160	(3)
.6326	1.163	.002	1.165	(2)
2619.6063	1.171	0.000	1.171	(2)

UV OBSERVATIONS

JD 243	(a−v)	Cor.	(Δm) Cor.	n
2531.6206	1m914	0m209	2m123	(3)
.6545	2.050	.116	2.166	(2)
.6732	2.055	.088	2.143	(3)
2532.6227	1.952	.196	2.148	(3)
.6565	2.021	.111	2.132	(3)
.6854	2.067	067	2.134	(3)
2533.6131	1.812	.215	2.027	(3)
.6384	1.918	.138	2.056	(3)
.7597	2.003	.009	2.012	(3)
2534.6646	0.987	.034	1.021	.....
6703	0.981	.030	1.011	.....
.7715	0.768	.001	0.769	.....
.7793	0.757	.001	0.758	.....
.8997	0.587	.010	0.597	.....
.9084	0.510	.010	0.520	.....
2552.6845	0.366	.000	0.366	.....
2553.6575	0.359	000	0 359	.....
2554.6306	0.347	.000	0.347	.....
2572.6791	0.963	.002	0.965	.....
.6856	0.999	.001	1.000	.....
.7842	1.136	.031	1.167	.....
.7917	1.012	0.039	1.051	.....

a plot of the fraction of eclipse versus time. It is obvious that the systematic displacement between the two sets of observations is of considerable significance in understanding the nature of the eclipse mechanism. Certainly, the existence of such a displacement makes the idea of a simple geometrical eclipse seem untenable. This point will be treated more fully in a general discussion of the system to be undertaken in collaboration with Dr. F. E. Roach.

The observed depth of eclipse at 4500 A was 0.539 mag., and in the ultraviolet, 1.784 mag. Thus, in the former case, the K component supplies 0.609 of the light of the system; in the latter, 0.193.

It is of interest to see whether the color corrections found to be necessary will make any significant difference in the interpretation of the earlier observations. Generally

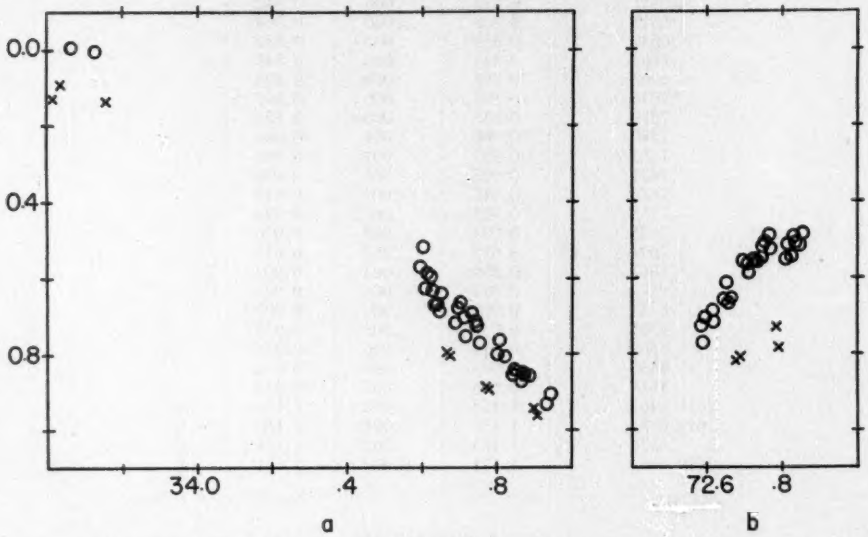

FIG. 2.—Observations during (*a*) ingress and (*b*) egress. *Ordinate:* fraction of eclipse; *abscissa:* JD 2432500. *Circles*, observations in blue; *crosses*, UV observations.

speaking, the corrections to the observations will be insignificant, since they were made at about 4500 A. In this region the correction will usually be less than 0.01 mag.; only when the observations were made well away from the zenith will these be as great as 0.02 mag., and results based on discrepancies of this size have not generally been seriously considered. There is, however, one discussion of the system which perhaps should be modified in the light of these results. This is a discussion by Kopal,[5] in which the results of various observers are combined to form a light-curve showing the changes during the partial phases of the ingress of the 1939–1940 eclipse. In this the existence of a tremendous opaque cloud in the atmosphere of the K star is postulated because of an irregular fluctuation found in one position of the light-curve. The evidence for this irregularity was based on a combination of the observations of Roach with those of Bruck and Green.[6] It now appears that serious doubt must be cast on the reality of the fluctuation. Bruck and Green had published no observations except those during the partial phases of the eclipse; there was thus no way of precisely determining the effective wave length of their instrument. Because both they and Roach worked with potassium-hydride cells

[5] *Ap. J.*, **103**, 310, 1946.

[6] *L'astronomie*, **54**, 38, 1940.

on reflecting telescopes, the assumption was made that the effective wave lengths of the two sets of observations must be the same. But the present investigations were made with precisely the same telescope and photometer as that used by Roach, with only two changes—the use of a different photocell and an aluminum surface on the mirror. Both cells had potassium-hydride surfaces, and both were made by Kunz at approximately the same time; that used by Roach had a quartz envelope, while the one I used was inclosed in Corex. Yet the depth of eclipse observed in 1947–1948 was 0.539 mag., while that found by Roach was 0.472. This indicates a difference of effective wave length of at least 100 A and casts serious doubt on the validity of the assumption that these two sets of observations can be properly combined by simply assuming that the effective wave lengths were the same. Actually, the light-loss indicated by Bruck and Green, expressed as fraction of eclipse, can be altered at will by slightly different assumptions of effective wave length. It seems probable that what is suggested by a comparison of the observations of Bruck and Green with those of Roach is simply a combination of the effects illustrated in Figures 1 and 2.

The only other evidence for the irregularity is the systematic departure of the first two of Roach's normals on the night of ingress (normals 7 and 8); these fall below a straight line passing through the remainder of his observations on that night. But these two normals were made at low altitudes; the discussion of these observations indicates that the correction of Roach's in the same manner requires adding 0.017 mag. to his first normal and 0.009 to his second; for the following ones, where the altitude was high, the corrections are negligible (of the order of 0.002 mag. or less); only in the last is a correction of +0.011 mag. indicated. When so treated, none of Roach's normals falls more than 0.01 mag. from a straight line passing through them; they fall even more closely to a smooth curve which departs slightly from the line in the direction required by a uniform eclipse (i.e., one free from irregular fluctuations). Thus there is no real indication of any irregularity in the ingress of the 1939–1940 eclipse.

Two further comments should be made concerning the observations in the partial phases. The first is that, in order to make the ultraviolet observations, it was necessary to apply appreciably higher voltage to the cell than was used in making the observations at 4500 A. Under normal conditions there was no disadvantage attached to this, except that, for maximum precision, it is desirable to wait for a few minutes after the application of the voltage before commencing observation. In the effort to get the maximum number of observations during the partial phases, it was not always possible to do this; the pressure, of course, increased toward the end of the night. Thus the last two ultraviolet observations, especially on the night of the ingress, should be weighted somewhat lower than the earlier ones.

The second comment concerns the shape of the light-curve during the egress. The last seven observations fall about 0.06 mag. below the value indicated from the earlier ones. At first glance, this seems to indicate a "plateau" in the light-curve. However, a more careful inspection shows that the increase from 0.80 to 0.93 mag. was appreciably more rapid than the smooth decrease 38 days earlier, and it seems more reasonable to suppose the observations between JD 2432572.7 and 2432572.8 are systematically too high by about 0.02 m g. This could conceivably be caused by an increase in the intrinsic brightness of the K star. Such an interpretation is perhaps also to be favored, since irregular fluctuations of such an amplitude have been reported by earlier workers.

In this connection it is important to see what information is gained by the observation at the shorter wave length; unfortunately, the evidence here is not conclusive. The last two ultraviolet observations fall somewhat below their expected position, and the second is considerably lower than the first, indicating an actual decrease of brightness. For the reason previously stated, these two observations must be considered with some caution; however, the differences indicated by them are larger than the expected error, even under these comparatively unfavorable circumstances. Obviously, the behavior in the ultra-

violet is of considerable importance; but, from the present observations, it seems inadvisable to attempt a further discussion. Attention is called to these peculiarities in the hope that the system was being observed simultaneously elsewhere and that additional information, if thus afforded, might cast further light on these complexities. The only definite evidence which can be drawn is that the behavior at egress was observably different from that at ingress.

I am indebted to Dr. F. E. Roach for helpful comments and suggestions. Observing assistants were paid in part by a grant from the Penrose Fund of the American Philosophical Society and in part by the Steward Observatory.

THE ECLIPSING BINARY U SAGITTAE*

D. H. McNAMARA
Berkeley Astronomical Department, University of California
Received June 21, 1951

ABSTRACT

A series of 148 spectrograms of U Sagittae have been obtained with the McDonald and Mount Wilson spectrographs. The *H* lines give systematically different velocities from the other star lines at certain phases in the cycle. The orbital elements and radial-velocity-curve have been determined from all the star lines present except the *H* lines and the *Ca* II K line. The *H* velocities are controlled primarily by measurements of the cores present within the *H* lines, which are usually displaced to the red or violet of the center of the broad *H* wings. Near phase 0.88*P* the *H* asymmetries change from red-displaced cores to violet-displaced cores without any apparent change in the displacement of the *H* velocities from above the velocity-curve. From phase 0.88*P* to phase 0.93*P* neither the *H* cores nor the center of the *H* wings gives velocities consistent with the other star lines. The discordant *H* velocities can be only partially explained on the basis of absorption in gaseous streams. Very rapid changes in the *H*-line velocities are present at phases 0.73, 0.125, and 0.20*P*.

I. INTRODUCTION

The variability of U Sagittae[1] was discovered by Schwabe[2] in 1901. A study of the light-variations proved it to be an Algol-type variable, ranging in light from magnitude 6.5 to magnitude 9.8. A considerable number of photometric and spectroscopic investigations have followed the discovery. References to the work completed on this star prior to 1930 have been given by Joy.[3]

Recently Struve[4] has made a detailed spectroscopic study of the rotation effect in this system. His observations revealed strong asymmetrical *H* lines which failed to take part in the pronounced rotational disturbance displayed by the other star lines. These results are in agreement with those found for U Cephei[5] and other similar binary systems. The present investigation was planned to supplement the earlier observations.

II. THE OBSERVATIONS

The majority of the observations presented here were made by me in the latter part of August, 1950, with the Cassegrain spectrographs of the McDonald Observatory. The 500-mm camera was used with glass prisms, which gives a dispersion of 26 A/mm at $H\gamma$; and a few plates were obtained near minimum light with the Cassegrain glass $f/2$ spectrograph combination, which gives 75 A/mm at $H\gamma$. I am also indebted to Dr. Struve for obtaining 22 coudé (10 A/mm) plates at the Mount Wilson Observatory. The coudé plates were secured on three consecutive nights on which McDonald plates were also obtained and therefore provide a valuable check on some of the details of the radial-velocity-curve. In addition to the above plates, a few of the Cassegrain quartz spectrograms (40 A/mm at $H\gamma$) obtained by Struve[6] in 1949 were used to advantage in the determination of the velocity-curve.

A list of the star lines used to determine the radial velocity is presented in Table 1.

* This investigation was made possible by a co-operative arrangement with the McDonald and Mount Wilson Observatories.

[1] HD 181182; $\alpha = 19^h14^m4$; $\delta = +19°26'$ (1900); Sp. B9.

[2] *A.N.*, **157**, 79, 1901.

[3] *Ap. J.*, **71**, 336, 1930.

[4] *M.N.*, **109**, 492, 1949.

[5] O. Struve, *Ap. J.*, **99**, 222, 1944.

[6] *M.N.*, **109**, 495, 1949.

Four *H* lines in addition to those given in Table 1 were measured on the coudé plates. All the lines are very broad and diffuse.

The radial velocities determined from 148 plates are presented in Table 2. The heliocentric phases given in the third column of Table 2 were computed with the aid of the formula

$$\text{Principal minimum} = 2{,}417{,}130.4170 + 3.3806184E - 0.0162 \text{ day}.$$

The correction −0.0162 day was obtained by J. Irwin[7] from photoelectric observations made on October 2.0 and 9.0, 1949. The fourth column refers to the radial velocities determined from the *H* lines; and the fifth column contains the radial velocities determined from all the star lines except the *H* lines and the K line of *Ca* II.

Upon examination of the results of the radial-velocity determinations, it became apparent that the *H* lines and the *Ca* II K line give different velocities from the mean velocity of the other star lines at various phases in the cycle. As Struve[8] has already pointed

TABLE 1

STAR LINES MEASURED IN U SAGITTAE

H	*He* I	*Si* II	*Ca* II
3835.39	3819.61	3862.59	3933.66
3889.05	4026.20	4128.05	*Fe* II
3970.04	4471.50	4130.88	4233.17
4101.74	*Si* II	*Mg* II	
4340.47	3853.66	4481.23	
4861.33	3856.02		

out, the source of the discrepancy for the *Ca* II K line can be attributed to the blending of an interstellar line with the star line. On the Mount Wilson coudé plates the K line is distinctly double. Measurements of the interstellar component give a mean velocity of −19.7 km/sec. The discrepancy between the *H* lines and the other star lines can be accounted for in part by the absorption in gaseous streams usually associated with this type of binary. This point will be discussed in more detail later.

III. THE RADIAL-VELOCITY-CURVE

All the star lines listed in Table 1 except the *H* lines and the *Ca* II K line were used to determine the velocity-curve and orbital elements of the system. The observations were grouped into the eleven normal places given in Table 3. The Mount Wilson coudé plates have been given double weight. The period was regarded as known, and the other orbital elements were derived by means of Schlesinger's least-squares method. The final elements derived, as well as the results obtained by Joy[9] and Miss Fowler[10] from earlier observations, are given in Table 4. The values of O − C resulting from the least-squares solution are listed in the last column of Table 3. The velocity-curve is given in Figure 1. The crosses represent the velocities determined from all the star lines except *H* and the *Ca* II K line, and the circles refer to the *H* velocities. The probable error of a single observation of weight unity is ±3.9 km/sec. The uncertainty in the measurements can be attributed largely to the broad and diffuse nature of the lines.

A comparison of the present elements with those determined earlier reveals some noticeable differences. The most noteworthy is the apparent systematic change of the γ-axis in the three determinations. It should be pointed out that both Joy and Miss

[7] *M.N.*, **109**, 492, 1949.
[8] *M.N.*, **109**, 500, 1949.
[9] *Op. cit.*, p. 343.
[10] *Pub. Allegheny Obs.*, **3**, 14, 1916.

TABLE 2

RADIAL VELOCITIES OF U SAGITTAE

Plate	Date (1950) U.T.	Heliocentric Phase	Hydrogen Lines (Km/Sec)	All Lines except *H* and *Ca* II (Km/Sec)
CG				
8441	Aug. 19.1285	0.9275	+ 43.1	+ 29.1
8442	19.1437	.9320	+ 34.7	+ 25.6
8443	19.1590	.9365	+ 30.3	+ 34.9
8444	19.1812	.9431	+ 27.9	+ 31.4
8446	19.2326	.9583	+ 41.0	+ 38.3
8447	19.2486	.9630	+ 33.1	+ 42.4
8448	19.2667	.9683	+ 30.3	+ 56.0
8449	19.2882	.9747	+ 13.8	+ 67.4
8452	20.1097	.2177	−107.9	− 75.4
8453	20.1201	.2207	− 98.0	− 71.5
8454	20.1285	.2232	− 94.7	− 78.1
8455	20.1361	.2255	−104.2	− 73.4
8456	20.1458	.2283	− 97.2	− 79.7
8457	20.1618	.2331	− 86.9	− 84.3
8458	20.1771	.2376	− 86.7	− 82.8
8459	20.1833	.2394	−101.2	− 81.5
8460	20.1917	.2419	− 91.9	− 85.2
8461	20.2062	.2462	− 94.4	− 87.4
8462	20.2257	.2520	−100.6	− 85.8
8463	20.2354	.2548	− 89.4	− 88.2
8464	20.2458	.2579	− 92.1	− 76.0
8465	20.2639	.2633	− 87.9	− 69.9
8466	20.2847	.2694	− 92.0	− 92.5
8467	20.2972	.2731	− 89.2	− 79.3
8468	20.3090	.2766	− 94.5	− 86.5
8469	20.3306	.2830	−100.3	− 78.8
8470	20.3528	.2896	− 96.6	− 84.5
8471	21.1097	.5135	− 18.5	+ 0.3
8472	21.1181	.5159	− 13.4	− 6.7
8473	21.1278	.5188	− 12.8	− 8.1
8474	21.1465	.5243	− 13.7	− 17.5
8475	21.1667	.5303	− 9.6	+ 0.1
8476	21.1792	.5340	− 4.7	+ 0.2
8477	21.1924	.5379	+ 2.6	+ 4.3
8478	21.2174	.5453	− 0.2	+ 12.7
8479	21.2444	.5533	+ 10.1	+ 10.3
8480	21.2618	.5584	+ 4.9	+ 19.9
8481	21.2799	.5638	+ 16.2	+ 15.9
8482	21.3097	.5726	+ 18.0	+ 11.0
8483	21.3396	.5815	+ 24.6	+ 22.8
8484	22.1035	.8074	+ 62.2	+ 46.8
8485	22.1153	.8109	+ 65.6	+ 54.7
8486	22.1257	.8140	+ 64.3	+ 49.7
8487	22.1493	.8210	+ 66.8	+ 56.1
8488	22.1729	.8280	+ 66.0	+ 42.4
8489	22.1854	.8317	+ 65.1	+ 56.9
8490	22.1986	.8356	+ 58.4	+ 46.4
8491	22.2243	.8432	+ 54.9	+ 33.3
8492	22.2500	.8508	+ 57.9	+ 55.4
8493	22.2646	.8551	+ 60.2	+ 47.9
8494	22.2819	.8602	+ 46.5	+ 40.0
8495	22.3097	.8684	+ 51.0	+ 47.0
8496	22.3361	.8762	+ 49.4	+ 44.6
8497	23.1340	.1122	− 57.7	− 50.0
8498	23.1479	.1163	− 51.4	− 54.6
8499	23.1625	.1206	− 51.0	− 52.7
8500	23.1750	.1244	− 58.7	− 55.2
8501	23.1903	.1289	− 74.7	− 61.0
8502	23.2042	.1330	− 58.3	− 57.2
8503	23.2167	0.1367	− 70.9	− 58.9

TABLE 2—*Continued*

Plate	Date (1950) U.T.	Heliocentric Phase	Hydrogen Lines (Km/Sec)	All Lines except *H* and *Ca* II (Km/Sec)
CG				
8504	Aug. 23.2396	0.1435	− 74.1	− 63.3
8505	23.2611	.1498	− 70.2	− 64.0
8506	23.2729	.1533	− 77.7	− 60.7
8507	23.2979	.1607	− 84.6	− 74.1
8508	23.3243	.1685	− 80.1	− 67.9
8509	24.1840	.4228	− 41.1	− 44.2
8510	24.1958	.4263	− 50.7	− 48.0
8511	24.2215	.4339	− 44.5	− 43.2
8512	24.2479	.4417	− 41.9	− 39.4
8513	24.2639	.4465	− 38.9	− 33.8
8514	24.2806	.4514	− 39.8	− 40.6
8516	24.3153	.4616	− 30.5	− 34.4
8517	24.3326	.4668	− 25.3	− 21.4
8518	25.1521	.7092	+ 61.3	+ 59.7
8519	25.1646	.7129	+ 64.7	+ 55.0
8520	25.1778	.7168	+ 53.5	+ 55.1
8521	25.2382	.7347	+ 40.5	+ 60.3
8522	25.2660	.7429	+ 43.0	+ 56.8
8523	25.2826	.7478	+ 53.6	+ 57.5
8524	25.3021	.7536	+ 63.0	+ 63.4
8525	25.3222	.7595	+ 73.5	+ 53.9
8526	26.2743	.0411	− 61.1	− 54.2
8527	26.3007	.0489	− 48.2	− 50.7
8528	26.3201	.0546	− 56.9	− 50.1
8529	28.2000	.6107	+ 22.1	+ 39.3
8530	28.2160	.6154	+ 8.1	+ 28.2
8531	28.2312	.6199	+ 31.7	+ 32.9
8532	28.2472	.6247	+ 24.4	+ 33.3
8533	28.2618	.6290	+ 34.7	+ 45.0
8534	28.2778	.6337	+ 37.9	+ 41.2
8535	28.2951	.6388	+ 34.5	+ 37.5
8536	28.3111	.6436	+ 46.7	+ 37.0
8542	29.1174	.8821	+ 56.0	+ 45.4
8543	29.1278	.8852	+ 57.7	+ 40.0
8544	29.1375	.8880	+ 50.2	+ 42.0
8545	29.1562	.8936	+ 55.1	+ 33.0
8546	29.1778	.9000	+ 59.9	+ 39.9
8547	29.1903	.9037	+ 48.4	+ 37.4
8548	29.2014	.9069	+ 57.4	+ 29.5
8549	29.2167	.9115	+ 41.5	+ 36.3
8550	29.2326	.9162	+ 33.3	+ 33.6
8551	29.2514	.9217	+ 23.1	+ 30.5
8552	29.2701	.9273	+ 23.1	+ 25.1
8553	29.2937	.9343	+ 29.0	+ 16.1
8554	30.1854	.1980	− 73.3	− 58.9
8555	30.2069	.2043	− 78.6	− 73.3
8556	30.2264	.2101	− 82.1	− 72.4
8557	30.2500	.2171	− 91.7	− 79.2
8558	30.2799	.2259	−106.0	− 80.2
8559	30.3090	.2345	−106.0	− 84.9
8560	30.3299	.2407	− 91.6	− 76.8
8563	31.2097	.5010	− 8.9	+ 3.3
8564	31.2222	.5047	− 6.0	− 9.4
G *f*/2				
12586	26.2076	.0214	− 77.1	−107.3
12587	26.2257	.0267	− 59.4	− 91.1
12591	29.3229	.9429	+ 40.1	+ 46.3
12592	29.3299	.9449	+ 29.6	+ 62.8
12593	29.3375	.9472	+ 42.0	+ 54.3
12595	29.3535	.9519	+ 41.6	+ 59.2
12596	29.3646	0.9552	+ 33.0	+ 54.5

TABLE 2—*Continued*

Plate	Date (1950) U.T.	Heliocentric Phase	Hydrogen Lines (Km/Sec)	All Lines except *H* and *Ca* II (Km/Sec)
CD				
6450A	Aug. 23.1868	0.1278	− 65.6	− 63.2
6450B	23.2056	.1334	− 55.5	− 58.1
6450C	23.2222	.1383	− 80.4	− 64.8
6450D	23.2389	.1433	− 75.6	− 60.0
6450E	23.2569	.1486	− 76.1	− 58.2
6451A	23.2861	.1572	− 81.2	− 66.4
6451B	23.3021	.1619	− 85.9	− 65.5
6451C	23.3181	.1667	− 81.4	− 64.1
6451D	23.3347	.1716	− 81.6	− 67.7
6451E	23.3514	.1765	− 85.1	− 73.9
6451F	23.3687	.1817	− 85.1	− 69.7
6451G	23.3854	.1866	− 84.8	− 75.9
6451H	23.4049	.1924	− 75.7	− 74.7
6453A	24.1458	.4115	− 61.1	− 55.0
6453B	24.1736	.4197	− 52.0	− 47.2
6453C	24.2021	.4281	− 52.3	− 44.4
6453D	24.2312	.4368	− 52.4	− 42.8
6453E	24.2604	.4454	− 43.6	− 38.8
6458A	25.1896	.7203	+ 56.2	+ 48.4
6458B	25.2181	.7287	+ 52.5	+ 61.5
6458C	25.2437	.7363	+ 48.9	+ 57.9
6458D	25.2694	.7439	+ 40.7	+ 56.3
CQ	(1949) U.T.			
7712	July 31.1938	.3582	− 70.4	− 70.5
7713	31.1986	.3596	− 65.0	− 66.9
7714	31.2035	.3611	− 62.4	− 62.4
7717	31.3031	.3905	− 60.9	− 44.5
7718	31.3090	.3923	− 56.4	− 65.1
7719	31.3139	0.3937	− 52.2	− 58.9

TABLE 3

NORMALS

No.	Phase	Velocity (Km/Sec)	Wt.	O−C (Km/Sec)	No.	Phase	Velocity (Km/Sec)	Wt.	O−C (Km/Sec)
1	0.1371	−60.0	22	−1.0	7	0.5370	+ 3.9	14	+0.8
2	.1834	−71.1	21	+1.1	8	.6270	+36.8	8	0.0
3	.2331	−80.5	12	−0.1	9	.7335	+56.9	16	+0.1
4	.2689	−82.4	9	−0.6	10	.8298	+49.0	10	−2.4
5	.3759	−61.4	6	+1.8	11	0.8910	+39.1	12	+1.9
6	0.4352	−42.3	18	−0.9					

TABLE 4

SPECTROGRAPHIC ELEMENTS OF U SAGITTAE

	Fowler 1907–1911	Joy 1926–1928	Present Study 1950
P (days)	3.380603	3.38056	3.3806184
T (days after min.)	2.998	1.5960	1.02±0.13
ω	44°	260°	194°4±14.1
γ (km/sec)	−19.13	−15.1	−10.1
e	0.035	0.035	0.030±0.008
K (km/sec)	66.45	67.9	69.69±0.59
$a \sin i$ (km)	3.09×10^6	3.16×10^6	3.24×10^6

Fowler used all the spectral lines available for the determination of their sets of elements, including the *H* lines and the K line of *Ca* II. An inspection of Figure 1, however, reveals distinct discrepancies between the velocities given by the *H* lines and those given by the other lines in the star. This change in the γ-axis, however, should still be regarded as fairly certain, since, if the *H* lines were combined with the other star lines in this investigation, it would probably lead to a value of γ very close to the one adopted in Table 4. The large changes in the value of ω can probably be attributed to the large uncertainties

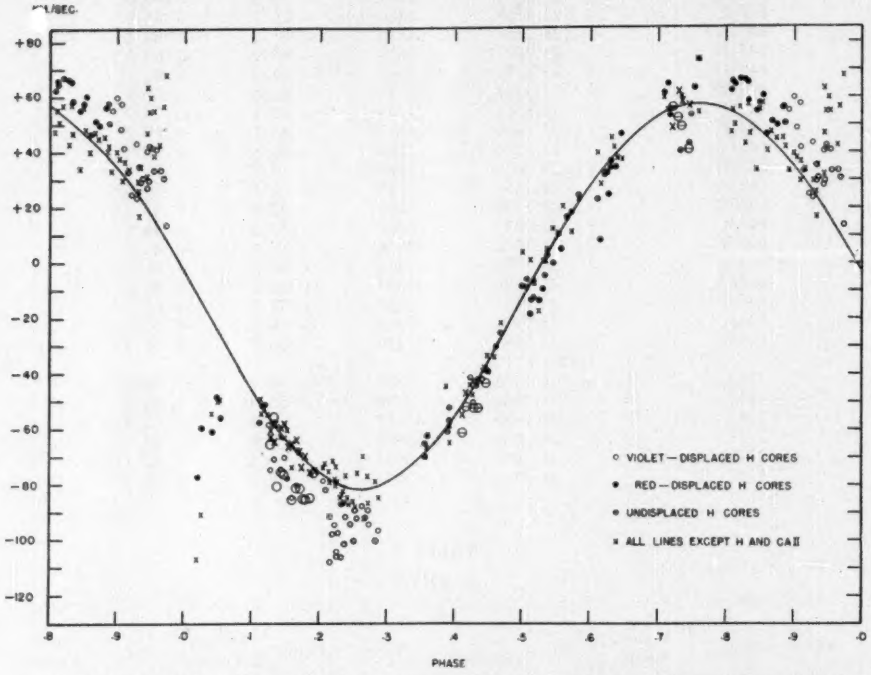

FIG. 1.—The radial-velocity-curve of U Sagittae is based on all the star lines present except the *H* lines and *Ca* II K line. The circles represent the *H* velocities, and the crosses represent the velocities given by all the lines except *H* and *Ca* II K. The large circles and large crosses represent coudé measures. Open circles indicate that the cores of the *H* lines are displaced to the violet side of the center of the broad wings, and closed circles indicate that the cores of the *H* lines are displaced to the red. Open circles intersected by a horizontal line indicate undisplaced cores. The cores are the features largely controlling the *H* velocities.

involved in obtaining an accurate value of this quantity, since the eccentricity is very small.

The slope of the velocity-curve of the fainter component has been determined by Joy[11] from spectra taken during the total eclipse. By comparing the slopes of the two velocity-curves, the mass ratio can be determined. The value of the mass ratio found by Joy is $m_1/m_2 = 3.3$. Since Joy included the *H* lines and the *Ca* II K line in the determination of the velocity-curve of the brighter component, an important question arises as to what extent the mass ratio would be altered if he had omitted these lines. From a consideration of the influence of these lines on changing the slope of the present velocity-curve and

[11] *Op. cit.*, p. 348.

assuming that the behavior of the star lines has not changed since Joy's investigation, it appears that the mass ratio would have been increased by no more than 0.3 if they had been omitted.

IV. DISCUSSION OF THE *H* LINES

The velocities determined from the *H* lines are shown in Figure 1 as circles. The large circles are Mount Wilson coudé measurements. An inspection of the *H*-line velocities at ingress reveals the failure of these lines to follow the pronounced straight-line trend of the rotational disturbance displayed by the other star lines. This confirms Struve's[12] 1949 observations. At egress the same effect appears to be present, although the present *H* velocities appear to be displaced about 10 km/sec, in the mean, below the velocities determined by Struve.

Between phases 0.14 and 0.30*P* we find that the *H* velocities fall considerably below the velocity-curve, and from phase 0.76 to 0.92*P* they are above the curve. On the rising branch of the velocity-curve, between phases 0.36 and 0.72*P*, the agreement between the velocity-curve and the *H* lines is much better, although a small negative displacement of the *H* velocities appears to be present. It is fairly certain that the *H* lines give velocities discordant with the other star-line measures throughout at least half the period.

The *H* lines show asymmetries at various phases in the cycle. In order to make a comparison with Hardie's[13] investigation of the distribution of asymmetries in U Cephei, the spectra were examined visually several times to ascertain the form of the asymmetries at various phases. In Figure 1 open circles indicate that the cores of the *H* lines are displaced to the violet side of the centers of the broad wings, and closed circles indicate that the cores of the *H* lines are displaced to the red. The open circles intersected by a horizontal line indicate undisplaced cores and the absence of strong cores within the *H* lines. It should be emphasized that the asymmetries have been estimated only from visual inspection and are therefore subject to some uncertainty. When the asymmetries are weak, it is difficult to ascertain in which direction the cores are displaced.

A comparison of the form and distribution of *H*-line asymmetries in U Sagittae at various phases with those of U Cephei reveals many striking similarities. At phase 0.75*P* the *H* lines display asymmetries, with the cores displaced to the red. Shortly after this, the asymmetries weaken and then change to strong violet asymmetries before first contact. After third contact the *H* lines display red asymmetries, which change over into violet asymmetries after the termination of the eclipse. This succession of events is identical to those described by Hardie[14] in U Cephei. Although no attempt has been made in Figure 1 to signify the strength of the asymmetries, the strongest asymmetries are present during the primary eclipse and near phases 0.25 and 0.75*P*. This is also in agreement with U Cephei. Apparently, the great advantage of studying these effects in U Sagittae is the ease with which it is possible to bring out the systematic velocity differences between the *H* lines and the other star lines. In U Cephei no significant systematic differences between the two sets of lines were found by either Hardie[14] or Struve[15] except during the phases when the rotational effect is observed.

The main difference in the *H* lines of the two systems appears to be in the magnitude of the asymmetries. The microphotometer tracings of the *H* lines in U Cephei made by Hardie indicate that the cores are displaced in the mean by 30 and 60 km/sec from the center of the wings at phases 0.6 and 2.0 days, respectively. In U Sagittae the *H* lines are displaced 18 and 12 km/sec from the velocity-curve at the corresponding phases of 0.25 and 0.75*P*. Rough settings on the wings and cores of *Hγ* and *Hδ* indicate that the cores are displaced from the center of the broad wings by 10–25 km/sec. This suggests that the center of the *H* wings would give velocities consistent with the other star lines at the

[12] *M.N.*, **109**, 496, 1949.
[13] *Ap. J.*, **112**, 545, 1950.
[14] *Ibid.*, p. 544.
[15] *Ap. J.*, **99**, 231, 1944.

above phases in the velocity-curve and indicates that the asymmetries are weaker in U Sagittae.

If the *H*-line measures were included, they would certainly distort the velocity-curve in the sense of raising the measured velocities near 0.75*P* and depressing them near 0.25*P*, but not nearly to the extent that they apparently influence the velocity-curve of U Cephei.

Struve[8] has pointed out that, just before the commencement of the primary eclipse (0.92*P*), when the *H* lines have violet cores, the velocities determined from the *H* lines are displaced considerably above the velocity measures of the other star lines. The present investigation confirms Struve's earlier observations and demonstrates that the discrepancy between the two sets of lines begins near phase 0.75*P*. The most remarkable result, however, is the observed change in the *H* cores from red asymmetries to violet asymmetries, without any apparent change in the red displacement of the *H* velocities. Rough settings on the wings and cores of $H\gamma$ and $H\delta$ on plates taken near phase 0.92*P* indicate that the cores are displaced about 20 km/sec to the violet of the center of the wings. Since the settings for the *H*-line velocities are made on the cores which are already located about 10 km/sec above the velocity-curve, we infer that the centers of the *H* wings are displaced about 30 km/sec above the velocity-curve at first contact. If the centers of the *H* wings were measured instead of the cores from phase 0.75 to phase 0.92*P*, the *H* velocities would probably remain nearly constant at approximately +60 km/sec.

One possible explanation of the peculiar behavior of the *H* lines described above is a hypothesis suggested by Struve[16] which combines rotation and Stark effect. This hypothesis requires the brighter component to be tidally distorted. In the tidal bulges the pressure will be lower and hence the Stark effect weaker. Therefore, the contribution to the *H* lines will be narrower in the bulges than those produced in the regions of higher pressure. At certain favorable phases in the velocity-curve, one of the tidal bulges will be receding while the area of high pressure is approaching, which will lead to unsymmetrical lines. The same will be true when the tidal bulge is approaching and the area of high pressure is receding, except that the asymmetry will be in the opposite sense. Hardie[17] has assumed two different dwarf-line profiles which represent the two pressure areas and has carried out graphical integrations for a rotating star. His results indicate that the hypothesis can account for the observed velocity discrepancies in U Cephei. The unsymmetrical lines, and hence the discordant *H* velocities, should occur near phases 0.125, 0.375, 0.625, and 0.875*P*. As we have already indicated, the proposed model does fit the observational evidence in the case of U Sagittae near phase 0.875*P*. There is no conclusive evidence, however, that this effect is present at the other phases in the velocity-curve. Indeed, at phase 0.125*P*, where the *H* lines have undisplaced cores, the *H*-line velocities appear to agree very well with the velocities determined from the other lines. Additional observations are required from phase 0.05 to phase 0.125*P*, in order to settle this question conclusively. At phase 0.375*P* the hypothesis predicts that the *H* velocities should be above the velocities of the other lines. Struve's 1949 observations, however, indicate a general agreement. Near phase 0.625*P* the *H* velocities appear to be slightly below the velocity-curve, which is the direction that the hypothesis predicts. It is of interest to note that some of the plates near this phase show striking red asymmetries, which indicates that the centers of the wings would have given an even larger discrepancy. However, as was pointed out before, a small negative displacement of the *H* velocities appears to be present along the entire rising branch of the velocity-curve.

One serious objection to the above hypothesis is furnished by the light-curve of U Sagittae. A photoelectric study of this system made by Irwin[18] has shown that there is

[16] *Pop. Astr.*, **58**, 7, 1950.

[17] *Op. cit.*, p. 548.

[18] Dissertation, University of California.

very little distortion of the primary star. It is also of interest to note the absence of this effect among close binaries in which no evidence of strong *H* cores has been found. Indeed, the presence of this peculiar behavior of the wings in a system such as U Sagittae, in which evidence for gas streams has also been found, might indicate a closer relationship between the two effects than we have been prepared to admit. Perhaps the gas streams may provide an appreciable area of low pressure, such as a small pseudo-elongation of the star.

Some very striking changes in the *H*-line velocities are exhibited in Figure 1. The most remarkable is the rapid decline and recovery near phase 0.74*P*. There seems to be little doubt that this is real and not due to errors in measurement, since the McDonald and Mount Wilson plates agree very well. Other rapid changes are also indicated near phases 0.125 and 0.21*P*. Apparently, the *H* lines change by as much as 25 km/sec in a period of less than 1 hour, while the velocities of the other lines remain nearly constant. These rapid changes can probably be attributed to the influence of the gaseous streams on the *H* lines.

An account[19] has already been given of the discovery of emission lines in the spectrum of U Sagittae. The absence of these features on spectrograms obtained earlier by Joy[3] and Struve[7] indicates that these features are unstable, as observations of similar emission lines in RW Tauri[20] had already suggested. U Cephei now remains the only carefully investigated binary system which displays sharp *H* cores superimposed on the normal stellar absorption lines, and yet fails to show strong emission lines. If our experience with U Sagittae is any guide, it is only a matter of time until spectra taken of U Cephei near totality will reveal their presence.

The observational part of this investigation was carried out primarily at the McDonald Observatory. I am indebted to Dr. Struve for many suggestions and to the staff of the McDonald Observatory for their help.

[19] D. H. McNamara, *Pub. A.S.P.*, 63, 38, 1951.

[20] W. A. Hiltner and R. H. Hardie, *Ap. J.*, 110, 438, 1949.

ON THE COLOR-MAGNITUDE DIAGRAM OF THE PLEIADES*

H. L. JOHNSON AND W. W. MORGAN
Yerkes and McDonald Observatories
Received July 25, 1951

ABSTRACT

A series of photoelectric observations of colors and magnitudes of 61 of the brightest members of the Pleiades is given. The observations were made with the 82- and 13-inch reflectors of the McDonald Observatory. A color-magnitude diagram from the new data is illustrated. The stars fall along a single, rather broad sequence having a sharp upturn for the brightest members; the McDonald observations do not confirm the fine structure found by Eggen. Attention is called to the desirability of further observations.

The results of O. J. Eggen[1] on the color-magnitude diagrams of various clusters are of the greatest interest, and the implications in the fields of galactic research and astrophysics are far-reaching.

Because of the importance of the discovery of fine structure, it is felt that additional evidence on the subject under a variety of observing conditions is of interest; a program of observations for a number of the Pleiades was therefore undertaken during the winter of 1950–1951; the observations were made by Johnson with the 13- and 82-inch reflectors of the McDonald Observatory.

The construction of the photometer is conventional. In order of increasing distance from the telescope, the essential parts are as follows: a large-field finding eyepiece, a focal-plane diaphragm, a high-power guiding eyepiece, filter slide, Fabry lens, and a 1P21 photomultiplier. Both the eyepieces are arranged so that they can be withdrawn from the light-beam while measurements are being made. The focal-plane diaphragms are 2, 3, 4, and 8 mm in diameter, corresponding to angular diameters of $15''$, $21''$, $30''$, and $60''$ with the 82-inch telescope, and $1'$, $1'.5$, $2'$, and $4'$ with the 13-inch telescope. The 2-mm diaphragm has been used for all 13-inch observations and for the 82-inch observations, with the exception of a few nights when the 3-mm diaphragm was necessary because of poor seeing. A Fabry lens is used to insure that the deflections will be independent of guiding so long as the star appears within the diaphragm.

The transmissions of the filters and the spectral response of the 1P21 photomultiplier have been measured with the monochromator of the Washburn Observatory; the over-all response of the photometer is given in Table 1 and Figure 1. The reflectivity of the very recently aluminized reflectors is not included. A radium-paint standard source has been included in the filter slide. A cast-iron magnetic shield was used with the 1P21 to reduce interference from such stray magnetic fields as may exist.

The amplifier was constructed by Johnson at the Washburn Observatory and is designed especially for the type of photometry reported here. This amplifier will be described in detail elsewhere, but the principal features are: very high stability, extremely linear relationship between input and output, and high gain. The amplifier is so designed that the gain depends only upon the ratios of the resistances of wire-wound resistors; this insures stable calibrations and linearity of scale. The calibrations and linearity of the amplifier have been checked several times; the maximum deviations (probably observational errors) are 0.2–0.3 per cent. The amplifier is therefore capable of measuring the output of the photomultiplier within a fraction of 1 per cent.

All measurements were recorded by a Brown Recording Potentiometer. The manu-

* *Contributions from the McDonald Observatory, University of Texas*, No. 205.

[1] See *Ap. J.*, 111, 65, 81, 414, 1950.

facturer states that the maximum error of the meter is one-quarter of 1 per cent of full scale. The average errors will, of course, be much smaller. Calibrations of the meter used show no deviations from linearity exceeding one-tenth of 1 per cent. No deflections smaller than about 20 per cent of full scale were used; the maximum error which could be introduced by the meter is therefore about one-half of 1 per cent (0.005 mag.). It is estimated that the average error introduced by the meter is 0.002 mag., at most.

Since the amplifier gain was always adjusted so that the "blue" deflections were all about the same size, the meter or amplifier errors cannot introduce appreciable errors into the magnitudes. Small systematic errors, of the size discussed above, will appear in the colors, but the amplifier and meter errors cannot introduce scatter.

No laboratory checks of the linearity of the photomultiplier have been made, although

TABLE 1

RESPONSE OF PHOTOMETER*

λ	Corning 9863 (Ultra-violet)	Corning 5030+ Schott GG13 (Blue)	Corning 3384 (Yellow)	λ	Corning 9863 (Ultra-violet)	Corning 5030+ Schott GG13 (Blue)	Corning 3384 (Yellow)
2983	0.51	0.00	.....	4459	.....	4.94	0.00
3190	3.51	.....	.....	4872	.....	.....	0.25
3410	5.49	.....	.....	4977	.....	2.10	1.27
3630	5.86	0.02	.....	5082	.....	.....	2.81
3780	4.64	0.48	.....	5187	.....	.....	3.87
3864	2.58	1.96	.....	5292	.....	.....	4.29
3959	0.80	4.74	.....	5500	.....	0.05	3.95
4058	0.11	.....	.....	6015	.....	.....	1.65
4157	0.00	.....	.....	6500	.....	.....	0.21
4257	.....	5.42	.....	7020	.....	.....	0.05

* Equal energy at all wave lengths.

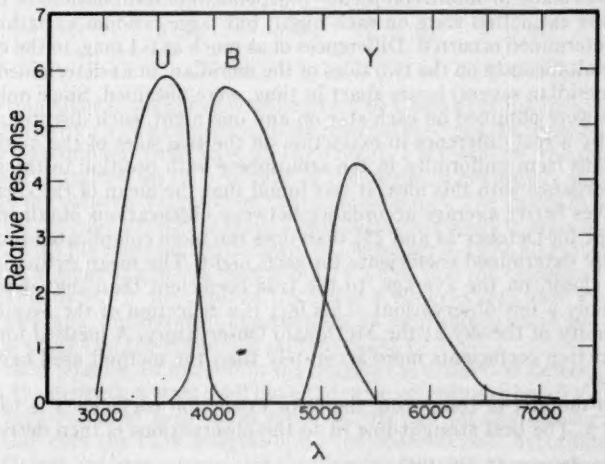

FIG. 1.—Response of the photometer to equal energy at all wave lengths

internal checks between the 82- and 13-inch telescopes indicate that the nonlinearity of the entire system cannot exceed 0.01 mag. over the entire range of brightness observed. There is, however, no reason to expect that any measurable nonlinearity should arise in the photomultiplier; independent checks for a number of tubes by R. W. Engstrom[2] and by Stebbins, Whitford, and Johnson[3] have not shown any significant deviations from linearity.

The deflections were taken in the following order: blue, yellow, ultraviolet, dark (if required), ultraviolet, yellow, blue. Next came the sky readings and standard source, if taken. All sky deflections were taken with the same diaphragm that was used for the stars. The sky corrections were made in two ways, depending upon whether the stars are scattered over the entire sky or clustered in one small region. Individual sky and standard light-source deflections were taken for all noncluster stars. For the cluster stars, sky and standard source deflections were taken only for every ten to fifteen stars, and the required corrections were interpolated for the intermediate stars.

After the deflections were corrected for sky, the observed colors, C_{y_0} and C_{u_0}, and the observed logarithmic deflections, log d_0, were computed as follows:

$$C_{y_0} = 2.5 \log \frac{y}{b};$$

$$C_{u_0} = 2.5 \log \frac{b}{u}; \qquad 1)$$

$$\text{og } d_0 = \log b .$$

The subscript 0 indicates quantities not corrected for extinction; the subscript is dropped when these corrections are made. The symbols y, b, and u designate the deflections obtained with the yellow, blue, and ultraviolet filters, respectively. Complete reductions for the colors of the stars were made before reductions for magnitudes were begun.

Six stars (10 Lac, η Hya, HR 875, HR 8832, α Ari, and β Cnc) were selected as extinction stars and secondary standards, and observations at widely different zenith distances were obtained for at least three of these stars on every night. At the beginning, an attempt was made to obtain completely independent determinations of the extinction for each of the extinction stars on each night, but large random variations in the extinction so determined occurred. Differences of as much as 0.1 mag. in the extinction determined simultaneously on the two sides of the meridian, or as determined on the same side of the meridian several hours apart in time, were obtained. Since only two to five observations were obtained on each star on any one night, such discordances could be caused, not by a real difference in extinction on the two sides of the meridian, but by local variations from uniformity in the atmosphere with position in the sky and with time. In accordance with this idea, it was found that the mean of the coefficients from all nights gives better average accordance between observations obtained on different nights (except for October 24 and 25) than does the more complicated process of using independently determined coefficients for each night. The mean extinction coefficient is therefore closer, on the average, to the true coefficient than that determined each night from only a few observations. This fact is a reflection of the excellent night-to-night uniformity of the sky at the McDonald Observatory. A method for determining nightly extinction coefficients more accurately than the method used heretofore is described below.

The usual method of computing the color extinction coefficients is to assume that $C_{y_0} = K \sec z$. The best straight-line fit to the observations is then derived, either by

[2] *J. Opt. Soc. America*, **37**, 420, 1947.

[3] *Ap. J.*, **112**, 469, 1950.

graphical means or by a least-squares solution. This procedure is the best that can be had for a single night, but, when observations on several nights are available, it completely disregards the fact that the color of an extinction star outside the atmosphere must be the same on all nights. To include the condition that all nights must lead to the same color for each extinction star should give a much greater leverage on the problem. Accordingly, this condition was included, and a least-squares solution for the color extinction coefficients for all nights simultaneously was made for each star. The results of this computation are tabulated in Table 2. The use of these coefficients reduces the

TABLE 2

EXTINCTION COEFFICIENTS

DATE (C.S.T.)	10 LAC	η HYA	HR 875	α ARI	HR 8832	β CNC
	Color					
Oct. 24, 1950	.....	0.157± 6	0.157± 8	0.113±5	.....	0.121±11
25, 1950	.....	.152± 6	.133± 9	.089±5	0.109±12	.119± 7
Nov. 11, 1950	0.107±3	.131± 7	.....	.....	.071± 6	.093±11
12, 1950	.121±3	.129± 6	.....	.....	.081± 6	.083±10
27, 1950	.127±2	.....	.....	.....	.084± 5	.....
Dec. 8, 1950	.133±2	.....	.128±10	.....	.076± 5	.....
24, 1950	.117±3	.132± 7	.114± 8	.068±4	.068± 6	.078±10
25, 1950	.133±6	.124± 7	.128±13	.073±7	.072± 9	.070±11
26, 1950	.116±3	.126± 5	.142±13	.092±7	.072± 6	.079± 8
Jan. 3, 1951	.....	.128± 8	.123±16	.065±6	.....	.080±14
4, 1951	.118±3	.124± 5	.124± 8	.072±4	.070± 6	.083± 9
5, 1951	.....	.131±11	.119± 9	.080±5	.....	.094±10
6, 1951	.107±3	.121± 5	.118±10	.059±5	.061± 5	.073± 7
7, 1951	0.110±3	0.122± 5	0.114± 9	0.062±4	0.067± 5	0.078± 7
	Magnitude					
Mean	0.101	0.101	0.092	0.081	0.091	0.082

discordances from night to night below those given by a mean extinction coefficient. The final results are nearly twice as accurate, from internal evidence, as those obtained from independently determined coefficients for each night. Furthermore, the differences between coefficients obtained for the two sides of the meridian are greatly reduced and, in fact, are within the values expected from the probable errors. The values in Table 2 have been adopted for the color determinations. These comments apply to stars scattered over the entire sky. With the exception of the night of December 8, 1950, all Pleiades observations were made at hour angles less than about $1\frac{1}{2}$ hours, and the calculated extinctions are practically identical. On the night of December 8, observations were made up to an hour angle of $4\frac{1}{2}$ hours, but frequent observations on local standards in the cluster provided adequate checks on the extinction on that night.

It has not been possible to include in the magnitude extinction determinations the condition that the extinction stars shall have the same magnitudes on all nights because the standard light-source *as used*, while quite satisfactory for any one night, was not sufficiently stable over the time interval of all the observations. Accordingly, a mean extinction coefficient has been adopted for the magnitudes; the values appear in Table 2.

The three filter bands—yellow, blue, and ultraviolet—permit the determination of

two colors and one magnitude. We shall assume, following Stebbins, Whitford, and Johnson,[3] that, for C_{y_0} and d_0, the following relationships between the observed quantities and those outside the atmosphere hold:

$$C_y = C_{y_0} - (k_1 + k_2 C_y) \sec z \,; \qquad (2)$$
$$\log d = \log d_0 + (k_3 + k_4 C_y) \sec z \,.$$

These assume that the extinction coefficients are linear functions of the color index, and

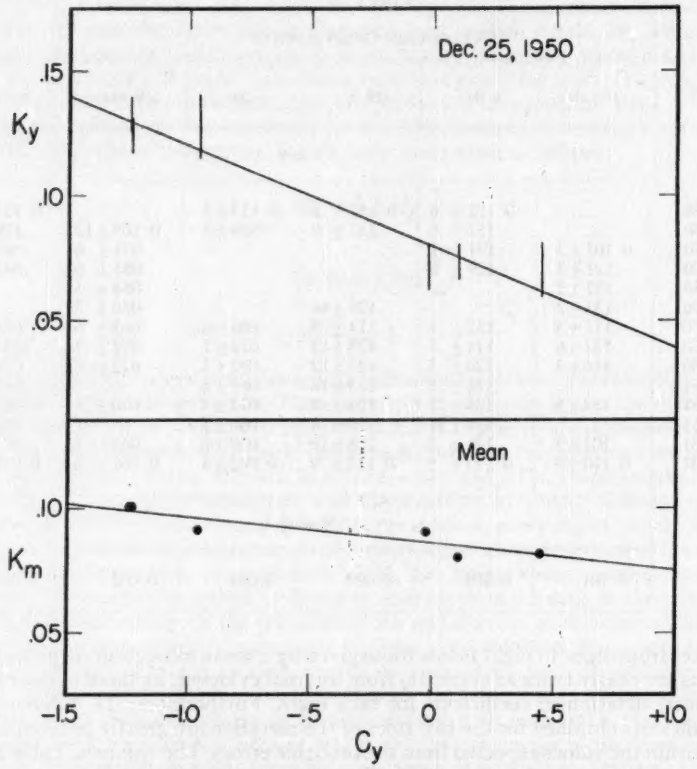

FIG. 2.—*a*, *upper*, The color extinction coefficient, K_y, on December 25, 1950; *b*, *lower*, the mean magnitude extinction coefficient, K_m.

Figure 2, *a* and *b*, shows that this assumption is satisfactory. The ultraviolet observations will be discussed in a later paper.

After log *d* is obtained, appropriate corrections for the amplifier gain for each star are made, and the result is converted to photoelectric magnitudes, m_p.

On July 6, 1950, at a meeting in Pasadena attended by Bowen, Baade, Baum, Minkowski, and Pettit, of the Mount Wilson and Palomar Observatories; Eggen, Kron, and Weaver, of the Lick Observatory; Whitford, of the Washburn Observatory; and Johnson, now at Yerkes and McDonald Observatories, the magnitudes and colors given by Stebbins, Whitford, and Johnson[3] for the nine stars NPS 6, 2r, 10, 4r, 13, 8r, 16, 19, and

12r were adopted as standards for all future photoelectric work. It was agreed that the values given by Stebbins, Whitford, and Johnson for these nine stars define a color-magnitude system as nearly on the International system as can be obtained with a limited number of stars. This new color-magnitude system, which we shall designate as the (*P*, *V*) system, has been used in the comparisons with the North Polar Sequence reported here. Following Kron,[4] we shall adopt *P* and *V* as the photographic and visual magnitudes on the (*P*, *V*) system. The ultraviolet observations will add an ultraviolet magnitude, *U*, to be defined in a later paper. Again following Kron,[4] we shall adopt $P - V$ as the color index on the (*P*, *V*) system.

TABLE 3

COLORS AND MAGNITUDES OF NINE NPS STARS WHICH DEFINE (*P*, *V*) SYSTEM

DATE	NPS 6	NPS 10	NPS 4r	NPS 2r	NPS 13	NPS 16	NPS 19	NPS 8r	NPS 12r
	C_y								
No. of obs.	13	13	13	13	5	5	5	5	2
Oct. 24, 1950..	−0.874	−0.773	+0.016	+0.512	.....	.....	.....	.....	.....
25, 1950..	−0.870	−0.779	+0.011	+0.542	.....	.....	.....	.....	.....
Nov. 11, 1950..	−0.853	−0.738	+0.025	+0.515	−0.696	−0.556	−0.492	+0.035	.....
12, 1950..	−0.868	−0.738	+0.024	+0.533	.....	.....	.....	.....	.....
27, 1950*.	−0.842	−0.766	+0.033	+0.524	−0.695†	−0.543†	+0.473†	+0.066†	+0.312
Jan. 6, 1951..	−0.859	−0.733	+0.039	+0.550	.....	.....	.....	.....	.....
___ 7, 1951..	−0.839	−0.742	+0.015	+0.524	−0.695	−0.591	−0.434	+0.058	.....
$\overline{C_y}$.....	−0.859	−0.753	+0.023	+0.529	−0.695	−0.558	−0.468	+0.056	+0.312
$P-V$‡.....	+0.06	+0.12	+1.02	+1.56	+0.24	+0.32	+0.41	+1.02	+1.27
$P-V$§.....	+0.022	+0.137	+0.983	+1.535	+0.200	+0.350	+0.448	+1.019	+1.298
	Δm_p								
Oct. 24, 1950..	−0.009	+2.049	+1.985	+0.640	.....	.....	.....	.....	.....
25, 1950..	+0.021	+2.057	+1.997	+0.671	.....	.....	.....	.....	.....
Nov. 11, 1950..	−0.003	+2.048	+1.977	+0.641	+3.309	+4.378	+5.492	+4.179	.....
12, 1950..	−0.024	+2.045	+1.999	+0.658	.....	.....	.....	.....	.....
27, 1950*.	+0.012	+2.052	+1.983	+0.617	+3.328†	+4.404†	+5.474†	+4.178†	+6.540
Jan. 6, 1951..	+0.040	+2.083	+1.987	+0.662	.....	.....	.....	.....	.....
___ 7, 1951..	−0.044	+2.019	+2.007	+0.716	+3.370	+4.402	+5.504	+4.225	.....
Δm_p.....	0.000	+2.051	+1.992	+0.659	+3.337	+4.396	+5.491	+4.195	+6.541
P‡.....	7.15	9.17	9.24	7.90	10.51	11.56	12.66	11.43	13.80
P§.....	7.14	9.20	9.21	7.93	10.49	11.56	12.67	11.42	13.79

* Observations with the 82-inch on this night, all others 13-inch.

† Double weight was given to those values of the fainter stars that were observed with the 82-inch.

‡ From Stebbins, Whitford, and Johnson, *Ap. J.*, **112**, 469, 1950.

§ Values computed from formula (4).

Observations on the nine stars defining the (*P*, *V*) system were obtained on seven nights. The colors and magnitudes observed are given in Table 3, where C_y designates the "natural" photoelectric color and Δm_p designates the difference

$$\Delta m_p = m_p - m_p\,(\text{NPS 6}) - \frac{\sum_i (\overline{m_{p_i}} - m_{p_i})}{N}, \qquad (3)$$

[4] *Ap. J.*, 113, 324, 1951.

where i ranges for each night over the stars NPS 6, 10, 4r, 2r, and as many of the extinction stars as were observed on that night, and N is the total number of such stars observed on that night. The third term is necessary to avoid making the assumption that the values obtained for NPS 6 on each night are exact.

The following two equations relating the natural photoelectric system and the (P, V) system were assumed:

$$\begin{aligned} P - V &= A + BC_y\,, \\ P &= m_p(\text{NPS 6}) + \Delta m_p + D(P - V)\,. \end{aligned} \tag{4}$$

Least-squares solutions gave the following values for the coefficients:

$$\begin{aligned} A &= +0.958 \pm 0.007 \text{ (p.e.)}\,, \\ B &= +1.090 \pm 0.013 \text{ (p.e.)}\,, \\ D &= +0.085 \pm 0.009 \text{ (p.e.)}\,, \\ m_p(\text{NPS 6}) &= \quad 7.139 \pm 0.008 \text{ (p.e.)}\,. \end{aligned} \tag{5}$$

These formulae represent the (P, V) system satisfactorily over the range of color available in the standards [$+0.06 \leqslant (P - V) \leqslant +1.56$]; but for the blue stars a considerable extrapolation is required. We shall assume that the straight-line extrapolation is satisfactory for all stars, regardless of color.

The next step was to determine the values on the (P, V) system for the extinction stars. The values of C_y and Δm_p for these six stars are given in Table 4. Values of C_y are given on fourteen nights, but values of Δm_p are given on only seven. The addition of color observations on the seven nights on which the North Polar Sequence was not observed is legitimate, since careful nightly determinations of color extinction coefficients have been made and the color determinations and reductions have been made in a differential manner so that variations in the photomultiplier and amplifier gains cancel out. All other reductions to the (P, V) system were made through these six stars, which may be considered to be the standard stars for this work.

The internal probable errors derived from the individual observations from which Tables 3 and 4 are constructed are:

$$\begin{aligned} C_y &: \text{p.e.} = \pm 0.005 \text{ mag.} \begin{pmatrix}\text{one obs.}\\ \text{unit air mass}\end{pmatrix}, \\ m_p &: \text{p.e.} = \pm 0.012 \text{ mag.} \begin{pmatrix}\text{one obs.}\\ \text{unit air mass}\end{pmatrix}. \end{aligned} \tag{6}$$

There is no significant difference between the North Polar Sequence and the other stars, when the difference in air mass (sec z) is considered. There is no internal evidence to indicate that any of the four brightest NPS stars (except possibly NPS 2r) or the six secondary standards are variable by an amount larger than the errors of observation. Evidence showing the possible variability of NPS 2r is presented below.

If we assume that the average air mass at which observations were made is $\overline{\sec z} = 1.5$, the average probable errors for a single observation are:

$$\left.\begin{aligned} C_y &: \overline{\text{p.e.}} = \pm 0.008 \text{ mag.} \\ m_p &: \overline{\text{p.e.}} = \pm 0.018 \text{ mag.} \end{aligned}\right\} \text{for one observation}\,. \tag{7}$$

The probable errors on the system as defined by the six secondary standard stars are:

$$\left.\begin{aligned} P - V &: \overline{\text{p.e.}} = \pm 0.009 \text{ mag.} \\ P &: \overline{\text{p.e.}} = \pm 0.018 \text{ mag.} \end{aligned}\right\} \text{ for one observation .} \qquad (8)$$

It should be emphasized that these are internal probable errors and that the probable errors of the coefficients in the equations of transformation to the (P, V) system must be considered if the external probable errors are to be computed.

The nightly values of C_y for the Pleiades stars are given in Table 5. In the determina-

TABLE 4

MAGNITUDES AND COLORS FOR EXTINCTION STARS

DATE	10 LAC	η HYA	HR 875	HR 8832	α ARI	β CNC
	C_y					
Oct. 24, 1950	.....	−1.246	−0.959	.....	+0.111	+0.441
25, 1950	.....	−1.234	−0.974	−0.017*	+0.097	+0.446
Nov. 11, 1950	−1.238	−1.213	.....	−0.032	.....	+0.446
12, 1950	−1.236	−1.236	.....	−0.022	.....	+0.426
27, 1950†	−1.235	.....	−0.937*	−0.023	.....	.....
Dec. 8, 1950†	−1.238	.....	−0.960	−0.014	.....	.....
24, 1950‡	−1.234	−1.221	−0.961	−0.023	+0.113	+0.451
25, 1950‡	−1.228	−1.263	−0.959	−0.026	+0.116	+0.413
26, 1950‡	−1.236	−1.244	−0.933	−0.037	+0.127	+0.412
Jan. 3, 1951	.....	−1.245	−0.959	.....	+0.108	+0.443
4, 1951	−1.238	−1.235*	−0.946	−0.030	+0.114	+0.454*
5, 1951	.....	−1.239	−0.970	.....	+0.108	+0.438
6, 1951	−1.240	−1.230	−0.947	−0.030	+0.108	+0.440
7, 1951	−1.237	−1.228	−0.952	−0.032	+0.106	+0.450
$\overline{C_y}$	−1.236	−1.236	−0.955	−0.026	+0.111	+0.438
$P-V$	−0.389	−0.389	−0.083	+0.930	+1.080	+1.435
No. of obs.	27	32	31	29	30	32
	Δm_p					
Oct. 24, 1950	.....	−3.190	−2.014	.....	−4.175	−2.295
25, 1950	.....	−3.185	−2.050	−0.775*	−4.180	−2.305
Nov. 11, 1950	−2.616	−3.174	.....	−0.733	.....	−2.275
12, 1950	−2.607	−3.183	.....	−0.728	.....	−2.299
27, 1950	−2.611	.....	−2.036*	−0.729	.....	.....
Jan. 6, 1951	−2.632	−3.210	−2.075	−0.726	−4.172	−2.312
7, 1951	−2.631	−3.200	−2.074	−0.732	−4.148	−2.278
$\overline{\Delta m_p}$	−2.619	−3.190	−2.050	−0.737	−4.169	−2.294
m_p	4.521	3.950	5.090	6.403	2.971	4.846
P	4.488	3.917	5.083	6.482	3.062	4.968
No. of obs.	12	18	14	13	14	18

* Only one observation; weight, ½.

† 82-inch, full aperture.

‡ 82-inch, effective aperture = 24 inches. All others, 13-inch.

TABLE 5

PLEIADES COLORS, C_y
(1950–1951)

Eggen No.	Dec. 8*	Oct. 25	Nov. 12	Jan. 4	Jan. 3	Jan. 6	Dec. 24†	Dec. 25†	Oct. 24	Mean	$P-V$
3	−0.805									−0.801	+0.085
	−0.797										
5	−0.836									−0.839	+0.043
	−0.842										
7	−0.574									−0.574	+0.332
8	−0.767									−0.771	+0.118
	−0.774										
9	−0.501									−0.499	+0.414
	−0.496										
10	−1.084		−1.076	−1.087		−1.092	−1.077			−1.084	−0.224
	−1.086										
11				−1.161		−1.154	−1.137			−1.151	−0.297
13	−0.403									−0.409	+0.512
	−0.414										
15	−0.702									−0.705	+0.197
	−0.708										
16	−1.111		−1.108	−1.118		−1.117	−1.096			−1.113	−0.255
	−1.128										
17			−1.136	−1.158		−1.147	−1.136			−1.144	−0.289
18	−0.587									−0.597	+0.307
	−0.606										
19	−0.817									−0.817	+0.067
20	−0.674									−0.685	+0.211
	−0.695										
21	−0.432									−0.432	+0.487
22	−0.873		−0.869							−0.873	+0.006
	−0.877										
23	−0.486									−0.489	+0.425
	−0.491										
24	−0.514									−0.516	+0.396
	−0.518										
25			−1.106	−1.120		−1.110	−1.093			−1.107	−0.249
26	−0.844									−0.844	+0.038
27	−1.069		−1.077							−1.076	−0.215
	−1.081										
28	−1.058		−1.054							−1.060	−0.197
	−1.068										
31				−1.109		−1.099	−1.094			−1.101	−0.242
32	−0.393									−0.396	+0.526
	−0.399										
33	−0.946									−0.946	−0.073
34‡	−0.689			−0.678	−0.704	−0.695	−0.688	−0.670		−0.687	+0.209
35	−0.310									−0.310	+0.620
36	−0.564									−0.564	+0.343
39	−0.395									−0.395	+0.527
40‡	−1.024		−0.998	−1.026		−1.030	−1.013	−0.999	−1.016	−1.015	−0.148
41	−0.741									−0.742	+0.149
	−0.743										
42	−0.570									−0.568	+0.339
	−0.566										
43	−1.005									−1.007	−0.140
	−1.008										
44	−0.831				−0.843					−0.837	+0.046
	−0.837										

* On the night of December 8, 1950, control of the extinction was insured by frequent checks upon the three tertiary standards, Nos. 34, 40, and H 669. The extinction coefficients determined for this night from the stars 10 Lac, HR 875, and HR 8832 have proved to be satisfactory. In all cases where two or more observations of a star were made, the time interval separating the individual observations was about 4 hours, except for the tertiary standards, which were observed at intervals of about 1½ hours. In most cases the individual observations were made at considerably different zenith distances; the excellent agreement between the individual observations again shows that the extinction coefficients adopted for this night are correct. All individual observations on this night are given, except for the tertiary standards, for which the mean values are given. 82-inch, full aperture.

† 82-inch, effective aperture = 24 inches.

‡ Tertiary standard.

TABLE 5—*Continued*

Eggen No.	Dec. 8*	Oct. 25	Nov. 12	Jan. 4	Jan. 3	Jan. 6	Dec. 24†	Dec. 25†	Oct. 24	Mean	*P−V*
45	−0.991									−1.001	−0.133
	−1.011										
46	−0.883		−0.879						−0.878	−0.880	−0.001
	−0.880										
47	−0.973		−0.956							−0.969	−0.098
	−0.977										
48‡		−1.132	−1.115	−1.139	−1.152	−1.143	−1.110		−1.118	−1.130	−0.274
49	−0.498									−0.497	+0.416
	−0.495										
50	−0.490									−0.488	+0.426
	−0.486										
51	−0.677									−0.675	+0.222
	−0.675										
	−0.672										
52	−0.565									−0.566	+0.341
	−0.567										
53	−0.478									−0.478	+0.437
	−0.478										
54	−1.103		−1.107	−1.116		−1.121	−1.094		−1.109	−1.109	−0.251
	−1.115										
55	−0.472									−0.472	+0.444
56	−0.916		−0.900							−0.907	−0.031
	−0.915										
	−0.902										
57	−0.421									−0.422	+0.498
	−0.423										
58	−0.748									−0.753	+0.137
	−0.757										
59			−1.111	−1.133		−1.133	−1.115			−1.123	−0.266
60	−1.114		−1.098	−1.131		−1.127	−1.099			−1.115	−0.257
	−1.123										
61	−0.820									−0.820	+0.064
62	−0.942									−0.939	−0.066
	−0.936										
63	−1.066		−1.060							−1.060	−0.197
	−1.053										
64	−0.852		−0.854							−0.857	+0.024
	−0.865										
65	−0.602									−0.602	+0.302
	−0.602										
67	−1.086		−1.077							−1.082	−0.221
68	−0.953		−0.943							−0.955	−0.083
	−0.969										
69	−0.906		−0.898							−0.898	−0.021
	−0.889										
70	−0.943									−0.951	−0.079
	−0.958										
71	−0.656									−0.652	+0.247
	−0.647										
H 597	+0.136									+0.136	+1.106
H 569	+0.202									+0.202	+1.178
H 669‡	+0.685			+0.652	+0.651	+0.640	+0.679	+0.665		+0.662	+1.680
H 993	−0.868									−0.872	+0.007
	−0.875										

tion of these values the only corrections made to the observed colors are those for extinction, using the extinction coefficients listed in Table 2. The quantity $\overline{C_y}$ is the straight mean of the nightly values of C_y, with no night corrections. Double weight was given December 8, if two or more observations were made on that night. The values of $(P - V)$ were obtained directly from $\overline{C_y}$ through equations (4) and the coefficients in equations (5). Small night corrections ($\sim$0.01 mag.) could have been made on the assumption that the colors of the tertiary standards must be the same on all nights, but, in the interests of simplicity, these corrections were omitted.

For the determination of the magnitudes, four Pleiades stars (Nos. 40, H 669, 34, and 48) were chosen as tertiary standards for the cluster, and the mean magnitudes, $\overline{m_p}$, were determined for these stars from the secondary standards. Thereafter, these mean values for the Pleiades standards were used on each night to determine the nightly values of m_p, given in Table 6. This procedure takes account of nightly variations of extinction in the Pleiades region from the mean extinction given in Table 2. The quantity $\overline{m_p}$ is found directly from the nightly values of m_p, with no night corrections. For the correction from $\overline{m_p}$ to P, the value of D given in equations (5) has been used.

The observations on December 8, 1950, were made with the 82-inch telescope and a 2-mm focal-plane diaphragm corresponding to an angular diameter of 15″. The largest sky correction on this night, for the faintest star, was about 1 per cent. For the 13-inch observations of the Pleiades, the diaphragm was 2 mm in diameter, or 1′ in angular diameter, and the largest sky correction for the faintest Pleiades star observed with the 13-inch was about 2 per cent. The sky corrections were therefore so small that accurate knowledge of the sky background, which is likely to be quite variable in the Pleiades, was unnecessary.

The new color-magnitude diagram is illustrated in Figure 3; it should be compared with Eggen's own observations,[1] which have been replotted in Figure 4. In order to plot the sequence lines of Eggen on the McDonald observations, it is necessary to transform Eggen's colors to the $(P - V)$ system. The relationship between the two systems is shown in Figure 5. The relationship defined by the solid line was used for the transformation; it was then possible to examine the fit between Eggen's sequences as redrawn and the McDonald observations. This is illustrated in Figure 6. For comparison, Eggen's own observations[1] and sequences are illustrated in Figure 7.

An inspection of Figures 3 and 6 fails to indicate fine structure in the McDonald observations. There is certainly no marked preference of the plotted points for the lines as drawn in Figure 6; nor does there seem to be any reason for drawing additional lines—other than a rather broad, smooth relationship between color and magnitude for the main sequence as a whole—together with the well-known sharp upturn at the bright end.

Now, if the McDonald magnitudes and colors were less accurate than those of Eggen, the fine structure observed by the latter might be masked. A comparison with a third series is therefore of interest.

Figure 8 gives an intercomparison between the magnitudes of Eggen,[5] Johnson (as listed in the present paper), and those of Binnendijk.[6] The agreement between Johnson and Binnendijk is as good as could be expected when the heterogeneous sources of the latter are kept in mind. After a correction in zero point of around 0.1 mag. has been made, the probable error of the observations is in approximate agreement with Binnendijk's own estimate of the accuracy of his catalogue. It appears that the accidental errors of the magnitudes of both Johnson and Binnendijk are somewhat lower than those of Eggen.

[5] Corrections to the magnitudes of five of the stars have been communicated by Eggen (unpublished). The revised values are: No. 15, 8.79; No. 20, 8.84; No. 41, 8.52; No. 58, 8.53; and No. 71, 9.13. The published values have been used in the present discussion.

[6] *Ann. Sterrew. Leiden*, Vol. 19, No. 2, 1946.

TABLE 6

PLEIADES MAGNITUDES, m_p
(1950–1951)

Eggen No.	Dec. 8*	Oct. 24	Nov. 12	Jan. 4	Jan. 3	Jan. 6	Dec. 24†	Dec. 25†	Mean	P
3	8.311								8.31	8.32
	8.306									
5	8.104								8.09	8.10
	8.079									
7	9.361								9.36	9.39
8	8.261								8.26	8.26
	8.249									
9	10.198								10.20	10.24
	10.203									
10	5.245		5.244	5.256		5.245	5.234		5.24	5.22
	5.225									
11				3.435		3.432	3.416		3.43	3.40
13	10.846								10.84	10.88
	10.836									
15	8.749								8.74	8.76
	8.735									
16	5.391		5.394	5.416		5.415	5.396		5.40	5.38
	5.391									
17			4.014	4.023		4.032	4.015		4.02	4.00
18	9.259								9.26	9.28
	9.254									
19	8.091								8.09	8.10
20	8.777								8.77	8.79
	8.759									
21	10.561								10.56	10.60
22	7.163		7.157						7.16	7.16
	7.165									
23	10.078								10.08	10.12
	10.083									
24	9.793								9.79	9.82
	9.791									
25			3.623	3.641		3.639	3.626		3.63	3.61
26	7.887								7.89	7.89
27	5.551		5.541						5.54	5.53
	5.543									
28	6.225		6.229						6.22	6.21
	6.217									
31				3.948		3.964	3.928		3.95	3.93
32	10.923								10.90	10.95
	10.883									
33	7.273								7.27	7.27
34‡	8.277			8.251	8.294	8.282	8.274	8.288	8.28	8.30
35	10.767								10.77	10.82
36	9.578								9.58	9.61
39	10.993								10.99	11.04
40‡	6.663	6.678	6.679	6.668		6.667	6.663	6.665	6.67	6.66
41	8.519								8.51	8.52
	8.501									
42	9.761								9.75	9.78
	9.743									
43	6.850								6.85	6.84
	6.843									
44	7.695				7.674				7.68	7.69
	7.685									
45	7.136								7.13	7.12
	7.130									

* Checks on the magnitude extinction on December 8, 1950, were made in the manner described in a footnote to Table 5. 82-inch, full aperture. All individual observations on this night are given, except for the tertiary standards, for which the mean values are given.

† 82-inch, effective aperture = 24 inches.

‡ Tertiary standard.

TABLE 6—*Continued*

Eggen No.	Dec. 8*	Oct. 24	Nov. 12	Jan. 4	Jan. 3	Jan. 6	Dec. 24†	Dec. 25†	Mean	*P*
46	7.744	7.767	7.754						7.75	7.75
	7.747									
47	6.701		6.721						6.70	6.70
	6.694									
48‡		2.618	2.613	2.622	2.585	2.611	2.604		2.61	2.59
49	10.247								10.25	10.28
	10.244									
50	9.630								9.63	9.66
	9.626									
51	8.447								8.45	8.47
	8.447									
	8.466									
52	9.428								9.42	9.45
	9.420									
53	10.491								10.49	10.52
	10.485									
54	5.195	5.211	5.204	5.214		5.203	5.196		5.20	5.18
	5.197									
55	10.411								10.41	10.45
56	6.898		6.914						6.90	6.90
	6.898									
	6.906									
57	10.793								10.79	10.83
	10.781									
58	8.478								8.48	8.49
	8.476									
59			3.386	3.388		3.372	3.353		3.38	3.35
60	4.843		4.849	4.866		4.840	4.842		4.85	4.83
	4.845									
61	8.167								8.17	8.17
62	7.451								7.45	7.44
	7.443									
63	6.398		6.403						6.40	6.38
	6.396									
64	7.979		7.971						7.98	7.98
	7.981									
65	9.358								9.36	9.38
	9.358									
67	5.939		5.943						5.94	5.92
68	7.441		7.449						7.44	7.44
	7.438									
69	7.378		7.389						7.39	7.38
	7.395									
70	6.848								6.85	6.84
	6.845									
71	9.044								9.04	9.06
	9.034									
H 597	9.776								9.78	9.87
H 569	8.762								8.76	8.86
H 669‡	7.973			7.983	7.969	7.967	7.988	7.960	7.97	8.12
H 993	9.138								9.14	9.14
	9.138									

A similar intercomparison of the colors of the three observers is given in Figure 9. Figure 10 illustrates a comparison between the colors of Eggen,[1] Johnson, and Hertzsprung.[7] This last comparison is not independent of that with Binnendijk, since the latter used Hertzsprung's colors in his compilation.[8]

Additional evidence on the accuracy of the McDonald magnitudes and colors is given

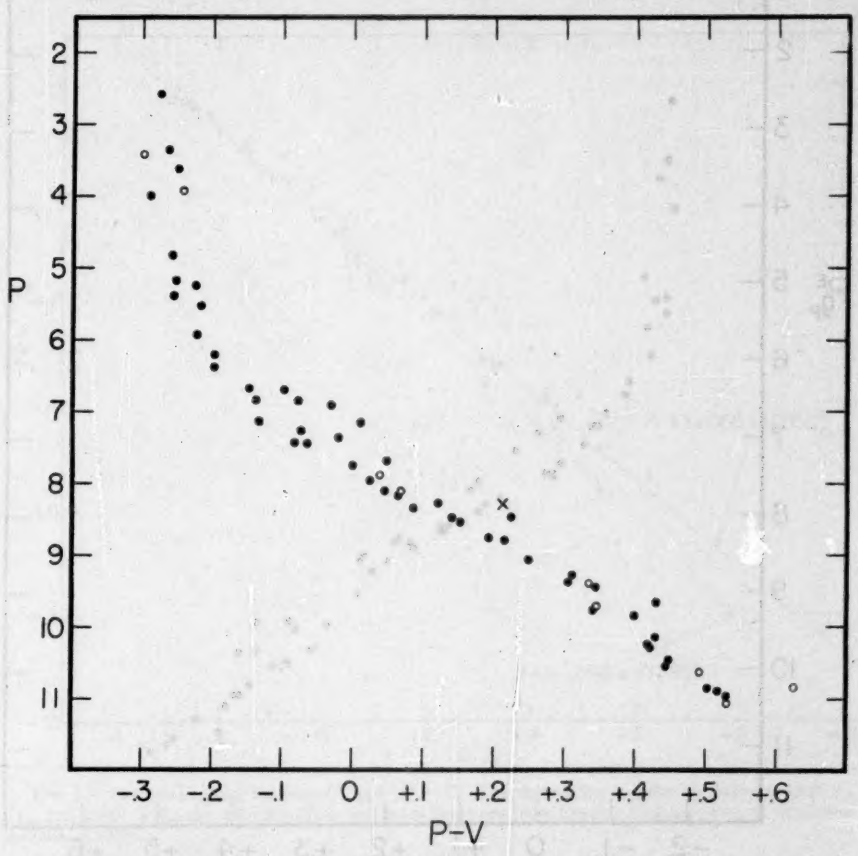

FIG. 3.—The color-magnitude diagram for the Pleiades from the McDonald data. The cross indicates the position of the reddened A0 star, No. 34. The open circles designate stars in Eggen's Area C; all other stars are in Eggen's Areas A and B.

in Figure 11, where comparisons are made for the same stars as observed with the 13- and 82-inch[9] telescopes at McDonald. The light-flux measured by the photometer differs by about 4 mag. for the same star with the two instruments; a critical check of the linearity

[7] *Effective Wavelengths of Stars in the Pleiades* (Copenhagen, 1923).

[8] It should be noted that the resolution in the color-magnitude diagrams is much more sensitive to the accuracy of the colors than to the magnitudes. Only gross errors in the latter can affect color-magnitude arrays appreciably.

[9] Full aperture.

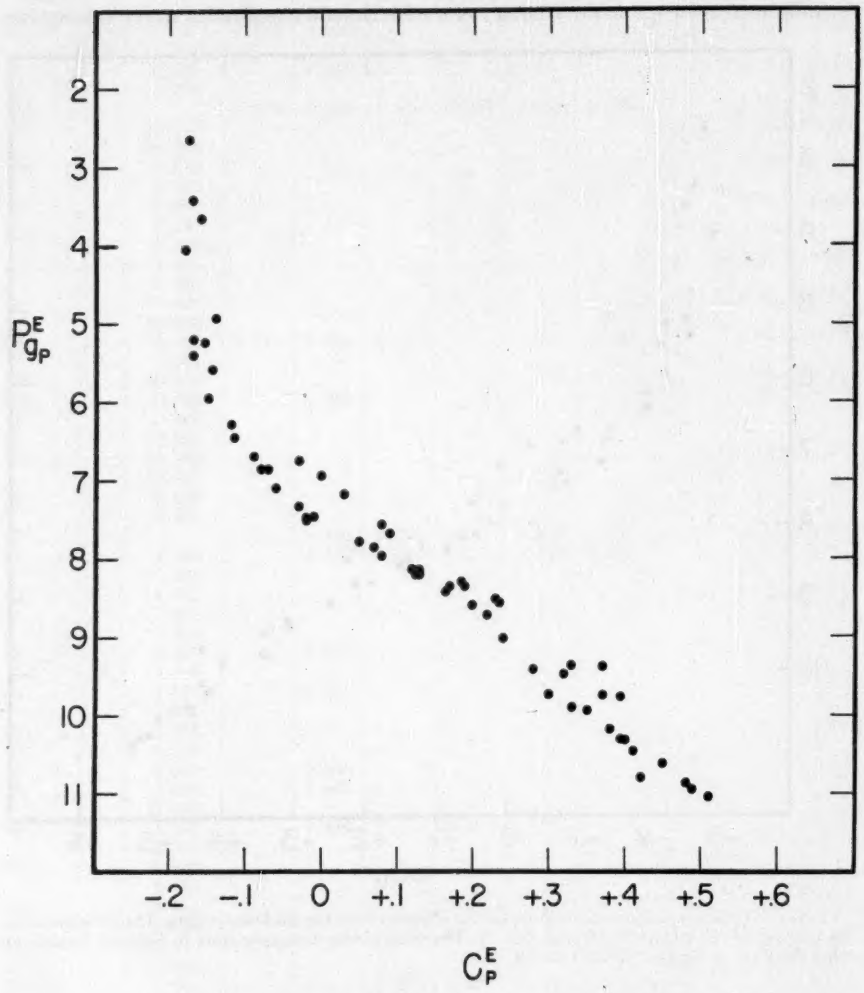

FIG. 4.—The color-magnitude diagram for the Pleiades from Eggen's data

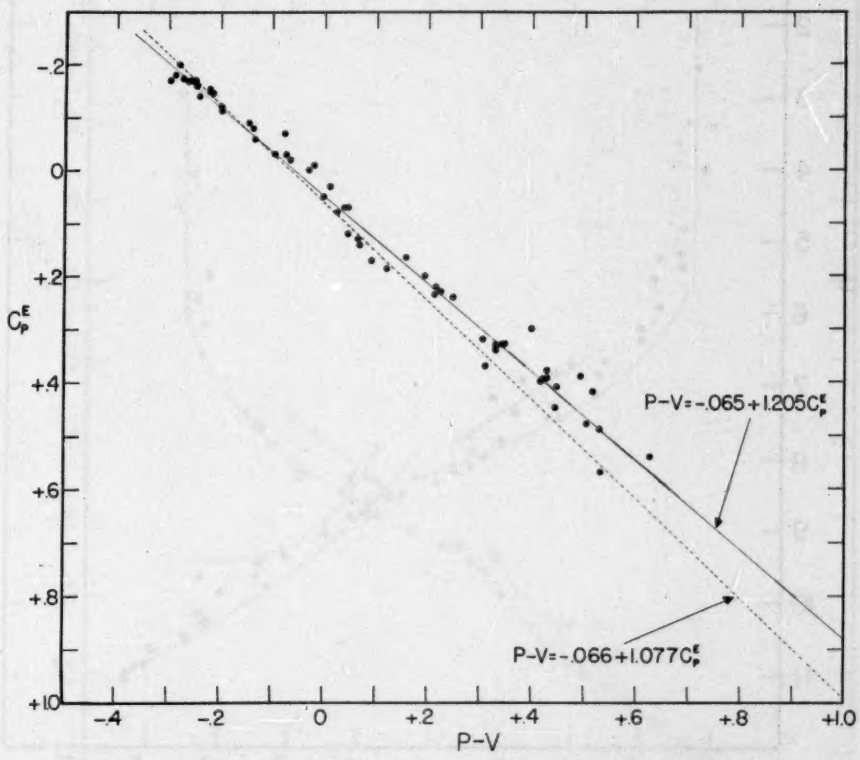

FIG. 5.—The relationship between C_p^E and $(P - V)$. The dotted line is given by Johnson (*Ap. J.*, 112, 240, 1950), while the solid line is the best transformation from Eggen's Pleiades colors to the International system.

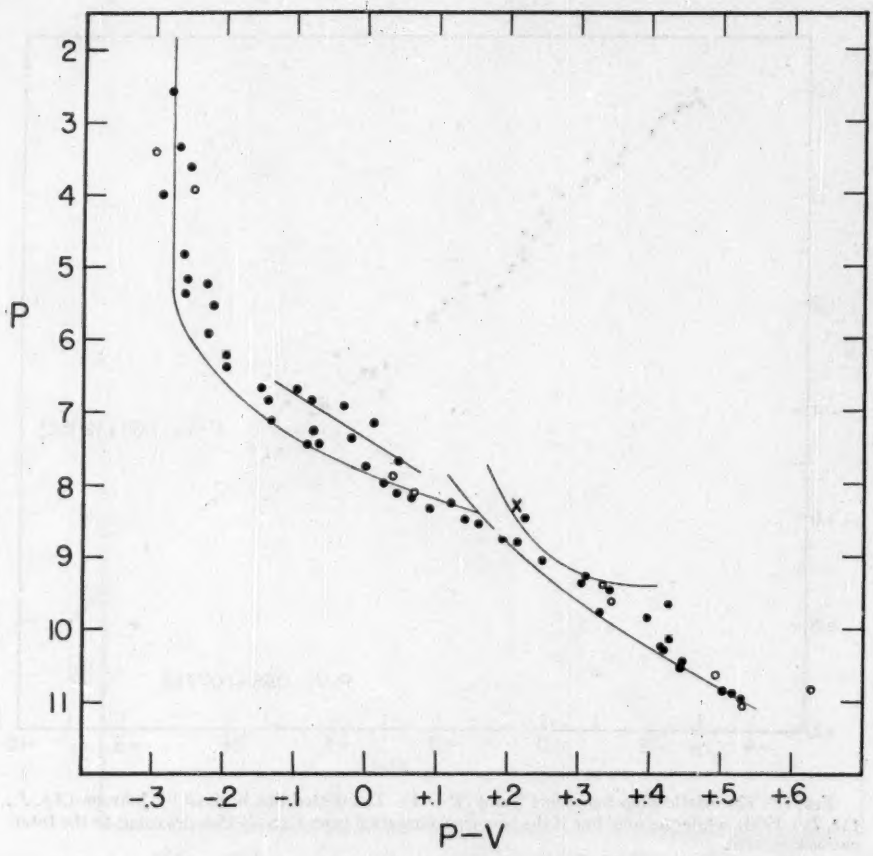

FIG. 6.—The color-magnitude diagram for the Pleiades from the McDonald data. The sequences are Eggen's transformed to the International system by the following equations: $P = P^{E}g_{p} - 0.02$; $P - V = -0.065 + 1.205\ C^{E}_{p}$. The cross designates the reddened A0 star, and the open circles stars in Eggen's Area C.

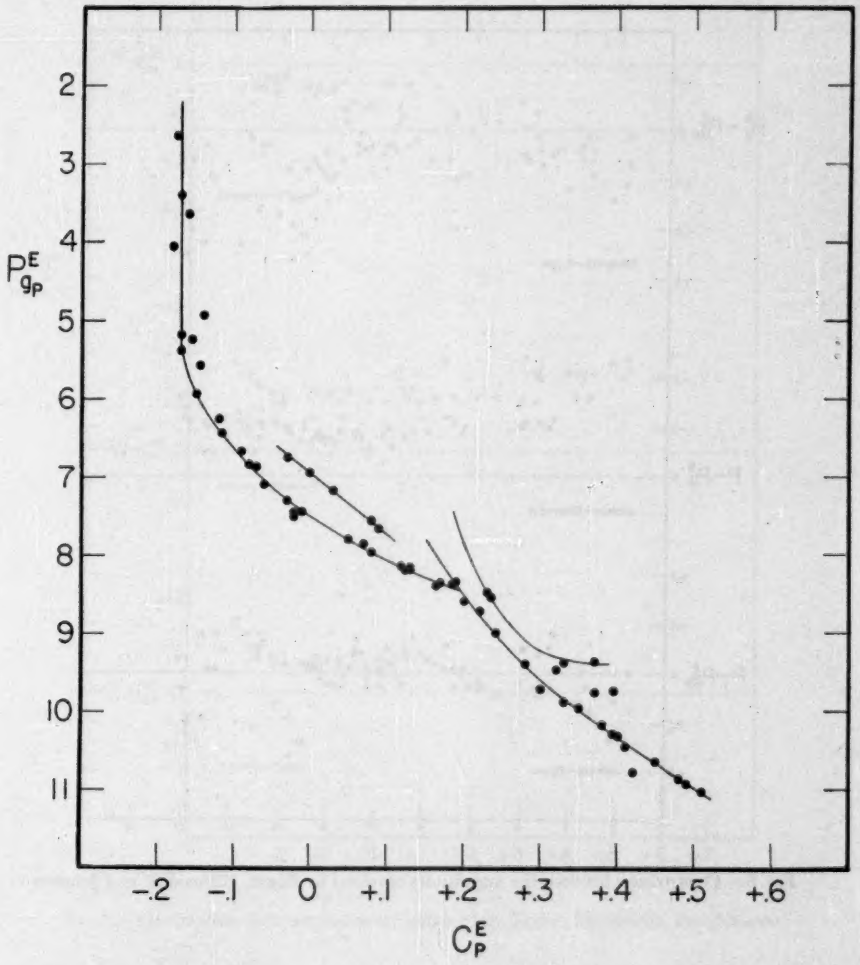

FIG. 7.—The color-magnitude diagram for the Pleiades from Eggen's data. The sequences are Eggen's

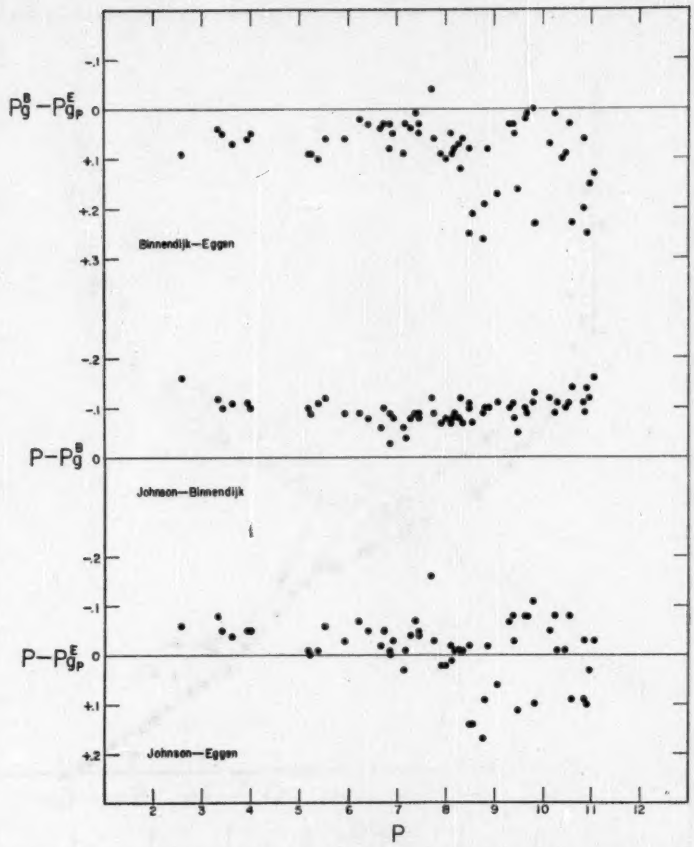

FIG. 8.—Comparisons between the magnitudes obtained by Eggen, Binnendijk, and Johnson

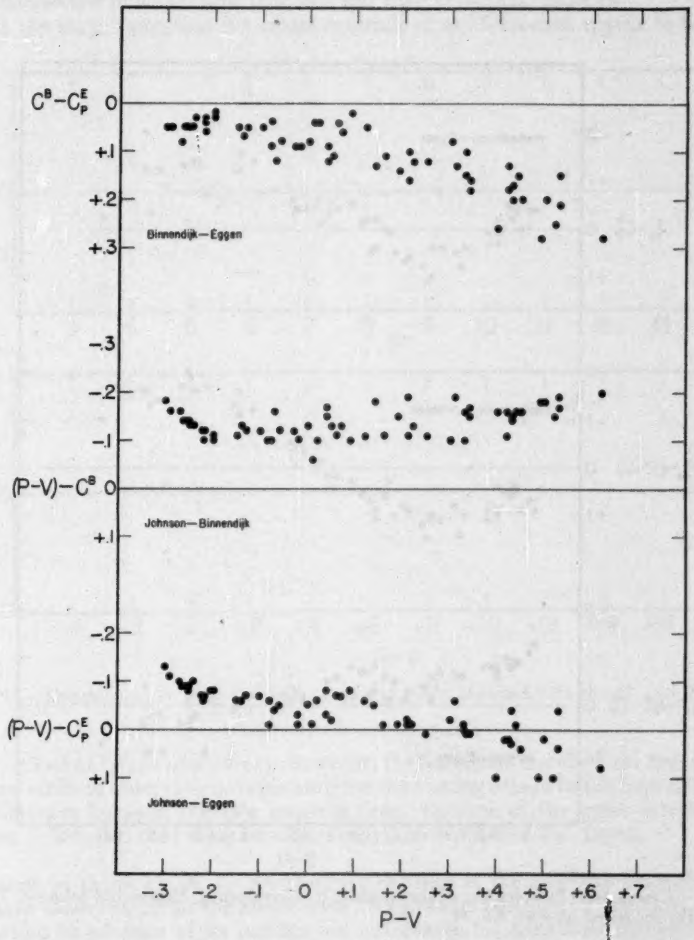

FIG. 9.—Comparisons between the colors obtained by Eggen, Binnendijk, and Johnson

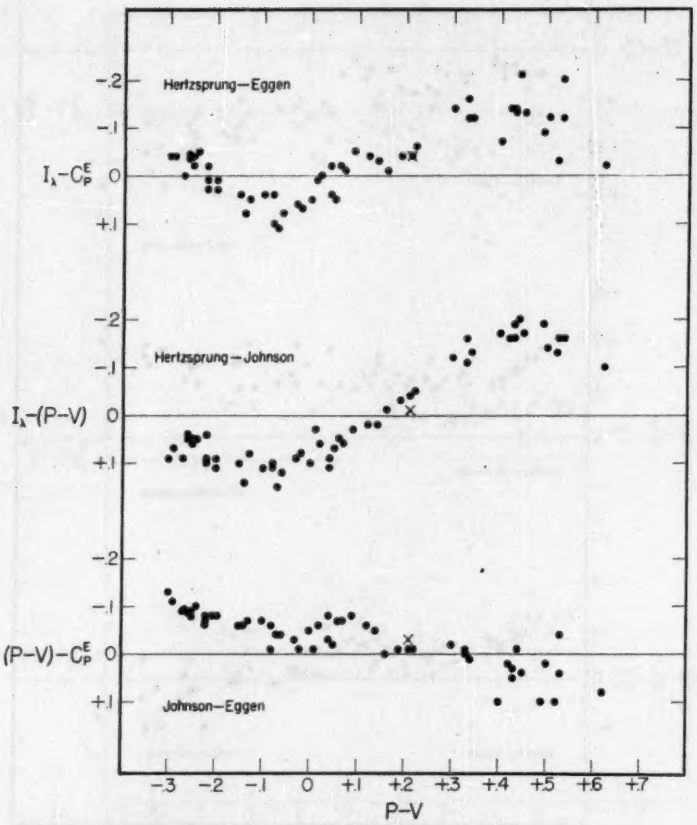

FIG. 10.—Comparisons between the colors obtained by Hertzsprung, Eggen, and Johnson. The cross represents the reddened A0 star, No. 34.

of response is therefore afforded by such a comparison. The excellent agreement in both magnitude and color for the two series is strong evidence for high systemic and accidental accuracy of the McDonald results. The open circle designates NPS 2r; its large residual in the magnitude plot indicates that this star may be slightly variable.

Both the magnitudes and the colors determined at McDonald appear to be at least

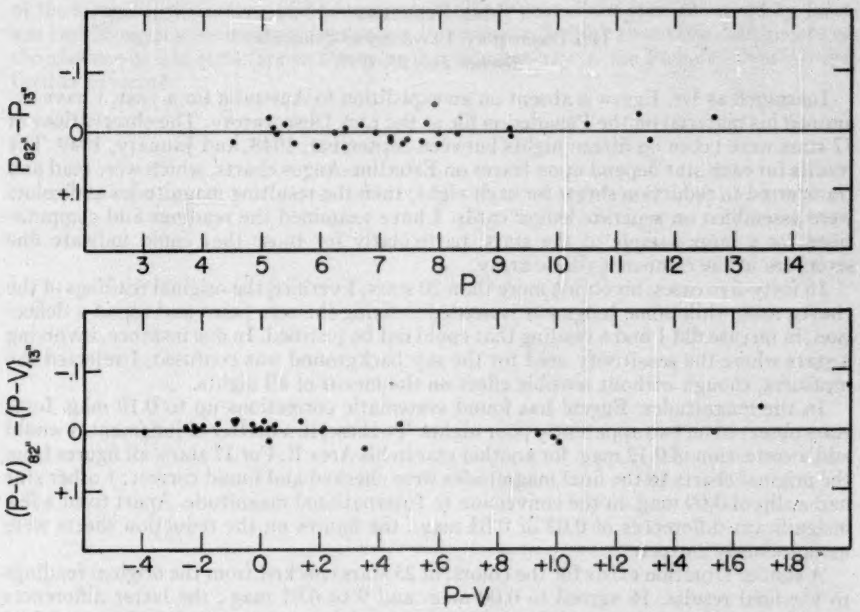

FIG. 11.—Comparisons between the magnitudes and colors obtained with the 82- and 13-inch telescopes.

equal to those of Eggen in accuracy; however, the former do not show the fine structure.

A new series of observations is planned for the coming season in the hope of resolving the differences between the two investigations. Because of the great interest of the problem, it is hoped that other observers may also reobserve the cluster.

We wish to thank Dr. A. E. Whitford for the loan of the amplifier belonging to the Washburn Observatory for the above work. We are also indebted to Dr. G. E. Kron for information in advance of its publication concerning his simplified nomenclature for magnitudes and colors. Many of the computations were carried out by Mr. Stewart Sharpless and Mrs. Mildred Provin.

NOTE ON OLIN J. EGGEN'S OBSERVATIONS OF THE PLEIADES

JOEL STEBBINS
Lick Observatory, University of California
Received July 25, 1951

Inasmuch as Dr. Eggen is absent on an expedition to Australia for a year, I have examined his material on the Pleiades on file at the Lick Observatory. The observations of 77 stars were taken on fifteen nights between September, 1948, and January, 1949. The results for each star depend upon traces on Esterline-Angus charts, which were read and transferred to reduction sheets for each night; then the resulting magnitudes and colors were assembled on separate ledger cards. I have examined the readings and computations for a large sample of the stars, particularly for those that could indicate fine structure in the color-magnitude array.

In forty-five cases, involving more than 20 stars, I verified the original readings of the charts, and, while some judgment is needed in fixing the zero point and top of a deflection, in no case did I find a reading that could not be justified. In one instance, involving 4 stars where the sensitivity used for the sky background was confused, I rejected the measures, though without sensible effect on the means of all nights.

In the magnitudes, Eggen[1] has found systematic corrections up to 0.19 mag. for 7 stars observed on two apparently poor nights. To these, in a matter of judgment, I would add a correction of 0.12 mag. for another star in his Area B. For 17 stars, all figures from the original charts to the final magnitudes were checked and found correct; 1 other star had a slip of 0.09 mag. in the conversion to International magnitude. Apart from a few insignificant differences of 0.02 or 0.03 mag., the figures on the reduction sheets were monotonously correct.

A similar situation exists for the colors: of 25 stars checked from the original readings to the final results, 16 agreed to 0.00 mag. and 9 to 0.01 mag., the latter differences caused partly by neglected decimals. In 4 other stars, two errors of 0.02, one of 0.04 and one of 0.05 mag., were found, the last for a star at the lower limit of the eleventh magnitude. I rejected 1 star because of discordant colors on the two poor nights.

From the night-to-night residuals, including all the poor ones, we have the accompanying table of probable errors. Since nearly all the stars were observed on two or

PROBABLE ERRORS ACCORDING TO MAGNITUDE

	Range of Magnitude				
	2.65–5.9	6.0–7.9	8.0–8.9	9.0–9.9	10.0–11.08
No. obs.	36	34	36	42	39
No. stars	12	14	15	17	14
P.E. 1 obs., mag.	±0.015	±0.024	±0.014	±0.026	±0.025
P.E. 1 obs., color	±0.010	±0.011	±0.007	±0.009	±0.012

three nights, the errors in the magnitudes are negligible in the color-magnitude array, and the probable error of a resulting color was usually considerably less than ±0.01

[1] *Ap. J.*, **114**, 522, n. 5, 1951.

mag., a precision not exceptional in photoelectric work. Hence final errors of several hundredths of a magnitude in the colors should rarely occur.

My present judgment is that Eggen's measures give strong evidence for the existence of the bright blue-dwarf sequence in the Pleiades but that the data are insufficient to confirm in the Pleiades the bright-dwarf sequence that he found in the Hyades. In view of the foregoing discussion, and because some 60 per cent of the stars observed by Johnson and Morgan were measured on only a single night, I think that their conclusions on the absence of fine structure in the color-magnitude array in the Pleiades should await further evidence.

NOTES

TRANSITION PROBABILITIES FOR C_2 AND N_2^+*

In a previous paper in this *Journal*,[1] the author reported the results of semitheoretical calculations of transition probabilities for C_2 and N_2^+. These calculations were made with the ordinary dipole-length form of the dipole transition operator. Following the suggestion of Professor Chandrasekhar, the calculations have been repeated with the dipole-velocity form of the transition operator but with the same approximate methods and orbitals as before.[2]

The dipole-velocity calculations showed a remarkably different dependence upon the assumed degree of $s - p$ hybridization in the orbitals concerned from that shown by the dipole-length calculations. For a given choice of the effective nuclear charges, the two methods agree in a very limited region of hybridization. Hence, by making a reasonable choice for the effective Z values, one can obtain an estimate of hybridization completely independent of the semiempirical choice kindly supplied by Professor Mulliken in the previous calculations.

The "best" choice of hybridizations is somewhat higher than that suggested by Mulliken and leads to the following "best" choices for f-numbers:

C_2, Swan bands, $^3\Pi_g \leftarrow {}^3\Pi_u$, $f = 0.18$;

C_2, Deslandres, D'Azambuja system, $^1\Pi_g \leftarrow {}^1\Pi_u$, $f = 0.23$;

N_2^+, first negative system, $^2\Sigma_u^+ \leftarrow {}^2\Sigma_g^+$, $f = 0.18$.

It will be noted that these values are about 40 per cent higher than those previously suggested by the author and roughly seventy-five times those suggested by Lyddane, Rogers, and Roach.[3]

The net effect of these results is to reduce considerably the estimates of C_2 (and possibly CN) concentrations wherever these are based upon absolute intensity measurements of these transitions. Complete details of these calculations will be published elsewhere.

HARRISON SHULL

DEPARTMENT OF CHEMISTRY
IOWA STATE COLLEGE
July 26, 1951

ON THE SPECTRUM OF AC ANDROMEDAE

The general features of the light-variations of the star AC And[1] resemble those of cluster-type cepheids but show such rapid changes from cycle to cycle that it is not possible to characterize the light-curve by a simple period. In his photometric study of the

* *Contributions from the Institute for Atomic Research and Department of Chemistry, Iowa State College, Ames, Iowa*, No. 144. This work was supported in part by the Ames Laboratory of the Atomic Energy Commission.

[1] H. Shull, *Ap. J.*, **112**, 352, 1950.

[2] See S. Chandrasekhar, *Ap. J.*, **102**, 223, 395, 1945; S. S. Huang, *Ap. J.*, **108**, 354, 1948, for applications of the dipole-velocity method in the case of atoms.

[3] *Phys. Rev.*, **60**, 281, 1941.

[1] $\alpha = 23^h13^m4$; $\delta = +48°14'$ (1900). Discovered by Guthnick and Prager in 1927.

star, N. T. Florja[2] showed that the observed light-oscillations could be represented fairly well by the superposition of two light-curves of the RR Lyr type, with periods 0.525 and 0.711 day and photographic amplitudes 0.77 and 1.16 mag., respectively. More recently, M.A. Lurie[3] has rediscussed Florja's interpretation, with the addition of new observations, and has essentially verified the correctness of the earlier analysis. On the basis of his discussion, Florja suggested that the object in question could be a close double star, with both components being cluster-type cepheids. Were this the true physical nature of AC And, it would be a unique object among all known short-period pulsating stars. For this reason the writer and Dr. O. Struve obtained a few spectrograms of the object with the Cassegrain spectrograph of the McDonald 82-inch reflector. The faintness of the star ($m_{pg} \sim 11.0$) required the use of the 180-mm camera and the quartz optics, a combination which gives a dispersion of 120 A/mm at K.

The spectrum of the object, in the five plates obtained, appears to be similar to that of the cluster cepheids with later spectral type (SW And may be given as prototype).[4] By using the standard line-intensity ratios, spectral types around F6, with giant characteristics, may be assigned, although the metallic lines, in general, appear to be weaker than in the spectra of standard bright stars (ι Peg). It has been noticed also that the

TABLE 1

OBSERVATIONS OF AC ANDROMEDAE

Plate Q $f/2$	Date July, 1949	Sp.	V* (Km/Sec)	Δm (Mag.)
12007.....	5.378	F5	−85	−0.3
12010.....	10.367	F6	−35	0.0
12011.....	10.417	F6	−60	−0.2
12017.....	13.364	F6	−85	−0.4
12023.....	17.299	F5	−80	−0.6

* A radial velocity of −70 km/sec has been published by A. E. Joy (*Pub. A.S.P.*, **50**, 303, 1938).

faint metallic lines do not appear in every plate so sharp and well defined as those observed on July 10, notwithstanding the nearly equal quality of the spectrograms. The plates obtained were measured for radial velocity, and the results are given in Table 1. The internal consistency of the measures indicates that the observational uncertainty of the radial velocities is about 15 km/sec, corresponding to a mean standard deviation in the micrometer settings of only 1.5 μ at $H\delta$. The eye estimates of the brightness of the variable at the times of observation are also given in Table 1, relative to the minimum light observed.

On the basis of the present spectroscopic data and ignoring the position of our times of observation on the light-curve, it is not possible to decide definitely whether the star is a binary or not. The former possibility, however, is made improbable by the information provided by our spectra of July 5, 13, and 17, in all of which the lines appear with the same degree of sharpness and indicate nearly the same radial velocity and spectral class. It should be recalled, in this context, that "typical" cluster cepheids have, in the mean, a range in radial velocity of about 80 km/sec and a variation in spectral type of nearly a whole class. While further spectroscopic material is obtained to ascertain the physical nature of AC And, rather than consider it as a binary, it would seem more appropriate to classify it in the same class of pulsating stars to which AI Vel belongs. The spectrum

[2] *A.J.U.S.S.R.*, **14**, 11, 1937.

[3] *Variable Stars, Akad. Nauk. SSSR*, **7**, 182, 1950.

[4] Cf. G. Münch and L. Rivera Terrazas, *Ap. J.*, **103**, 371, 1946.

of this star, recently studied by G. Herbig,[5] with fair certainty excludes the possibility of being a binary with two components of nearly the same brightness. The light-variations of AI Vel, on the other hand, although they have not been studied so extensively as those of AC And, also show rapid changes from cycle to cycle.[6]

GUIDO MÜNCH

YERKES OBSERVATORY
August 11, 1951

A USEFUL LUMINOSITY DISCRIMINANT IN THE LATE K AND EARLY M GIANTS

The separation of dwarf K5–M2 stars from the giants spectroscopically is a relatively simple matter. A number of features located in the ordinary photographic region can be used, and in the green and yellow regions the strong absorption of *MgH* and the D lines of *Na* are especially useful. Supergiants of classes K5–M2 can also be accurately segregated from giants and dwarfs on spectrograms of moderate dispersion; up to the present time, however, this has usually been done by the use of the blue region.

In the light of recent work which emphasizes the value of the M giants for problems of galactic research, it appears worth while to re-examine the problem of the separation of late-type supergiants and giants in the regions lying at longer wave lengths. The green region, in particular, appears to be especially useful for this problem.

Figure 1 illustrates the visual region of several K5–M2 stars. An inspection of the interval λλ 5175–5270 shows several blended features which are sensitive to changes in absolute magnitude—in spite of the fact that the dispersion of the original plates (obtained with the parallax spectrograph of the 40-inch telescope) is only around 260 A/mm in this region. The upper spectrum is of 61 Cyg A (dK5); the following three are of giants of classes K5, M0, and M2, respectively (α Tau, β And, χ Peg); the two at the bottom of the illustration are of supergiants of classes cK5 and cM2 (ψ^1 Aur, α Ori).

The broad, deep blend near λ 5175 in dK5 changes in appearance in the giant stars and degenerates to a much narrower feature at cK5. Even more striking, however, is the change with luminosity in the ratio of the blends at λ 5206 and λ 5250; the former is very much the stronger in the dwarf and normal giants, while the two features are approximately equal in intensity in the supergiants illustrated. The pair of features at λ 5250 and λ 5270 also show marked variations in relative intensity with luminosity due to the increase in strength of λ 5250 with increasing luminosity.

The changes with luminosity appear to be due principally to blends including one or more members of the $a^5D - z^7D^o$ multiplet of *Fe* I; the behavior of the lines of this multiplet thus resembles that of several other intersystem multiplets of *Fe* I located in the ordinary photographic region and having the same lower term—the lowest of the *Fe* I spectrum.

The use of the above ratios should result in a considerable decrease in exposure time in comparison with the blue region and should thus permit extension of the spectroscopic parallax method to fainter giants in this interval of spectrum.

W. S. FITCH
W. W. MORGAN

YERKES OBSERVATORY
June 21, 1951

[5] *Ap. J.*, **110**, 156, 1950.

[6] Cf. F. Zagar, *B.A.N.*, **8**, 169, 1937; and A. van Hoof, *B.A.N.*, **8**, 172, 1937.

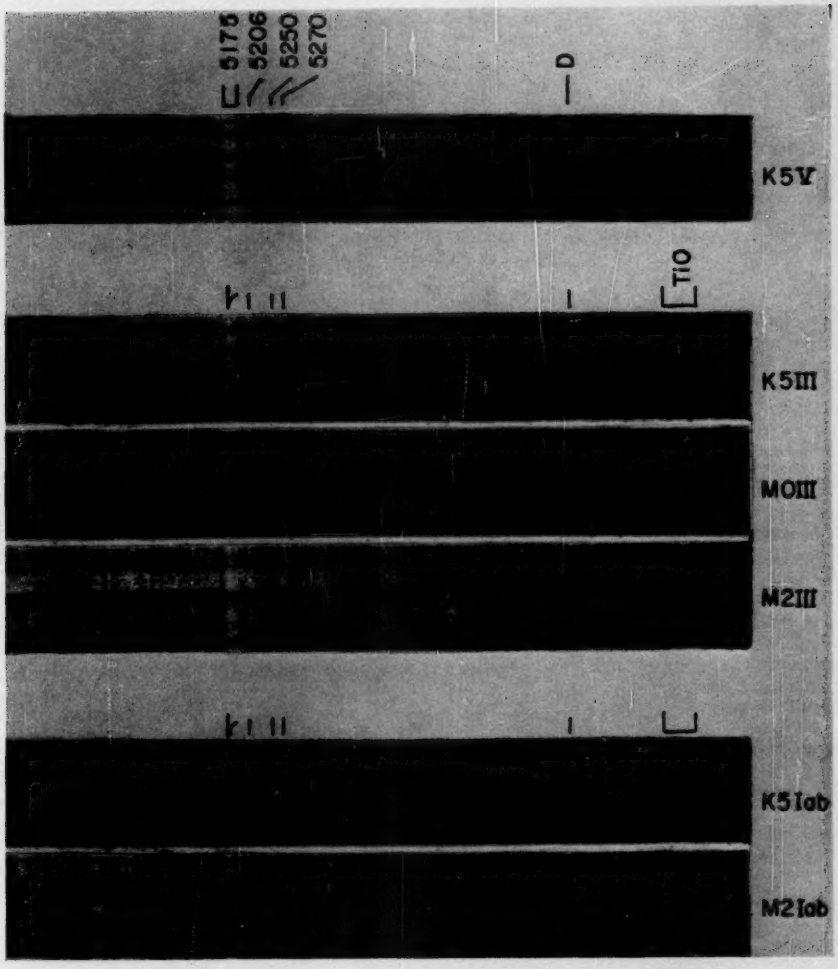

FIG. 1.—Some luminosity effects in the visual region for stars in the spectral range K5–M2

REVIEWS

Stellar Evolution. By OTTO STRUVE. Princeton: Princeton University Press, 1950. Pp. 266+xiv. $4.00.

In 1949 the Vanuxem Lectures at Princeton were given by Professor Otto Struve. On these lectures was based a book which Struve has entitled *Stellar Evolution*. In this he has set out the views to which he has been led by spectroscopic studies, particularly of double stars.

The book is divided into three long sections. The first, entitled "Probing the Stars' Chemical Composition," is a general introduction to the ideas later developed. Since the book is intended for a wider audience than professional astronomers, the section ranges over a great deal of observational and theoretical astronomy. Among the subjects discussed are the determination of stellar luminosities, radii, and masses; the mass-luminosity and Hertzsprung-Russell diagrams; the hydrogen content of stars, as determined from the theory of stellar structure; the composition of stellar atmospheres; the curve of growth of spectral lines; Baade's stellar populations I and II; and many others. This section is packed with information, and, if a reader skims carelessly through any part, he is liable to overlook something which may be vitally important later. The conclusion drawn from the general survey, and in particular from the rapidity with which early-type stars exhaust their sources of energy, is that stars of types O, B, and A evolve fairly rapidly and are soon removed from the upper left-hand portion of the H-R diagram. A few of them, it is suggested, become red giants, but most slide along the main sequence, losing mass as they go.

The second section discusses the evolution of single stars. This again treats a number of general subjects, such as the generation of energy by the conversion of hydrogen into helium, the formation of stars in interstellar clouds, and the rotational breakup of stars. But the distinctive note of the book is struck in a discussion of the star Pleione, in which Struve suggests that this and many other rapidly rotating stars are surrounded by rapidly rotating rings or shells. This he relates to von Weizsäcker's cosmogonic theories, according to which a star, soon after formation, gets rid of its excess angular momentum by shedding material, mainly in the direction of the rotational motion, from a turbulent envelope which surrounds it. The shells around Pleione and similar stars are, he suggests, the means by which such stars lose their excess mass and angular momentum and develop from early to late main-sequence stars. Most O, B, and A stars are supposed to evolve in this way; the few which rotate slowly are unable to lose mass and develop into red giants.

The third and longest section is entitled "The Origin and Development of Close Binary Stars"; it is, however, mainly a discussion of the observations of such stars, with a few evolutionary suggestions at the end. It begins with a general discussion of binaries, particularly of spectroscopic binaries, and a classification of the different types of eclipsing variables. Then the general properties of W Ursae Majoris and β Lyrae binaries are considered, with detailed discussions of numerous individual systems. It is emphasized that nebulous rings are normally found in association with close binaries, sometimes surrounding both stars, sometimes around the brighter component only; the rings rotate with the stars but also show irregular motions and motions predominantly outward from the binary. On the basis of this discussion a tentative course of evolution of close binaries is proposed. A massive, rapidly rotating star is supposed to condense from interstellar material; because of rotational instability, this splits to form a massive early-type pair; matter continually ejected in expanding rings reduces the mass until a late-type W Ursae Majoris pair results; more mass is lost, and a catastrophic reunion of the pair finally leads to a single star with planets. Arguments are examined for and against the hypotheses that rotational fission can occur in stars and that close binaries are in no way different from distant pairs.

As mentioned earlier, the book is intended for physicists, chemists, geologists, etc., as well as astronomers. But it is not, in the usual sense of the term, a popular book. Readers must be warned that they cannot hope to extract full value from the book by a single reading; it contains far too much meat. It is the kind of book which needs and deserves re-reading.

At the same time, Struve has perhaps made it rather more difficult than was necessary. He sometimes treats side issues with an unnecessary degree of detail. Sometimes (as in the last thirty pages) he puts forward his ideas with such apparent hesitation and uncertainty as to make it difficult to understand what he really does mean. Finally, sometimes (and particularly in the third section) the book shows signs of overhasty preparation, in that different subsections are not well co-ordinated. On pages 169–171 a classification of eclipsing binaries is described; no use whatever is made of this later. The discussion on pages 248–251 is really a repetition of that on pages 232–239, without new ideas. And, to descend to more trivial details, frequent reference is made to P Cygni type phenomena (e.g., on pp. 21, 106, 116, 117, 131, 143, 148) without any clear explanation of what these phenomena may be.

In this book Struve has advanced from his own proper field of stellar spectroscopy into the field of theory—even of speculative theory. He is, of course, treading on dangerous ground; dynamical problems cannot be discussed on spectroscopic evidence alone. A theorist will want to ask many questions before he can accept Struve's proposed scheme of evolution. I personally feel that the arguments against this scheme (set out by Struve in full detail) are stronger than those in its favor, especially as I believe that the use of the Reynolds criterion on page 151 is invalid, and I do not believe that rotational fission of stars is theoretically possible. But these are matters which must be left to later discussion. The value of the book does not appear to me to rest on the correctness or otherwise of the few tentative conclusions to which the author comes. It consists rather in the way in which he has brought together facts of many different kinds, in the vivid picture which he gives of processes in double stars, and in the challenge to readers to try to interpret the facts. Too often, observers and theoretical workers live apart from each other; we must be grateful to anyone who attempts to bridge the gulf. Personally, I am very glad to have been able to read the book.

T. G. COWLING

University of Leeds
Leeds, England

Modern Interferometers. By C. CANDLER. London: Hilger & Watts, Ltd., 1951. Pp. 502. $9.75.

Two-thirds of this book deals with interferometers in the usual meaning of the word; in the remainder, monochromatic radiation, applications of thick plates and thin films to interferometry, diffraction gratings, and refractometers are treated. The work is descriptive of instruments and their methods of use, but it includes some theoretical discussion. Each chapter is followed by a bibliography. In the Preface it is noted that, because of wartime conditions, many articles were not available during the preparation of the manuscript, which may account for some regrettable omissions from the text.

The book assembles information relating to the design, the construction, and (in smaller degree) the application of spectroscopic apparatus. The use of interference phenomena in testing lenses and prisms, in gauges for metrology, and in various forms of refractometers is developed in detail. Tables of numerical data, graphs, line drawings, and halftone illustrations are freely used. The instrument shop, rather than the spectroscopic laboratory, makes itself felt in the text. The reader may surmise that the applications of interferometers are not always discussed from personal experience. References sometimes apply to the work of a recent investigator instead of the originator of the idea.

The diagram on page 303 is erroneous in showing equal maximum intensities for the fringes corresponding to various coefficients of reflection. Although absorption in the metallic films has no effect on resolving power in the Fabry-Perot etalon, as the writer notes elsewhere, the reduced intensity of the fringes formed by thick films is a serious limitation to the usefulness of the etalon. The discussion of absorption in metallic films on pages 311–314 is of little practical value. Fabry and Buisson (1919) showed that, in the useful range of thickness, the absorption of silver is very nearly constant.

Emphasis is given to the use of the Twyman prism interferometer (an adaptation of the Michelson form) in compensating for the inhomogeneity of the glass by local refiguring of the prism faces. But in small prisms this procedure is not necessary, and in large ones the results are disappointing when the observations extend over a long range of wave lengths, as in a stellar spectrograph. This is one reason why plane diffraction gratings (not transmission replicas, as Candler supposes) are increasingly used in stellar spectroscopy.

Chapter xv, "Ruling a Diffraction Grating," attempts too much. Ten pages here are drawn from J. A. Anderson's valuable article in the *Dictionary of Applied Physics* (1923). The very few readers who will seriously use this material will read the original article and take it as a point of departure from which to draw their own designs. Contrary to his expressed belief, the author might, by inquiry, have obtained specific information on modern developments.

The discussion of astigmatism in concave gratings and of methods for correcting it is excellent. Another method, using a cylindrical lens behind the slit, might well have been included.

In a paragraph on the index of refraction of air (p. 460), we read: "Finally many stellar and solar lines are emitted by matter at very low pressure, so that the refractive index of air must be known before they can be identified in terrestrial sources." Here the author has confused the slight displacement of a spectral line which is produced by a change of 1 atm. in the pressure affecting the emitting or absorbing source with the variation of wave length as dependent on changes in the refractivity of the medium in which the measurement is made. As is well known, neither of these effects is important in the identification of stellar and solar lines.

For the refractivity of gases, three chapters present the application of the Fabry-Perot etalon, the Rayleigh refractometer, and that of Jamin. Six interesting pages are given to the relation of group velocity to phase velocity.

On page 421 under Figure 17.5 we read: "The plate is placed at the center of curvature of the grating, not on the Rowland circle." This is an obvious slip; the correct statement is given on page 422.

The merits of *Modern Interferometers* are very considerable. In wealth of detail and in extent of scope the book is unique in the reviewer's experience. Metrologists, master-opticians, designers of spectroscopic apparatus, and spectroscopists concerned with high resolution will find and use its valuable features.

HAROLD D. BABCOCK

Mount Wilson and Palomar Observatories